



**HAL**  
open science

# Non-coding RNAs as prognostic biomarkers of cardiac arrest

Francesca Maria Stefanizzi

► **To cite this version:**

Francesca Maria Stefanizzi. Non-coding RNAs as prognostic biomarkers of cardiac arrest. Human health and pathology. Université de Lorraine, 2022. English. NNT : 2022LORR0294 . tel-04126952

**HAL Id: tel-04126952**

**<https://hal.univ-lorraine.fr/tel-04126952>**

Submitted on 13 Jun 2023

**HAL** is a multi-disciplinary open access archive for the deposit and dissemination of scientific research documents, whether they are published or not. The documents may come from teaching and research institutions in France or abroad, or from public or private research centers.

L'archive ouverte pluridisciplinaire **HAL**, est destinée au dépôt et à la diffusion de documents scientifiques de niveau recherche, publiés ou non, émanant des établissements d'enseignement et de recherche français ou étrangers, des laboratoires publics ou privés.



**UNIVERSITÉ  
DE LORRAINE**

**BIBLIOTHÈQUES  
UNIVERSITAIRES**

## AVERTISSEMENT

Ce document est le fruit d'un long travail approuvé par le jury de soutenance et mis à disposition de l'ensemble de la communauté universitaire élargie.

Il est soumis à la propriété intellectuelle de l'auteur. Ceci implique une obligation de citation et de référencement lors de l'utilisation de ce document.

D'autre part, toute contrefaçon, plagiat, reproduction illicite encourt une poursuite pénale.

Contact bibliothèque : [ddoc-theses-contact@univ-lorraine.fr](mailto:ddoc-theses-contact@univ-lorraine.fr)  
*(Cette adresse ne permet pas de contacter les auteurs)*

## LIENS

Code de la Propriété Intellectuelle. articles L 122. 4

Code de la Propriété Intellectuelle. articles L 335.2- L 335.10

[http://www.cfcopies.com/V2/leg/leg\\_droi.php](http://www.cfcopies.com/V2/leg/leg_droi.php)

<http://www.culture.gouv.fr/culture/infos-pratiques/droits/protection.htm>

## Ecole Doctorale BioSE (Biologie-Santé-Environnement)

### Thèse

Présentée et soutenue publiquement pour l'obtention du titre de

**DOCTEUR DE L'UNIVERSITE DE LORRAINE**

**Mention : « Sciences de la Vie et de la Santé »**

par **Francesca Maria STEFANIZZI**

## **Les ARNs non-codants comme biomarqueurs pronostiques de l'arrêt cardiaque**

**14 Décembre 2022**

### **Membres du jury :**

<b>Rapporteurs :</b>	<b>Mme. Florence PINET</b>	PhD, HDR, Inserm UMR-1167 Institut Pasteur de Lille, Lille, France.
	<b>Mme. Cécile VINDIS</b>	PhD, HDR, Inserm UMR-1048, Institute for Cardiovascular and Metabolic Diseases, Toulouse, France.
<b>Examineurs :</b>	<b>M. Bruno CHARPENTIER</b>	PhD, HDR, Prof., Inserm UMR-7365 CNRS-UL IMoPA, Université de Lorraine, Vandœuvre-lès-Nancy, France.
	<b>M. Yvan DEVAUX</b>	PhD, HDR, Unité de Recherche Cardiovasculaire, Luxembourg Institute of Health, Strassen, Luxembourg. <b>Directeur de thèse</b>
	<b>M. Nicolas DEYE</b>	MD-PhD, Inserm UMR-S 942, Réanimation Médicale et Toxicologique, Hôpital Lariboisière, Paris, France.
<b>Membres invités :</b>	<b>M. Niklas NIELSEN</b>	MD-PhD, Prof., Department of Anesthesia and Intensive Care, Clinical Sciences, Lund University and Helsingborg Hospital, Lund, Sweden.

## Ecole Doctorale BioSE (Biologie-Santé-Environnement)

### Thèse

Présentée et soutenue publiquement pour l'obtention du titre de

**DOCTEUR DE L'UNIVERSITE DE LORRAINE**

**Mention : « Sciences de la Vie et de la Santé »**

par **Francesca Maria STEFANIZZI**

## **Non-coding RNAs as prognostic biomarkers of cardiac arrest**

**14 December 2022**

### **Membres du jury :**

<b>Rapporteurs :</b>	<b>Mme. Florence PINET</b>	PhD, HDR, Inserm UMR-1167 Institut Pasteur de Lille, Lille, France.
	<b>Mme. Cécile VINDIS</b>	PhD, HDR, Inserm UMR-1048, Institute for Cardiovascular and Metabolic Diseases, Toulouse, France.
<b>Examineurs :</b>	<b>M. Bruno CHARPENTIER</b>	PhD, HDR, Prof., Inserm UMR-7365 CNRS-UL IMoPA, Université de Lorraine, Vandœuvre-lès-Nancy, France.
	<b>M. Yvan DEVAUX</b>	PhD, HDR, Unité de Recherche Cardiovasculaire, Luxembourg Institute of Health, Strassen, Luxembourg. <b>Directeur de thèse</b>
	<b>M. Nicolas DEYE</b>	MD-PhD, Inserm UMR-S 942, Réanimation Médicale et Toxicologique, Hôpital Lariboisière, Paris, France.
<b>Membres invités :</b>	<b>M. Niklas NIELSEN</b>	MD-PhD, Prof., Department of Anesthesia and Intensive Care, Clinical Sciences, Lund University and Helsingborg Hospital, Lund, Sweden.



## Acknowledgments

I would first like to thank my supervisor, Dr Yvan Devaux, who welcomed me into his team. Thank you for having taught me so much and for having given me the opportunity to embark on this journey that has made me grow enormously, not only professionally but also and perhaps above all personally. You have always demanded the maximum from me, and this has allowed me to go beyond my expectations very often. I thank you for all this, I really do.

I would also like to thank the CORE programme of the Luxembourg National Research Fund (FNR) which believed in the validity of this project and funded it (grant # C17/BM/11613033).

A special thanks go to the cardiac arrest patients and their families who, despite the difficult time, allowed the creation of the two clinical trials, TTM and TTM2, on which this research project was based. Therefore, many thanks to Dr Niklas Nielsen and all the members of the TTM-trial and TTM2-trial. Without the contribution of all these parties, this project would never have existed.

In addition, I would like to thank all the team members of the cardiovascular research unit who have supported me over these 4 years not only in all technical matters related to this research, but also emotionally, in the most difficult moments you have been my rock. Thank you all, Melanie, Andrew, Antonio, Christelle, Lu, Amela, Shounak, Shubhra, Bernadette and Tania. You all contributed in different ways to make a cold and rainy day in Luxembourg warmer and sunnier, which for a southern Italian is no small thing! With some of you a beautiful friendship started, which I hope to continue after this experience. Also, Melanie and Andrew, a special thank you for helping in the revision of this thesis. I would like to thank you not only for your hard work and dedication that made this manuscript better, but also for your moral support throughout the writing process. You never stopped believing in me and I thank you immensely for all this!

Thank you also to the members of my thesis committee, Dr Nicolas Deye and Dr Bruno Charpentier, who meticulously reviewed the progress of this research over these 4 years and gave a lot of useful inputs. Thank you also to all the other members of my thesis jury, Dr Florence Pinet, Dr Cecile Vindis and Dr Niklas Nielsen for accepting this role and helping to improve this research work.

Thank you to the various members of the BioSE doctoral school who have had the patience to guide me through the bureaucratic procedures of the university over the years.

Finally, thanks to all my friends and family, who from different parts of the world have always been present during this journey and have lived with me all the victories, struggles, fears and insecurities. Thank you all for your presence and encouragement. You always find a way to make me smile and I am really grateful to have you in my life.

Lastly, a special thanks needs to go to my parents who have always believed in my life choices and supported them even when they were not fully in agreement. I hope that I have succeeded in meeting your expectations and that I will continue to do so.

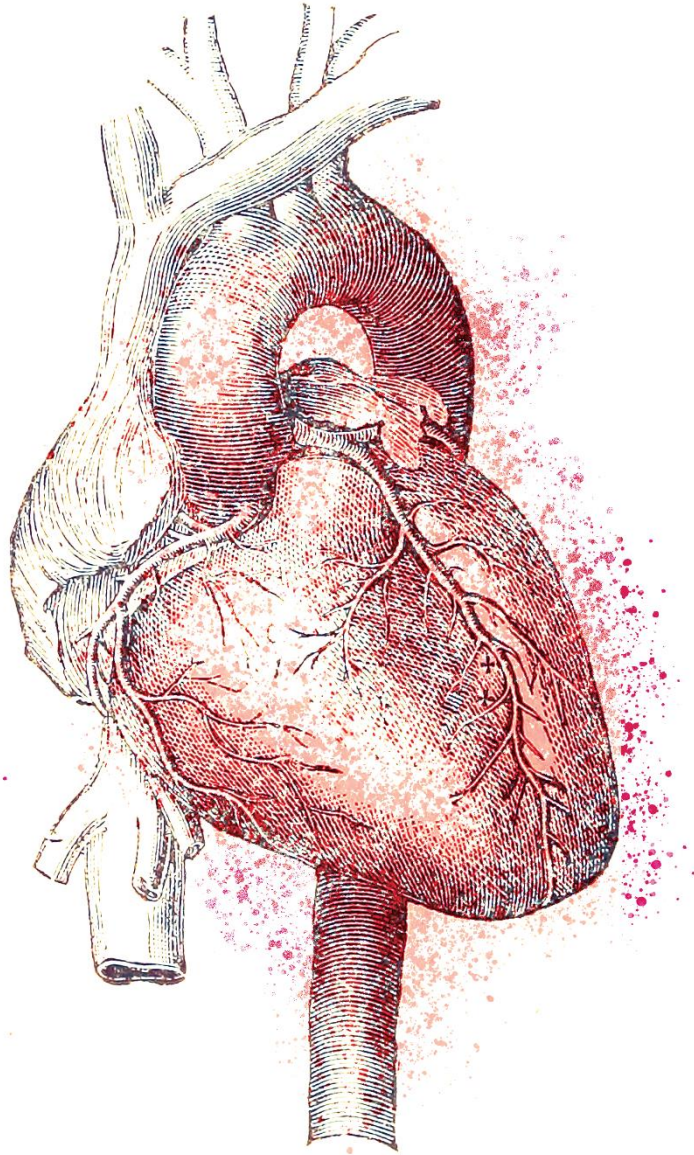


FIG. 55.—The Heart and the Large Vessels

Artwork by Sofia Carenzi

## List of work

### ○ Publications related to this thesis

#### *Appendix I:*

Salgado-Somoza, A., **Stefanizzi, F.M.**, Stammet, P., Erlinge, D., Friberg, H., Nielsen, N., & Devaux, Y. (2018). Non-Coding RNAs to Aid in Neurological Prognosis after Cardiac Arrest. *Non-coding RNA*, 4(4), 42.

STATUS: *published*

#### *Appendix II:*

**Stefanizzi FM**, Nielsen N, Zhang L, et al. Circulating Levels of Brain-Enriched MicroRNAs Correlate with Neuron Specific Enolase after Cardiac Arrest-A Substudy of the Target Temperature Management Trial. *Int J Mol Sci*. 2020;21(12):E4353.

STATUS: *published*

#### *Appendix III:*

Stefanizzi F.M., Zhang L., Salgado-Somoza A., Dankiewicz J., PhD, Stammet P., Hassager C., Wise M.P., Friberg H., Cronberg T., Hundt A., Kjaergaard J., Nielsen N., Devaux Y. Circular RNAs to predict clinical outcome after cardiac arrest. *Journal of Intensive Care Medicine Experimental*.

STATUS: *accepted*

### ○ Publications not related to this thesis

Jusic, A.; Salgado-Somoza, A.; Paes, A.B.; **Stefanizzi, F.M.**; Martínez-Alarcón, N.; Pinet, F.; Martelli, F.; Devaux, Y.; Robinson, E.L.; Novella, S.; on behalf of the EU-CardioRNA COST Action. Approaching Sex Differences in Cardiovascular Non-Coding RNA Research. *Int. J. Mol. Sci.* 2020, 21, 4890.

Acharya S, Salgado-Somoza A, **Stefanizzi FM**, Lumley AI, Zhang L, Glaab E, May P, Devaux Y. Non-Coding RNAs in the Brain-Heart Axis: The Case of Parkinson's Disease. *Int J Mol Sci*. 2020 Sep 6;21(18):6513. doi: 10.3390/ijms21186513. PMID: 32899928; PMCID: PMC7555192.

Sweaad WK\*, **Stefanizzi FM\***, Chamorro-Jorganes A, Devaux Y, Emanuelli C; EU-CardioRNA COST Action CA17129. Relevance of N6-methyladenosine regulators for transcriptome: Implications for development and the cardiovascular system. *J Mol Cell Cardiol*. 2021 May 13; 160:56-70. doi: 10.1016/j.yjmcc.2021.05.006. Epub ahead of print. PMID: 33991529.

## Dissemination activities and scientific missions

### ○ Scientific mission

- ✓ Short-term scientific mission (STSM) of 4 weeks (03/2019) in the laboratory of professor Emanuela Costanza at the Myocardial Function Department, National Heart & Lung Institute, Imperial college of London.

### ○ Oral presentations

- ✓ Printemps de la Cardiologie recherche fondamentale & clinique Groupe de Réflexion pour la Recherche Cardiovasculaire (GRRC) et Société Française de Cardiologie (SFC) meeting, Grand Palais in Lille (France, 1-3/4/2019).
- ✓ Journée scientifique de l'école doctorale BioSE 2021 (France, 02/06/2021).

### ○ Poster presentations

- ✓ 3rd International Symposium on Frontiers in Molecular Science - RNA Regulatory Networks, Pavilhao do conhecimento, Lisbon (Portugal, 26-28/06/2019).
- ✓ 3rd COST Action CardioRNA WG Meeting, School of Medicine Yeditepe University, Istanbul (Turkey, 16-18/10/2019).
- ✓ 4th COST Action CardioRNA MC and WG meeting 2020, Maastricht University - Medical center (MUMC+), Maastricht (Netherlands, 12-14/02/2020).
- ✓ ESC Congress 2020 - The Digital Experience (online – 29/08-1/09/20).
- ✓ Journée de l'école doctorale BioSE 2020, Amphithéâtre Lepois - Campus Brabois Santé (France, 12/11/2020).
- ✓ Cardio Genomics 2021 (online – 20/03/21).
- ✓ ISHR 2021 (online - 29/06-01/07/21).
- ✓ Noncoding RNA World from Mechanism to Therapy (online – 21-23/07/21).
- ✓ PhD days 2021 -University of Luxembourg (online – 07/10/2021).

## Abbreviations

<b>95% CI</b>	95% of confidence interval
<b>AED</b>	automated external defibrillator
<b>AHA</b>	American Heart Association
<b>AIC</b>	Akaike's information criterion
<b>AP</b>	alkaline phosphatase
<b>AUC</b>	area under the curve
<b>BNP</b>	B-Type Natriuretic Peptide
<b>cDNA</b>	complementary DNA
<b>CDR1as</b>	cerebellar degeneration-related protein 1 antisense
<b>ceRNA</b>	competing endogenous RNA
<b>C-index</b>	concordance index
<b>circRNA</b>	circular RNA
<b>CoCl<sub>2</sub></b>	Cobalt(II) chloride hexahydrate
<b>COPD</b>	chronic obstructive pulmonary disease
<b>CPC</b>	Cerebral Performance Category
<b>CPR</b>	cardiopulmonary resuscitation
<b>CRP</b>	C-reactive protein
<b>CT</b>	computerized tomography
<b>DWI</b>	diffusion-weighted imaging
<b>EEG</b>	electroencephalography
<b>EV</b>	extracellular vesicle
<b>FISH</b>	fluorescent in situ hybridization
<b>FPKM</b>	fragments per kilobase of transcript per million
<b>GFAP</b>	glial fibrillary acidic protein
<b>hnRNPs</b>	heterogeneous nuclear ribonucleoproteins
<b>HR</b>	hazard ratio
<b>IBBL</b>	Integrated Biobank of Luxembourg
<b>ICU</b>	intensive care unit
<b>IDI</b>	integrated discrimination improvement

<b>IHCA</b>	in-hospital cardiac arrest
<b>IL6</b>	interleukin 6
<b>IRES</b>	internal ribosome entry site
<b>LDH</b>	lactate dehydrogenase
<b>lncRNA</b>	long non-coding RNA
<b>LPS</b>	lipopolysaccharide
<b>LRT</b>	likelihood-ratio test
<b>m6A</b>	N6-methyladenosine methylation
<b>MALAT1</b>	metastasis-associated lung adenocarcinoma transcript 1
<b>MI</b>	myocardial infarction
<b>MICRA</b>	Myocardial Infarction-associated Circular RnA
<b>miRISC</b>	miRNA-induced silencing complex
<b>miRNA</b>	micro-RNA
<b>MRI</b>	magnetic resonance imaging
<b>mRNA</b>	messenger RNA
<b>mRS</b>	modified Rankin Scale
<b>NaCl</b>	sodium chloride
<b>ncRNA</b>	non-coding RNA
<b>NEAT1</b>	nuclear enriched abundant transcript 1
<b>Nfl</b>	neurofilament light
<b>NIH</b>	National Institutes of Health
<b>NRI</b>	net reclassification index
<b>NSE</b>	neuron-specific enolase
<b>OD</b>	optical density
<b>OHCA</b>	out-of-hospital cardiac arrest
<b>OR</b>	odd ratio
<b>ORF</b>	open reading frame
<b>PBMC</b>	peripheral blood mononuclear cell
<b>PBS</b>	phosphate buffered saline
<b>PCAS</b>	post- cardiac arrest syndrome
<b>PCI</b>	percutaneous coronary intervention

<b>PCT</b>	Procalcitonin
<b>PEA</b>	pulseless electrical activity
<b>piRNA</b>	piwi-interacting RNA
<b>Pol II</b>	RNA polymerase II
<b>PPP</b>	plasma pure platelet
<b>PQ</b>	platelets
<b>PRP</b>	plasma rich platelet
<b>QALY</b>	quality adjusted life year
<b>qPCR</b>	quantitative polymerase chain reaction
<b>RBP</b>	RNA-binding protein
<b>RNase R</b>	ribonuclease R
<b>RNA-seq</b>	RNA sequencing
<b>ROC</b>	receiver operating characteristic
<b>ROSC</b>	return of spontaneous circulation
<b>rRNA</b>	ribosomal RNA
<b>RT</b>	reverse transcription
<b>S100B</b>	S100 calcium-binding protein B
<b>siRNA</b>	small interfering RNA
<b>snoRNA</b>	small nucleolar RNA
<b>snRNA</b>	small nuclear RNA
<b>SSEP</b>	somatosensory evoked potential
<b>TNT</b>	Troponin T
<b>tRNA</b>	transfer RNA
<b>TTM</b>	Targeted temperature management trial
<b>TTM2</b>	Targeted temperature management trial 2
<b>UCHL1</b>	ubiquitin C-terminal hydrolase-L1
<b>UTR</b>	untranslated region
<b>VF</b>	ventricular fibrillation
<b>VT</b>	ventricular tachycardia
<b>WLST</b>	withdrawal of life-sustaining treatment

## List of Tables

<i>Table 1. Modified Rankin Scale.</i>	32
<i>Table 2. Cerebral Performance Categories.</i>	32
<i>Table 3. List of antisense LNA<sup>TM</sup> GapmeRs (QIAGEN) used to transfect THP-1 cells.</i>	69
<i>Table 4. List of primer pair sequences and respective annealing temperatures for qPCR measurements.</i>	72
<i>Table 5. Primer pairs used to clone circNFAT5 into a pcDNA 3.1(+) vector.</i>	74
<i>Table 6. Primer pairs used to clone circNFAT5 and NFAT5 into a pEZX-MT05 vector.</i>	74
<i>Table 7. Demographic and clinical characteristics of the 50 TTM patients subjected to miRNA sequencing.</i>	81
<i>Table 8. Demographic and clinical characteristics of the 46 TTM patients (discovery cohort).</i>	86
<i>Table 9. List of differentially expressed circRNAs (left) and lncRNAs (right) identified in the RNA-seq of the 46 TTM patients.</i>	88
<i>Table 10. Spearman correlations between 5 circRNAs and 1 lncRNA with established prognostication markers of cardiac arrest.</i>	90
<i>Table 11. Demographic and clinical characteristics of 542 TTM patients (validation cohort).</i>	91
<i>Table 12. Candidate performance to predict 6-month neurological outcome in TTM validation cohort using CPC score.</i>	97
<i>Table 13. Candidate performance to predict 6-month neurological outcome in TTM validation cohort using mRS score.</i>	98
<i>Table 14. Candidate performance to predict 6-month survival in TTM validation cohort.</i>	101
<i>Table 15. Correlation between circNFAT5 and white blood cell markers in the RNA-seq data of the 46 TTM patients.</i>	103
<i>Table 16. Correlation between linear NFAT5 and white blood cell markers in RNA-seq data of 46 TTM patients.</i>	104
<i>Table 17. Spearman correlations between circNFAT5 or linear NFAT5 and the three proteins predicted to interact with linear NFAT5 and known to be involved in hypertonic responses.</i>	114
<i>Table 18. Predicted miRNAs with binding sites on circNFAT5.</i>	121
<i>Table 19. Spearman correlations between circNFAT5 or linear NFAT5 and the predicted miRNAs binding circNFAT5 in the 23 TTM patients common to the two RNA-seq datasets.</i>	122
<i>Table 20. RBPs predicted by RBPmap database to bind circNFAT5 at the junction point.</i>	125
<i>Table 21. Demographic and clinical characteristics of 674 TTM2 patients.</i>	129
<i>Table 22. Candidate performance to predict 6-month neurological outcome in TTM2 patients.</i>	133
<i>Table 23. Candidate performance to predict 6-month survival in 674 TTM2 patients.</i>	135



## List of Figures

<i>Figure 1. OHCA chain of survival.</i>	26
<i>Figure 2. Components of multimodal prognostication.</i>	34
<i>Figure 3. Schematic overview of some methods used to assess the biomarker potential of a molecule under study.</i>	44
<i>Figure 4. Central dogma of molecular biology.</i>	47
<i>Figure 5. Translation machinery.</i>	49
<i>Figure 6. Classification of RNA molecules.</i>	51
<i>Figure 7. Canonical pathway of miRNA biogenesis.</i>	52
<i>Figure 8. Classification lncRNAs according to their genomic origin.</i>	53
<i>Figure 9. Functions of lncRNAs.</i>	54
<i>Figure 10. CircRNAs biogenesis.</i>	55
<i>Figure 11. Functions of circRNAs.</i>	57
<i>Figure 12. ncRNAs in inflammatory signalling response.</i>	60
<i>Figure 13. Circulating ncRNAs in cardiovascular diseases.</i>	62
<i>Figure 14. CircRNAs in cardiovascular diseases.</i>	63
<i>Figure 15. Cloning of circNFAT5 pcDNA 3.1(+) vector.</i>	73
<i>Figure 16. Primer pair positions used to clone circNFAT5 and the corresponding linear portion of NFAT5 in a pEZX-MT05 vector.</i>	74
<i>Figure 17. Scatter plots showing correlations between NSE and levels of miR-9-3p, miR-124-3p, and miR-129-5p 48 h after ROSC.</i>	82
<i>Figure 18. Univariate (a) and multivariable (b) logistic regression analysis to evaluate the potential of miR9-3p, miR124-3p and miR129-5p in predicting neurological outcome.</i>	83
<i>Figure 19. Study flow chart TTM-trial.</i>	85
<i>Figure 20. Bar graphs showing the confirmed circularity of 5 circRNAs identified in the RNA-seq data of the discovery cohort.</i>	89
<i>Figure 21. Box plots showing the differential expression of the 5 circRNAs and 1 lncRNA in the discovery cohort according to the neurological outcome of the patients (CPC1 or CPC5).</i>	89
<i>Figure 22. Differential expression levels of 5 circRNAs and 1 lncRNA in the 542 TTM patients of the validation cohort.</i>	93
<i>Figure 23. Univariate logistic regression analyses to predict 6-month neurological outcome in TTM validation cohort.</i>	94
<i>Figure 24. Multivariable logistic regression analyses using CPC score to predict 6-month neurological outcome in the TTM validation cohort.</i>	95
<i>Figure 25. Multivariable logistic regression analyses to predict neurological outcome in TTM validation cohort using mRS score.</i>	96
<i>Figure 26. Kaplan-Meier curves in the TTM study at 6 months after CA, using Youden index as cut-off value.</i>	99

Figure 27. Univariate Cox proportional hazards for 9 independent variables plus selected candidates for survival prediction in the TTM validation cohort.....	99
Figure 28. Multivariable Cox proportional hazards for predicting 6-month survival in TTM validation cohort..	100
Figure 29. Expression profiles of circNFAT5 in blood compartments of three healthy volunteers.....	105
Figure 30. Amplification curves of circNFAT5 in serum samples from cardiac arrest patients.....	106
Figure 31. Expression levels of circNFAT5 and linear NFAT5 transcript in three different cell lines.....	106
Figure 32. Modulation of circNFAT5 expression under normoxic and hypoxic conditions in different cell lines..	107
Figure 33. Modulation of circNFAT5 expression after CoCl <sub>2</sub> treatment in different cell lines.....	108
Figure 34. Expression profiles of circNFAT5 after treatment of THP-1 cells with LPS.....	109
Figure 35. Expression profiles of circNFAT5 after treatment of jurkat cells with anti-CD3/CD28.....	110
Figure 36. Schematic representation of the system used to study the hypothetical relationship between NFAT5 and circNFAT5.....	111
Figure 37. Intracellular localisation of circNFAT5 and linear NFAT5 in SHSY5Y and jurkat cells.....	112
Figure 38. THP-1 cells treated with NaCl.....	114
Figure 39. Expression levels of linear NFAT5, circNFAT5, S100A4, ZFP36L1 and SLC38A2 after silencing of linear NFAT5.....	115
Figure 40. THP-1 cells treated with NaCl after silencing linear NFAT5.....	116
Figure 41. Expression levels of linear NFAT5, circNFAT5, S100A4, ZFP36L1 and SLC38A2 after silencing of circNFAT5 with antisense LNA <sup>TM</sup> gapmeR in THP-1 cells.....	117
Figure 42. Overexpressing circNFAT5 in jurkat cells.....	118
Figure 43. Protein-coding potential of circNFAT5.....	120
Figure 44. Scatter plots showing the correlation between circNFAT5 or linear NFAT5 and miR-144-3p.....	123
Figure 45. Luciferase assay to test the potential binding between miR-144-3p and circNFAT5 in HEK293 cells.	124
Figure 46. Bar graphs representing qPCR measurements of miR-144-3p in HEK293, jurkat, THP-1 and SH-SY5Y cell lines.....	125
Figure 47. Scatter plots showing the correlation between circNFAT5 (a.) or linear NFAT5 (b.) and RBPs predicted to bind circNFAT5 at the junction point in the RNA-seq data of TTM.....	126
Figure 48. Scatter plots showing the correlation between circNFAT5 or linear NFAT5 and YTHDC2 in the RNA-seq data of TTM.....	127
Figure 49. Study flow chart TTM2-trial.....	128
Figure 50. Differential expression levels of 3 selected circRNAs in 674 TTM2 patients.....	130
Figure 51. Univariate (a.) and multivariable (b.) logistic regression analyses to predict 6-month neurological outcome in TTM2-trial using mRS score.....	132
Figure 52. Kaplan-Meier curves to predict 6-month survival in TTM2 patients.....	134
Figure 53. Univariate (a.) and multivariable (b.) Cox proportional hazards for 8 independent variables and 3 candidate circRNAs for predicting 6-month survival in the TTM2-trial.....	134
Figure 54. Best predictors identified in TTM-trial and TTM2-trial.....	135

# Table of Contents

<b>Résumé de dix pages en française</b> .....	14
<b>Contexte</b> .....	14
<b>Résultats et conclusions</b> .....	16
Première étude: les miARN circulants enrichis dans le cerveau sont en corrélation avec le biomarqueur NSE après un arrêt cardiaque.....	16
Deuxième étude: identification de ARNInc et ARNcirc comme potentiels biomarqueurs pronostiques post-ACEH. ....	17
• <i>Phase de découverte</i> .....	17
• <i>Validation des six candidats sélectionnés chez les patients TTM</i> .....	18
• <i>Caractérisation moléculaire de circNFAT5</i> .....	19
• <i>Validation de 3 ARNcirc chez des patients de TTM2</i> .....	22
<b>Introduction</b> .....	24
<b>1. Cardiac arrest</b> .....	25
<b>1.1 Definition, classification and epidemiology</b> .....	25
<b>1.2 The chain of survival</b> .....	26
<b>1.3 Outcome after cardiac arrest</b> .....	31
<b>1.4 Prognostication of outcome after cardiac arrest</b> .....	34
<b>1.5 Therapeutic approaches</b> .....	37
<b>1.6 The burden of cardiac arrest</b> .....	39
<b>2. Biomarkers</b> .....	40
2.1 Statistical evaluation of new biomarkers .....	42
2.2 Biomarkers to prognosticate the outcome after cardiac arrest.....	45
<b>3. Transcriptome</b> .....	47
3.1 Coding RNAs (mRNAs).....	48
3.2 Non-coding RNAs .....	50
3.3 Blood transcriptome .....	58
3.3.1 Circulating RNAs.....	58
3.3.2 RNAs in blood cells.....	59
<b>4. NcRNAs after cardiac arrest</b> .....	61
<b>Objectives</b> .....	64
<b>Materials and methods</b> .....	66
<b>1. Cohorts of patients: TTM and TTM2</b> .....	67
<b>2. Cell biology</b> .....	67
<b>2.1. Cell cultures</b> .....	67

2.1.1.	<i>SH-SY5Y: Human Neuroblastoma Cell Line</i> .....	67
2.1.2.	<i>Jurkat: Human T lymphoblast cell line</i> .....	67
2.1.3.	<i>THP-1: Human monocytic cell line</i> .....	68
2.1.4.	<i>HEK293: Human embryonic kidney cell line</i> .....	68
2.1.5.	<i>Hela: Human cervical cancer cell line</i> .....	68
<b>2.2.</b>	<b>Cell treatments</b> .....	<b>68</b>
2.2.1.	<i>Hypoxia</i> .....	68
2.2.2.	<i>Cobalt(II) chloride hexahydrate (CoCl<sub>2</sub>)</i> .....	68
2.2.3.	<i>Sodium chloride (NaCl)</i> .....	68
2.2.4.	<i>Lipopolysaccharide (LPS)</i> .....	69
2.2.5.	<i>ImmunoCult™ Human CD3/CD28 T Cell Activator</i> .....	69
<b>2.3.</b>	<b>Nucleofection</b> .....	<b>69</b>
<b>2.4.</b>	<b>Transfection procedures</b> .....	<b>69</b>
2.4.1.	<i>Transfection of antisense LNA™ GapmeRs for circNFAT5 and NFAT5</i> .....	69
2.4.2.	<i>Transfection of pcDNA 3.1(+)<i> vector containing circNFAT5 sequence</i></i> .....	70
<b>2.5.</b>	<b>Nuclear and cytoplasm fractionation</b> .....	<b>70</b>
<b>2.6.</b>	<b>Fluorescent In Situ Hybridization (FISH)</b> .....	<b>70</b>
<b>3.</b>	<b>Molecular biology</b> .....	<b>71</b>
<b>3.1.</b>	<b>RNA extraction</b> .....	<b>71</b>
3.1.1.	<i>From Blood samples</i> .....	71
3.1.2.	<i>From cell cultures</i> .....	71
<b>3.2.</b>	<b>Retro transcription (RT)</b> .....	<b>71</b>
<b>3.3.</b>	<b>Quantitative PCR (qPCR)</b> .....	<b>71</b>
<b>3.4.</b>	<b>RT and qPCR with miRCURY system</b> .....	<b>72</b>
<b>3.5.</b>	<b>Cloning procedures</b> .....	<b>72</b>
3.5.1.	<i>Using pcDNA 3.1(+)<i> vector</i></i> .....	72
3.5.2.	<i>Using pEZX-MT05 vector</i> .....	74
<b>3.6.</b>	<b>Sanger Sequencing</b> .....	<b>75</b>
<b>3.7.</b>	<b>Western blot</b> .....	<b>75</b>
<b>4.</b>	<b>Biochemistry</b> .....	<b>75</b>
4.1.	<i>Lactate Dehydrogenase (LDH) assay</i> .....	75
4.2.	<i>Luciferase assay</i> .....	76
4.3.	<i>Ribonuclease R (RNase R) treatment</i> .....	76
<b>5.</b>	<b>Bioinformatical analyses</b> .....	<b>76</b>
<b>6.</b>	<b>Biostatistical analyses</b> .....	<b>77</b>
<b>Results</b>	.....	<b>79</b>

<b>1. Circulating Levels of Brain-Enriched MicroRNAs Correlate with Neuron Specific Enolase after Cardiac Arrest—A Substudy of the Target Temperature Management Trial .....</b>	<b>80</b>
<b>2. LncRNAs and circRNAs as prognostic biomarkers after cardiac arrest .....</b>	<b>84</b>
<b>2.1. Discovery study: selection of candidates lncRNAs and circRNAs.....</b>	<b>85</b>
<b>2.2. Biomarker potential assessment of the selected candidates in the whole TTM cohort</b>	<b>91</b>
<b>2.3. Molecular characterisation of circNFAT5 .....</b>	<b>102</b>
<b>2.4. Validation of the biomarker potential of 3 circRNAs in TTM2-trial .....</b>	<b>127</b>
<i>Discussion</i> .....	136
<i>Conclusions and future perspectives</i> .....	143
References.....	146
Appendix I .....	168
Appendix II .....	185
Appendix III .....	195
Abstract .....	240
Résumé.....	241

## Résumé de dix pages en française

### Contexte

L'arrêt cardiaque est l'une des principales causes de décès dans le monde [1-4]. En Europe, on dénombre en moyenne 100 cas d'arrêts cardiaques extrahospitaliers (ACEH) pour 100 000 personnes par an. Dans 50 à 60% des cas, une réanimation a été tentée et dans environ 8% des cas seulement, les survivants sont sortis de l'hôpital [5].

Après un ACEH, la prise en charge des patients comateux admis aux soins intensifs met l'accent sur l'identification et le traitement du syndrome post arrêt cardiaque (SPAC). En général, les patients qui reprennent conscience rapidement après le retour de circulation spontanée (RCS) ou dans les 4 premiers jours de leur séjour aux soins intensifs [6] présentent une évolution favorable après un ACEH. Dans les cas les plus sévères, la prédiction d'une évolution défavorable après un ACEH peut conduire à l'arrêt du traitement de maintien en vie.

L'identification de la cause de l'arrêt cardiaque ainsi qu'un pronostic précis post-ACEH sont essentiels pour fournir aux patients les thérapies les plus appropriées et prévenir l'arrêt prématuré des traitements de maintien en vie. Actuellement, les thérapies post-ACEH se concentrent sur le traitement des symptômes du SPAC. En pratique, le niveau de gravité du SPAC varie considérablement d'un patient à l'autre, de sorte que les thérapies existantes doivent être adaptées aux besoins de chaque patient individuellement et dans un délai précis après l'ACEH [7]. Les lésions et dysfonctionnements induits par un ACEH touchent majoritairement le cerveau et le système cardiovasculaire et jouent un rôle majeur dans la survie du patient après un ACEH. En effet, les lésions et dommages au cerveau peuvent se poursuivre pendant plusieurs heures post-RCS. Cette période constitue une fenêtre thérapeutique potentielle pendant laquelle il est possible de limiter les lésions et dommages induits par un ACEH [8]. La fièvre, température corporelle égale ou supérieure à 37,8°C, est associée à une évolution neurologique défavorable après un ACEH. La principale thérapie recommandée pour protéger le cerveau de dommages supplémentaires est le contrôle ciblé de la température corporelle entre 32 et 36°C (hypothermie) chez les patients comateux post-RCS [9]. Bien que l'on ne sache pas encore exactement comment l'abaissement de la température corporelle peut protéger le cerveau, il a été décrit que l'hypothermie peut réduire le stress oxydatif, l'inflammation et la mort cellulaire programmée [10].

Deux des principales études cliniques sur l'effet de l'hypothermie chez les patients ayant souffert d'un arrêt cardiaque ont été utilisées dans ce travail, c'est-à-dire les études TTM (Target Temperature Management) (NCT01020916) et TTM2 (NCT02908308). Brièvement, dans l'étude TTM, les 2 contrôles ciblés de la température corporelle testés, 33°C ou 36°C, ont montré des effets bénéfiques similaires sur l'état de santé des patients quel que soit la température utilisée [11]. Dans l'étude TTM2, l'hypothermie (contrôle ciblé de la température à 33°C) a été comparée au traitement précocement la fièvre (normothermie;  $\leq 37,5^\circ\text{C}$ ). Aucun effet bénéfique additionnel significatif n'a été observé sur l'état de santé des patients entre normothermie et hypothermie à 33°C dans cette étude [12]. Par conséquent, les résultats de ces deux études suggèrent que le traitement précoce de la fièvre après le RCS améliore l'évolution du patient et non l'utilisation d'un contrôle ciblé à une température corporelle précise (33°C ou 36°C).

Les tests et examens utilisés pour prédire l'évolution neurologique des patients post-ACEH doivent être précis et présenter des taux de faux positifs et faux négatifs les plus faibles possible. En effet, un pronostic incorrect pourrait conduire à l'arrêt des traitements de maintien en vie chez des patients

ayant encore une chance de survie. Par conséquent, une approche multimodale combinant les résultats d'examens cliniques, de la neuro-imagerie, d'investigations électrophysiologiques ainsi que des mesures de biomarqueurs est la meilleure approche à utiliser pour obtenir le pronostic le plus précis possible. Actuellement, le pronostic neurologique des victimes d'un arrêt cardiaque est encore trop imprécis et nécessite des études complémentaires. Afin d'aider les cliniciens, de nouveaux tests et examens doivent être identifiés pour établir un pronostic plus précis sur l'évolution de l'état de santé des patients post-RCS. L'identification de biomarqueurs sanguins supplémentaires dont les mesures, couplées aux procédures déjà standardisées, permettraient d'améliorer le pronostic neurologique post-ACEH et d'aider les cliniciens dans la prise de décision de maintenir ou d'arrêter les traitements post-ACEH.

Les lésions cérébrales provoquées par un arrêt cardiaque influencent la fonction neurologique et peuvent altérer la récupération à long terme d'un patient. Cette fonction neurologique est mesurée et classifiée à l'aide d'échelles. Bien que ces échelles ne soient pas utilisées actuellement pour le pronostic des patients, elles sont essentielles à des fins de recherche pour évaluer de nouveaux biomarqueurs et traitements, formuler des recommandations et comparer l'évolution des patients [13]. Les deux échelles les plus couramment utilisées sont les catégories de performance cérébrale (CPC) [14] et l'échelle de Rankin modifiée (mRS) [15]. Les scores CPC vont de 1 (récupération complète) à 5 (décès), tandis que les scores mRS vont de 0 (aucun symptôme) à 6 (décès). Un score CPC de 1-2 ou mRS de 0 à 3 sont généralement considérés comme des indicateurs d'une bonne évolution neurologique, tandis qu'un score CPC de 4-5 ou mRS de 4 à 6 représente une évolution neurologique défavorable. Bien que ces deux échelles soient largement utilisées, le mRS semble pouvoir mieux distinguer les lésions cérébrales légères versus modérées par rapport à l'échelle CPC [15, 16].

A ce jour, les biomarqueurs utilisés en clinique pour aider au pronostic post-ACEH sont actuellement d'origine protéique. Parmi ceux-ci, l'énolase spécifique des neurones (*Neuron Specific Enolase*; NSE) est actuellement considérée comme le meilleur biomarqueur sanguin et reste le seul recommandé par les directives cliniques [9, 17, 18]. Cependant, l'ère des " *Omiques* " a permis d'identifier d'autres molécules, notamment les acides ribonucléiques (ARN), comme potentiels nouveaux biomarqueurs utiles en clinique pour le diagnostic et le pronostic de diverses maladies [19-21]. Parmi ces ARN, la sous-catégorie des ARN non codants (ARNnc) représente un groupe hétérogène de molécules d'ARN ayant des fonctions de régulation [22, 23]. En effet, les ARNnc peuvent réguler directement ou indirectement l'expression des gènes à différents niveaux avec des profils d'expression spatio-temporels spécifiques [24-27]. De plus, en fonction de leur longueur, les ARNnc peuvent être divisés en deux grandes familles, les petits ARNnc de moins de 200 nucléotides (nt), dont les représentants les plus connus sont les microARN (miARN), et les longs ARNnc (ARNlnc) de plus de 200 nt de long, qui comprennent notamment la sous-famille des ARN circulaires (ARNcirc) [28].

Plusieurs catégories d'ARNnc, en particulier les miARN, les ARNlnc et les ARNcirc, ont été considérés dans ce présent travail de thèse. L'étude de ces ARNnc a été menée dans le compartiment sanguin. En effet, parmi les fluides corporels, le sang représente le principal canal de transmission des signaux à travers le corps. De plus, la collecte du sang ainsi que son analyse représentent une procédure relativement non invasive et largement pratiquée en routine clinique [29-32]. Les molécules d'ARN présentes dans les cellules sanguines et celles qui circulent librement dans le sang constituent une source potentielle de biomarqueurs [33]. En fait, le potentiel biomarqueur de divers ARNnc a déjà été identifié dans de nombreuses maladies cardiovasculaires telles que l'infarctus du myocarde, l'insuffisance cardiaque et la fibrillation auriculaire [34, 35]. Les miARN font partie des ARNnc circulants les plus étudiés dans les maladies cardiovasculaires. Dans le contexte de l'arrêt cardiaque, le laboratoire où ce travail a été réalisé a déjà identifié et étudié les miR-21, miR-122-5p, et miR-124-3p

comme biomarqueurs potentiels pour aider au pronostic des patients victimes d'un ACEH [36, 37]. En lien avec ce présent travail de thèse, un article de synthèse a été publié en 2018 dans la revue " Non-Coding RNA " (Annexe I) et décrit les ARNnc comme biomarqueurs potentiels après un arrêt cardiaque [17]. Découvert récemment, les ARNcirc y sont décrits comme réservoir de biomarqueurs potentiels en raison de leurs caractéristiques intrinsèques. En effet, les ARNcirc présentent une structure circulaire, en boucle fermée de manière covalente, qui les rend particulièrement résistants aux attaques destructrices des exonucléases [38-40]. Le potentiel des ARNcirc en tant que biomarqueurs a déjà été évalué dans des maladies cardiovasculaires telles que l'insuffisance cardiaque et les accidents vasculaires cérébraux [41-43]. Cependant, rien n'est connu quant à leur utilité potentielle comme biomarqueurs dans l'arrêt cardiaque.

Dans ce travail de thèse de doctorat, le potentiel pronostique des ARNnc a été investigué après un arrêt cardiaque.

## Résultats et conclusions

### Première étude: les miARN circulants enrichis dans le cerveau sont en corrélation avec le biomarqueur NSE après un arrêt cardiaque.

Dans cette première étude, l'objectif était d'évaluer si les miARNs identifiés dans de précédents travaux du laboratoire étaient capables de prédire le degré de lésions neuronales post-ACEH. Pour cela, une analyse de corrélation a été réalisée entre les taux de NSE, biomarqueur utilisé actuellement en clinique, et des miARN trouvés dans la circulation 48 h après le RCS. Pour cette analyse, les données de séquençage des petits ARN (" miRNA-seq ") ont été obtenues à partir d'échantillons plasmatiques provenant de deux groupes de patients issus de l'étude TTM : 25 ayant un score CPC de 1 et 25 ayant un score CPC de 5, 6 mois après l'ACEH.

Parmi les données de séquençage, seuls les miARN ayant au moins 5 comptages dans plus de 12 patients provenant du même groupe CPC 1 ou CPC 5 ont été analysés. Ensuite, les 673 miARN sélectionnés ont été corrélés avec plusieurs caractéristiques démographiques et cliniques présentées dans le tableau 7 de ce manuscrit ou le tableau 1 de l'annexe II [44]. Les coefficients de corrélation supérieurs à 0,6 ont été considérés pour cette étude. Par conséquent, en considérant l'ensemble de ces 50 patients, une corrélation significative a été identifiée entre la NSE et les miR-9-3p, miR-124-3p et miR-129-5p avec des coefficients de corrélation de 0,64 (valeur  $p=6,48E-07$ ), 0,69 (valeur  $p=5,16E-08$ ) et 0,61 (valeur  $p=3,58E-06$ ), respectivement. Lorsque les patients ont été dichotomisés en fonction de leur résultat neurologique, CPC1 versus CPC5, des corrélations significatives ont également été observées mais uniquement dans le groupe à évolution neurologique défavorable (CPC5), et cela avec des coefficients de corrélation encore plus élevés. En effet, des coefficients de corrélation de 0,86 (valeur- $p = 3,50E-08$ ), 0,74 (valeur- $p = 2,08E-05$ ) et 0,71 (valeur- $p = 6,09E-05$ ) ont été observés dans le groupe CPC5 pour miR-9-3p, miR-124-3p et miR-129-5p, respectivement. De plus, des modèles d'analyse de régression logistique univariée et multivariée ont évalué le potentiel de ces 3 miARN dans la prédiction de l'évolution neurologique à 6 mois après un ACEH chez ces 50 patients. Ces analyses ont montré que ces 3 miARN étaient des prédicteurs indépendants de l'évolution neurologique à 6 mois, comme on peut l'observer sur la figure 18 de ce manuscrit ou sur la figure 2 de l'annexe II [44].

Les résultats de cette première étude suggèrent que miR-9-3p, miR-124-3p et miR-129-5p pourraient contribuer au pronostic de l'évolution neurologique post-ACEH. Dans la littérature, ces 3 miARN sont décrits dans plusieurs processus physiologiques du cerveau tels que le développement, la différenciation et la plasticité [45-48]. Leur présence dans la circulation sanguine après un arrêt cardiaque pourrait suggérer leur libération suite à la mort cellulaire du cerveau et la rupture de la barrière hémato-encéphalique. Cependant, la capacité de ces miARN à prédire les lésions cérébrales



ainsi que leurs fonctions biologiques lors d'un ACEH nécessitent des études supplémentaires. En fait, dans le cadre de ce travail, le séquençage d'ARN a été effectué sur un petit nombre de patients, 50 au total. Pour cette raison, les analyses multivariées ont été effectuées en ajoutant seulement une variable à la fois afin d'éviter de biaiser celles-ci. C'est pourquoi, il n'a pas été possible de générer un modèle utilisant simultanément tous les paramètres démographiques et cliniques dans ces analyses. De plus, ces analyses ont été effectuées sur des échantillons collectés à un seul moment, 48 h après le RCS, qui représente le moment où la NSE atteint son pic dans la circulation et présente donc la valeur pronostique la plus élevée [49]. Cependant, il se peut que des patients soient décédés d'autres causes que les lésions cérébrales post-ACEH et donc, que cela puisse avoir un impact sur la corrélation observée entre les 3 miARN et la NSE. Aussi, les dosages de miARN ont été réalisés dans les échantillons plasmatiques et comparés aux taux de NSE provenant du sérum pris au même moment. Comme ces patients ont montré des niveaux comparables de miARN dans le plasma et le sérum, il est fort probable que la différence d'origine des dosages entre miARN et NSE ne représente pas un problème majeur.

En conclusion, cette première étude a indiqué un potentiel pronostique des miR-9-3p, miR-124-3p et miR-129-5p dans la détection de l'étendue des dommages cérébraux chez les patients après un ACEH. Les résultats de cette étude ont été publiés dans le journal *International Journal of Molecular Sciences* en 2020 et sont rapportés dans l'annexe II de ce travail [44].

#### Deuxième étude: identification de ARNlnc et ARNcirc comme potentiels biomarqueurs pronostiques post-ACEH.

Dans cette deuxième étude, l'accent a été mis sur la modulation de l'expression des ARNlnc et ARNcirc présents dans les cellules sanguines des patients après un ACEH. En effet, ces dernières années, un intérêt croissant a été porté à la famille des ARNlnc, dont les représentants les plus connus sont les ARNlnc linéaires et les ARNcirc [34]. Ceux-ci peuvent moduler l'expression d'autres gènes à différents niveaux [50] et présentent une plus grande spécificité d'expression selon le type de tissu ou le stade de différenciation par rapport aux miARN [39, 51-54]. De plus, la structure fermée des ARNcirc, sans extrémité libre, les rend particulièrement résistants aux attaques des exonucléases et donc plus stables que toute autre molécule d'ARN. Ceci leur confère donc un avantage particulier et permet une détection potentiellement plus aisée de cette sous-catégorie d'ARNnc [38-40]. Dans les maladies cardiovasculaires, il a déjà été reporté des dysrégulations de profils d'expression d'ARNlnc ainsi que leur potentiel comme biomarqueurs, notamment lors d'insuffisance cardiaque ischémique [22, 34, 50, 55]. Une hypothèse similaire a été émise dans le cadre de l'arrêt cardiaque dans ce travail et qui suggérerait que des ARNlnc et/ou ARNcirc pourraient avoir un potentiel de biomarqueurs pronostiques [17].

Il a été également décrit dans la littérature qu'en plus des lésions cérébrales, l'inflammation systémique est une composante importante du SPAC et est cruciale pour la récupération après un arrêt cardiaque [56-58]. Il existe des études rapportant l'association de l'expression altérée des ARNnc dans différents compartiments du sang avec une inflammation incontrôlée [59-63]. Par conséquent, l'objectif de cette étude a été d'identifier des ARNlnc et des ARNcirc provenant des cellules sanguines comme potentiels biomarqueurs pronostiques de l'ACEH et qui pourraient être potentiellement impliqués dans la réponse inflammatoire déclenchée au cours du SPAC.

##### ○ Phase de découverte

Dans un premier temps, le séquençage des longs ARN (" RNA-seq ") a été réalisé et comparé entre deux groupes de 23 patients de l'étude TTM dont les échantillons ont été collectés 48 h après le RCS. Le premier groupe de 23 patients avaient un score CPC de 1 et le second groupe, 23 patients un score CPC de 5, 6 mois après l'ACEH. Les patients de ces 2 groupes ont été appariés par le sexe. À partir des

données de ce séquençage, 41 ARNlnc et 28 ARNcirc présentant des niveaux d'expression différentiels significatifs ont été identifiés. Parmi ceux-ci, 7 ARNlnc présentant des niveaux d'expression acceptables (*fragments per kilobase of transcript per million fragments mapped* >10) ont été présélectionnés.

Pour confirmer ces résultats, des paires d'amorces spécifiques ont été générées et validées pour ces candidats présélectionnés en PCR quantitative (qPCR). L'amplification d'un produit PCR spécifique n'a été possible que pour 1 seul des 7 ARNlnc présélectionnés, c'est-à-dire pour lnc-IL1R1-1:2. Quant aux 28 ARNcirc, des paires d'amorces ont été optimisées pour amplifier uniquement les formes circulaires des ARNcirc. Grâce au test de résistance à l'exonuclease RNase R, la forme circulaire a été confirmée pour 5 ARNcirc candidats : circAGO2, circDLG1, circDNM2, circFAM13b et circNFAT5. Par conséquent, ces 5 ARNcirc et lnc-IL1R1-1:2 ont été les candidats sur lesquels cette deuxième étude s'est concentrée. Ces 6 candidats ont également été mesurés par qPCR sur les 46 patients utilisés lors de la phase de découverte, sur lesquels les données du séquençage ont été générées. Des tendances similaires ont été observées entre les résultats du séquençage et ceux de qPCR : une augmentation des niveaux d'expression de lnc-IL1R1-1:2, circAGO2, circDNM2, circFAM13b et circNFAT5 chez les patients présentant une évolution neurologique défavorable. Par contre, pour circDLG1, la diminution des niveaux d'expression observée en séquençage n'a pas été confirmée en qPCR chez les patients présentant une évolution neurologique défavorable.

Ensuite, les données de séquençage ont été utilisées pour corréler les niveaux d'expression de ces 6 candidats avec des marqueurs décrits dans le cadre de l'arrêt cardiaque, tels que NSE et S100 entre autres, afin de mieux comprendre dans quel(s) processus physiopathologique(s) les candidats ARNlnc et ARNcirc pourraient potentiellement être impliqués. Dans ces analyses de corrélations, circDNM2 a montré les coefficients de corrélation les plus forts, et les corrélations les plus élevées ont été observées avec des marqueurs de lésions cérébrales et d'inflammation, avec des coefficients de corrélation de 0,491 (valeur-p = 0,001) et 0,494 (valeur-p = 0,001) avec la NSE et la procalcitonine respectivement.

○ Validation des six candidats sélectionnés chez les patients TTM

Ensuite, les 6 candidats sélectionnés lors de la phase de découverte TTM ont été mesurés par qPCR chez les 542 autres patients de l'étude TTM. Des analyses d'expression différentielle de ces 6 candidats ont été réalisées en fonction de l'évolution neurologique à 6 mois en utilisant soit l'échelle CPC ou l'échelle mRS.

Quel que soit l'échelle utilisée, les résultats obtenus par séquençage et par qPCR lors de la phase de découverte ont été confirmés chez les autres patients TTM utilisés dans cette phase de validation pour tous les candidats étudiés, à l'exception de circDLG1. Dans cette phase de validation, une augmentation de circDLG1 a été observée dans le groupe des patients à évolution défavorable par rapport aux patients à évolution favorable, c'est-à-dire des résultats inverses par rapport aux résultats de séquençage obtenus lors de la phase de découverte. Une dichotomisation supplémentaire des patients en fonction de la température du contrôle ciblé (33°C ou 36°C) ou du sexe n'a montré aucune expression différentielle pour aucun candidat, sauf pour circDNM2 pour lequel des niveaux significativement plus élevés ont été observés dans le groupe traité à 33°C.

Des analyses prédictives ont été réalisées par régression logistique univariée avec les données d'expression de ces candidats 48 h après le RCS ainsi que l'état neurologique à 6 mois. Ces analyses ont montré que tous les candidats étaient des prédicteurs de l'évolution neurologique à 6 mois. Des analyses multivariées ont également été réalisées en tenant compte des 9 variables suivantes dans le modèle de base : âge, sexe, premier rythme cardiaque monitoré, réanimation cardio-pulmonaire par des témoins, choc circulatoire à l'admission, contrôle thermique ciblé, délai entre l'arrêt cardiaque et

le RCS, taux de lactate sérique initial et taux de NSE. Après ajustement avec ces 9 variables démographiques et cliniques, seul circNFAT5 est resté un prédicteur indépendant de l'évolution neurologique à 6 mois, avec des rapports de cotes (*Odd Ratio* ; OR) [Intervalle de Confiance ; IC à 95%] de 1,39 [1,07-1,83 ; 2,0E-02] en utilisant l'échelle CPC et de 1,40 [1,07-1,84 ; 0,016] en utilisant l'échelle mRS. Le critère d'information d'Akaike (*Akaike Information Criterion* ; AIC) permet d'évaluer dans quelle mesure un modèle s'adapte aux données. Plus l'AIC est petit, plus le modèle est adapté aux données. Dans cette étude, ce critère a montré la valeur la plus faible lorsque circNFAT5 était ajouté au modèle de base, ce qui veut dire que l'ajout de circNFAT5 au modèle clinique améliore significativement le pronostic de l'évolution neurologique post-ACEH.

Des analyses de survie ont également été réalisées à l'aide de courbes de survie de Kaplan-Meier et de modèles de risques proportionnels de Cox. Les courbes de survie de Kaplan-Meier ont montré pour tous les candidats une probabilité de survie plus faible lorsque les patients présentaient des niveaux de candidats post-ACEH supérieurs au seuil défini par l'indice de Youden. Après ajustement avec les mêmes variables précédemment mentionnées, seuls circNFAT5 et circFAM13b sont restés des prédicteurs indépendants de la survie à 6 mois avec des rapports de hasards (*Hazard Ratio* ; HR [IC 95 % ; valeur-p]) de 1,23 [1,07-1,42 ; 0,004] et 1,27 [1,10-1,46 ; 1,2E-03]), respectivement. De plus, l'ajout de circNFAT5 au modèle contenant les variables démographiques et cliniques permet l'obtention d'un AIC le plus faible par rapport au modèle seul ou aux modèles avec l'ajout d'un des autres candidats ARNInc (*Likelihood ratio test* valeur-p = 3.91E-04 ; *Wald test* valeur-p = 8.62E-74 ; *C-index* = 0.85). Cela signifie donc que circNFAT5 est le meilleur candidat pour améliorer le modèle de survie dans cette phase de validation TTM.

Un article scientifique décrivant les ARNcirc identifiés dans la phase de découverte et la validation d'un candidat circARN (circNFAT5) dans l'étude TTM a été accepté par le journal *Intensive Care Medicine Experimental*. La version de cet article acceptée par la revue se trouve à l'annexe III.

- Caractérisation moléculaire de circNFAT5

Parmi les différents candidats étudiés, circNFAT5 s'est avéré le meilleur candidat identifié dans l'étude TTM. C'est pourquoi la troisième partie de cette étude s'est concentrée sur la caractérisation moléculaire de cet ARNcirc. Au moment où cette étude a été menée, il n'existait aucune connaissance sur les origines et les fonctions de circNFAT5. Il s'agissait donc d'une étude préliminaire qui devra être approfondie grâce à des études supplémentaires.

Étant donné que les mesures de circNFAT5 dans l'étude TTM ont été effectuées à partir d'échantillons de sang prélevés grâce à des tubes PAXgene™, il a été supposé que circNFAT5 était principalement exprimé dans les cellules sanguines. Par conséquent, des analyses de corrélation avec divers marqueurs de cellules sanguines ont été réalisées afin d'aider à identifier les types de cellules sanguines exprimant circNFAT5. De plus, circNFAT5 a également été mesuré dans le plasma, le sérum ainsi que dans des sous-populations de globules blancs isolés à partir de sang provenant de trois volontaires sains. Les résultats ont confirmé l'absence ou la très faible présence de circNFAT5 dans le compartiment extracellulaire du sang (plasma et sérum). Au niveau des cellules sanguines, les analyses de corrélation ont montré des corrélations positives significatives notamment avec les marqueurs des monocytes/macrophages et des lymphocytes T. Par conséquent, les modèles cellulaires *in-vitro* sélectionnés pour ce travail ont utilisés des lignées cellulaires de lymphocytes (jurkat) et de monocytes (THP-1). Une troisième lignée cellulaire représentant une lignée de cellules neuronales, nommée SH-SY5Y, a été également ajoutée pour étudier une association potentielle entre circNFAT5 et les lésions cérébrales après un ACEH. Les mesures de circNFAT5 dans ces trois lignées cellulaires par qPCR ont montré des profils d'expression similaires. Celles-ci ont donc été utilisées pour l'ensemble de l'étude de caractérisation moléculaire menée dans ce travail.

Etant donné que les lésions cérébrales ischémiques hypoxiques après un arrêt cardiaque sont une cause majeure de mortalité et de déficience neurologique chez les survivants [64], deux types d'expériences *in-vitro* ont été réalisées pour imiter une condition hypoxique : d'une part la chambre hypoxique (1% O<sub>2</sub>) et d'autre part une alternative chimique, le chlorure de cobalt (CoCl<sub>2</sub>). Dans les deux cas, le facteur de croissance de l'endothélium vasculaire (*Vascular Endothelial Growth Factor* ; VEGF) a été utilisé comme contrôle positif de la condition hypoxique. Les trois lignées cellulaires ont été incubées pendant 24 h et 48 h dans la chambre hypoxique ou traitées au CoCl<sub>2</sub>. Aucun changement significatif des niveaux d'expression de circNFAT5 n'a été observé dans toutes les conditions testées, sauf pour les cellules jurkat. En effet, 48 h après l'incubation dans la chambre hypoxique, une diminution significative des niveaux de circNFAT5 a été observée pour ces cellules. Une tendance similaire a également été observée dans les cellules sanguines jurkat et THP-1 après un traitement avec CoCl<sub>2</sub>, bien que ces changements ne soient pas significatifs. Dans les cellules neuronales SH-SY5Y, une augmentation non significative a été observée dès 24 h après le traitement avec CoCl<sub>2</sub>. En conclusion, les résultats obtenus après incubation dans la chambre hypoxique ne corroborent pas les résultats observés après traitement CoCl<sub>2</sub>. Par conséquent, d'autres conditions susceptibles d'affecter les niveaux de circNFAT5 liés au SPAC ont été étudiées.

Il est bien connu qu'après une réanimation, la réoxygénation induit la production d'espèces réactives de l'oxygène et la libération de cytokines pro-inflammatoires qui déclenchent la migration de cellules immunitaires telles que les macrophages et les lymphocytes T vers le cerveau [65]. Dans ce contexte, il se pourrait que circNFAT5 puisse être impliqué dans le processus inflammatoire déclenché après un arrêt cardiaque. Afin d'étudier cette hypothèse, des cellules lymphocytaires jurkat ont été activées *in-vitro* avec un mélange d'anticorps anti-CD3/CD28 pendant 4 h, 24 h et 48 h. Ces anticorps se fixent sur les récepteurs cellulaires : CD3, essentiel pour activer le complexe TCR (récepteur des cellules T), et CD28, molécule co-stimulatrice nécessaire pour initier la prolifération des cellules T [66]. Dans ces conditions, une cytokine appelée facteur de nécrose tumorale (*Tumor Necrosis Factor alpha* ; TNF-alpha) est également produite par les lymphocytes T [67] et a donc été utilisée comme contrôle positif dans ces expériences. Une surexpression significative du TNF-alpha a été observée dès 4 h après le début du traitement et confirme l'activation de ces cellules par les anticorps anti-CD3/CD28. Dans ces mêmes expériences, les niveaux d'expression de circNFAT5 ont commencé à augmenter dès 24 h et ont montré des niveaux d'expression plus élevés après 48 h de traitement. Par conséquent, il est donc possible que circNFAT5 soit impliqué dans le processus inflammatoire déclenché après un arrêt cardiaque. Cependant, des études complémentaires sont nécessaires pour confirmer cette hypothèse et pour mieux comprendre le rôle que circNFAT5 pourrait jouer dans le processus inflammatoire post-ACEH.

Dans les bases de données, la séquence de circNFAT5 est constituée par un seul exon. Celui-ci correspond au dernier exon du transcrit linéaire de NFAT5. Afin de mieux comprendre si circNFAT5 possède un rôle fonctionnel propre ou est simplement un sous-produit de l'expression de NFAT5 linéaire, un modèle a été développé en utilisant un outil moléculaire permettant de diminuer l'expression de la forme linéaire NFAT5 (transfection avec un antisens LNA<sup>TM</sup> GapmeR ciblant spécifiquement NFAT5 linéaire) et couplé avec un activateur connu pour augmenter les niveaux d'expression de circNFAT5. Malheureusement, ce modèle n'a pas pu être appliqué à la lignée cellulaire jurkat qui est trop difficile à transfecter. C'est pourquoi, un autre modèle cellulaire a été recherché pour tester cette hypothèse.

Dans la littérature, NFAT5 est un facteur de transcription connu pour être activé suite à un stress osmotique, notamment par un traitement avec du chlorure de sodium (NaCl) [68, 69]. La lignée monocyttaire THP-1 a été choisie pour tester si le stress osmotique, via un traitement au NaCl, pouvait

également moduler l'expression de circNFAT5 dans la lignée cellulaire THP-1. Dans ces expériences, les cellules traitées avec du NaCl ont montré une augmentation du niveau d'expression de NFAT5 linéaire, comme décrit dans la littérature, mais également une augmentation du niveau d'expression de circNFAT5. Ces conditions expérimentales utilisant du NaCl ont donc été choisies pour étudier la relation entre NFAT5 linéaire et circNFAT5 dans la lignée cellulaire THP-1. C'est ainsi que les cellules THP-1 ont d'abord été transfectées avec un antisens LNA™ GapmeR afin de diminuer spécifiquement l'expression de NFAT5 linéaire, et ensuite traitées au NaCl. En présence de cet antisens, circNFAT5 a eu tendance à diminuer également. Cependant cette diminution n'était pas significative. De plus, en présence du NaCl, une augmentation des niveaux d'expression de circNFAT5 a été observée indépendamment de la présence ou de l'absence de l'antisens ciblant NFAT5 linéaire. Ces résultats suggèrent donc que circNFAT5 n'est pas un simple sous-produit de la surexpression de NFAT5 linéaire et possède donc très probablement une fonction propre et indépendante du transcrite linéaire. Cependant, le modèle testé dans ce travail a montré une grande variabilité entre les expériences. Les résultats obtenus quant à la régulation de l'expression de circNFAT5 devront donc être confirmés par des expériences additionnelles.

S'il est possible que circNFAT5 puisse avoir une fonction propre, celle-ci reste à investiguer. Au sein des ARNcirc, quatre fonctions principales ont été identifiées : la régulation des gènes parentaux, la production de protéines, le phénomène de séquestration des miARN et la séquestration de protéines [70].

Par conséquent, dans la section suivante de ce travail, les différentes fonctions possibles de circNFAT5 ont été abordées. Dans un premier temps, des expériences de gain et de perte de fonction de circNFAT5 ont été réalisées pour évaluer un effet potentiel sur le gène parental linéaire NFAT5. Aucune modulation du niveau d'expression de NFAT5 linéaire n'a été observé après avoir, soit diminué l'expression de circNFAT5 avec un antisens LNA™ GapmeR ciblant spécifiquement le point de jonction de circNFAT5 ; soit surexprimé circNFAT5 grâce à la transfection d'un vecteur d'expression codant pour circNFAT5. Ces résultats suggèrent donc que circNFAT5 ne régule pas le gène parental.

Bien que les ARN circulaires appartiennent à la famille des ARNnc, il est apparu récemment que certains de ceux-ci peuvent coder pour des protéines. En effet, la présence de cadres de lecture ouverts, d'éléments IRES (*Internal Ribosome Entry Site*) et de modifications post-transcriptionnelles type N6-méthyladénosine (m6A) dans la séquence d'un ARNcirc sont des indications d'un potentiel élevé à coder pour des protéines [71]. Afin de déterminer si circNFAT5 pouvait avoir un tel potentiel codant, ces éléments ont d'abord été investigués. Malgré la prédiction d'un potentiel cadre de lecture ouvert, l'absence de motifs IRES, la faible prédiction de sites de méthylation m6A ainsi que la très faible capacité de codage pour des protéines semblaient déjà exclure la capacité de circNFAT5 à coder une protéine. Néanmoins, une étude préliminaire *in-vitro* a été menée pour confirmer ces données. Pour ce faire, des cellules HeLa ont été transfectées avec un vecteur d'expression codant pour circNFAT5. Ensuite, une analyse par western blot a été réalisée en adaptant le protocole pour la détection de protéines de très petite taille. Les résultats de western blot n'ont pas montré la présence de protéine au poids moléculaire prédit pour circNFAT5 et supporte l'hypothèse que circNFAT5 ne semble pas coder pour une protéine.

Ensuite, la capacité de circNFAT5 à séquestrer les miARN a été évaluée. Tout d'abord, des analyses ont été réalisées pour prédire les miARN capables de lier la séquence de circNFAT5. Sur les 19 miARN identifiés, seuls deux, miR-144-3p et miR-139-5p, étaient capables de lier la séquence de circNFAT5 au niveau du point de jonction. Seuls ces deux miARN sont donc capables de reconnaître spécifiquement la séquence de circNFAT5 et non sa forme linéaire. Entre les 50 échantillons séquencés lors de la première étude de ce travail (miRNA-seq) et les 46 échantillons séquencés dans la deuxième étude (RNA-seq), 23 patients étaient communs. Par conséquent, les données de ces 23 patients provenant

de ces deux séquençages ont été utilisées pour effectuer des analyses de corrélation entre les niveaux d'expression des miARN précédemment identifiés et circNFAT5. Les résultats ont montré une corrélation négative significative entre les niveaux d'expression de miR-144-3p et de circNFAT5, ce qui peut suggérer un effet séquestrant de circNFAT5 pour ce miARN. Cette hypothèse a ensuite été étudiée *in-vitro* avec un test de luciférase dans des cellules HEK293. Les résultats du test de luciférase ont indiqué une interaction possible entre le miR-144-3p et circNFAT5, mais pas entre le miR-144-3p et NFAT5 linéaire. Bien que ces résultats soient très prometteurs, ils doivent être considérés avec prudence et leur exactitude doit être confirmée dans d'autres systèmes.

Enfin, la capacité de circNFAT5 à séquestrer les protéines a été évaluée seulement par des analyses de prédiction. En effet, parmi les protéines identifiées à partir de la base de données RBPmap (<http://rbpmap.technion.ac.il/>), seules les protéines ZNF326, RC3H1 et KHDRBS2 ont présenté un site de liaison prédit spécifiquement sur le point de jonction de circNFAT5. De plus, des analyses de corrélation ont été effectuées en utilisant les données de séquençage des ARN totaux des 46 patients de l'étude TTM (RNA-Seq). Ces analyses n'ont montré aucune corrélation significative entre les niveaux d'expression des ARN messagers codants pour ces protéines et circNFAT5. Des analyses supplémentaires sont donc nécessaires pour continuer à évaluer le potentiel de séquestration de circNFAT5 pour les protéines identifiées dans cette partie.

Enfin, pour identifier de potentielles interactions indirectes entre des ribonucléoprotéines (RNP) et circNFAT5, la base de données RBPDB (<http://rbpdb.cabr.utoronto.ca/>) a été utilisée dans ce travail pour identifier les 403 RNP présentes chez l'homme. Grâce aux données de séquençage des ARN totaux sur les 46 patients de l'étude TTM (RNA-Seq), des analyses de corrélation ont été réalisées entre les niveaux d'expression des ARN messagers codants pour ces 403 RNP et circNFAT5 ou sa forme linéaire NFAT5. Parmi toutes les RNP examinées, YTHDC2 était la seule RNP à être significativement corrélée avec circNFAT5 dans le groupe CPC5 ( $r=0,637$ ; valeur  $p=0,001$ ) et sans corrélation avec la forme linéaire NFAT5. Cependant, la relation potentielle entre circNFAT5 et YTHDC2 n'a pas été étudiée davantage dans ce travail. Il serait donc intéressant de poursuivre ces études pour comprendre par quel(s) mécanisme(s) circNFAT5 et YTHDC2 pourraient être liés.

- Validation de 3 ARNcirc chez des patients de TTM2

Pour finaliser la deuxième étude de ce travail, les trois principaux candidats identifiés dans l'essai TTM, c'est-à-dire circNFAT5, circDNM2 et circFAM13b, ont été mesurés chez les 674 patients de l'étude TTM2 pour lesquels des échantillons d'ARN étaient disponibles 48 heures après le RCS. Dans cette étude, seule l'échelle neurologique mRS était disponible à 6 mois post-ACEH. Celle-ci a donc été utilisée pour dichotomiser les patients en fonction de leur évolution neurologique. En considérant l'ensemble des patients, peu importe le contrôle ciblé de la température utilisé (hypothermie à 33°C ou normothermie  $\leq 37,5^\circ\text{C}$ ), une augmentation significative de circDNM2 et de circFAM13b a été observée chez les patients dont l'évolution neurologique était défavorable. En considérant uniquement les patients du groupe normothermie, seule une augmentation significative de circNFAT5 a été mesurée dans le groupe dont l'évolution neurologique était défavorable. Cependant, aucune différence dans les niveaux d'expression de circNFAT5 n'a été observée lorsque les patients ont été séparés en fonction de la température du contrôle ciblé.

À l'instar de ce qui a été rapporté précédemment pour l'étude TTM, des analyses prédictives de l'évolution neurologique et de la survie à 6 mois après l'arrêt cardiaque ont également été menées dans le cadre de l'étude TTM2. Des analyses multivariées ont été réalisées pour l'étude TTM2 en considérant tous les paramètres démographiques et cliniques précédemment décrits pour l'étude TTM, à l'exception de la NSE dont les taux n'étaient pas disponibles au moment de la réalisation de

cette étude. Il est donc impossible de comparer les résultats des modèles générés dans l'étude TTM avec ceux de l'étude TTM2 présentés ci-dessous.

Lors des analyses de régression logistique univariées réalisées pour TTM2, les 3 ARNcirc candidats étaient des prédicteurs de l'évolution neurologique dans le groupe normothermie. Après ajustement avec les 8 variables précédemment introduites, tous les ARNcirc ont été confirmés comme prédicteurs de l'évolution neurologique à 6 mois dans le groupe normothermie avec des OR de 1,29 [1,00-1,65 ; 0,045], 1,53 [1,19-2,00 ; 0,001] et 1,39 [1,09-1,79 ; 8,52E-03] respectivement pour circNFAT5, circDNM2 et circFAM13b. Cependant, cette capacité prédictive est perdue pour ces 3 candidats lorsqu'on considère uniquement les patients traités par hypothermie. Lorsque tous les patients de l'étude TTM2 sont considérés, cette capacité prédictive est également perdue pour circNFAT5 et circFAM13b mais reste présente pour circDNM2. Chez les patients du groupe normothermie, une valeur prédictive additionnelle a été confirmée pour chacun des candidats par une diminution de l'AIC par rapport au modèle clinique de base. Parmi ces candidats, circDNM2 a montré les meilleurs résultats pour améliorer le modèle d'évolution neurologique dans le groupe normothermie.

Dans cette étude TTM2, les courbes de Kaplan-Meier ont montré un risque de décès significativement plus élevé chez les patients dont les taux de circNFAT5, circDNM2 et circFAM13b étaient supérieurs à la valeur seuil identifiée par l'indice de Youden. Les modèles à risques proportionnels de Cox ont confirmé que les taux de circNFAT5, circDNM2 et circFAM13b sont des prédicteurs indépendants de la survie à 6 mois dans le groupe normothermie avec des HR de 1,24 [1,05-1,47 ; 0,013], 1,34 [1,14-1,59 ; 5,11E-04] et 1,29 [1,09-1,53 ; 3,09E-03], respectivement. Cependant, dans les modèles de survie, tous les candidats ont perdu leur capacité à prédire la survie lorsqu'on considère tous les patients ensemble (hypothermie et normothermie) ou seulement les patients du groupe hypothermie. Néanmoins, circDNM2 a de nouveau été identifié comme le candidat le plus performant pour prédire la survie à 6 mois chez les patients en normothermie de cette étude TTM2.

En conclusion, ce travail de thèse a été réalisé grâce aux échantillons et aux données de deux des plus grands essais cliniques multicentriques de patients victimes d'un ACEH (TTM et TTM2). De plus, la collecte, le stockage et le traitement des échantillons sanguins de ces patients ont été effectués de manière homogène selon des protocoles validés par une biobanque centrale. Toutes les mesures ont été effectuées dans le même laboratoire, évitant ainsi la variabilité inter-laboratoire pour la mesure des candidats étudiés. Parmi les principales limites de cette seconde étude, tous les candidats ont été mesurés 48 h après le RCS. D'autres candidats avec des profils d'expression plus précoces pourraient également être détectés plus tôt et aider plus rapidement au pronostic après le RCS. De plus, dans ce travail, aucune analyse n'a été réalisée en combinant les différents candidats étudiés. Bien que le rôle joué par circNFAT5 dans le contexte de l'arrêt cardiaque n'ait pas été totalement élucidé, les données présentées dans ce travail ont fourni des indications sur la régulation de circNFAT5 dans les cellules sanguines en conditions basales et après différents stimuli, sur la relation potentielle entre cet ARNcirc et son homologue linéaire ainsi que sur ses possibles mécanismes d'action. Pour terminer, ce travail est la première étude ayant pour but d'identifier des ARNinc et des ARNcirc en tant que biomarqueurs pronostiques de l'évolution neurologique après un arrêt cardiaque.

# *Introduction*



## 1. Cardiac arrest

### 1.1 Definition, classification and epidemiology

The American Heart Association (AHA) and the American College of Cardiology have defined cardiac arrest as the cessation of cardiac activity and subsequent disruption of blood circulation and organ oxygenation [72]. Death becomes final and irreversible if corrective measures are not taken within minutes. When the heartbeat stops there is a short window of time in which severe organ damage is not yet definitive and apparent death is reversible, during this time, the patient can be resuscitated. The term cardiac arrest describes this window of opportunity, where resuscitation is still possible. However, the brain is the most vulnerable organ affected by a lack of oxygen and severe neuronal damage can occur within minutes after oxygen deprivation [73]. Once cardiac arrest passes the threshold where brain activity is irreversibly lost, counter measures are futile and death ensues. This chain of events is known as sudden cardiac death [72].

Commonly, cardiac arrests are classified into in-hospital cardiac arrest (IHCA) and out-of-hospital cardiac arrest (OHCA) due to differences mainly in patient characteristics, cardiac arrest circumstances and intervention times [74, 75]. Usually, IHCA result from another disease for which the patient is hospitalized. These patients can benefit from a rapid treatment since they are already under surveillance. On the other hand, OHCA often occur in isolated and unwitnessed situations. As such, rapid intervention is unlikely for these patients and their chances of survival are significantly reduced.

Cardiac arrest represents the third leading cause of death in Europe [1-3]. Although cases of OHCA vary greatly from one country to another, the latest guidelines from the European Resuscitation Council reported an incidence of 67-170 OHCA per 100,000 population per year. Resuscitation is attempted in 50-60% of OHCA cases and the survival rates of these patients at hospital discharge are on average 8% [5]. Similarly to OHCA incidence rates, the global incidence of IHCA vary considerably between countries. In Europe, a number of cases ranging from 1.5 to 2.8 per 1,000 hospital admissions has been estimated with a survival rate of 15% to 34% at 30 days of hospital discharge [5].

Cardiac arrests can originate from primary cardiac pathologies. In this regard, over 90% of cardiac arrest cases originate from coronary heart disease [76] or cardiomyopathies [77]. The remaining 5-10% of cardiac arrests occur due to arrhythmogenic, mechanical or other causes [77]. However, cardiac arrests can also have non-cardiac origins. Trauma, drug overdose, hypothermia, severe infections, pulmonary embolism and intracranial haemorrhage are some of the non-cardiac aetiologies [72].

Risk of cardiac arrest significantly rises with age, reflecting the elevated incidence of coronary heart disease and other cardiovascular complications. Indeed, by the age of 45, cases of sudden cardiac death increase dramatically, with about 75% of sudden cardiac deaths occurring above the age of 65 [78, 79]. Additionally, men appear to have a three to four-fold higher probability to have a cardiac arrest than women [80]. Other factors such as family history and lifestyle can also predispose to cardiac death.

Despite advances in the field, identifying the cause of a cardiac arrest remains challenging even when an autopsy is performed [81]. Therefore, it is fundamental to continue to find new approaches to better identify at high-risk individuals.

## 1.2 The chain of survival

In 1991, the concept of the chain of survival was introduced as a sequence of actions that, if taken rapidly, could increase the survival rate of patients who have had a cardiac arrest outside the hospital setting [82]. The chain highlights the importance and the need of early defibrillation and cardiopulmonary resuscitation (CPR) manoeuvres to maximise the chance of patient survival.

Although the chain of survival is suitable for both types of cardiac arrest (IHCA and OHCA), the differences in the two events affects the links in the chain and the type of health care provided at each stage. Indeed, for patients with OHCA, arrest usually represents the primary event, while for patients with IHCA it usually reflects the heart's response to severe systemic disease (such as cardiac injury, kidney dysfunction, thrombosis and others [2]). Therefore, the patient can be monitored before the event occurs and preventive interventions can be applied [83]. Thus, response times are shorter in IHCA compared to OHCA and medical staff can provide immediate and simultaneous treatments in response to IHCA. For this reason, more attention must be paid to patients with OHCA since they have a higher risk of dying if prompt interventions are not taken.

As such, for the purpose of this thesis, we will focus on the OHCA chain of survival.

Over the years, the chain of survival has been updated several times, but the message conveyed in each link has remained unchanged. The latest version, released by the AHA in 2020, shows six links (Figure 1), two more than the original version [84]. Any bystander can perform the first three links of the chain while the last three require the intervention of health professionals. The optimal application of each link in the chain can greatly improve the chance of survival and the outcome of the patient.

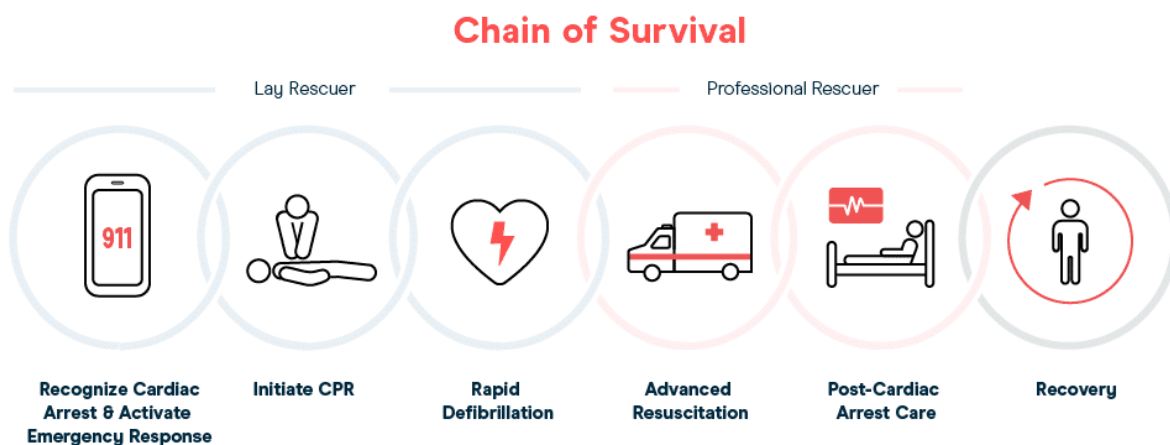


Figure 1. OHCA chain of survival. Image taken from: <https://avive.life/blog/chain-of-survival/>.

As illustrated in Figure 1 the links within the latest Chain of Survival include:

### 1. Activation of the emergency response

The chain of survival begins with the recognition of the emergency by the person with symptoms or a bystander who can call for help.

The first link underlines the importance of recognition of a cardiac arrest event and rapid activation of the emergency response system in the hope of receiving an early treatment.

Contrary to its name, sudden cardiac arrest is rarely sudden [85]. Indeed, many patients present warning symptoms long before cardiac arrest occurs [85]. However, most of the time the patient misinterprets or ignores these symptoms until the collapse occurs [85]. For this reason, an efficient emergency response alongside improved education of the general public in terms of what to do when an emergency occurs, are crucial elements for early hospitalisation and chance of recovery [82, 86].

## *2. High-quality CPR*

The second link in the chain of survival is the initiation of basic CPR to support breathing and circulation of the patient until advanced resuscitation treatments can be initiated.

An external cardiac massage and artificial ventilation of the lungs can keep the patient alive by ensuring oxygenation of the central nervous system and of the myocardium [86]. However, for CPR to be effective, it must be started as soon as possible after the patient collapses. Ideally, CPR begins immediately upon recognition of a cardiac arrest and simultaneously with the alerting of the emergency services [87].

The initiation of early basic life support increases the chances of the patient being in a state of ventricular fibrillation when the medical professionals arrive and therefore, to be successfully defibrillated [86].

Equally important is the quality of CPR performed. For this reason, in 2010 the AHA guidelines focused their attention on the methods to be used to ensure optimal CPRs [88]. Five main components ensure high-quality CPR:

- I. Chest compression fraction: It is important to minimise pauses during chest compressions [88, 89].
- II. Chest compression rate: a chest compression rate of 100 to 120/min is recommended [88].
- III. Chest compression depth: The minimum chest compression recommended in adults is 50 mm [90-92].
- IV. Chest recoil: it is necessary that the chest wall releases completely after each compression [92].
- V. Ventilation: excessive ventilation must be avoided (< 12 breaths/min) [92].

These parameters can help trained rescuers to optimise CPR performance, which results in a higher probability of survival for the patient [92].

## *3. Defibrillation*

Defibrillation is the therapy used to restore normal heart rhythm in patients with cardiac arrest. Therefore, it represents a key link in the chain of survival.

A defibrillator delivers a dose of electrical current that shocks the heart by converting the rhythm from ventricular fibrillation or pulseless ventricular tachycardia to a normal beat. Thus, this intervention can significantly increase the survival chances of these patients [93, 94]. However, to be effective, heart defibrillation must occur within 3-5 minutes after collapse [95]. In fact, the patient's chances of survival have been shown to decrease by 7-10% for every minute spent without receiving CPR or defibrillation [93].

The most used devices are automated external defibrillators (AEDs). Unlike regular defibrillators, an AED can automatically diagnose heart rhythm and determine if a shock is needed. Therefore, AEDs are highly accurate and easy to use, minimising training required for their use and consequently increasing the number of people who can manipulate them [82, 96, 97]. Public access to AED's is becoming more common, however, there are still not enough devices and persons trained to use them [98]. Less than 12% of cardiac arrest patients receive a shock before the arrival of the emergency responders [87]. For this reason, it is important that the rescuer calls for help as soon as possible and continues to deliver CPR until the arrival of the emergency service.

#### *4. Advanced resuscitation*

The remaining links in the chain of survival relate to actions that should be undertaken by medical professionals. Advanced resuscitation consists of a series of interventions and protocols that professional responders provide to stabilise the patient prior to the arrival at the hospital. These interventions include the administration of medications, advanced airway procedures, heart rhythm monitoring, and initiation of transcutaneous pacing [87]. However, similarly to the delivery of CPR, advanced life support should be provided within the first 9 minutes of the cardiac arrest in order for the patient to have the best chance of survival [99].

#### *5. Post-cardiac arrest care*

Post-cardiac arrest care consists of a series of practices that aim to increase patients' chances of survival by minimising the effects of the post-cardiac arrest syndrome (PCAS). Therefore, this fifth link in the chain of survival is critically important for the long-term outcome of the patient. PCAS is a condition whose aetiology, although not completely understood, appears to be dominated by global ischemic-hypoxic injury and a systemic inflammatory response [100, 101]. PCAS represents a major determinant of high morbidity and mortality if return of spontaneous circulation (ROSC) is not achieved rapidly after onset of cardiac arrest [7]. The syndrome is characterised by four major components and severity may vary from individual to individual [7].

The four major components of the PCAS can be classified as:

##### *I. Brain injury*

The brain more than any other organ in the body is affected by ischemia/reperfusion injury which leads to both neuronal necrosis and apoptosis [102]. In particular, the reoxygenation/reperfusion period can exacerbate the level of neuronal damage due to the production of free radicals and mitochondrial injury [103]. Pyrexia [104-106], hyperglycaemia [106-108], and seizures [109] are other

factors that highly affect the levels of brain injury and for which precise neuroprotective strategies should be applied.

## II. Myocardial dysfunction

Myocardial dysfunction can also significantly reduce the survival rate after cardiac arrest [110]. Changes in heart rate and blood pressure can be seen immediately after ROSC and are usually reversible [111-113], thus with appropriate monitoring these conditions can be detected and immediate treatment strategies adapted [114, 115].

## III. Systemic ischemic-reperfusion response

The systemic ischemic-reperfusion response manifests mainly through impaired oxygen delivery and utilization, imbalanced vasoregulation, intravascular volume depletion and increased susceptibility to infection [7]. CPR can partially reverse the oxygen store depletion generated after onset of cardiac arrest, however endothelial activation and systemic inflammation can still occur [116, 117] increasing the risks of multi-organ failure, infection and ultimately death [118, 119]. As previously mentioned, blood reperfusion to ischemic organs can worsen organ damage due to the production of free radicals [103, 117]. The heart and brain are particularly at risk for these harmful effects because of their high metabolic activity [117]. However, in most cases the adverse clinical manifestations of ischemia/reperfusion injury are responsive to treatment strategies such as ischemic preconditioning, pharmacological treatment, medical gases and vitamin therapy [117].

## IV. Persisting precipitating pathology

Persisting acute pathology can cause or contribute to the pathophysiology of cardiac arrest. Cardiovascular diseases, pulmonary diseases, brain disease, intoxication, infection and hypothermia are among the precipitating causes of cardiac arrest [7]. For instance, it has been reported that approximately 50% adults with OHCA suffer an acute myocardial infarction (MI) [120, 121]. When combined, these acute pathologies can exacerbate PCAS (and/or vice versa), which makes diagnosis difficult.

Major post cardiac arrest care focuses on mitigating the brain injury. However, PCAS is a complex and heterogeneous condition and death can occur from multi-organ dysfunction. Therefore, the development of multidisciplinary protocols could critically improve patient outcome [122]. An optimal hospital care is yet not defined, nevertheless, there is an increasing interest in identifying and optimising practices that can improve the likelihood of patient survival. Prognostication strategies and treatment approaches used in post-cardiac arrest care to improve patient's outcome will be discussed in chapter 1.4 and 1.5 respectively.

## 6. Recovery

In 2020, the AHA guidelines added the recovery phase as the last link in the chain of survival to highlight the importance of rehabilitation and surveillance for cardiac arrest survivors after hospital discharge [87]. Indeed, a patients' recovery from cardiac arrest continues after hospitalization. Many survivors experience physical, neurological, cognitive, emotional, and even social problems that persist after

hospital discharge [123]. As the number of survivors is on the rise, long-term rehabilitation plans need to be organized. Therefore, the guidelines recommend providing a comprehensive, multidisciplinary assessment and support to the survivors and caregivers before being discharged from the hospital in order to facilitate their return to daily activities [87].

### 1.3 Outcome after cardiac arrest

Approximately half of the OHCA survivors present long-term neurocognitive impairment [124, 125]. Primary neurological injury is determined by the severity and duration of ischaemia during cardiac arrest. The longer someone remains in cardiac arrest, the lower the chances of survival with a favourable neurological outcome are. Resuscitation of those patients allow restoring cardiac and cerebral function, however the heart is able to tolerate ischemia better than the brain. Thus, even when resuscitation is successful, the risk of the patient not recovering from brain damage remains high [126-128].

Comatose patients are hospitalised in the intensive care unit (ICU) where the attention is focused on identification and treatment of PCAS. Concomitantly, several prediction tools (listed in chapter 1.5) are used to assess the likelihood of neurological recovery of the patient. The best outcomes are reported in patients who regain consciousness rapidly after ROSC or within the first 4 days of ICU [6]. For the most severe cases, the prognostication of unfavorable neurological outcome might ultimately lead to withdrawal of life-sustaining treatment (WLST). In fact, more than 70% of comatose OHCA patients die before hospital discharge due to WLST after assessment of severe neurological injury [129]. However, it should be acknowledged that to date the practice of WLST varies greatly among countries [130]. Worldwide variability of WLST could be due to geographical, cultural and religious factors, as well as to the characteristics of patients, physicians and intensive care facilities [131]. National regulations may also differ, in fact in some countries the suspension of ventilation is prohibited while in others terminal sedation is allowed [131]. Therefore, finding an international consensus on end-of-life decision-making is necessary to harmonise and improve the quality of care for these patients [131].

Death before hospital discharge may also occur due to refractory hemodynamic shock, comorbid withdrawal of care or respiratory failure [129]. Ultimately, in 4-10% of OHCA cases, cardiac arrest leads to brain death [129, 132].

Despite improvements in pre-hospital care and post-cardiac arrest management, the number of patients who completely recover after cardiac arrest it is still too low and severe brain damage after cardiac arrest remains a major concern among physicians. Mounting evidence shows that early initiation of high-quality CPR and thus, a shorter duration of the ischemic condition, can reduce brain damage and can significantly improve the likelihood of better long-term neurological outcome [128, 133-136]. Worldwide, 8.8% of OHCA patients who underwent CPR survive at hospital discharge [128]. Furthermore, a significant improvement in the survival rate at discharge of those who underwent CPR was reported over a 40-year period, from 8.6% in 1976-1999 to 9.9% in 2010-2019 [128].

Clinicians are often required to determine the long-term recovery of those patients by using scales that measure the neurologic function of cardiac arrest survivors. These scales are not useful in the hours immediately following cardiac arrest when outcome predictions and end-of-life decision-making needs to be taken. However, they are extremely useful for research purposes such as comparing outcomes, evaluating new therapies, and formulating recommendations [13]. The Utstein Resuscitation Registry template for OHCA recommend the use of either the modified Rankin Scale (mRS) [15] or the Cerebral Performance Categories (CPC) [14] to measure the level of neurological and physical disability of cardiac arrest survivors [137]. The mRS scale was originally developed for stroke and later modified for

the determination of outcome after cardiac arrest. It includes seven scores, from no symptoms (mRS=0) to dead (mRS=6) (Table 1).

<i>Score</i>	<i>Activity level</i>	<i>Description</i>
<b>0</b>	No symptoms	
<b>1</b>	No significant disability	Able to perform all previous activities despite symptoms
<b>2</b>	Slight disability	Able to look after own affairs without assistance but unable to perform all previous activities
<b>3</b>	Moderate disability	Able to walk without assistance but requires some help
<b>4</b>	Moderately severe disability	Unable to walk unassisted and unable to attend to own bodily needs unassisted
<b>5</b>	Severe disability	Requires constant nursing care and attention, bedridden and incontinent
<b>6</b>	Dead	

Table 1. Modified Rankin Scale. Table adapted from [15, 138].

The CPC scale is instead adapted from the Glasgow Outcome Scale and includes five scores (Table 2), from no or minor disabilities (CPC=1) to dead (CPC=5) (Table 2).

<i>Score</i>	<i>Activity level</i>	<i>Description</i>
<b>1</b>	Good cerebral performance	Conscious, able to work, alert, might have mild neurologic or psychologic deficits.
<b>2</b>	Moderate cerebral disability	Conscious, sufficient cerebral function for independent activities of daily life and work in sheltered environment.
<b>3</b>	Severe cerebral disability	Conscious, required daily assistance because of impaired brain function. Range from ambulatory state to severe dementia or paralysis.
<b>4</b>	Coma or vegetative state	Any degree of coma without the presence of all brain death criteria. Unresponsive, unaware of surroundings, no interaction with environment.
<b>5</b>	Dead	Certified brain death or dead by traditional criteria.

Table 2. Cerebral Performance Categories. Table adapted from [14, 139].

According to the Utstein criteria a CPC score of 1 to 2 or a mRS score of 0 to 3 is indicative of good neurological outcome and conversely, a CPC score of 3 to 5 or a mRS score of 4 to 6 as poor outcome [140]. As, neurological outcome can evolve between 1 and 6 months after cardiac arrest [141, 142], it is important to select an optimal timing when assessing the neurological function [137], to ensure that the brain injury has stabilized. The Utstein guidelines recommends evaluating neurological outcome



with the CPC or mRS scale at hospital discharge or 30 days after cardiac arrest. Further assessments are suggested as supplementary considering the difficulties of the health care system in collecting information for such long-term follow-up [140].

Although the two scoring systems are widely used, the mRS score appears to be more sensitive in discriminating between mild and moderate brain injuries than the CPC score [15, 16] and therefore favored by the International Liaison Committee on Resuscitation [143].

## 1.4 Prognostication of outcome after cardiac arrest

Prognostication of neurological outcome after cardiac arrest is a crucial component of the post-cardiac arrest care that might ultimately lead to WLST. For this reason, neuroprognostication tools are required to be accurate and deliver results with the lowest possible false-positive rate.

Many demographic and clinical parameters have been associated with poor outcome such as, time from collapse to start of CPR [144, 145], the time from start of CPR to ROSC [144], age [146, 147], gender [148] and type of initial rhythm [149]. However, none of these factors are sensitive enough to be considered as an outcome predictor alone. Even the most reliable predictors are not 100% accurate. Therefore, to obtain more precise prognostications the guidelines recommend the use of a multimodal approach that combines different parameters to assess the level of neurological damage [9].

To add another layer of complexity, clinicians are asked to prognosticate as soon as there is certainty of the neurological outcome. This drives precision medicine and helps avoid causing additional suffering to the relatives and patients, for whom a poor outcome is confirmed. Unfortunately, even with the use of multimodal approaches the results of the various tests performed might not align. This can be due to the use of some medications that could alter the results of the tests or to a non-optimal test performance time. In cases where the neurological outcome is uncertain, early prediction can be dangerous, thus the guidelines recommend prognosticating the neurological outcome not earlier than 72 h after admission to the ICU [9].

A multimodal prognostication includes clinical examinations, neuroimaging, biomarker measurements and electrophysiological investigations (Figure 2). All these tests will be described below with the exception of biomarkers. As the main topic of this research project, an entire chapter was dedicated to biomarkers used in outcome prognostication after cardiac arrest.

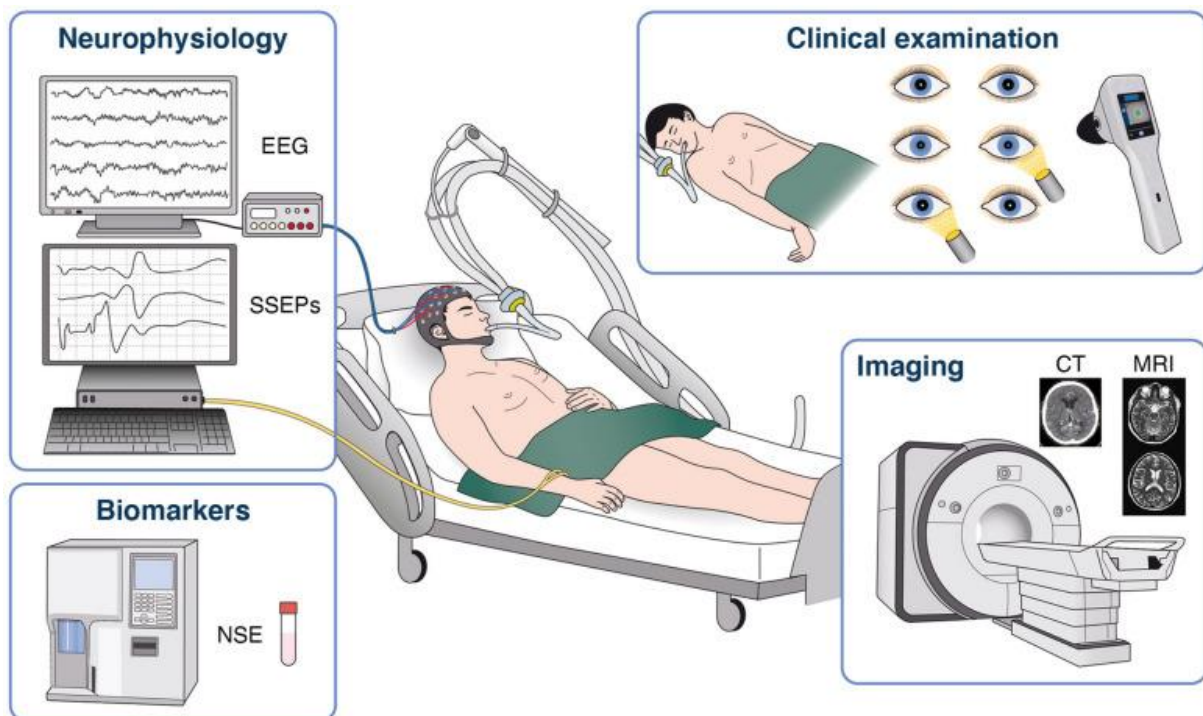


Figure 2. Components of multimodal prognostication. Image taken from [9].

- Clinical examinations

Pupillary light reflex and corneal reflex are among the most reliable neurological examinations for outcome prognostication after cardiac arrest [150-153]. Shortly after cardiac arrest, pupillary light reflex and corneal reflex are absent, however these reflexes are soon recovered in survivors. Patients with persistent absence of brainstem reflexes are predicted to have an unfavourable outcome [152, 154-156].

Other clinical signs like the presence of status myoclonus [109, 157] and motor responses to pain [158] can also be indicators of poor neurological outcome [158]. However, several cofounders such as sedatives and seizures can affect the reliability of these tests and consequently increase the false positive rate of the prognostication [158]. Therefore, the guidelines recommend the use of neurological examinations for outcome prognostication of cardiac arrest patients not earlier than 72 h after ROSC [9].

- Neuroimaging

Neuroimaging is mainly used to assess the structural damage caused by the cardiac arrest or alternative aetiologies of the arrest.

Computerised tomography (CT) scan is the most widely available and used neuroimaging technique for early prognostication following cardiac arrest. This technique focuses mainly on the loss of gray-white matter ratio as a predictor of poor neurological outcome [159, 160]. Usually, the density of the gray matter is higher than the white, so in case of severe brain injury the gray-white matter ratio is reduced [9]. Furthermore, this parameter can be measured on hospital admission as the reduction of gray-white matter ratio occurs early after cardiac arrest. It has been reported that the reduction of the gray-white matter ratio can prognosticate poor outcome already 1h after ROSC with high specificity [158].

Magnetic resonance imaging (MRI) is another widely accepted tool used to prognosticate the outcome of cardiac arrest patients. MRI measures the level of brain injury as abnormalities in the diffusion-weighted imaging (DWI) sequences [161]. Many studies have shown that the widespread of DWI lesions is associated with unfavourable neurological outcome [161-163].

Despite the fact that MRI has a higher soft tissue resolution than CT scan and can give a more robust assessment of brain damage, it is challenging to use in unstable patients and is generally not performed earlier than 48 h after ROSC [9, 161]. This limits its applicability for an early prognostication [9]. Moreover, the combined use of CT scan and MRI, rather than their single use, appear to improve the sensitivity of the prognostication [164].

The use of neuroimaging techniques is advantageous because they can be performed blindly and the results are not affected by the presence of sedatives. However, there is no standardisation in the methodologies used to measure brain damage, so the results are difficult to reproduce limiting their use to experienced neuroradiologists [9].

- Electrophysiological investigations

Electroencephalography (EEG) is one of the most extensively used tools to evaluate coma depth and levels of brain damage after cardiac arrest. It consists of a series of electrodes placed on the patient's scalp for detection of abnormalities in the brain's electrical waves. Therefore, this technique is non-invasive and easy to use even in unstable patients. Different malignant EEG patterns such as generalised suppression to  $< 20 \mu\text{V}$  or burst-suppression pattern associated to generalized epileptic discharges have been associated with poor neurological outcome [165]. Furthermore, unfavourable EEG patterns can predict the outcome of cardiac arrest patients already 24 h after ROSC with high specificity [166]. Unfortunately, the lack of a unified classification system for categorising the malignant EEG patterns and the susceptibility of this technique to sedatives, anti-epileptic drugs, hypothermia treatment and metabolic disorders limit the accuracy and therefore the application of the technique [165, 167-169].

Accordingly, a more reliable electrophysiological test appears to be the somatosensory evoked potential (SSEP). SSEP consists of "stimulating electrodes" and "recording electrodes", the former stimulates a peripheral nerve whilst the latter records the response of the nervous system to the stimulus. The best studied evoked potential in outcome prognostication after cardiac arrest is the N20 component of the SSEP. SSEP components are usually defined according to their polarity (positive/negative) and typical peak latency, measured in milliseconds. As such, the N20 component indicates a negative cortical response at 20 milliseconds after the median nerve stimulation. A bilateral absence of the N20 potentials after median nerve stimulation is a reliable predictor of poor outcome in unresponsive cardiac arrest survivors with high specificity if measured from 24 h to one week after ROSC [9, 170-175].

Unlike EEG, SSEPs are less influenced by sedatives [176], however there are other limiting factors to consider. For instance, muscle activity can affect the quality of recording and mislead in the interpretation of the results. This factor can be easily resolved using neuromuscular blocking agents [9, 176, 177]. Additionally, SSEPs are not available in all hospital and the widespread implementation of this technique requires advanced neurological training to be performed and interpreted accurately [9, 122]. Furthermore, it seems that SSEPs and EEG are less reliable in predicting the outcome of patients treated with hypothermia [178-181]. Therefore, the guidelines recommend performing these tests after rewarming of the patients and after sedative components have been cleared [9].

The sensitivity of both techniques remain unacceptably low and further studies are required to decrease the false-positive rates of these applications [166, 175, 176, 182].

## 1.5 Therapeutic approaches

Early identification of the precipitating cause of cardiac arrest as well as accurate prognostication are of paramount importance to provide the patient with the most appropriate and specific therapies and prevent premature withdrawal of care. Treatment plans should focus in reverting the pathophysiological manifestations of PCAS. The severity of PCAS varies widely among patients, therefore therapies must be tailored to their needs within a precise time frame for execution [7].

Brain injury and cardiovascular dysfunctions are the main determinants of long-term survival after cardiac arrest. Brain damage continues in the hours and days following ROSC providing a window for therapeutic interventions [8]. Fever, considered as a core temperature above 37°C, is common in the first 72 h after cardiac arrest and is associated with unfavourable neurological recovery [105]. Targeted temperature management has been a key component of neuroprotection after cardiac arrest for several years [183-185] and the current guidelines suggest the use of targeted temperature regimen of 32-36°C in unresponsive patients after ROSC [9]. The mechanisms towards which mild hypothermia protects the brain are still unclear, however there is growing evidence that lowering core temperature can reduce oxidative stress, inflammation and programmed cell death [10].

Several clinical trials have studied the effects of targeted temperature management after OHCA. The targeted temperature management trial (TTM-trial, NCT01020916) randomised 950 OHCA patients treated for 28 h at the targeted temperature of 33°C or 36°C followed by a slow rewarming phase [11]. Of the 950 patients, 939 were included in the primary analysis. The results of this study showed non-beneficial effects of using a targeted temperature of 33°C compared to the 36°C [11]. More recently, a follow-up study of the TTM-trial, the TTM2-trial (NCT02908308), compared targeted hypothermia (33°C) with targeted normothermia (early treatment of fever) in 1900 patients and showed no difference in survival and neurological outcome improvement by using one of the selected treatments [12]. These studies may have created some confusion among physicians, but what they most likely indicate is that the level of mild hypothermia selected is not as crucial as previously thought, however early fever treatment after ROSC might be the important determinant for the long-term favourable outcome of these patients. Further evidence on the benefits of fever control will be required to confirm this hypothesis.

Both the TTM-trial and TTM2-trial cohorts are used in this thesis and will be discussed more in detail in the following sections.

Among other pathophysiological manifestations of the hypoxic–ischaemic brain injury, seizures are present in 20–30% of cardiac arrest patients admitted at the ICU [9, 109]. There are several subtypes of seizures, the most common one is myoclonus [109, 157]. It is also common for a patient to present different seizure subtypes, which are usually associated with poor outcomes [109]. However, it has been reported favourable to recovery in patients with early status myoclonus [109, 157]. Therefore, the presence of myoclonus alone should not be considered for outcome prediction and treatment of seizures with anticonvulsants and sedative drugs is recommended by the current guidelines [9].

Post-resuscitation myocardial dysfunction occurs in approximately two-thirds of patients [186] and begins to gradually resolve after 72 h [187]. Early echocardiography allows identifying the type of pathology and the levels of myocardial dysfunction which can guide haemodynamic management [9]. In this regard, arterial hypotension is another indicator of poor outcome [188, 189] and continuous

monitoring of arterial pressure is suggested to identify and treat hypotension with intravenous fluids [9, 190].

Coronary angiography and, where indicated, percutaneous coronary intervention (PCI) performed early after ROSC are well known to improve the neurological outcome and survival at discharge [191, 192] and therefore should be considered in all patients in whom acute coronary syndrome is suspected [9]. Patients with severe neurological damage may not benefit from PCI, even when treatment is successful. Indeed, performing PCI might delay other important post-resuscitation care, such as targeted temperature, which these patients could benefit from [193]. However, the absence of an accurate prognostic tool early after ROSC makes it difficult to identify these patients at hospital admission [9].

Many other therapies have contributed to save many lives over the years, however there is still room for improvement especially in the selection of patients who can benefit most from certain therapies.

## 1.6 The burden of cardiac arrest

For every single patient hospitalised after OHCA, the economic burden of health care resources is substantial. Starting from the emergency phone assistance for bystanders CPR, the ambulance team, emergency physicians and ultimately the specialists in the ICU who tailor all possible treatments that patients could benefit from, a single cardiac arrest requires the intervention of numerous health care professionals only in the acute phase of this condition. In this regard, Hamel et al. published a study in 2002, showing that continuing aggressive treatments in non-traumatic comatose patients after 3 days substantially increases treatment costs especially for patients at high risk of having an unfavourable outcome [194]. In fact, they estimated an average of \$ 140,000 (\$ 1998) per quality adjusted life year (QALY) for high-risk patients and \$ 87,000 / QALY for low-risk patients [194].

The economic burden continues also after the acute phase of cardiac arrest. A study reported that the cost of hospital rehabilitation of an anoxic brain injured patient could be in the region of \$ 44,181 for an average of 41.5 days [195]. Furthermore, the prevalence of patients remaining in a persistent vegetative state or with a certain degree of disability after cardiac arrest has a huge impact on the patients, their families and the society [196]. In fact, approximately half of survivors present cognitive impairments [124, 125] and the return-to-work rate varies from 29% to 79% [197-200].

Further improvement in the quality of CPR and use of AEDs could drastically reduce the economic burden of cardiac arrest by reducing the incidence of post-cardiac arrest syndrome and therefore the healthcare resources needed for the long-term survival of these patients. Furthermore, more accurate and early prognostication methods could further reduce the economic and social burden and could help clinicians target patients who would benefit most from invasive, costly and time-consuming therapies, while avoiding additional unnecessary pain for the families of patients with certain unfavourable outcomes.

## 2. Biomarkers

In 2001 the National Institutes of Health (NIH) Biomarkers Definition Working Group defined biomarker as “a characteristic that is objectively measured and evaluated as an indicator of normal biological processes, pathogenic processes, or pharmacologic responses to a therapeutic intervention” [201]. Thus, molecular, histologic, radiographic, and physiologic characteristics can be measured in tissues or body fluids and provide diagnostic, prognostic or therapeutic information about a particular disease or condition [202].

Previously, biomarkers were mostly physiological indicators such as heart rate, body temperature, pulse, and blood pressure [203]. However, as advances in molecular medicine have provided a profound understanding of healthy and diseased conditions, the term biomarker is increasingly becoming synonymous with molecular biomarker [203, 204]. Molecular biomarkers include molecules such as nucleic acids, peptides, proteins and lipids. These biomarkers have the additional potential of stratifying a population based on the specific genotype associated with a disease, for instance. Consequently, molecular biomarkers can help predict individuals more susceptible to a given disease and help drive precision care [205]. Indeed, the discovery and development of effective molecular biomarkers is of paramount importance for the advancement in precision medicine. Precision medicine, also known as personalised medicine, refers to a form of medicine that recognises a disease or the risk of developing a disease and adapts precise interventions based on genetic, environmental, and lifestyle factors of the patients resulting in a specific and efficient prevention or treatment of the disease in question [203, 206].

Regardless of their role and classification, an ideal biomarker should present the following characteristics:

- Practicality: it should be easy to measure, ideally in a non-invasive way [207].
- Robustness: it should not be influenced or modified by physiological variations [208].
- Accuracy: it should be able to identify only patients with a precise disease or condition [209, 210].
- Reproducibility: the biomarker potential should be confirmed in independent studies [211].
- Cost effectiveness: the costs from measuring a biomarker should be low.

While promising new biomarkers are constantly being discovered and some are validated and used in the clinical setting, only a few exhibit highly satisfactory performance [212]. Therefore, there is still an unmet need to find better performing biomarkers for the diagnosis, prognosis and/or treatment of specific diseases.

As mentioned above, the molecular profile of human diseases allows for a more complete picture of the mechanisms and risk factors associated with a specific condition [20]. In particular, the advances made in the field of "omics" which includes, among others, genomics, epigenomics, transcriptomics, proteomics, metabolomics and lipidomics, allow the identification of new clinically useful molecular biomarkers [19-21]. Nowadays, several high-throughput techniques are available depending on the molecular level at which these markers are studied [21]. For instance, gene expression microarrays and RNA sequencing (RNA-seq) are two main high-throughput methodologies used for transcriptome screening [213, 214]. Of the two, RNA-seq is more sensitive in quantifying RNA molecules, allowing for the detection of rare or poorly expressed transcripts [21, 213]. Furthermore, unlike microarrays, which detect only known pre-selected sequences, RNA-seq sequences the entire transcriptome thus allowing the discovery of new RNA molecules and variants [21, 213]. However, the cost of RNA-seq are still high and therefore prohibitive for many researchers. In either case, these techniques allow the selection of a defined number of transcripts, which can be further investigated with more affordable and targeted methods. Indeed, the preferred technique used to quantify the expression of specific RNA molecules



in large numbers of samples is reverse transcription (RT) followed by quantitative polymerase chain reaction (qPCR). The RT process is essential for the conversion of RNA into complementary DNA (cDNA) which can be recognised by the DNA polymerase and thus act as template for the qPCR reaction [215]. Differently from the traditional PCR, RT-qPCR uses fluorescent dyes, such as SYBR green, which intercalate into the newly generated DNA and, upon excitation, emit more fluorescence than its unbound form [216]. The fluorescent signal revealed is directly proportional to the levels of the specific RNA molecule measured in the sample. Therefore, RT-qPCR monitors the increase in the amplified piece of cDNA from which the amount of starting material is extrapolated [217]. As such, if the results of an RT-qPCR show significant differential expression of a given RNA molecule under two different conditions (i.e. healthy and diseased individuals), this RNA may have a biomarker potential. However, a significant differential expression is not sufficient for a molecule to be used as biomarker. Thus, different biostatistical tools have been developed for processing, analysing, and efficiently evaluating the performance of new molecular markers [218]. Some of these methodologies, which have been used in this research project, are summarised in chapter 2.1.

Regardless of the type of molecular biomarker studied, an important aspect to consider is the quality and integrity of the samples analysed, which can significantly influence the results of the analyses performed [21]. It is therefore important to follow the recommended protocols for collection and storage of specific types of samples [219-221]. This applies also to RNA samples. Indeed, after RNA extraction from bio specimens, the samples should be stored at -80°C in RNase-free water and multiple freeze-thaw cycles should be avoided to prevent RNA degradation [222].

In addition, the accessibility of samples must also be considered when studying new molecular biomarkers. Indeed, tissue samples are not easy to obtain, especially in healthy individuals. In this regard, the identification of biomarkers in body fluids has the advantage of being a less invasive approach than the collection of tissue samples, while being able to reflect pathological changes originating from different organs [223]. Therefore, circulating molecules in body fluids represent advantageous biomarker reservoirs. As this thesis focuses on the study of RNA molecules, more details on circulating RNAs are presented in chapter 3.3.

Finally, present and future technological developments in biomarker detection and validation aim to improve the healthcare system by assisting clinical decisions and reducing the economic burden of many complex diseases, enabling progress towards precision medicine [224, 225].

## 2.1 Statistical evaluation of new biomarkers

Several statistical tools have been developed to study the performance of new molecular biomarkers. For instance, when measuring an RNA molecule under different conditions, such as healthy and diseased individuals, having a statistically significant difference in the expression levels of the molecule under those conditions is the minimum requirement to be considered a potential biomarker. Different tests can be performed to evaluate this statistically significant difference according to the dataset at disposal. Indeed, when the analysed dataset follows a normal distribution usually the test performed is a student's t-test. If the opposite is true, the Mann-Whitney U test is preferred. Regardless of the method used, the differential expression of the molecule is considered to be statistically significant when  $p\text{-value} < 0.05$ . However, statistical significance alone is not sufficient for the new potential biomarker to have clinical significance as well. To this end, model performance measures are required.

The accuracy of a biomarker can be measured in terms of its sensitivity and specificity. A sensitive biomarker is able to identify only the patients that truly have the disease/condition (true positives) [210]. On the contrary, a specific biomarker is able to exclude individuals without the disease/condition (true negatives) [210]. Therefore, an ideal biomarker would present high sensitivity and high specificity [210]. One method commonly used to evaluate the performance of a biomarker in classifying patients is the receiver operating characteristic (ROC) curve. ROC curves are probability curves that map true positive rates (sensitivity) against false positive rates (1-specificity) at various threshold settings [226]. The calculation of the area under the curve (AUC), also known as concordance index (C-index), gives the information about the performance of a biomarker in dichotomising patients [226]. AUC values range from 0 to 1. The closer is the AUC to 1 the better the biomarker is in classifying patients, conversely an AUC of 0.5 is indicative of a random predictor. However, AUC evaluates the performance of a biomarker without specifying an optimal threshold, which is important to define for clinical applications. A threshold is considered optimal when able to classify most of individuals correctly. One of the most common approaches used to select an optimal threshold value is the Youden index method [227]. The Youden index calculates the difference between true positive and false positive rates over all possible threshold values. Therefore, the optimal biomarker threshold is the value that maximises sensitivity and specificity and therefore, the Youden index [227].

Even when a biomarker shows excellent performance, it may not be clinically useful if it does not improve the risk stratification of a population obtained with other clinical and biological predictors [210]. These other predictors could include characteristics relevant to a given disease such as age, sex, or other already identified biomarkers [210]. Thus, the use of a risk prediction model that combines several "classic" predictors is extremely important to determine the usefulness of the new biomarker studied [210]. For this purpose, two models are produced and compared, one containing the "classic" predictors (basal model) and another one with the same predictors plus the biomarker to test (basal model + biomarker) [210]. Multivariable regression models, such as multivariable logistic regression and multivariable cox proportional hazard, are methods used for the development of risk-prediction models [228]. Multivariable regression models allow examining several independent variables (e.g. age, gender, biomarker) and determining those that best predict a specific outcome (e.g. diseased or not diseased) [229]. This differs from univariate regression models where instead the relationship between one outcome and one predictor (independent variable) is calculated [229]. The results of logistic regression analyses are reported in odd ratios (ORs) with 95% of confidence intervals (95% CIs). The OR provides information on the risk that a given predictor is associated with the outcome, while the 95% CIs indicate the range in which the relative risk is present in 95% of cases [230]. Cox proportional hazard models are favoured when it is important to consider the time to event, for example the survival of a patient at a given time point [228]. In fact, cox proportional hazard evaluates the effect of one (univariate analysis) or more independent variables (multivariable analysis) upon the

time a certain outcome takes to happen [231]. The effect sizes of cox proportional hazard models are hazard ratios (HRs) with 95% CIs. The HRs can be defined as the hazard rates of an event happening at a specific time [231]. Therefore,  $HR > 1$  indicate a higher risk of death and contrarily an  $HR < 1$  indicate a lower risk.

Along with cox proportional hazard models another method often considered when performing survival analyses is the Kaplan-Meier survival curve. This method calculates the survival probability of patients at different time intervals [232, 233]. If the goal of survival analysis is to estimate the ability of a new biomarker to predict survival, the first thing to do is to identify a biomarker threshold. This can be done as described previously using the Youden index. Patients are then divided into two groups based on their biomarker level, whether it is below or above the threshold. Other two parameters required for the analysis are the time to event, also known as serial time, meaning the time from when the patient is enrolled in the study until the endpoint (for example the end of a clinical trial) and the status of the patients at the end of their serial time [232]. Therefore, survival curves are reported considering the number of patients who died in each time interval [232]. Finally, the statistical difference between the survival curves of the two groups is assessed using the log rank test [232, 234]. This is a nonparametric method used to test the null hypothesis that there is no difference between the populations of the two survival curves [234-236]. However, because the log rank is a test of significance, it cannot estimate the size of the difference between the groups like the cox regression models [237]. Furthermore, unlike cox regression models, Kaplan-Meier curves can take into account only one variable (i.e. biomarker evaluated) and therefore cannot estimate the covariate-adjusted survival, resulting in a limited clinical usability [232, 233]. Nevertheless, Kaplan-Meier curves are useful to provide information about the survival time of patients that present different levels of the biomarker evaluated [233].

Furthermore, the Akaike Information Criterion (AIC) is used to estimate the quality of a prediction model. Contrary to the previous methods, the AIC does not indicate the significance of a model, but it helps to determine which model among those being compared best fits the available data [238]. Indeed, the AIC tries to balance the fit of a model with its simplicity, by adding a penalty term for each variable included in the model [239]. This avoids the overfitting of complex models. Thus, the AIC value indicates the amount of information lost in a model; the less information is lost (lower AIC value) the better the model performs [239].

Another commonly used test to assess the prognostic or diagnostic value of a biomarker is the likelihood-ratio test (LRT). In fact, the LRT evaluates the goodness of fit between two models, for example, the baseline model and the model containing the biomarker tested [238]. If the more complex model (basal model + new biomarker) fit the dataset significantly better than the simpler model (basal model), it means that the tested biomarker adds a significant contribution to the model [210].

Like the LRT, the Wald test is another test of significance commonly used to estimate the performance of a new biomarker. However, unlike LRT, which requires at least two models, the Wald test can estimate the fit of a single model [240]. In fact, if the Wald test performed on the model containing the new biomarker is not significant ( $p\text{-value} > 0.05$ ), then the biomarker can be removed from the model without damaging the fit of the model. Conversely, if the Wald test is significant ( $p\text{-value} < 0.05$ ), it means that the new biomarker is an independent predictor of the outcome studied and therefore its inclusion in the model improves its fit [240].

Two further sound statistical methods for evaluating the usefulness of a new biomarker are the net reclassification index (NRI) and the integrated discrimination improvement (IDI) [241, 242]. Both these

measures have been proposed to assess the incremental value of a biomarker in reclassifying patients by comparing two models, one with and one without the new biomarker [241, 242].

The NRI uses reclassification tables and quantifies the biomarker improvement by using risk categories (patients with event and patients with no event) [241]. Therefore, a positive score is assigned to patients that are correctly reclassified in the new model (basal model + biomarker). On the contrary, patients incorrectly reclassified in the two risk category groups are negatively scored while no score is assigned to patients which remain in the same risk category. Subsequently, the scores in each risk category group are summed and divided by the number of patients per group. Finally, the sum of the two values obtained represent the NRI value.

Differently from NRI, the IDI uses the difference in discrimination slopes between the two models being compared to evaluate the biomarker performance [243]. A discrimination slope is considered as the difference in the mean of prediction probabilities for patients with events and the mean for the ones without event [241, 243]. Put in other words, the IDI value is the difference between the integrated differences of sensitivities and one minus specificities of the two models compared [241]. Thus, the IDI is defined as  $IDI = (IS_{new} - IS_{old}) - (IP_{new} - IP_{old})$ . In the equation, IS is the integrated of sensitivity and IP is the corresponding integrated of one minus specificity [242].

In conclusion, several methods should be considered when evaluating the performance and clinical applicability of a new biomarker in order to strengthen the validity of the obtained results (Figure 3).

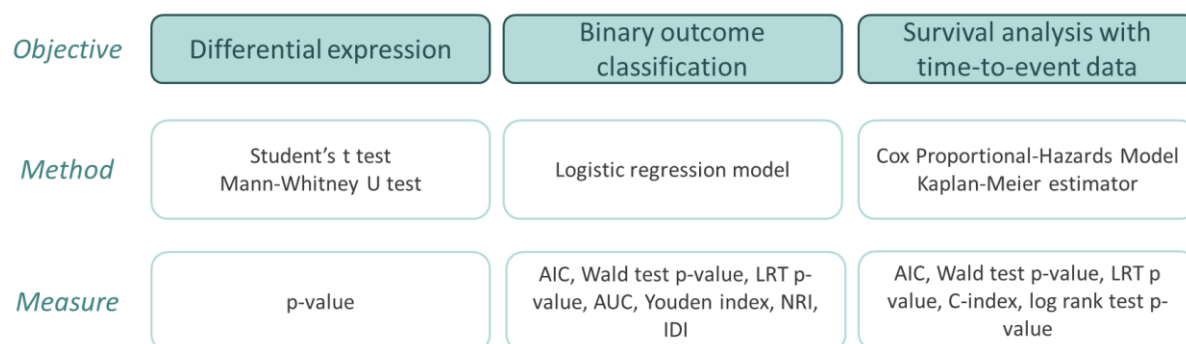


Figure 3. Schematic overview of some methods used to assess the biomarker potential of a molecule under study.

## 2.2 Biomarkers to prognosticate the outcome after cardiac arrest

As anticipated in chapter 1.4, the current European guidelines recommend the use of a multimodal approach in cardiac arrest prognostication, which includes the measurement of molecular biomarkers among the other tests described previously [9].

Several protein biomarkers have been identified in the bloodstream following a brain injury, as measures of the extent of damage [244]. Among them, neuron specific enolase (NSE) is the gold standard and the only biomarker recommended by the current clinical guidelines [9]. NSE is a specific enolase-isoenzyme found mainly in neurons and neuroendocrine cells that converts 2-phosphoglycerate to phosphoenolpyruvate [245, 246]. NSE has a biological half-life of 24 h, thus increasing levels of NSE after this time might suggest a continuous release of NSE in the blood meaning persistent neurological injury [247, 248]. Indeed, elevated serum levels of NSE are found in several malignancies and after traumatic or non-traumatic brain injury [249]. In the context of prognostication after cardiac arrest, a decrease in NSE is observed at 24 h after ROSC in patients with a good neurological outcome, and an increase in patients with a poor neurological outcome with a peak at 48-96 h [9, 49, 246, 250-252]. The increase in NSE values within 72 h after ROSC is a reliable predictor of poor outcome [9, 158, 253]. However, as there is still no consensus on the timing and threshold value to be used, it is recommended to perform several NSE measurements. From numerous studies, the threshold values predicting for poor outcome range from 33 to 120 µg/l when measured within 72 h after ROSC with specificity and sensitivity ranging from 75 to 100% and 7.8 to 83.6% respectively [9, 158, 246]. Alternatively, it has been proposed to use NSE ratios over the absolute values, to quantify the protein changes over time. Indeed, it has been reported that an increase > 1.0 of 48:24 hour and 72:24 hour NSE ratios correlates with poor neurological outcome [248]. In order to reduce the variability of NSE values it is also important to appropriately handle and store the samples. Indeed, NSE can also be found in erythrocytes and platelets [246, 254]. In case of haemolysis, higher levels of serum NSE can be found besides the presence of brain damage [246, 255]. Therefore, it is important to measure the degree of haemolysis prior to analyse the levels of NSE and discard samples with elevated haemolysis [9, 256]. Additionally, serial NSE measurements can also minimize the presence of these outliers [9]. However, it is exactly for these reasons that the guidelines recommend measuring NSE in combination with other tests when prognosticating the outcome of cardiac arrest patients [9].

Another biomarker widely studied is S100 calcium-binding protein B (S100B) [257-259]. S100B is an acidic Ca<sup>2+</sup> - binding protein mainly expressed by astroglial cells with a half-life of approximately 25 minutes [260]. Compared to NSE, S100B has a lower molecular weight, which allows it to cross the blood-brain barrier and be released in the bloodstream more rapidly [245]. As such, S100B has a higher sensitivity than NSE for detecting brain damage [245]. However, the usability of this protein as a prognostic biomarker after cardiac arrest is limited by its presence in other cells outside the brain tissue, such as muscle fibres, adipocytes, melanocytes and chondrocytes [261-265]. Therefore, S100B could detect other peripheral injuries other than brain damage [262]. For instance, after cardiac arrest, elevated serum levels of S100B could be due to skeletal injuries from chest compression and defibrillation or renal dysfunction from hypoperfusion [260-262]. Furthermore, it appears that S100B does not add value to the current prognostication models used [266]. Due to these reasons, S100B is not recommended in the current guidelines [9].

Among many newly studied biomarkers of brain injury such as tau protein [267, 268], glial fibrillary acidic protein (GFAP) [268-270], and ubiquitin C-terminal hydrolase-L1 (UCHL1) [269], the most promising is neurofilament light (NfL) [271-274]. NfL is a cytoskeletal neuron-specific protein and represents the major intermediate filament protein of neurons and axons [271, 275]. Elevated levels of NfL in the blood has been found in several chronic neuronal diseases as well as traumatic brain injury

[276-282]. Therefore, NfL is an established marker of brain damage. In the context of cardiac arrest, high levels of NfL have been found both in the cerebrospinal fluid [283] and in the bloodstream [272, 273, 284]. In the TTM-trial, high serum levels of NfL were shown to be stable from 24 to 72 h and presented high sensitivity for poor neurological outcome [272]. When compared to NSE and S100B, NfL was the most performant predictor at 24 h, 48 h and 72 h [272]. Other studies have confirmed NfL as a reliable predictor of neurological outcome after cardiac arrest and its superiority to NSE [244, 273, 284, 285] which might be due, in part, to the fact that NfL is less sensitive than NSE to haemolysis [272]. Further studies are required to confirm the accuracy of NfL as well as to establish an international threshold value to use for long-term prognostication after cardiac arrest. However, the higher performance observed in different studies compared to NSE and S100B could allow the addition of NfL to the current multimodal approaches [285].

Additionally to brain injury biomarkers, biomarkers of other pathologies including cardiac injury (e.g. troponin T, N-terminal pro-B-type natriuretic peptide and copeptin) [286-289] and systemic inflammation (e.g. procalcitonin and interleukin-6) [290, 291] are associated with neurological outcome, however they show limited accuracy [17, 244].

Although many of the aforementioned biomarkers have prognostic potential, NSE is the only one recommended by guidelines and with a long history of use in clinical practice [9, 17, 18]. Moreover, all the prognostic biomarkers mentioned have protein origins. However, as discussed at the beginning of chapter 2 the omics era and particularly the development of high-throughput technologies have allowed the identification of other molecules, such as RNAs, able to serve as biomarkers in the discovery and prognostication of diseases. Before delving into the role of RNAs in cardiovascular diseases and their biomarker potential in chapter 4, an adequate introduction on transcriptome is required and will be presented in the next chapter.

### 3. Transcriptome

The term transcriptome refers to the complete set of RNA molecules encoded by the genome in a specific cell or tissue.

The central dogma of molecular biology formulated in 1958 by Francis Crick explains the flow of genetic information, from DNA to RNA, to obtain a functional product, a protein [292] (Figure 4). This suggested that the primary role of the RNA was to transfer the genetic information from DNA to protein. Consequently, these RNA molecules took the name of messenger RNAs (mRNA). However, after 65 years following the formulation of the central dogma of molecular biology, it became clear that RNAs can also have regulatory functions within the cell without necessarily being translated into proteins. Therefore, RNA molecules can mainly be categorised into protein coding RNAs (mRNAs) and non-protein coding RNAs (ncRNAs).

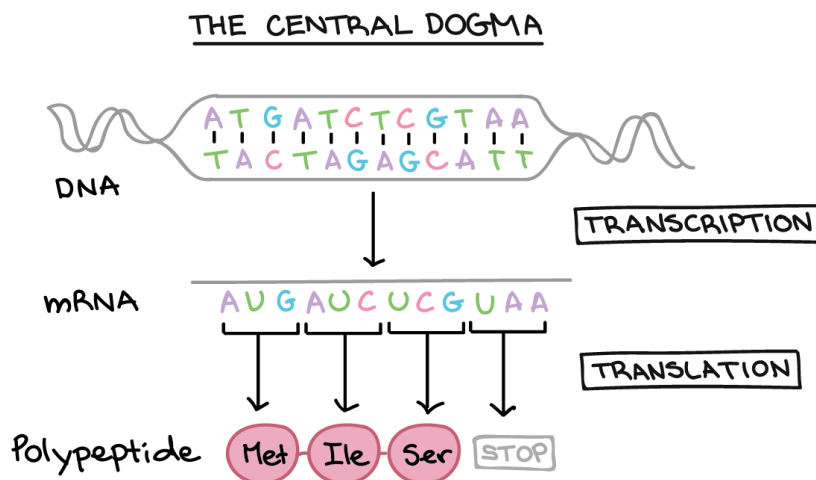


Figure 4. Central dogma of molecular biology. Image taken from: <https://www.khanacademy.org/science/ap-biology/gene-expression-and-regulation/translation/a/intro-to-gene-expression-central-dogma>.

Multicellular organisms have the same genetic information in every cell. However, the transcriptomic profile differs from cell types and tissues. Furthermore, the transcriptome can change during the different stages of cell differentiation [293, 294] and due to external environmental conditions [295]. Alternative splicing and RNA editing among other events allow more than one variant of RNA to be produced from the same gene [294, 296]. Thus, transcriptome analyses can reveal genes that are actively expressed at a given time and in a specific cellular state, as well as changes in gene expression that may reflect or contribute to disease. Therefore, by studying the transcriptome, researchers can capture what is happening inside a specific cell, giving a level of understanding that the genome alone cannot provide.

In the human genome, less than 3% of the entire transcriptome is composed of mRNAs and more than 80% of ncRNAs [297-299]. Although the distinction of these two types of RNA seems simple enough, it is actually much more complex than previously thought as recent discoveries have shown that many RNA molecules can have regulatory functions as ncRNAs or function as mRNAs and thus encode proteins [300].

### 3.1 Coding RNAs (mRNAs)

An mRNA is a single-stranded RNA molecule that carries genetic information to be translated into a protein. The molecular process that turns DNA into RNA is called transcription and takes place in the cell nucleus. When mRNAs are transcribed, they leave the nucleus and enter the cytoplasm where they are used as templates for protein synthesis, in a process called translation.

RNA polymerase II (Pol II) is the enzyme that synthesises a strand of RNA using DNA as template. Pol II catalyse the addition of nucleotides in 5' to 3' direction of the growing sequence of mRNA [301]. However, in order to initiate the transcription process Pol II needs to recognise the promoter region of the gene transcribed, located prior the gene. Proteins called transcription factors mediate the recognition and binding of Pol II. Transcription factors regulate gene expression by either enhancing or repressing the binding of Pol II on the promoter of the gene.

The termination of the transcription generates a primary transcript mRNA (pre-mRNA) which needs to be further processed before being translocated in the cytoplasm and translated into a protein [301]. To increase their stability, the pre-mRNA molecules are capped and polyadenylated. The addition of a 5' cap (a modified guanine nucleotide) occurs co-transcriptionally and is mediated by the capping enzyme complex. Instead, the polyadenylation process consists of the cleavage of the pre-mRNA at the poly(A) site and addition of 100-200 adenosine residues at the 3'-end of the transcript. Furthermore, the pre-mRNA is made of coding sections, called exons, and non-coding sections, introns. The formation of mature mRNAs occurs when the introns are removed and the exons joined together, in a process called splicing. Alternative splicing can also occur and lead to the production of a different mature mRNA originating from the same pre-mRNA.

The mature mRNA is then ready to leave the nucleus and reach the cytoplasm where translation can begin. Proteins are made of amino acids. The nucleotides of mRNA are read in triplets called codons, and each codon corresponds to a specific amino acid (genetic code).

Translation requires the action of ncRNAs, such as ribosomal RNAs (rRNAs) and transfer RNAs (tRNAs) (Figure 5) [301]. Indeed, protein synthesis takes place inside ribosomes, which are complex molecules made up of rRNAs and proteins. tRNAs are instead used to recognise a specific codon and attach the matching amino acid to the growing peptide (Figure 5).

Translation termination occurs when a ribosome reaches the stop codon and then releases the protein.



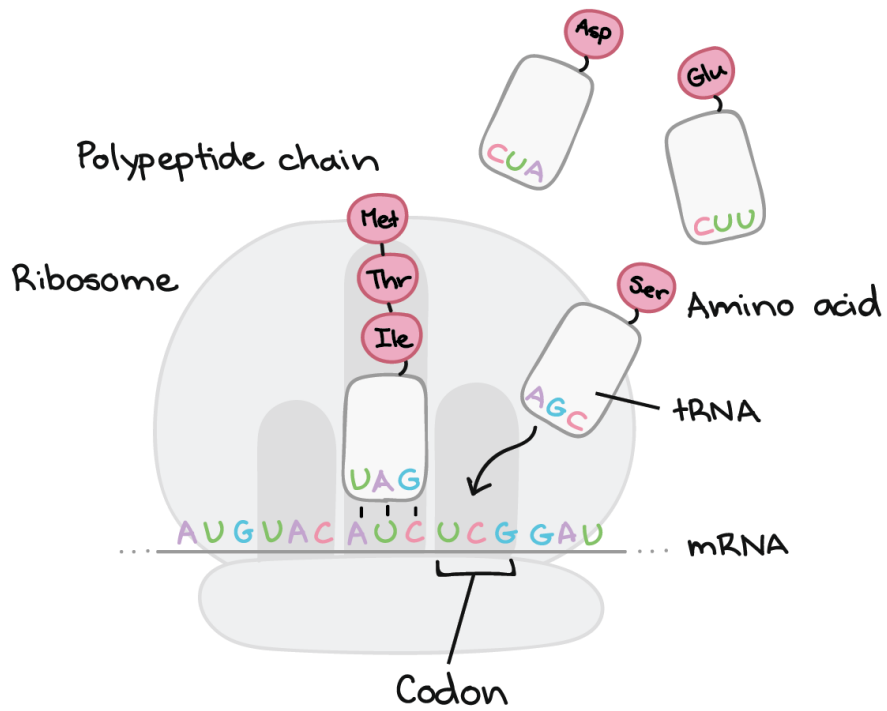


Figure 5. Translation machinery. Image taken from: <https://www.khanacademy.org/science/ap-biology/gene-expression-and-regulation/translation/a/intro-to-gene-expression-central-dogma>.

### 3.2 Non-coding RNAs

NcRNAs are a vast heterogeneous class of untranslated RNAs with key regulatory functions [22, 23]. They can interact with DNA, other RNAs and RNA-binding proteins (RBPs) and therefore can be versatile as proteins in the functions they execute [27]. Therefore, ncRNAs are involved in most of the cellular processes and they can mainly be classified into housekeeping ncRNAs and regulatory ncRNAs [24, 27] (Figure 6).

The housekeeping ncRNAs are ubiquitously expressed in cells and are essential for cell viability. Other than the aforementioned rRNAs and tRNAs, small nuclear (snRNAs) and nucleolar RNAs (snoRNAs) also belong to this category of ncRNAs (Figure 6). These RNAs play fundamental roles mainly in mRNA modification and splicing as well as protein synthesis [24].

Regulatory ncRNAs are direct or indirect regulators of gene expression at epigenetic, transcriptional and post-transcriptional levels with precise temporal and spatial patterns of expression [24-27]. Regulatory ncRNAs can be further classified based on their length into small ncRNAs and long ncRNAs [28] (Figure 6).

Small ncRNAs are ncRNA molecules with < 200 nucleotides (nt). The most widely studied small ncRNAs are microRNAs (miRNAs) which will be discussed in the following section. Other small ncRNAs include small interfering RNAs (siRNAs) and piwi-interacting RNAs (piRNAs). All these classes of small ncRNAs are mainly involved in gene silencing, however they differ for biogenesis, mechanism of action and the pathways they regulate [302, 303].

The second category of regulatory ncRNAs is represented by long ncRNAs with transcripts longer than 200 nt. Long ncRNAs can be further divided into subgroups according to their loci of origin. Furthermore, circular RNAs (circRNAs) are also classified as long ncRNAs. This heterogeneous class of long ncRNAs plays diverse roles in biological processes which will be further discussed in chapter 3.2.2 and 3.2.3.

For the purpose of this thesis work, separate chapters are dedicated to the biogenesis and function of each subtype of ncRNAs.

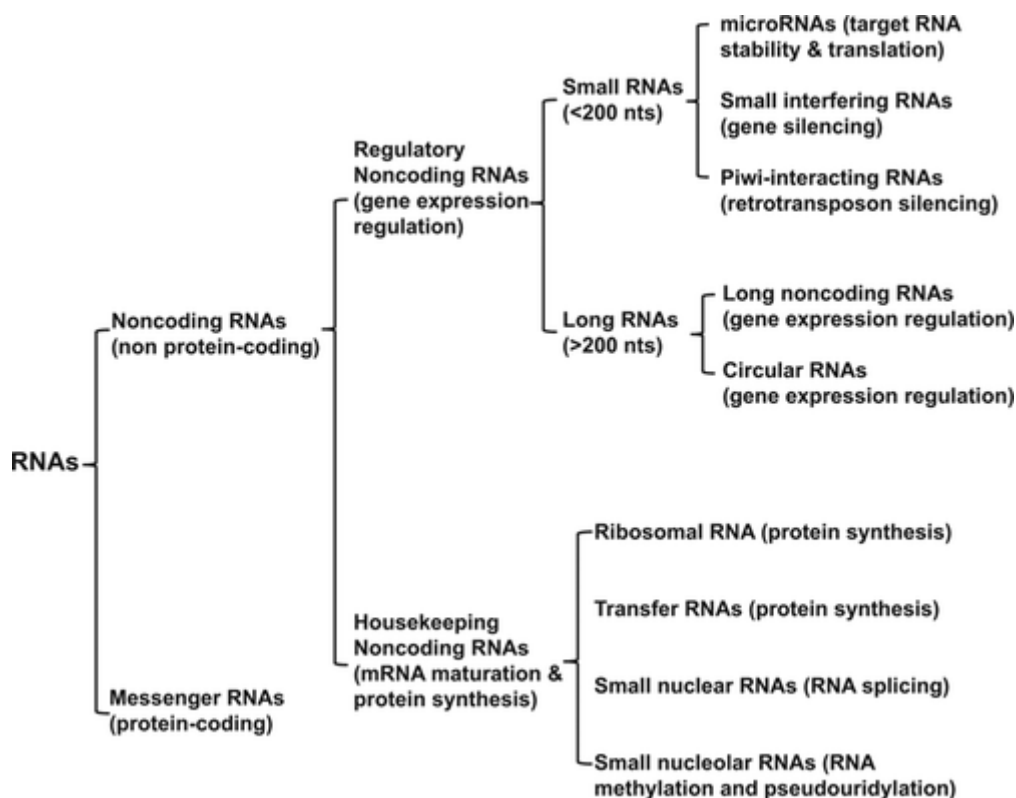


Figure 6. Classification of RNA molecules. Image taken from [27].

### 3.2.1 MiRNAs

MiRNAs are short (approximately 18-22 nt) single-stranded ncRNAs playing crucial roles in the post-transcriptional regulation of mRNAs [304]. Indeed, miRNAs bind to the 3' untranslated region (UTR) of the target mRNA inducing the cleavage of the mRNA or its translational repression [305]. In addition to their conventional role in mRNA silencing, evidence has shown that miRNAs can also influence the biogenesis and function of other RNA molecules in the nucleus [306, 307] or recruit ribonucleoprotein complexes to promote the translation of target mRNAs [308].

Several hundreds of miRNAs have been discovered in nearly all organisms, from viruses to animals [309, 310] (<http://www.mirbase.org/>), indicating the importance of their regulatory functions. Furthermore, closely related organisms present highly conserved miRNAs and target sites of miRNAs, indicating that similar processes are most likely regulated by the same conserved miRNAs [311, 312]. Although many miRNAs are highly conserved among organisms, many other new miRNAs can arise in single species contributing to development, phenotypic diversification and speciation processes [313-315]. Moreover, the number of miRNAs, their expression and target mRNAs seem to be highly correlated with the organismal complexity [312]. Therefore, the complexity of an organism can be estimated by the complexity of its miRNA network [312].

Genes encoding for miRNAs can be found in intragenic and intergenic regions throughout the genome and many of them are localised within clusters [313, 316]. The same or similar transcription factors usually regulate miRNAs belonging to the same cluster [317]. Additionally, clustered miRNAs appear to participate in common molecular pathways by targeting functional related genes [318-320].

MiRNA biogenesis is a multistep process that leads to the production of a functional RNA. The canonical pathway will be summarized below; however, it should be kept in mind that other non-canonical

pathways can lead to the generation of miRNAs [304]. Pol II transcribes the majority of miRNAs, while a minor group depends on the polymerase pol III [321, 322]. MiRNAs are transcribed into primary miRNAs (pri-miRNAs), precursors that similarly to mRNAs present 5' capping and 3' polyadenylation and have a typical stem-loop structure [305] (Figure 7). A nuclear complex, called microprocessor, mediates the first cleavage of the pri-miRNAs by the RNA endonuclease Drosha [323, 324]. This cleavage generates second precursors called pre-miRNAs. The pre-miRNAs then translocate in the cytoplasm, where a second RNA endonuclease, Dicer, cleaves the pre-miRNAs close to the terminal loop, producing RNA duplexes of about 22 nt [325]. These duplexes are then loaded into the Argonaute proteins assembling the miRNA-induced silencing complex (miRISC) [304, 326]. One strand of the duplex is degraded (passenger strand) while the other is retained in the complex (guide strand) and represent the mature functional miRNA [304, 327].

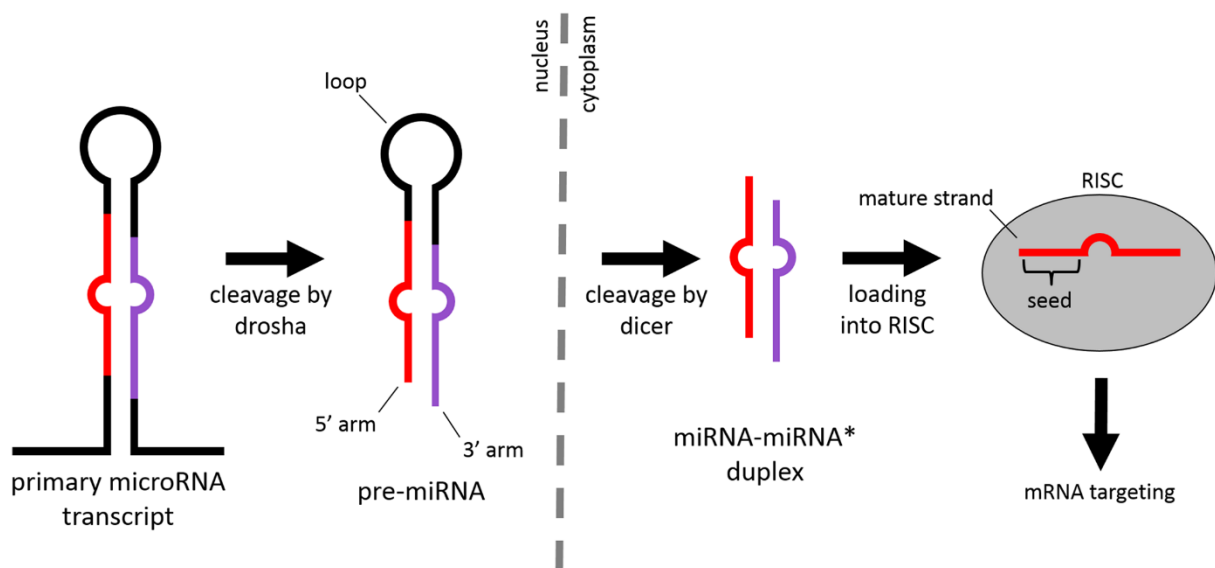


Figure 7. Canonical pathway of miRNA biogenesis. Image taken from: <https://doi.org/10.1371/journal.pone.0176596>.

### 3.2.2 lncRNAs

As mentioned above, lncRNAs are considered non-coding transcripts with a length greater than 200 nt. However, this broad description includes a large and heterogeneous group of transcripts that differ in biogenesis, genomic origin and function. Furthermore, recent discoveries also reported that some lncRNAs present open reading frames (ORFs) and therefore have protein coding potential [328-330]. However, the ability to generate small peptides does not exclude them from being also functional transcripts. Indeed, growing evidence reported that some transcripts can work both as protein templates and as lncRNAs, leading to a novel class known as bifunctional transcripts [300, 329, 331, 332].

Unlike miRNAs, lncRNAs exhibit high sequence variability between species [333-335]. However, several lncRNAs present evolutionarily conserved promoters, genomic positions and/or secondary structures indicating that, despite the large sequence divergence, they might preserve related functions [336-339].

One way to classify lncRNAs concerns their genomic origin [340]. Thus, lncRNAs can be categorised as (Figure 8):

- a. *Intergenic*: located between two protein-coding genes.

- b. *Intronic*: located inside an intron or a protein-coding gene.
- c. *Bidirectional*: located in the promoter region of a protein-coding gene but transcribed in the opposite direction.
- d. *Enhancer*: located in enhancer regions.
- e. *Sense*: transcribed in the sense strand of the protein-coding gene.
- f. *Antisense*: transcribed in the antisense strand of the protein-coding gene.

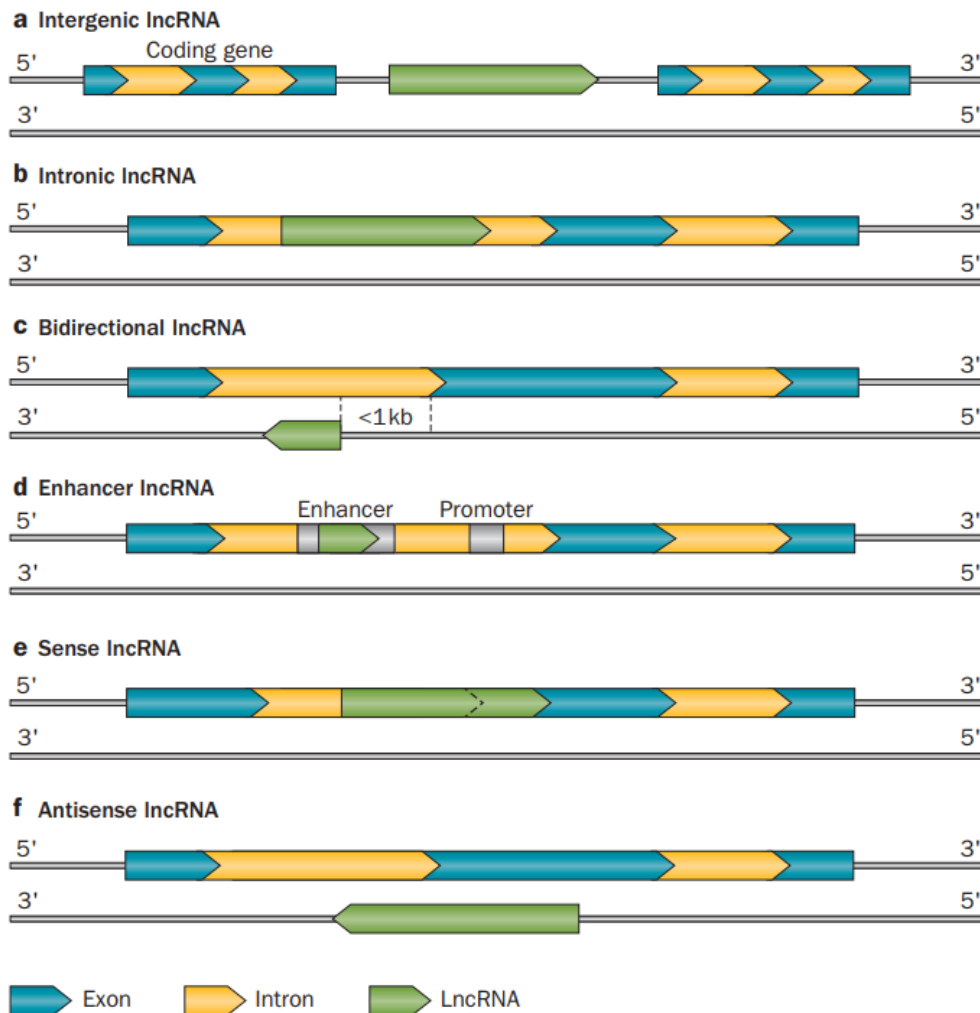


Figure 8. Classification lncRNAs according to their genomic origin. Image taken from [50].

lncRNAs present low expression patterns compared to protein-coding genes and have a high degree of tissue- and time- specificity [51-53]. They appear to play fundamental regulatory roles in almost every cellular process therefore their dysregulation is often related with some kind of disease [341-343].

Similar to miRNAs and mRNAs, lncRNAs are mainly transcribed by Pol II enzymes and undergo post-transcriptional processing and RNA editing, with capping, polyadenylation and splicing events [22, 51, 53]. Indeed, more than 98% of lncRNAs appear to be spliced and approximately 25% are alternatively spliced [53].

After biogenesis and processing, some lncRNAs translocate in the cytoplasm while others are retained in the nucleus [53]. Among the numerous lncRNAs detected in the human genome, only a small number have been characterised. This is mainly due to the fact that they can regulate gene expression

at different levels and through complex molecular mechanisms. Additionally, their low conservation among species makes it difficult to have appropriate cellular and animal models in order to investigate their functions [22].

Among the lncRNAs already characterised, the following four main functions have been identified (25855606) (Figure 9):

- Signal:** lncRNAs can regulate gene expression in response to specific stimuli.
- Decoy:** lncRNAs can bind regulatory factors or miRNAs preventing the binding to their targets and therefore altering their function.
- Guide:** lncRNAs can be required to localise specific proteins.
- Scaffold:** lncRNAs can assume a structural role by working as a platform to bring different proteins together.
- Enhancer:** lncRNAs can promote the interaction between enhancer and promoter regions of specific genes modulating their expression.

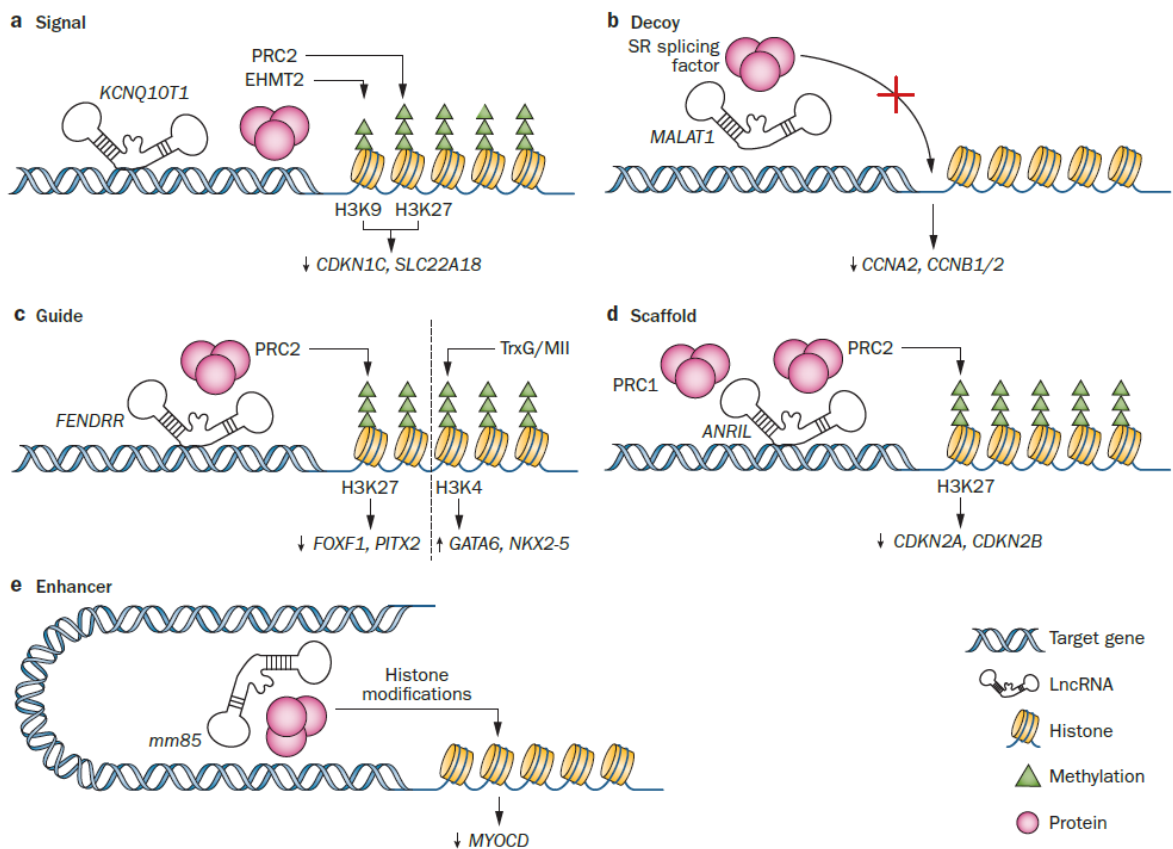


Figure 9. Functions of lncRNAs. Image taken from [50].

The majority of lncRNAs are multifunctional and can modulate the gene expression through different mechanisms of actions [50]. Nevertheless, the function of many lncRNAs is still unclear. Thus, deeper research on lncRNAs might bring the discovery of novel functions and improve the classification of this heterogeneous class of ncRNAs.

### 3.2.3 CircRNAs

CircRNAs represent the most novel subclass of lncRNAs. They are covalently closed single-stranded RNA molecules that play different roles in the regulation of gene expression [54, 344, 345]. They appear to be evolutionarily conserved and present tissue- and time- specific expression profiles [39, 54].

CircRNAs can arise from exons and introns and therefore can be classified as exonic, intronic or exonic-intronic circRNAs. They are produced by an alternative splicing event of pre-mRNAs called backsplicing in which the 3' and 5' ends join together producing a covalently closed RNA. Although backsplicing is usually less efficient than linear splicing [346], several mechanisms can promote the circularization and thus the production of circRNAs. Indeed, during circRNA biogenesis, a splice donor site (located downstream) is brought in close proximity to the splice acceptor site (located upstream) by base pairing of repeated inverted elements located in the flanking introns or by dimerization of RBPs [344, 347, 348] (Figure 10). Alternatively, circRNAs can be produced by lariat-driven circularization. Indeed, during exon skipping, a lariat containing the skipped exons is released. This lariat can escape degradation by de-branching enzymes and circularise generating an exonic circRNA or an exonic-intronic circRNA if the introns are removed or retained respectively [40, 349, 350].

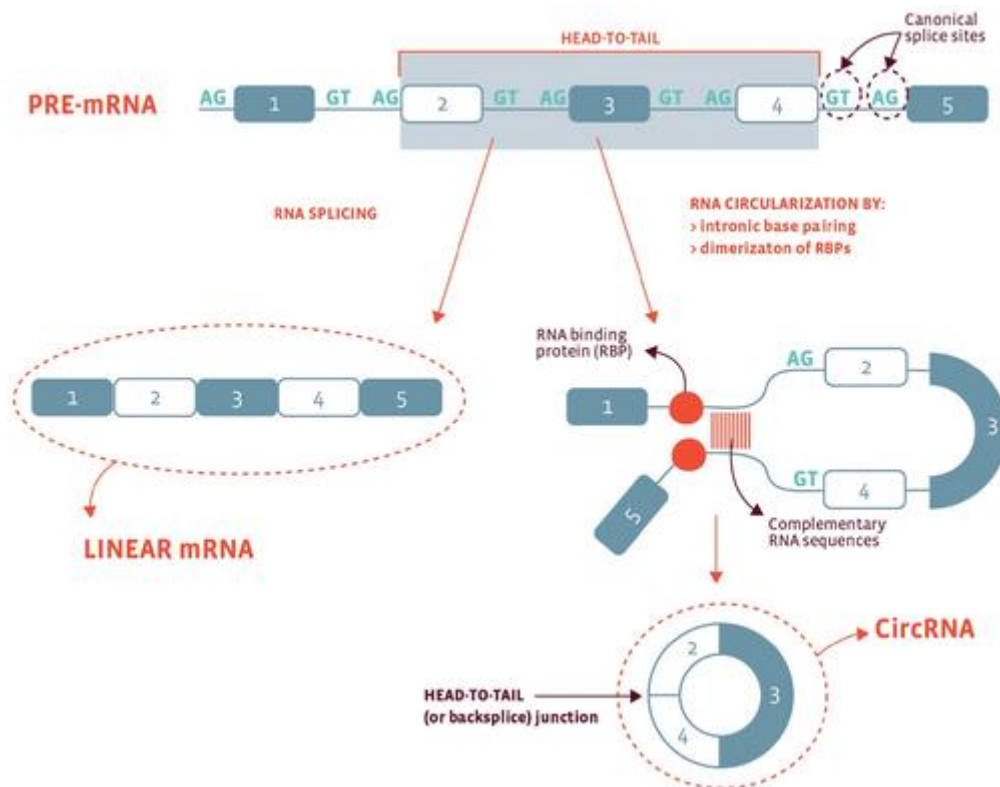


Figure 10. CircRNAs biogenesis. Image taken from [41].

Due to the lack of free ends, circRNAs are resistant to exonuclease digestion and therefore more stable than linear RNAs [38-40]. Indeed, the average half-life of circRNAs can be up to 48 h [38, 40] in contrast to their linear counterparts, which average is of 4-9h [351]. The mechanisms by which circRNAs are degraded are still largely unknown. Endoribonucleases appear to be the only enzymes able to degrade circRNAs. Indeed, it has been showed that the endonuclease RNase L is able to globally degrade circRNAs [352]. Furthermore, N6-methyladenosine (m6A) methylation appear to be the main mediator of circRNAs turnover by promoting their cleavage via RNase-P-multidrug associated protein complex [353].

After their biogenesis, circRNAs may remain in the nucleus or move to the cytoplasm to exert their regulatory functions (Figure 11). Increasing research has been dedicated to this class of ncRNAs for their unique structures and association to several pathological conditions [41, 354-358]. For instance, circRNAs appear to play important roles during cancer initiation and development and are therefore considered to be useful diagnostic biomarkers [359].

However, to date the biological functions of circRNAs are not fully identified. Many circRNAs contain miRNA binding sites, which allow them to sponge miRNAs and prevent them from binding the 3' UTR of the target mRNAs (figure 11.a). Thereby, circRNAs act as competing endogenous RNAs (ceRNAs) and indirectly regulate protein translation [360, 361]. However, to effectively sponge miRNAs, circRNAs need to present multiple miRNA sponging sites. For instance, it is well known that the circRNA, cerebellar degeneration-related protein 1 antisense (CDR1as), is an efficient inhibitor of miR-7 presenting more than 70 binding sites for this miRNA [362]. Growing evidence shows that CDR1as promotes tumour proliferation in several cancer types and therefore represents a potential target for cancer therapy [362]. The CDR1as/miR-7 axis was also detected in cardiomyocytes. It seems that overexpression of CDR1as may aggravate MI injury by increasing the infarcted area and that instead overexpression of miR-7 induces cardiomyocyte protection [363, 364]. Therefore, CDR1as could also be considered in the development of new therapeutic strategies to treat MI [363].

Other circRNAs contain protein-binding sites instead of miRNA binding sites and can therefore act as protein scaffolds to regulate their parental gene function or as protein sponges by sequestering and inhibiting their biological function [54, 361] (figure 11.b). CircFOXO3 can, for example, promote cardiac senescence by interacting with anti-senescence proteins such as Inhibitor of DNA binding 1 (ID1) and E2F transcription factor 1 (E2F1) and anti-stress proteins such as Hypoxia inducible factor 1 subunit alpha (HIF1a) and focal adhesion kinase (FAK), thereby preventing them from translocating into the nucleus and performing their functions [365]. However, when circFOXO3 is silenced, cellular senescence and apoptosis are reduced [365]. Furthermore, circFOXO3 can play a tumour suppressor role by binding proteins such as cyclin dependent kinase 2 (CDK2) and CDK-interacting protein 1 (p21), thereby blocking cell cycle progression in cancer [366]. It is therefore clear that circFOXO3 targets multiple proteins in different diseases. In addition, circFOXO3 can sponge several miRNAs [367] and is therefore a good representative of the complexity of action of many circRNAs.

Alternatively, circRNAs can regulate the transcription of their parental genes at multiple levels, through specific RNA-protein, RNA-DNA or RNA-RNA interactions. Indeed, some circRNAs, such as circEIF3J and circPAIP2, have been shown to promote transcription of their parental genes by retaining the small nuclear ribonucleoprotein U1 (snRNP) and further binding the Pol II transcription complex at the level of the parental gene promoter [368] (Figure 11.c). Other circRNAs can induce DNA hypomethylation at the promoter or regulate the intronic enhancer and thus activate transcription of the parental gene [369]. Other circRNAs inhibit the activation of their parental genes, such as circHuR which can bind the transcription factor CCHC-type zinc finger nucleic acid binding protein (CNBP) and thereby repress CNBP binding to the human antigen R (HuR) promoter [370].

Finally, although circRNAs are classified as ncRNAs, recent reports have demonstrated that some circRNAs present ORFs and could therefore be translated into small proteins through cap-independent mechanisms [329] (figure 11.d). It has been shown that the presence of internal ribosome entry site (IRES) elements as well as short sequences presenting m6A methylation modifications can efficiently induce circRNAs internal translation initiation [371, 372]. One of the first protein-coding circRNAs identified in eukaryotes is Myocardial Infarction-associated Circular RnA (MICRA), also known as circZNF609. MICRA has an ORF of 753 nt, shares the same start codon with the linear transcript and



terminates with an in-frame stop codon that is generated after circularization [373]. So far, however, the molecular roles played by MICRA-derived proteins remain largely unknown [373].

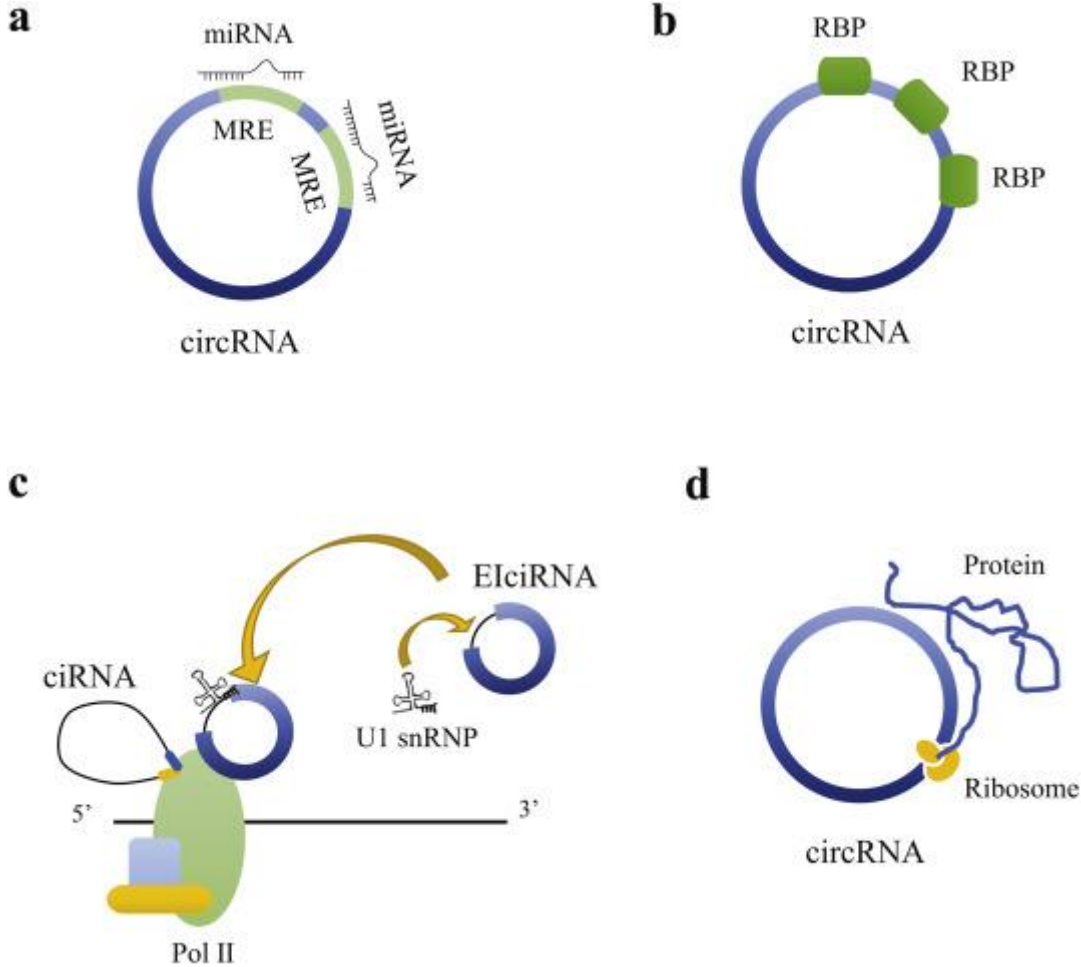


Figure 11. Functions of circRNAs. Image taken from [70].

### 3.3 Blood transcriptome

Body fluids, such as blood, saliva and urine, represent a circulating network developed by multicellular organisms to transport nutrients, remove waste and transmit signals to different cells and organs within an organism. Among the various body fluids, blood is the primary conduit for the transmission of signals throughout the body and is easily accessible [29]. Thus, blood contains useful information on an individual's physiological or pathological state and as such, blood analyses have the potential to identify biomarkers and therefore provide a better understanding on the development, progression or treatment of a given disease [29]. Therefore, a wide range of biomolecules including RNAs, are present in the blood for different purposes [30-32]. RNA molecules can be found freely circulating in the blood or confined in blood cells – both of which constitute useful biomarker resources [33].

#### 3.3.1 Circulating RNAs

The term circulating RNAs refers mainly to mRNAs and ncRNAs released from cells and freely circulating in body fluids. Although RNAs are considered unstable molecules, subjected to degradation by RNases activity, many highly stable RNAs have been found in the circulation [30, 31]. Indeed, circulating RNAs can be secreted by vesicle-dependent or vesicle-independent mechanisms that protect them from degradation [374].

Extracellular vesicles (EVs) are the most well studied way of communication between cells. Exosomes and microvesicles are some types of EVs that transport signalling biomolecules to distant recipient cells [375]. EVs contain large numbers of mRNAs and ncRNAs [31, 376]. Interestingly, the RNA profiles in the EVs can differ from their cells of origin, suggesting that the loading of RNA molecules into EVs is a selective sorting mechanism [30, 31, 377].

Alternatively, RNAs can be secreted from the cells in a vesicle-independent manner. Indeed, more than 90% of circulating miRNAs have been found associated with proteins outside of EVs [377]. Different RNA-protein complexes can be detected in body fluids. Among them Argonaute 2 [378, 379], Nucleophosmin 1 [380] and High-Density Lipoproteins [381, 382] have been shown to carry and protect miRNAs in extracellular compartments. Although the mechanisms by which these proteins interact and transport circulating miRNAs are still unclear, it appears that miRNA export is an active and energy-dependent process [380]. Furthermore, other RBPs forming similar complexes with miRNAs and other types of RNAs in the circulation may exist and need to be uncovered.

Although the study of circulating RNAs is attracting greater interest from the scientific community, many open questions remain. One of the most important gaps in our knowledge is the biological functions of circulating RNAs. The presence of several and selective sorting mechanisms suggest that some circulating RNAs might function as hormone-like molecules and play a role in cell-to-cell communication systems [383]. Indeed, there is evidence demonstrating that circulating RNAs can reach neighbouring or distant cellular compartments and modulate the activity of the recipient cells [375, 384-386]. However, circulating RNAs could also be passively released into the bloodstream during cell death and thus have no, or very little, biological function [387, 388]. For instance, proteins like cardiac troponins and creatine kinase are progressively released in circulation from damaged cardiomyocytes after acute MI [389]. Therefore, it could be hypothesised that similarly to these proteins, RNAs are also released in the bloodstream from injured organs in pathological conditions [390].

Despite their biological function, the strong correlation of circulating RNA expression patterns and disease status make these molecules valuable biomarkers for diagnosis, risk-stratification and

prognosis in several pathological conditions [22, 30, 374, 375]. Circulating ncRNAs are considered ideal biomarkers in cardiovascular disease for several reasons: 1) they are stable in body fluids and relatively easy to measure with high sensitivity, 2) they can be amplified, 3) they perform key regulatory functions and are dysregulated in disease conditions and 4) some of them have cellular and tissue-specific expression patterns and can therefore mark specific pathologies [30, 377].

In addition, it is important to bear in mind that the information derived from plasma or serum collection differs considerably from that of whole blood, as the former mainly reflects the portion of freely circulating RNA, while the latter is indicative of the intracellular RNA present in blood cells [391]. Therefore, the collection of different types of blood samples reflects the type of biomarker being sought in a specific disease.

### 3.3.2 RNAs in blood cells

Although the majority of the studies focus on circulating RNAs for the identification of new biomarkers, RNAs confined in blood cells also constitute a prime biomarker reservoir [33]. Indeed, in the context of cardiovascular disease, changes in the blood cells transcriptome might provide crucial information on the disease status and progression [33]. Inflammation plays a major role after an acute cardiac event, such as MI [392]. Indeed, if not properly regulated, inflammation can contribute to cardiac injury with mobilization and activation of leukocytes [393].

Emerging evidence shows that altered expression of ncRNAs in various blood components is frequently associated with uncontrolled inflammation [59-63]. Indeed, pro-inflammatory and anti-inflammatory ncRNAs have been shown to act in coordination to fine tune the inflammatory response (Figure 12). Furthermore, it is well recognised that the role of ncRNAs is essential in both innate and adaptive immune responses [394, 395]. For instance, miR-155 is induced in monocytes/macrophages stimulated with TLR/IFN $\gamma$  and drives their inflammatory response by repressing negative regulators of innate cell activation therefore maximising the inflammatory response [396-398]. Moreover, miR-155 appear to be a key player during B-cells proliferation and T cells differentiation [398-401], suggesting that miR-155 might be a suitable therapeutic target for the treatment of inflammatory and autoimmune disorders [401].

Similarly to miRNAs also lncRNAs participate in the regulation of the inflammatory signalling and their functional importance in the innate and adaptive immune response is starting to be recognised [402, 403]. Indeed, many lncRNAs, such as lincRNA-Cox2 and linc1992, have been shown to interact with heterogeneous nuclear ribonucleoproteins (hnRNPs) to activate or repress distinct classes of immune genes [404, 405]. However, lncRNAs regulate the inflammatory response in many other ways at both the transcriptional and post-transcriptional levels [403, 406, 407].

Even though much less is known about circRNAs, increasing evidence has illustrated the importance of circRNAs in immune-cell development, immune response and inflammatory response [408]. Indeed, due to their resistance to exonucleases it is hypothesized that circRNAs are responsible in the long-term regulation of gene and protein expression [407]. However, very little is known about their molecular mechanisms in immunological context. Therefore, further studies focusing on their biological functions might offer greater insight about their use as biomarkers in immune and inflammatory conditions [408].

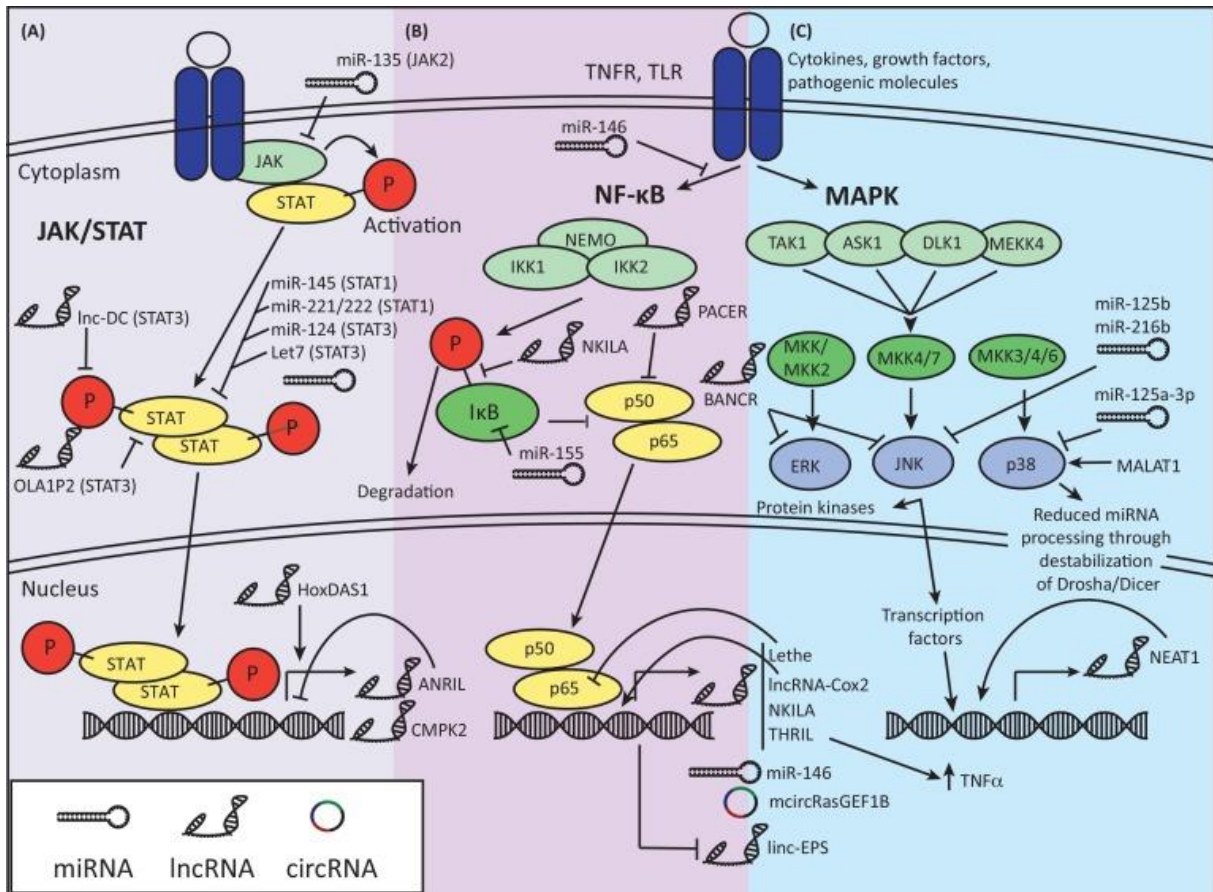


Figure 12. NcRNAs in inflammatory signalling response. Image taken from [407].

Lastly, it is necessary to note that transcriptional analyses of blood samples require the presence of stabilisers to prevent RNA from being degraded. In this context, the development of methods for collection and storage of whole blood samples, such as the PAXgene™ Blood RNA System, have made it possible to limit the degradation of intracellular RNA and thus also improve the reproducibility of the following transcriptional analyses [29, 33, 409, 410].

#### 4. NcRNAs after cardiac arrest

The essential regulatory role played by ncRNAs in cardiovascular disease is gaining recognition [411-414]. Indeed, numerous studies have already investigated the involvement of miRNAs, lncRNAs and circRNAs in cardiovascular physiology and pathology [34, 41, 357, 358, 414-419]. Furthermore, the biomarker potential of several ncRNAs in the blood have been identified in various cardiovascular conditions such as MI, heart failure and atrial fibrillation [34, 35] (Figure 13).

The most widely studied group of circulating ncRNAs in cardiovascular diseases are miRNAs [416, 417, 420, 421], although recently an increasing interest has been directed towards other regulatory ncRNAs such as lncRNAs and circRNAs [34].

In the context of cardiac arrest, a review article was published in 2018 in the journal *Non-Coding RNA* reporting on the current knowledge on the biomarker potential of ncRNAs in cardiac arrest and related diseases (Appendix I; [17]).

Among miRNAs, miR-21, miR-122-5p and miR-124-3p showed promising results in plasma human samples. Indeed, a small proof of concept study of 28 cardiac arrest patients, found miR-122-5p and miR-21 to be associated with poor neurological outcome and survival at 6-month follow-up [36]. In another separated small-scale study including 65 cardiac arrest patients, miR-124-3p a brain-enriched miRNA, was found to be upregulated in patients with poor neurological outcome [422]. These promising results allowed further validation of the biomarker potential of these candidates in larger patient cohorts. Indeed, in almost 600 patients from the TTM-trial the neurological outcome and survival prediction potential of miR-124-3p was confirmed [37]. Furthermore, the addition of miR-122-5p in a clinical model including miR-124-3p improved the outcome prediction of TTM patients [423]. This reinforced the concept that a miRNA panel reflecting different pathophysiological conditions can provide added values to the outcome prognostication of patients with a given disease. This has already been demonstrated in the outcome prediction of patients who have had MI and appears to be true in the context of cardiac arrest [423].

Dysregulation of lncRNA expression profiles has also already been reported in cardiovascular diseases such as ischemic heart failure [22, 34, 50, 55]. For example, patients with chronic heart failure showed higher levels of the mitochondrial lncRNA, LIPCAR, in plasma samples and elevated LIPCAR levels are associated with a higher risk of cardiovascular death [424, 425]. Furthermore, alteration of lncRNA expression profiles seems to be associated with outcome after MI [426]. Considering that cardiac arrest often occurs as a consequence of MI, it could be hypothesized that dysregulation of lncRNA profiles may also be associated with outcome after cardiac arrest [17]. Moreover, lncRNA profiles appear to be markedly altered in brain-related diseases [427-430]. Indeed, lncRNA profiles from a rat model with cardiac arrest reported 58 dysregulated brain lncRNAs after cardiac arrest [431]. Furthermore, models of traumatic brain injury in mice and rats demonstrated that several lncRNAs, including the well-known nuclear enriched abundant transcript 1 (NEAT1) and metastasis-associated lung adenocarcinoma transcript 1 (Malat1), could potentially be involved in the process of brain injury [432, 433]. However, the biomarker potential of lncRNAs in cardiac arrest patients has still to be clarified. Therefore, it is necessary to conduct further studies on human samples and elucidate the roles of these lncRNAs to evaluate their potential contribution in therapeutics development for prevention of neuronal death caused by cardiac arrest [17, 431].



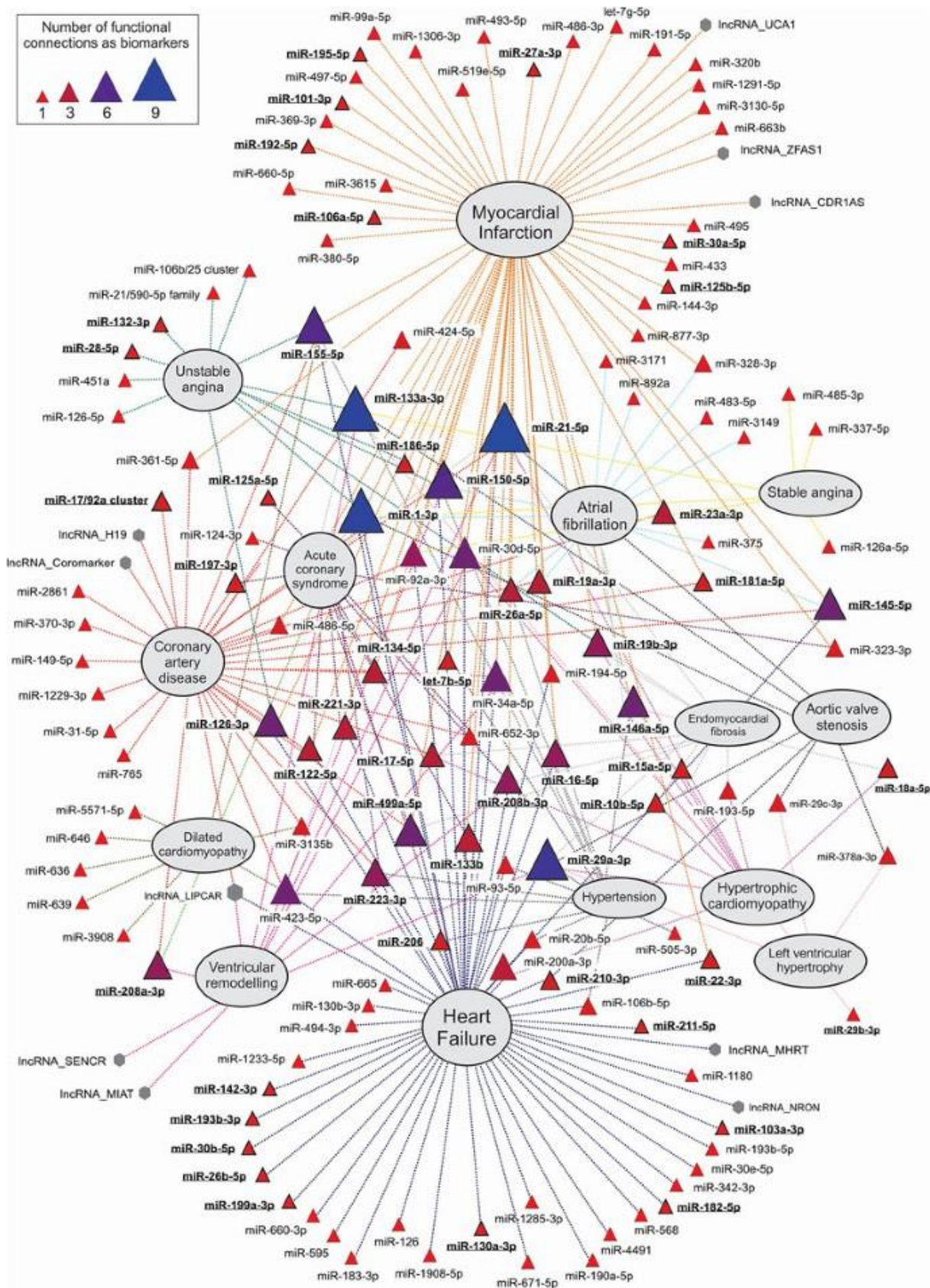


Figure 13. Circulating ncRNAs in cardiovascular diseases. Image taken from [34].

Finally, circRNAs have been proposed as a new class of candidate biomarkers in cardiovascular diseases such as heart failure and MI [41-43] (Figure 14). For instance, the circRNA MICRA has been found to be

a valuable predictor of heart failure development after MI [434, 435]. MICRA is able to predict left ventricular remodelling after acute MI and thus represents a potential new outcome prognostication biomarker of these patients [435]. Similarly to linear lncRNAs, animal models and *in-vitro* studies have demonstrated the involvement of circRNAs in the mechanisms underlying ischemic and traumatic brain injury [358, 436-439]. Although the biomarker potential of circRNAs has been studied in several diseases related to cardiac arrest [440], there is still no direct study reporting the prognostic value of circRNAs after cardiac arrest [17].

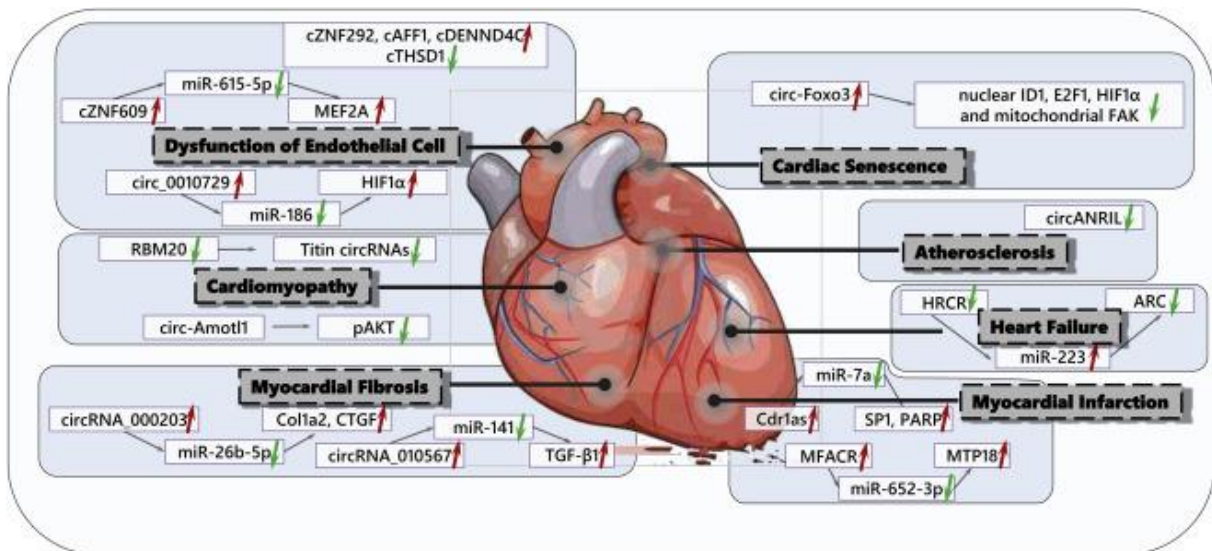


Figure 14. CircRNAs in cardiovascular diseases. Image taken from [441].

Several notable features make circRNAs an optimal reservoir of biomarkers. Firstly, circRNAs are highly stable due to their closed-loop structure which makes them resistant to degradation by exonucleases [38-40]. Indeed, the half-life of circRNAs in circulation appears to be much higher than their linear counterparts [70]. Secondly, the abundance of circRNAs in body fluids such as cerebrospinal fluid and blood appears to be greater than in other organs or compartments, allowing for minimally invasive detection in liquid biopsies [70]. Thirdly, highly cell-, tissue- and stage-specific expression patterns of circRNAs add further value for the use of this class of ncRNAs as biomarkers in specific diseases [70]. Finally, circRNAs are evolutionarily conserved, thus circRNAs found in rodent models have the potential to be confirmed in human samples and thus be used in new therapeutic strategies [39, 40, 54, 70].

Despite growing interest, the use of circulating ncRNAs as biomarkers for cardiovascular disease has not yet been implemented in current clinical practice. Therefore, further studies are needed to be able to apply these precious molecules in the clinical setting, especially the class of circRNAs that, as previously seen, appear to have high biomarker potential.

# *Objectives*



This doctoral research aimed to shed light on the prognostic potential of ncRNAs after OHCA to further improve the accuracy of prognostication after OHCA. The goals defined in this doctoral project were guided by the opportunity to access two of the largest clinical trials of patients after OHCA, the TTM-trial and the TTM2 trial.

Among the various ncRNAs identified so far, this work was focused on three classes, miRNAs, lncRNAs, and circRNAs, whose characteristics and functions have been extensively described in the introduction. Of these three classes, miRNAs represent the most studied group in the field of cardiovascular disease and cardiac arrest, while studies on lncRNAs and circRNAs are still at an early stage, although evidence on their potential as biomarkers in other cardiovascular diseases has already been reported.

Therefore, this work can be divided into two main studies. The first aimed to investigate the association between circulating miRNAs and NSE levels after OHCA and thus the ability of these miRNAs to reflect the level of neuronal damage in patients after OHCA. The second study, on the other hand, aimed to investigate the prognostic biomarker potential of lncRNAs and circRNAs that are mainly present in blood cells of OHCA patients, rather than circulating freely in the extracellular compartment of the blood. Therefore, the focus of this second study was to highlight the importance of the inflammatory response triggered after OHCA, in addition to the brain damage on which the first study was focused. Furthermore, although biomarker studies generally tend to limit themselves to the prognostic value of the identified biomarker, without defining its mechanism of action. In this second study, space was also given to functional studies among the identified candidates. Indeed, while anticipating that this research project would not be sufficient to comprehensively study the functions of the identified candidates, several preliminary studies were conducted, and it is hoped that the various hypotheses that emerged from the results can be more thoroughly investigated in future research.

# *Materials and methods*

## 1. Cohorts of patients: TTM and TTM2

The TTM-trial is an international, multicentre, randomized trial that enrolled 939 unconscious adults, in 33 sites between November 11, 2010 and January 10, 2013. These patients were admitted in the ICU after OHCA of presumed cardiac cause. The trial aimed to compare two different targeted temperature regimens (33 °C and 36 °C) on 6-month neurological outcome and survival until the end of the trial. Neurological outcome was assessed using mRS and CPC scores. Therefore, patients with none or moderate neurological damage (mRS 0-3 or CPC1-2) were classified as good neurological outcome, while patients with severe neurological damage, coma, or death (mRS 4-6 or CPC3-5) were classified as poor outcome. The TTM-trial is registered at [www.clinicaltrials.gov](http://www.clinicaltrials.gov) (NCT01020916).

Similar to the TTM-trial the follow-up TTM2-trial, was an international, multicentre and randomized trial that enrolled 1900 unconscious adults in a total of 60 locations between November 18, 2017 and January 20, 2020. The patients enrolled were admitted in the ICU after OHCA with a presumed cardiac or unknown cause. This second trial aimed at comparing targeted hypothermia (33 °C) versus targeted normothermia with early treatment of fever ( $\geq 37.8$  °C) on 6-month neurological outcome and survival. A second outcome of the trial was to assess health-related quality of life and survival at the end of the trial. In TTM2, the neurological outcome of the patients was established using the mRS score following the classification previously indicated for TTM. The TTM2-trial is registered at [www.clinicaltrials.gov](http://www.clinicaltrials.gov) (NCT02908308).

Both TTM- and TTM2-trials were performed within an ethical framework. Informed consent was waived and obtained from each patient or relatives, in line with the Declaration of Helsinki and the legislation of each participating country. Details of the designs, protocols, analyses and results of the two studies have already been extensively reported [12, 442, 443].

In both TTM and TTM2 trials, whole blood samples were collected in PAXgene™ Blood RNA tubes (PreAnalytiX) 48 h after ROSC. The samples were collected and stored at the Integrated Biobank of Luxembourg (IBBL) in compliance with the International Society for Biological and Environmental Repositories Best Practices and with International Organization for Standards (ISO 17025:2005).

## 2. Cell biology

### 2.1. Cell cultures

#### 2.1.1. *SH-SY5Y: Human Neuroblastoma Cell Line*

SH-SY5Y cells were maintained in DMEM medium (Lonza) containing 10% FBS (Lonza), 2 mM L-glutamine (Lonza) and 104 units of penicillin and  $\mu\text{g}$  of streptomycin per ml (Lonza). SH-SY5Y cells were subcultured at a concentration of  $2 \times 10^6$  cells/cm<sup>2</sup> in T-75 flasks (Corning®) and divided once 80-90% confluence was reached. During subculturing, cells were detached using a fresh solution of trypsin/EDTA (Lonza) for 2-5 minutes at 37°C. Subsequently, the trypsin was neutralised by adding a double volume of fresh complete medium. The detached cells were collected and centrifuged at 500 x g for 5 minutes at room temperature. Then, the pellet was resuspended in fresh complete medium in a new T-75 flask.

#### 2.1.2. *Jurkat: Human T lymphoblast cell line*

Jurkat cells were maintained in RPMI 1640 medium (Gibco) containing 10% FBS (Biowest), 2 mM L-glutamine (Lonza), 1x non-essential amino acids (Lonza) and 104 units of penicillin and  $\mu\text{g}$  of streptomycin per ml (Lonza). Cells were cultured at  $2 \times 10^5$  cells/mL in T-75 flasks (Corning®) and maintained at a maximum cell concentration of  $1 \times 10^6$  cells/ml. During subculture, cells were harvested

and centrifuged at 200 x g for 10 minutes at room temperature. The pellet was then resuspended in fresh complete RPMI medium in a new T-75 flask.

#### 2.1.3. THP-1: Human monocytic cell line

THP-1 cells were maintained under similar culture conditions as Jurkat cells, but with the addition of sodium pyruvate 1x (Lonza). The subculture protocol for THP-1 cells was the same as previously described for Jurkat cells.

#### 2.1.4. HEK293: Human embryonic kidney cell line

HEK293 cells were maintained in culture using the same complete medium as described for SH-SY5Y cells. Cells were cultured at a concentration of  $6 \times 10^3$  cells/cm<sup>2</sup> in T-75 flasks (Corning®). The subculture protocol was the same as previously described for SH-SY5Y cells.

#### 2.1.5. HeLa: Human cervical cancer cell line

HeLa cells were maintained in culture using the same complete medium as described for SH-SY5Y cells. Likewise, a subcultivation ratio of 1:6 was used following the protocol already described for SH-SY5Y cells.

## 2.2. Cell treatments

Antibiotics were removed 24 h before the start of each treatment to avoid biased results generated by the presence of antibiotics in culture rather than by the treatment itself [444, 445].

#### 2.2.1. Hypoxia

Jurkat and THP-1 were seeded at a concentration of  $1 \times 10^6$  cells/well and SH-SY5Y at  $5 \times 10^5$  cells/well in 6-well plates and incubated for 24 h and 48 h in normoxic (normal cell culture incubator) or hypoxic (hypoxia chamber; Eppendorf; 1% O<sub>2</sub>) conditions. At the end of the treatment, cells were harvested as previously described and resuspended in 700 µl of QIAzol Lysis Reagent (QIAGEN) for RNA extraction.

#### 2.2.2. Cobalt(II) chloride hexahydrate (CoCl<sub>2</sub>)

CoCl<sub>2</sub> (Sigma-Aldrich) was filtered before use with a 0.2 µm filter and used at a concentration of 20 µM and 200 µM for Jurkat and THP-1 cells and at a concentration of 200 µM for SH-SY5Y cells as established from previous laboratory experiments. Jurkat and THP-1 were seeded at a concentration of  $1 \times 10^6$  cells/well and SH-SY5Y at  $5 \times 10^5$  cells/well in 6-well plates and incubated for 24 h and 48 h with or without CoCl<sub>2</sub>. In the control condition without CoCl<sub>2</sub>, an equal volume of nuclease free water was added (Lonza). Cells were harvested following the protocols previously described for each cell line, the centrifuged pellet was resuspended in 700 µl of QIAzol Lysis Reagent (QIAGEN) and stored at -80 °C for RNA extraction.

#### 2.2.3. Sodium chloride (NaCl)

The 5 M NaCl solution (Sigma-Aldrich) was filtered through a 0.2 µm filter before use.  $1 \times 10^6$  THP-1/well were seeded in 6-well plates and incubated for 4 h, 8 h, 24 h and 48 h with 30 mM, 50 mM or 100 mM NaCl. Nuclease free water was added in the control condition without the addition of NaCl. Cells were harvested and centrifuged using the protocol previously described. 450 µl of medium was collected for each condition to perform LDH assay, described in the biochemistry section of the materials and methods. The pellet was resuspended in 700 µl of QIAzol Lysis Reagent (QIAGEN) and stored at -80 °C for RNA extraction.

#### 2.2.4. Lipopolysaccharide (LPS)

LPS (Sigma-Aldrich) powder was resuspended with THP-1 medium in a stock solution of 1 mg/ml.  $1 \times 10^6$  THP-1/well were seeded in 6-well plates and incubated for 2 h before treatment with LPS. Next, 100 ng/ml of LPS was added to the plates and incubated for 3 h, 6 h, 9 h, 24 h and 48 h. At the end of the treatment, the pelleted cells were resuspended in 700  $\mu$ l of QIAzol Lysis Reagent (QIAGEN) and stored at -80 °C for RNA extraction.

#### 2.2.5. ImmunoCult™ Human CD3/CD28 T Cell Activator

Jurkat cells were seeded at a concentration of  $2.5 \times 10^6$  cells/well. One hour after seeding the cells, 25  $\mu$ l/ $1 \times 10^6$  cells of ImmunoCult™ Human CD3/CD28 T Cell Activator (STEMCELL Technologies) was added in the medium for 4 h, 24 h and 48 h. The pelleted cells were then harvested and resuspended in 700  $\mu$ l of QIAzol Lysis Reagent (QIAGEN) and stored at -80 °C for RNA extraction.

### 2.3. Nucleofection

Jurkat cells were nucleofected with the pcDNA 3.1 (+) vector containing circNFAT5 to study the effects of circNFAT5 overexpression. For this purpose,  $1 \times 10^6$  jurkat cells /well were seeded in 12-well plates. Cells were nucleofected with Amaxa® Cell Line Nucleofector® Kit V (Lonza) following the manufacturer's protocol specific for jurkat cells ([https://bioscience.lonza.com/lonza\\_bs/CH/en/Transfection/p/000000000000191667/Cell-Line-Nucleofector%E2%84%A2-Kit-V](https://bioscience.lonza.com/lonza_bs/CH/en/Transfection/p/000000000000191667/Cell-Line-Nucleofector%E2%84%A2-Kit-V)). The nucleofection protocol for high cell viability (Nucleofector® Program X-001) was selected using the Nucleofector® II device (Amaxa Biosystems). The cells were then incubated at 37°C and 5% CO<sub>2</sub> for 24 h. Upon completion of the experiment, the cells were harvested, RNA was extracted and overexpression of circNFAT5 was confirmed by qPCR.

### 2.4. Transfection procedures

#### 2.4.1. Transfection of antisense LNA™ GapmeRs for circNFAT5 and NFAT5

Antisense LNA™ GapmeRs were designed by QIAGEN to silence the expression of circNFAT5 and linear NFAT5 in THP1 cells. To specifically silence only circNFAT5, the antisense LNA™ GapmeR was designed on the junction site. For this purpose,  $1 \times 10^6$  THP-1 cells/well were seeded in 12-well plates and the concentration of antisense LNA™ GapmeR used was 50 nM and 30 nM for linear NFAT5 and circNFAT5, respectively. Details of the antisense LNA™ GapmeRs used are given in Table 3. THP-1 cells were transfected with RNAiMAX Transfection Reagent (Invitrogen) using one of the antisense LNA™ GapmeRs listed in Table 3 following the manufacturer's protocol. THP-1 cells were transfected for 24 h, 48 h and 72 h. Then, the cells were harvested and the RNA was extracted. The success of the experiment and thus the silencing of circNFAT5 and linear NFAT5 were confirmed by qPCR, performed as described in the molecular biology section.

Name	Cat. No.	Sequence
Antisense LNA™ GapmeR Control – negative control A	339515 LG00000002-DDA	-
Antisense LNA™ GapmeR Standard – circNFAT5	339511 LG00776719-DDA	TACAGTATATCCAGTT
Antisense LNA™ GapmeR Standard – linear NFAT5	339511 LG00784858-DDA	GACTGGTGTGCGAAAC

Table 3. List of antisense LNA™ GapmeRs (QIAGEN) used to transfect THP-1 cells.

#### 2.4.2. Transfection of pcDNA 3.1(+) vector containing circNFAT5 sequence

A vector overexpressing circNFAT5 using the pcDNA 3.1(+) backbone, was generated and transfected into HeLa cells to check the protein-coding potential of circNFAT5. The original pcDNA 3.1 (+) vector was used as negative control of the transfection. For this purpose, 150.000 HeLa cells/well were seeded in 6-well plates and transfected with the respective vectors for 24 h and 48 h. Two µg of vector were transfected with Lipofectamine™ 3000 Reagent (Invitrogen) following the manufacturer's protocol. Thereafter, cells were harvested, and both proteins and RNA were extracted for western blot and qPCR analysis. RNA extraction and qPCR measurements were performed following the protocols described below. For protein extraction, cells were first washed with 1X Phosphate Buffered Saline (PBS) (Lonza) and then incubated with 250 µl 1x Cell Lysis Buffer (Cell Signaling). The cells were collected in a 1.5 ml tube and the solution was passed 5 times through a 1 ml cold syringe. Then, the samples were centrifuged for 15 minutes at 4°C, at maximum speed. The supernatant was collected and the protein concentration was quantified using the Pierce™ BCA Protein Assay Kit (Thermo Scientific™) following the manufacturer's protocol and the spectrophotometer (POLARStar OPTIMA, BMG Labtech) at 562 nm wavelength. Then, the proteins were stored at -80 until western blot was performed.

### 2.5. Nuclear and cytoplasm fractionation

The Protein and RNA Isolation System (PARIS; Invitrogen) was used to isolate RNA from nuclear and cytoplasmic fractions. This method is based on the differential lysis of plasma and nuclear membranes with non-ionic detergents, followed by RNA isolation. Here, the PARIS kit was used to identify the intracellular localisation of circNFAT5 in Jurkat cells. For this purpose, 400.000 cells/ml were seeded in 6-well plates for 24 h. Then, the cells were harvested and the nuclear and cytoplasmic fractions were isolated following the manufacturer's protocol. Finally, RT and qPCR were performed. NEAT1 and β-actin were used to verify the purity of the nuclear and cytoplasmic fractions respectively.

### 2.6. Fluorescent In Situ Hybridization (FISH)

To validate the results of the cellular fractionation experiments, FISH was performed for circNFAT5 and NFAT5 in SH-SY5Y cells. Briefly, 25000 cells were plated on glass coverslips in a 24 well plate containing SH-SY5Y medium without the addition of antibiotics. The next day, the medium was removed and the cells were fixed in 500 µl of pre-chilled ethanol for 10 minutes at -20°C. Coverslips were then washed in nuclease free water before being incubated at 55°C for 10 minutes. During this step, 5' FAM or TAMRA labelled probes specific to circNFAT5 and NFAT5, respectively, were denatured at 95°C for 30 seconds. The probe sequences used in this study are GAATAGTTGTCAGGTCT for linear NFAT5 and TGAGAAAGTGTTGTC for circNFAT5, respectively. Following this step, the nuclease free water was removed and 250µl of hybridization buffer (H7782-6ML, Sigma Aldrich) and denatured probes at a concentration of 1/100 were added to the respective wells. Coverslips were then incubated for 4 h at 62°C. Following hybridization with gene specific probes, coverslips were serially washed three times in pre-warmed wash buffer (2 x SSC in PBS). The maximum amount of liquid was removed between washes, then coverslips were incubated for 5 minutes with DAPI (D9542, Sigma Aldrich) at a final concentration of 1/500. Coverslips were washed once in PBS before being mounted on glass slides using Fluoroshield (F6182, Sigma Aldrich). Glass slides were kept at 4°C in the dark until Z-Stack images were captured using an LSM880 Airy confocal microscope (Carl Zeiss A.G.). Images were then analyzed using the Zen Black software package (Zen 2.3 SP1).

### 3. Molecular biology

#### 3.1. RNA extraction

##### 3.1.1. From Blood samples

Total RNA was extracted from TTM and TTM2 PAXgene™ Blood RNA tubes at the IBBL using the PAXgene™ Blood miRNA Kit (PreAnalytiX) following the manufacturer's protocol. The optional DNase I step was included in all sample extractions to avoid contamination with genomic DNA.

Details of total RNA extraction from TTM plasma samples for short RNA sequencing are provided in the following article: "Association of Circulating MicroRNA-124-3p Levels With Outcomes After Out-of-Hospital Cardiac Arrest: A Substudy of a Randomized Clinical Trial" [37].

##### 3.1.2. From cell cultures

Total RNA was extracted following the manufacturer's protocol of the miRNeasy Micro kit (QIAGEN). The optional DNase I step was included in all experiments conducted to minimise the risk of genomic contamination. After extraction, the RNA was denatured for 5 minutes at 65 °C and stored on ice. The RNA amount was quantified using the spectrophotometer ND-1000 (NanoDrop® Technologies, Wilmington, USA).

#### 3.2. Retro transcription (RT)

Superscript™ II kit (Invitrogen) was used to retrotranscribe total RNA extracted from blood samples and from cell cultures. Precisely, 300 ng of RNA from TTM and TTM2 blood samples and 1 µg of RNA from cell culture experiments were retrotranscribed into cDNA. Each RT reaction included 1X RT buffer, 180 ng of random primers (Invitrogen), 2.5 mM of dNTPs (Invitrogen), 100 mM of dithiothreitol and 200 units of SuperScript™ II RT in a final volume of 20 µl. The reaction was incubated at 42 °C for 50 minutes followed by an inactivation by heating at 70 °C for 15 minutes. The cDNA was then stored at -20 °C. In each RT series, controls without reverse transcriptase allowed verifying the absence of genomic DNA amplification while controls without RNA allowed verifying the absence of contaminants in the mastermix.

#### 3.3. Quantitative PCR (qPCR)

The cDNA generated from both patient cohorts and cell experiments was diluted 10-fold and 4 µl were used per well for qPCR measurements. IQ™ SYBR® Green Supermix (BioRad, Nazareth, Belgium) contains a polymerase, four deoxyribonucleotides and SYBR® Green intercalant and was used to perform qPCRs. The sequences of the primer pairs (Table 4) were generated with Beacon Designer version 8.0 software (Premier Biosoft, USA) and their optimal annealing temperature and efficiency were determined prior to use. Divergent primer pairs were designed for the circRNAs of interest, which allowed specific amplification of circular and not linear RNAs. The primer pairs were used at a concentration of 0.3 µM in a final volume of 20 µl. When measuring TTM and TTM2 samples, each PCR plate contained an internal standard calibrator. This calibrator was used to correct for inter-plate variability during qPCR analysis. In addition, appropriate negative controls were added to each qPCR performed to check for potential contamination of the mastermix or sample. The qPCRs were performed using the CFX96 thermal cycler (Bio-Rad). SF3a1 was used as a housekeeping gene for normalisation in TTM and TTM2 measurements. For the cellular studies, SF3a1 or 18s were used as normalisers depending on the type of treatment and stability of the housekeeping gene. Target

expression values were determined using the relative quantification method ( $\Delta\Delta C_t$ ) with CFX Maestro 1.1 software (Bio-Rad), followed by log<sub>2</sub> transformation and scaling.

Name	Forward primer	Reverse primer	Hybridation T°
<i>18s</i>	CGGCGACGACCCATTCTGAAC	GAATCGAACCTGATTCCCCGTC	64
<i><math>\beta</math>-actin</i>	AGAAAATCTGGCACCACACC	GGGTGTTGAAGGTCTCAA	60
<i>Caspase 3</i>	TTTTTCAGAGGGGATCGTTG	CGGCTCCACTGGTATTTTA	58
<i>circAGO2</i>	TTAACAGGGAAATCGTGGA	AGGTGCAAGTGCTTGTC	54
<i>circDLG1</i>	AAACACCAACTTACCCAAC	GTATTCTCAGCAGGGACT	54
<i>circDNM2</i>	AGAGGAGACAGAGCGAAT	CGTAAGTCCTTCTCGTCAA	54
<i>circFAM13b</i>	ATTGTGATGGGGAAGGAT	GATATATGGGTGCTGGGT	60
<i>circNFAT5</i>	AGATTGATTTGCTTGTTTC	TGAGAAAGAAGTGTTGTC	58
<i>IL4</i>	ATGGGTCTCACCTCCCAACT	TGTCTGTTACGGTCAACTCGG	62
<i>Inc-IL1R1-1:2</i>	TTTGAGAGGTGAAGGGGCTC	TACAGTCAGAGTTGCCAGCA	62
<i>MYB</i>	CAGAAGAACAGTCATTTGATGG	TAACGCTACAGGGTATGGAA	58
<i>NEAT1</i>	CATCTGACTGACTATGACTG	CATATCGTATCTGTAAGCCTAT	60
<i>NFAT5</i>	CATCTCAAACATAGCAGGAAA	GAATAGTTGTCAGGGTCTCT	58
<i>PCNA</i>	CAACGAGGCTGCTGGGATA	TCTTCATTGCCGGCGCATT	60
<i>S100A4</i>	ACTTGGACAGCAACAGGGAC	GCTGCTTATCTGGGAAGCCT	60
<i>SF3a1</i>	GATTGGCCCCAGCAAGCC	TGCGGAGACAACTGTAGTACG	60
<i>SLC38A2</i>	CTTGCCGCCCTCTTTGGATA	ACAGCCAGACGGACAATGAG	54
<i>TNF<math>\alpha</math></i>	ATCAAACAGGACAGAGTTG	ATCAAACAGGACAGAGTTG	60
<i>VEGF<math>\alpha</math></i>	ATCAAACAGGACAGAGTTG	GAGCCAGTTGTAAGATGC	58
<i>ZFP36L1</i>	AGTTCGCACACGGCATCCA	CGGCGCTCTTCAGCGTT	56

Table 4. List of primer pair sequences and respective annealing temperatures for qPCR measurements.

### 3.4. RT and qPCR with miRCURY system

The miRCURY system (QIAGEN) was used for the detection by qPCR of the miRNA, miR-144-3p, predicted to bind circNFAT5. At first, an RT was performed using the miRCURY LNA RT Kit (QIAGEN) on 200 ng of total RNA. Next, miR-144-3p was measured by qPCR using miRCURY LNA SYBR Green PCR Kit (QIAGEN) following the manufacturer's protocol. The forward primer used for miR-144-3p detection was also purchased by QIAGEN (GeneGlobe ID: YP00204754).

### 3.5. Cloning procedures

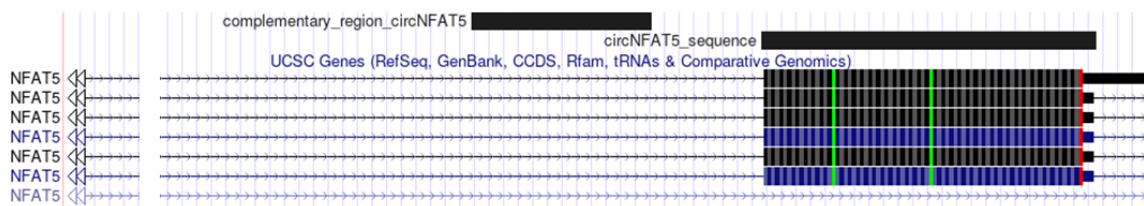
#### 3.5.1. Using pcDNA 3.1(+) vector

The circNFAT5 sequence was cloned into a pcDNA 3.1(+) vector flanked by complementary opposite regions. The purpose of these regions was to increase the circularization efficiency of circNFAT5 in *in-vitro* experiments. The complementary regions originate from the intronic region upstream of circNFAT5, approximately 200 bp before the start of the transcript (Figure 15.a). Primer pairs have been designed to amplify a first insert, ranging from 215 bp upstream to 61 bp downstream of the transcript (circNFAT5\_KpnI/circNFAT5\_Sall) (Figure 15.b). A second primer pair was designed also to amplify a second insert of 134 bp representing the complementary region (circNFAT5\_compl\_PmeI/circNFAT5\_compl\_Sall) (figure 15.b). This second insert was positioned in the opposite direction downstream of the transcript into the vector (figure 15.b). The sequences of the



primers are shown in Table 5. The primers were designed using Beacon Designer software version 8.0 (Premier Biosoft, USA) and were modified to contain the specific sequences recognised by the restriction enzymes. The first insert contained the sequences for KpnI (ggtacc; New England BioLabs) and Sall (gtcgac; New England BioLabs) and the second sequences for PmeI (gtttaaac; New England BioLabs) and Sall. The inserts were amplified using 100 ng of genomic DNA from HEK293, with Q5<sup>®</sup> High-Fidelity DNA Polymerase (New England BioLabs) following the manufacturer's protocol. The amplified products were separated on a 1% agarose gel at 100 V for approximately 20 minutes. The bands were cut and purified using the NucleoSpin<sup>™</sup> Gel and PCR Clean-up Kit according to manufacturer's instructions (Macherey-Nagel<sup>™</sup>). The concentration of the purified amplicons was measured with the ND-1000 spectrophotometer. One µg of each insert was cut using the specific restriction enzymes described above. Similarly, 5 µg of pcDNA 3.1(+) vector was opened with the restriction enzymes KpnI and PmeI using CutSmart<sup>®</sup> buffer according to the manufacturer's protocol (New England BioLabs). A second purification step was performed before the two inserts were ligated into the vector with T4 DNA Ligase (New England BioLabs) following the manufacturer's protocol. For the ligation reaction a molar ratio of 1:3 (vector: inserts) was used following the ligation calculator (<https://nebicalculator.neb.com/#!/ligation>). The TOP10 (F') competent bacteria were then transformed with the generated vector. A colony PCR with OneTaq<sup>®</sup> DNA Polymerase (New England BioLabs) and further separation of the amplicons with a 1% agarose gel allowed the selection of colonies containing the correct insert length. Finally, the correct cloning sequence was confirmed by Sanger sequencing (described below).

a.



b.

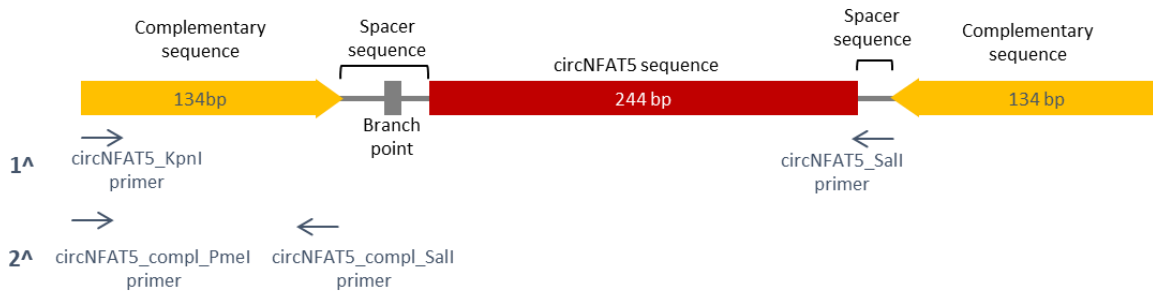


Figure 15. Cloning of circNFAT5 pcDNA 3.1(+) vector. **a.** genomic position of the complementary region sequence and circNFAT5 sequence to be cloned into the pcDNA 3.1(+) vector. **b.** Graphical representation of the cloning procedure with sequence lengths and primer pair locations.

Name	Sequence	Annealing T
cNFAT5-KpnI	catctaggtaccTAAGATGAATTCCAGTGC	62
cNFAT5-Sall	catctagtcgaCTGTTAAGAAGAATAAAATCTGATGCT	62
cNFAT5comp-PmeI	catctagttaaaccTAAGATGAATTCCAGTGC	62
cNFAT5comp-Sall	catctagtcgacGATTCATGAAAAGATATTATTAGTTGTTGG	62

Table 5. Primer pairs used to clone circNFAT5 into a pcDNA 3.1(+) vector. The primers contain a sequence that recognises a specific restriction enzyme (in red): KpnI (ggtacc), Sall (gtcgac) or PmeI (gtttaaacc). The optimal annealing temperature selected for each primer pair is indicated in the last column.

### 3.5.2. Using pEZX-MT05 vector

MYB, circNFAT5 and the corresponding linear sequence of NFAT5 were cloned into the pEZX-MT05 vector (GeneCopoeia™) to perform the luciferase assay. The cloning procedure follows that previously described for cloning into the pcDNA 3.1(+) vector. Primer pairs were designed using Beacon Designer software version 8.0 (Premier Biosoft). The orientation of the primers designed for circular and linear NFAT5 is shown in Figure 16. Sequences recognising the AsiSI and XhoI restriction enzymes were integrated into the sense and antisense primer pairs respectively for each gene to be integrated into the vector (Table 6). The optimal annealing temperature selected for amplification of the inserts is also shown in Table 6. The inserts were amplified using 30 ng cDNA from SH-SY5Y cells.

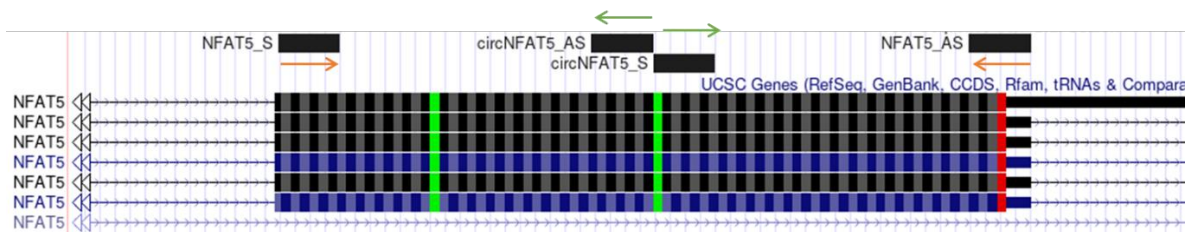


Figure 16. Primer pair positions used to clone circNFAT5 and the corresponding linear portion of NFAT5 in a pEZX-MT05 vector. Divergent primers were designed for circNFAT5 in green and convergent primers for linear NFAT5 in orange.

Name	Sequence	Annealing T
circNFAT5_LUC_S	catatcgcgatcgcATGCCAGAGAATTCTCCACT	62
circNFAT5_LUC_AS	catatcctcgagTTGCTGAGAAAAGAAGTGTG	62
NFAT5_LUC_S	catatcgcgatcgcCTGTAGTCAGCTTTTAACC	72
NFAT5_LUC_AS	catatcctcgagATATCCAGTTAAAAGGAGCC	72
MYB_LUC_S	catatcgcgatcgcGACATTTCCAGAAAAGCATTATG	58.7
MYB_LUC_AS	catatcctcgagTTTGTAGGTTAAAATAAGGGCAC	58.7

Table 6. Primer pairs used to clone circNFAT5 and NFAT5 into a pEZX-MT05 vector. The primers include a sequence (in red) recognising the restriction enzymes of AsiSI (gcgatcgc) and XhoI (ctcgag) for the sense (S) and antisense (AS) primers respectively. The optimal annealing temperature of the respective primer pairs is shown in the last column.

### 3.6. Sanger Sequencing

Sanger sequencing was used to validate the correct sequence of newly generated plasmids or qPCR-amplified products. For the latter, samples were purified with NucleoSpin™ Gel and PCR Clean-up Kit (Macherey-Nagel™) and quantified with the ND-1000 spectrophotometer before sequencing commenced. The BigDye™ Terminator v3.1 Cycle Sequencing kit (Applied Biosystems™) was used for the sequencing reactions following the manufacturer's protocol. Afterwards, the samples were purified with the Agencourt® CleanSeq® kit (Beckman Coulter) following the manufacturer's protocol. This step allowed the removal of unincorporated dyes, nucleotides and other contaminants. Finally, the sequencer (ABI PRISM 3100, Applied Biosystems) was used to analyse the samples.

### 3.7. Western blot

This procedure was performed to test the protein-coding potential of circNFAT5. The protocol was modified for the detection of very small proteins. First, 10 µg of proteins were added into a 6X loading buffer containing dithiothreitol and sodium dodecyl sulphate. The solution was then denatured for 5 minutes at 98°C and loaded into a 15% polyacrylamide gel. The ladder used was precision plus protein dual color (Bio-Rad, #161-0374). The proteins migrated in the polyacrylamide gel for about 2 h at 70V. Then, the proteins were transferred to a polyvinylidene difluoride membrane at 100V for 1 h. An additional polyvinylidene difluoride membrane was added below the first one to prevent very small proteins from crossing the first membrane. Then, the proteins were cross-linked with a 0.4 % paraformaldehyde solution for 30 minutes. Next, the membranes were washed with water twice and incubated with No-Stain™ Protein Labelling Reagent (Invitrogen) for 10 minutes. This reagent allows all proteins present on the membranes to be visualised. Following this, three more washes with water were performed before the bands were revealed with the iBright 1500 (Invitrogen). In addition, a positive control was performed to ensure that the western blot procedure was successful. The anti-SNCA antibody previously standardised in our laboratory was used as a positive control here. Therefore, the membranes were incubated with a blocking solution (5% milk in TBST 1X) for 1 h, followed by overnight incubation with the anti-SNCA primary antibody (BD Biosciences) diluted 1/1000 in 5% milk. Next, the membranes were washed and incubated with donkey anti-mouse secondary antibody (Jackson ImmunoResearch) diluted 1/2000 in 5% milk for 1 h. Then, the membranes were washed 5 times and the bands were visualised and analysed using the universal imaging mode on the iBright 1500 machine.

## 4. Biochemistry

### 4.1. Lactate Dehydrogenase (LDH) assay

The Cytotoxicity Detection Kit (Sigma-Aldrich) was used in this work to quantify the potential cytotoxic effect of NaCl on cells. Indeed, the lactate dehydrogenase (LDH) assay allows measuring the activity of the LDH enzyme that is released from lysed cells. LDH is a stable enzyme present in all cells and is rapidly released into the cell culture supernatant when the plasma membrane is damaged.

To perform the LDH assay, approximately 300 µl of supernatant was collected from each experimental condition and centrifuged at 1000 x g for 10 minutes to remove cell debris. Then, the supernatant was transferred to a new 1.5 ml tube and the procedure was conducted according to the manufacturer's protocol. The assay was performed in a 96-well plate using 100 µl of culture supernatant for each condition. Each condition was tested in duplicate. The maximum amount of LDH enzyme activity releasable from the cells was determined by adding Triton-X100 to the cells prior to harvest and used as a positive control in the final calculation of the cytotoxicity rate. The negative control was instead

obtained from fresh cell culture medium. LDH activity was measured with a spectrophotometer (POLARStar OPTIMA) at 492 nm wavelength. The cytotoxicity percentage of each experimental condition was calculated with the following equation, after averaging the optical density (OD) of the duplicates:

$$\text{Cytotoxicity \%} = \frac{(\text{sample OD} - \text{negative control OD})}{(\text{Positive control OD} - \text{negative control OD})} \times 100$$

## 4.2. Luciferase assay

A luciferase assay was performed to verify the potential binding of miR-144-3p on the circNFAT5 junction site. For this purpose, 80.000 HEK293/well were seeded in a 48-well plate with 200  $\mu$ l of complete medium without antibiotic. The cells were transfected for 48 h with 120  $\mu$ g of pEZX-MT05 vectors containing MYB, circNFAT5 or linear NFAT5 and 30 ng of pre-miR-144-3p or scramble (Applied Biosystems) using Lipofectamine 2000 (Invitrogen). Transfection was performed following the manufacturer's protocol. The original pEZX-MT05 vector without modification was used as the negative control of the experiment. pEZX-MT05 containing MYB, a known target of miR-144-3p, was used as the positive control of the experiment. Luciferase activity was performed using the Secrete-Pair™ Dual Luminescence Assay Kit (GeneCopoeia™) following the manufacturer's protocol and a spectrophotometer (POLARStar OPTIMA).

## 4.3. Ribonuclease R (RNase R) treatment

RNase R treatment was used to confirm the circularity of circRNAs. Indeed, RNase R is a 3' to 5' exoribonuclease that can digest linear single-stranded RNAs but not circular ones. Following RNA extraction, 500 ng of RNA was treated with 1.5 units of RNase R (Epicentre) or the same volume of water (mock treatment) and 20 units of RNaseOut™ Recombinant Ribonuclease Inhibitor (Invitrogen) in 1 $\times$  RNase R buffer, for a final volume of 8  $\mu$ l. Then, the RNA was incubated for 20 minutes at 37°C and placed on ice before RT was performed.

## 5. Bioinformatical analyses

Small RNA sequencing was performed on 50 plasma samples from TTM patients 48 h after ROSC. Sequencing details have already been extensively reported and can be found in Appendix II [44].

With respect to whole transcriptome RNA sequencing, 46 whole blood samples from TTM-trial were sequenced using the HiSeq platform (Illumina, San Diego, CA) with 2 x 50 bp of read length. A strand-specific RNA-Seq library was prepared from these samples using the Ovation Human Blood RNA-Seq Library Systems (NuGEN Technologies, San Carlos, USA). After trimming the adapter sequences, quality control of the RNA-seq data was performed using the FastQC tool (<https://www.bioinformatics.babraham.ac.uk/projects/fastqc/>). Next, the reads were aligned to the GRCh38 human reference genome with STAR using the default set-up [446]. For linear RNAs, transcript counting and differential expression analysis was performed using cufflinks and cuffdiff [447] with the protein coding transcripts from GENCODE28 ([https://www.encodegenes.org/human/release\\_28.html](https://www.encodegenes.org/human/release_28.html)) and lncRNAs from LINCipedia 5.5 high confidence set [448] as reference. For circRNAs identification, DCC was used with default set-up [449] and DESeq2 [450] was used to identify the differentially expressed circRNAs. The linear RNAs (protein coding and lncRNAs) detected with at least 5 reads and the circRNAs detected with at least 2 reads in

at least half samples of CPC1 or CPC5 group were kept for differential expression analysis. CircRNAs and the lncRNAs with  $p < 0.05$  and  $\log_2$  fold change  $> 0.5$  or  $< -0.5$  were selected for further validation by qPCR. In addition, fragments per kilobase of exon per million mapped fragments (FPKM)  $> 10$  was used to filter out the lowly expressed lncRNAs.

The protein-coding potential of circNFAT5 was tested using the web server <http://cpc2.gao-lab.org/>. In addition, the presence of potential IRES sequences was predicted with irespy (<https://irespy.shinyapps.io/IRESpy/>) and IRESbase (<http://reprod.njmu.edu.cn/cgi-bin/iresbase/index.php>).

MicroRNAs predicted to bind circNFAT5 at or near the junction were identified with <http://mirdb.org/>. Target Scan Human ([https://www.targetscan.org/vert\\_80/](https://www.targetscan.org/vert_80/)), on the other hand, was used to predict miR-144-3p target genes.

Finally, RBPmap database (<http://rbpmap.technion.ac.il/>) was used to identify potential proteins that can bind circNFAT5, and the RBPDB database (<http://rbpdb.ccb.utoronto.ca/>) was used to identify all RBPs in Homo sapiens to correlate with circNFAT5 and linear NFAT5 in the RNA-seq data.

## 6. Biostatistical analyses

For all the statistical analyses performed in this study a p-value  $\leq 0.05$  was considered as statistically significant.

Correlation analyses for continuous variables were performed using Spearman correlation. All skewed continuous variables were  $\log_2$  transformed and scaled.

Chi-squared test or Fisher's exact test were used to compare the differences of categorical characteristics between 2 groups of patients while T-test or Mann-Whitney U test was used to compare the difference between 2 groups for continuous variables. Furthermore, paired t-test was used to determine the statistical significance between two different conditions in the biological replicates of the *in-vitro* experiments. All the tests mentioned so far were performed using SigmaPlot (Sigma-Aldrich, version 12.5).

The ability of candidate lncRNAs and circRNAs to predict neurological outcome was evaluated by logistic regression analysis. For this purpose, patients were dichotomized into two groups according to their CPC score and/or mRS score. Therefore, patients with CPC 1-2 or mRS 0-3 were categorized as good outcome group and patients with CPC 3-5 or mRS 4-6 as poor outcome group. Both univariate and multivariable logistic regression analyses were performed. For generating clinical models in multivariable analyses, the same variables considered in previous publications [37, 49, 423] were selected in this study. These variables are age, sex, first monitored rhythm, bystander CPR, circulatory shock on admission, targeted temperature regimen, time from cardiac arrest to ROSC, initial serum lactate levels and NSE levels. In the TTM2-trial, NSE measurements were not available at the time this study was conducted, therefore for this patient cohort, multivariable analyses were performed using 8 variables instead of the 9 listed above. MissForest R package [451] was used to impute missing data of the selected variables. Forest plots, showing ORs with 95% CI, were generated for both univariate and multivariable analyses using Microsoft Excel. The LRT was used to compare the model with and without the candidate tested. Furthermore, the AIC and Wald test were used to estimate the fit of the models generated. NRI and IDI were instead used to test the ability of each candidate to reclassify patients misclassified by the clinical models. All these analyses were performed in R studio software

version 1.3.9594.0.3 using the following packages: ROCR, HmiscPredictABEL, rms, lme4 and matrixStats.

To determine the ability of each candidate to predict survival, cox proportional hazards regression models were run. Harrell's C-index (concordance index) was calculated to evaluate univariate and multivariable models. As for logistic regression analyses, LRT was used to compare different cox models with and without the specific candidate tested. In addition, AIC and Wald tests were used to measure the quality of the generated cox models. The survival analyses were performed using survival and lme4 R packages with R studio software version 1.3.9594.0.3.

AUC was determined for each candidate and was used to calculate the Youden index, following the formula: Youden index = sensitivity + specificity - 1. The Youden index allowed the identification of a cut-off value for each candidate that was subsequently used to generate Kaplan-Meier curves with Sigma Plot 12.5.

# *Results*

## 1. Circulating Levels of Brain-Enriched MicroRNAs Correlate with Neuron Specific Enolase after Cardiac Arrest—A Substudy of the Target Temperature Management Trial

In recent years, the study of the origins and functions of miRNAs has provided insights into their potential use in clinical practice as markers of disease [452]. In the context of OHCA, several miRNAs have already been identified as potential prognostic biomarkers, including miR-122-5p, miR-124-3p, and miR-21, which were previously studied in the same laboratory where this research was conducted [36, 37]. Some of these miRNAs, such as miR-124-3p, appear to be released from the brain into the bloodstream following disruption of the blood-brain barrier. Although the release of miRNAs from the brain should occur immediately after ROSC [453], it is still not well understood whether the levels of circulating miRNAs can reflect the extent of brain damage in patients and thus have considerable prognostic biomarker potential.

To this end, the aim of this first study was to evaluate the potential correlation between circulating levels of miRNAs and NSE measured 48 h after ROSC. Therefore, 2 groups of 25 plasma samples from TTM patients with neurological outcome of CPC1 or CPC5 6 months after OHCA were subjected to miRNA sequencing.

The results of the following study have been published in the *International Journal of Molecular Sciences* on June 19, 2020 and are shown in Appendix II [44].

The demographic and clinical characteristics, comorbidities, arrest conditions and laboratory measures of the 50 total patients and patients separated according to neurological outcome (CPC1 or CPC5) are shown in Table 7. The two groups of patients were sex-matched, but in the group with poor outcome, the average age of patients was higher than that of the group with good outcome. In addition, the CPC5 group had a higher frequency of arrhythmias, a longer time from cardiac arrest to ROSC and higher levels of markers such as brain natriuretic peptide, creatinine, procalcitonin, S100 and NSE (Table 7).



	ALL	Outcome patients		p-value
		CPC 1 (n=25)	CPC 5 (n=25)	
BIOMETRICS				
<b>Age</b>	<b>63 (59 - 74)</b>	<b>62 (59 - 69)</b>	<b>70 (60 - 80)</b>	<b>0.04</b>
Sex	41 (82%)	21 (84%)	21 (84%)	1
COMORBIDITIES				
Arterial hypertension	21 (42%)	10 (40%)	11 (44%)	1
Chronic heart failure	3 (6%)	1 (4%)	2 (8%)	1
Diabetes	3 (6%)	1 (4%)	2 (8%)	1
Ischemic Heart disease	11 (22%)	3 (12%)	8 (32%)	0.17
Transient Ischemic Attack or Stroke	4 (8%)	2 (8%)	2 (8%)	1
Asthma or Chronic obstructive pulmonary disease	5 (10%)	1 (4%)	4 (16%)	0.35
<b>Previous arrhythmia</b>	<b>11 (22%)</b>	<b>2 (8%)</b>	<b>9 (36%)</b>	<b>0.04</b>
Previous myocardial infarction	8 (16%)	2 (8%)	6 (24%)	0.25
ARREST CONDITIONS				
Bystander witnessed arrest	41 (82%)	22 (88%)	19 (76%)	0.46
Bystander cardiopulmonary resuscitation	37 (74%)	19 (76%)	18 (72%)	1
<b>Time from CA to ROSC (mins)</b>	<b>22 (19-30)</b>	<b>20 (17-22)</b>	<b>30 (22-37)</b>	<b>0.01</b>
Shock on admission	8 (16%)	3 (12%)	5 (20%)	0.7
ST segment elevation myocardial infarction	29 (58%)	16 (64%)	13 (52%)	0.57
Shockable rhythm	46 (92%)	25 (100%)	21 (84%)	0.11
First monitored rhythm	44 (88%)	24 (96%)	20 (80%)	0.19
LABORATORY MEASUREMENTS				
pH	7.25 (7.15-7.32)	7.29 (7.18-7.33)	7.21 (7.13-7.29)	0.22
Lactate (mmol/L)	4.9 (2.95-8.73)	4.8 (3.1-7.2)	5 (2.9-9.5)	0.99
<b>Brain natriuretic peptide (NT-proBNP, pg/mL)</b>	<b>1857 (946-2932)</b>	<b>1327 (407-1872)</b>	<b>2324 (1494-4009)</b>	<b>0.005</b>
Copeptin (pmol/L)	48.74 (25.4-112.87)	53.43 (27.43-119.73)	31.63 (23.63-82.95)	0.49
<b>Creatinine (mg/dL)</b>	<b>0.99 (0.82-1.47)</b>	<b>0.9 (0.71-1.08)</b>	<b>1.33 (0.89-1.55)</b>	<b>0.007</b>
C-reactive protein (µg/mL)	143.4 (102.54-201.23)	142 (115.1-192.31)	144.79 (100.29-205.56)	0.96
Interleukin 6 (pg/mL)	166.65 (73.77-336.8)	120.3 (73.01-295.4)	196.3 (76.88-545)	0.33
<b>Neuron Specific Enolase (ng/mL)</b>	<b>27 (17-57)</b>	<b>20 (15-29)</b>	<b>60 (20-110)</b>	<b>0.003</b>
<b>Procalcitonin (µg/L)</b>	<b>1.11 (0.4-3.61)</b>	<b>0.64 (0.34-1.38)</b>	<b>3 (0.57-5.27)</b>	<b>0.02</b>
<b>S100 (S100A1B and S100BB, µg/L)</b>	<b>0.12 (0.07-0.21)</b>	<b>0.09 (0.07-0.14)</b>	<b>0.16 (0.1-0.26)</b>	<b>0.04</b>

Table 7. Demographic and clinical characteristics of the 50 TTM patients subjected to miRNA sequencing. Medians (range) are shown for continuous variables, and numbers (percentage) for categorical variables. All laboratory measurements presented in this table were taken 48 h after ROSC, except pH and lactate, which were measured at admission. The characteristics of the two groups of patients (CPC1 - CPC5) were compared using the Wilcoxon signed-rank test for continuous variables and Fisher's exact test for categorical variables. Statistical significance was considered as p-value < 0.05 and are highlighted in bold. Abbreviations: CA: cardiac arrest; ROSC: return of spontaneous circulation.

The sequencing results were published in the Gene Expression Omnibus under the reference number GSE74198. Only miRNAs expressed with more than 5 counts in more than 12 samples from at least one

of the two patient groups were considered for further analysis. Thus, a total of 673 miRNAs were correlated with the variables mentioned in Table 7. A threshold coefficient of 0.6 was considered as a significant correlation between miRNAs and the continuous variables analysed. Of the 673 miRNAs analysed, considering all 50 patients, only miR-9-3p, miR-124-3p and miR-129-5p showed significant correlation with NSE, with correlation coefficients of 0.64 (p-value=6.48E-07), 0.69 (p-value=5.16E-08) and 0.61 (p-value=3.58E-06), respectively (Figure 17.a). When patients were dichotomized according to neurological outcome at 6 months after OHCA, no significant correlation was found between the 3 miRNAs and NSE levels in the CPC1 group (Figure 17.b). However, when considering only the CPC5 group, the correlation coefficients between the 3 miRNAs and NSE were even stronger than in the 50 patients as a whole, with coefficients of 0.86 (p-value=3.50E-08), 0.74 (p-value=2.08E-05) and 0.71 (p-value=6.09E-05) for miR-9-3p, miR-124-3p and miR-129-5p, respectively (Figure 17.c).

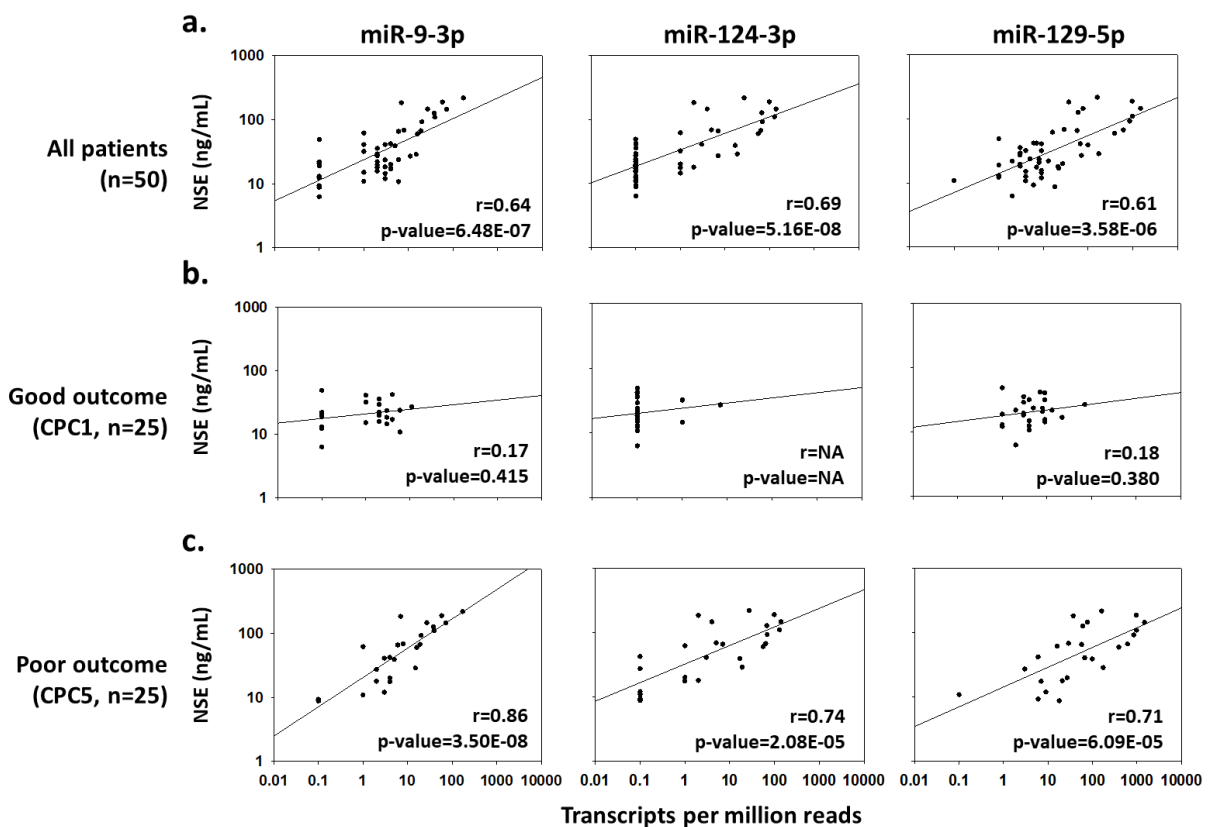


Figure 17. Scatter plots showing correlations between NSE and levels of miR-9-3p, miR-124-3p, and miR-129-5p 48 h after ROSC. Correlations were performed considering all 50 patients who underwent sequencing (a); only patients with neurological outcome CPC1 (b) or only patients with CPC5 (c). For each correlation, the correlation coefficient (r) and p-values are shown in the plot. NA stands for not applicable and refers to cases where only a few patients had miRNA values above the detection level.

In addition, miR-124-3p and miR-129-5p were significantly correlated with time from cardiac arrest to ROSC in the CPC5 group with a coefficient of 0.66 (p-value=3.16E-04) and 0.67 (p-value=2.70E-04), respectively. These miRNAs were not correlated with time from cardiac arrest to ROSC in the CPC1 group, and miR-9-3p was not correlated with time to ROSC in either patient group (CPC1: r = -0.19, p-value=0.355; CPC5: r = 0.53, p-value = 0.006). Among the comorbidities listed in Table 7, no correlation was found with these 3 miRNAs, either considering all patients or separating them according to neurological outcome.

Subsequently, logistic regression analyses were used to evaluate the potential of the 3 miRNAs in predicting neurological outcome in the 50 TTM patients at 6 months after cardiac arrest. Univariate logistic regression analysis showed that the 3 miRNAs were all predictors of neurological outcome (Figure 18.a.). Furthermore, after adjustment with each of the 27 variables listed in Table 7, the 3 miRNAs were still independent predictors of neurological outcome (Figure 18.b.).

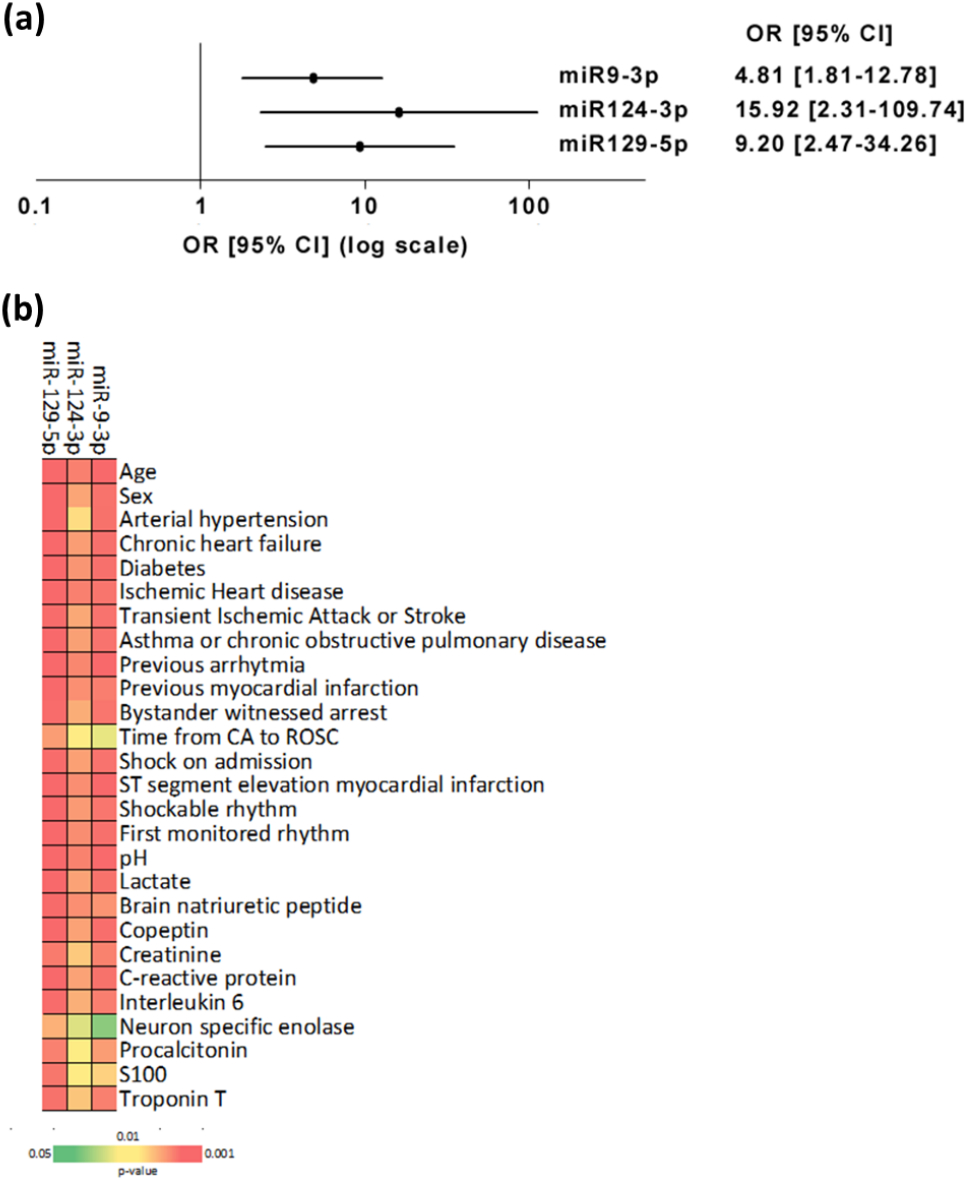


Figure 18. Univariate (a) and multivariable (b) logistic regression analysis to evaluate the potential of miR9-3p, miR124-3p and miR129-5p in predicting neurological outcome. **a.** univariate analysis was presented as a forest plot showing odds ratios (ORs) ± 95% confidence intervals (CIs) for predicting neurological outcome. **b.** multivariable logistic regression models were generated with one miRNA and one demographic or clinical variable at a time and represented as heatmap showing statistical significance. The colour scale ranges from p-value=0.05 (green) to p-value=0.001 (red) with p-value=0.01 (yellow) as the midpoint.

## 2. LncRNAs and circRNAs as prognostic biomarkers after cardiac arrest

As mentioned in the previous chapter, the potential use of miRNAs as prognostic biomarkers after cardiac arrest is now acknowledged.

Following this line of research, other ncRNAs, such as lncRNAs and circRNAs, could have similar prognostic potential after cardiac arrest. Indeed, as previously reported, dysregulation of lncRNA and circRNA expression levels has already been reported in several cardiac arrest-related diseases [22, 34, 50, 55, 440]. However, so far there is still no evidence for the prognostic potential of lncRNA and circRNA after cardiac arrest [17].

Unlike miRNAs, both lncRNAs and circRNAs are able to modulate gene expression at different levels [50] and have greater tissue and stage specificity than miRNAs [39, 51-54]. In addition, the closed structure of circRNAs makes them particularly resistant to attack by exonucleases and thus more stable than all other forms of linear ncRNAs, which results in easier detection of this class of ncRNAs [38-40].

Considering the various characteristics of lncRNAs and circRNAs, it was hypothesised that lncRNAs and circRNAs may also play roles as biomarkers, aiding in the prognostication of patients after cardiac arrest. Furthermore, because systemic inflammation after ischemia/reperfusion plays an important role in the recovery of patients after cardiac arrest [56-58], attention was turned to the modulation of lncRNA and circRNA in the immune response after cardiac arrest. Therefore, shifting the focus from studying circulating ncRNAs in plasma to ncRNAs in blood cells from PAXgene™ whole blood samples.

An article containing the results of circRNAs identified in the discovery phase and the validation of one circRNA (circNFAT5) in the TTM-trial was accepted by the *Intensive Care Medicine Experimental* journal. The journal-accepted version of the article is shown in Appendix III.

## 2.1. Discovery study: selection of candidates lncRNAs and circRNAs

PAXgene™ whole blood samples collected 48 h after ROSC from the TTM-trial were used for this study. As shown in the study flow chart, of the 939 patients enrolled in the TTM-trial, RNA samples were available at 48 h for 588 of the 643 recruited at the biobank (Figure 19). Among these 588 RNA samples, two sex-matched groups of 23 were sequenced and used in the discovery phase for identification of potential lncRNAs and circRNAs. One of the two groups included patients that completely recovered 6 months after the cardiac arrest (CPC1) while the other included patients that died at the same time point (CPC5). The remaining 542 RNA samples were used for the validation phase, to confirm the biomarker potential of the selected lncRNAs and circRNAs in the entire TTM cohort (Figure 19).

Although the CPC score was used in the discovery phase to dichotomize patients, current guidelines favour the mRS score [143], which was also the only one reported for the TTM2 cohort (considered later in this thesis work). Therefore, it was decided to keep the CPC score to dichotomize patients in the discovery phase, but to use both CPC and mRS scores in the validation phase of the TTM cohort. Indeed, this would allow a better comparison between the two cohorts TTM and TTM2 at a later stage.

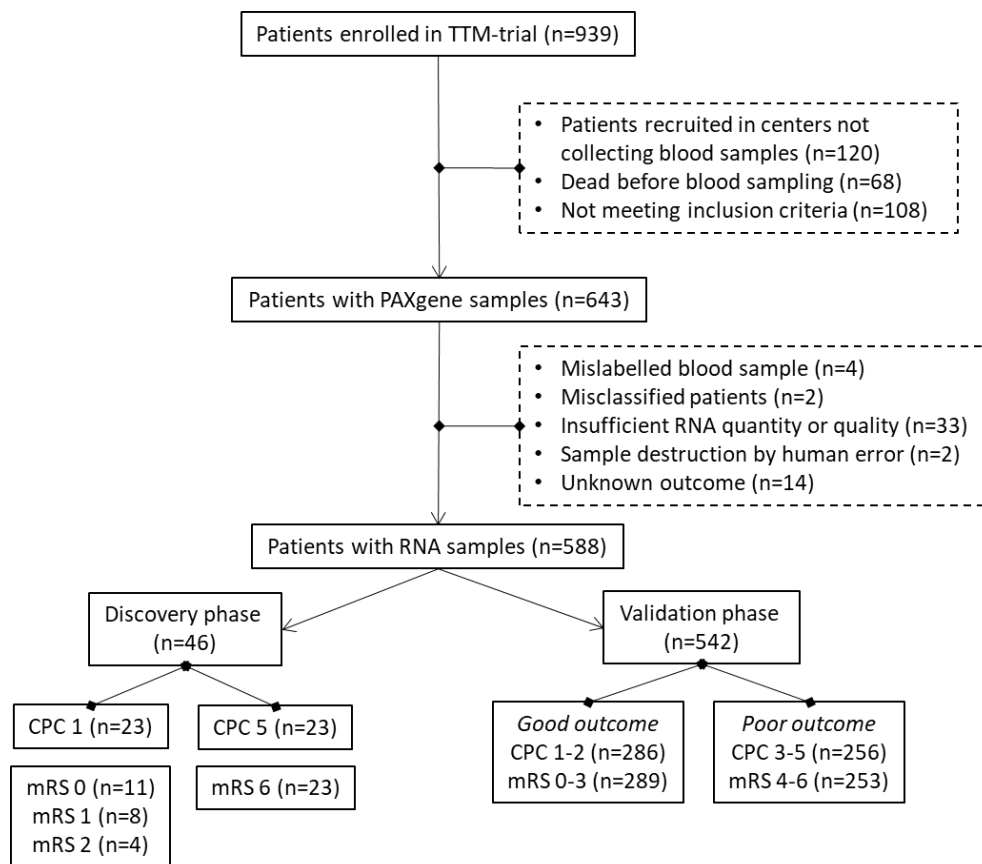


Figure 19. Study flow chart TTM-trial. Abbreviations: CPC = cerebral performance category; mRS = modified Rankin Scale.

The demographic and clinical characteristics of the discovery cohort are shown in Table 8. Unlike the CPC1 group, patients in the CPC5 group were significantly older and with a longer time from OHCA to ROSC (Table 8). Despite these, no other significant differences were observed in the characteristics considered.

Characteristics	Neurological outcome		p-value
	CPC1 (n=23)	CPC5 (n=23)	
<b>Age, years</b>	61 (41 - 80)	74 (53- 90)	<b>0.002</b>
<b>Sex</b>			1.000
Male	20 (87 %)	19 (82.6 %)	
Female	3 (13 %)	4 (17.4 %)	
<b>Co-morbidities</b>			
Hypertension	7 (30.4 %)	11 (47.8 %)	0.190
Diabetes mellitus	2 (8.7 %)	5 (21.7 %)	1.000
Known IHD	3 (13 %)	12 (52.2 %)	0.093
Previous MI	2 (8.7 %)	9 (39.1 %)	0.502
Heart failure	1 (4.3 %)	2 (8.7 %)	1.000
COPD	1 (4.3 %)	4 (17.4 %)	0.174
Previous cerebral stroke	1 (4.3 %)	3 (13 %)	1.000
<b>First monitored rhythm</b>			0.865
VF or non-perfusing VT	22 (95.7 %)	18 (78.3 %)	
Asystole or PEA	1 (4.3 %)	4 (17.4 %)	
ROSC after bystander	-	1 (4.3 %)	
<b>Witnessed arrest</b>	20 (87 %)	20 (87 %)	0.356
<b>Bystander CPR</b>	16 (69.6 %)	17 (74 %)	0.318
<b>Time from CA to ROSC (mins)</b>	20 (8 - 45)	29 (11 - 65)	<b>0.020</b>
<b>Initial serum lactate (mmol/l)</b>	3.2 (0 - 17)	4.7 (0 - 16)	0.244
<b>Shock on admission</b>	2 (8.7 %)	8 (34.8 %)	0.111

Table 8. Demographic and clinical characteristics of the 46 TTM patients (discovery cohort). The patients were dichotomized according to CPC score in CPC1 group and CPC5 group. Continuous variables are reported as median (range) while categorical variables are reported as number (frequency). Abbreviations: IHD = ischemic heart disease; MI = myocardial infarction; COPD = chronic obstructive pulmonary disease; VF = ventricular fibrillation; VT = ventricular tachycardia; PEA = pulseless electrical activity; ROSC = return of spontaneous circulation; CPR = cardiopulmonary resuscitation; CA = cardiac arrest.

Analysis of the RNA-seq data from the discovery cohort identified 41 lncRNAs and 28 circRNAs with significant differential expression levels (Table 9). The selection criteria for circRNA and lncRNA are given in the Materials and Methods section. Of the 41 lncRNAs identified, only 7 had FPKM >10 and were therefore pre-selected. Optimal primer pairs, correct amplified product by sequencing, and detectable levels in whole blood samples were obtained for only one lncRNA, lnc-IL1R1-1:2. As for circRNAs, optimal primers amplifying the correct product with detectable levels in whole blood samples were tested for each of the 28 circRNAs selected by RNA-seq. Then, the circularity of 5 of these circRNAs, circAGO2, circDLG1, circDNM2, circFAM13b, and circNFAT5, was confirmed by RNase R assay in whole blood samples from 2 sets of 8 cardiac arrest patients (Figure 20). These 5 circRNAs and lnc-IL1R1-1:2 were then measured in the discovery cohort by qPCR (Figure 21). The qPCR results showed for all selected candidates the same tendency to increase in the CPC5 group as observed in RNA-seq, with the exception of circDLG1. Indeed, while in the RNA-seq data circDLG1 was decreasing in CPC5 patients, the qPCR data showed the opposite trend (Figure 21). Although a statistically significant increase in the CPC5 group was observed only for circFAM13b and circDNM2, all 6 candidates were measured in the entire TTM cohort in order to obtain more reliable results from a larger sample size.

CircRNAs				LncRNAs			
ID_circRNAs	Counts	log2FoldChange	p-value	ID_lncRNAs	FPKM	log2FoldChange	p-value
circAFF2	28.88	0.62	0.007	<b>NEAT1:15</b>	<b>187.31</b>	<b>1.09</b>	<b>0.039</b>
circARHGGEF12	9.13	1.02	0.006	<b>NEAT1:26</b>	<b>72.51</b>	<b>1.32</b>	<b>0.026</b>
circFRMD4A	8.6	-0.57	0.015	<b>lnc-CLEC4D-2:1</b>	<b>61.73</b>	<b>0.55</b>	<b>0.006</b>
circDLG1	8.49	-0.62	0.012	<b>lnc-PI3-1:2</b>	<b>18.73</b>	<b>-0.49</b>	<b>0.013</b>
circWNK1	5.87	0.92	0.001	<b>lnc-BRF1-31:16</b>	<b>14.32</b>	<b>2.26</b>	<b>0.037</b>
circFAM13b	5.74	1.15	8.23E-05	<b>NEAT1:27</b>	<b>13.55</b>	<b>1.83</b>	<b>0.003</b>
circITGAL	4.87	0.83	0.017	<b>lnc-IL1R1-1:2</b>	<b>11.06</b>	<b>0.44</b>	<b>0.019</b>
circTFDP1	4.15	0.98	0.009	NEAT1:25	6.82	1.9	0.017
circFCHO2	4.01	0.88	0.021	lnc-BRF1-9:3	6.16	1.48	0.049
circDPY19L1P1	3.98	0.92	0.021	lnc-HECA-1:9	4.71	2.91	0.042
circCCDC9	3.72	0.88	0.004	lnc-GALNT14-3:1	2.27	2.15	0.008
circPROSC	3.09	0.95	0.016	lnc-ADIPOQ-3:4	2.11	2.44	0.049
circDNAJC6	2.72	0.74	0.049	lnc-TEX9-2:1	2.05	-2.59	0.047
circCHD2	2.63	-0.78	0.034	lnc-C21orf62-4:3	2.03	3.47	0.005
circFOXK2	2.35	1.19	0.002	lnc-METTL2B-3:16	1.91	-4.24	0.017
circNFAT5	2.17	0.99	0.024	lnc-STRBP-2:1	1.89	-1.42	0.015
circSPI1	2.05	1.26	0.001	lnc-CECR2-8:1	1.76	-1.21	0.041
circPOLE2	2.04	1.19	0.014	lnc-CASZ1-3:1	1.58	-2.18	0.006
circRIPK1	2	1.15	0.012	NEAT1:22	1.28	3.14	0.036
circCDC73	1.95	0.89	0.044	lnc-ATP2A2-5:1	1.28	-1.18	0.036
circNUP50	1.9	0.86	0.047	lnc-PAQR9-3:3	1.23	1.8	0.042
circDNM2	1.77	1.34	0.007	lnc-HECA-1:8	1.23	2.98	0.017
circMYO1F	1.74	1.5	0.004	lnc-TSSK3-1:1	1.2	-1.13	0.044
circR3HDM1	1.69	1.04	0.04	lnc-ARL11-1:1	1.19	-1.41	0.023
circDOPEY2	1.63	1.97	2.39E-04	lnc-ADRA2C-1:1	1.16	-1.2	0.048
circAGO2	1.52	0.9	0.045	lnc-LCE3A-1:1	1.12	-1.34	0.033
circTMEM65	1.32	2.07	3.29E-04	lnc-STIL-7:1	1.02	-1.09	0.048
circFAM193A	1.13	-1.19	0.036	lnc-CYP7B1-7:1	1.02	-1.25	0.028
				lnc-FBXL16-1:1	1	-1.53	0.009
				lnc-JHY-2:1	1	-1.09	0.049
				lnc-RRP1B-1:1	0.99	-1.81	0.046
				lnc-ANGPTL4-2:1	0.98	-1.61	0.004
				lnc-RNASE4-1:1	0.98	-1.4	0.032
				lnc-PEX19-4:2	0.87	8.39	0.009
				lnc-ADARB2-1:1	0.79	-1.22	0.026
				lnc-SLC12A7-2:1	0.79	-1.13	0.037
				lnc-ORC4-2:1	0.73	-1.18	0.033
				CCNT2-AS1:20	0.71	2.22	0.045
				NEAT1:29	0.65	2.49	0.047
				lnc-MRPL11-1:14	0.59	2.53	0.05
				lnc-CYB5RL-4:1	0.52	-5.47	0.019

Table 9. List of differentially expressed circRNAs (left) and lncRNAs (right) identified in the RNA-seq of the 46 TTM patients. A positive log2 fold-change indicates a higher level in patients with poor outcome (CPC 5) than in those with good outcome (CPC 1). Highlighted in bold are the lncRNAs with FPKM >10. Abbreviation: FPKM = Fragments Per Kilobase of transcript per Million mapped reads.



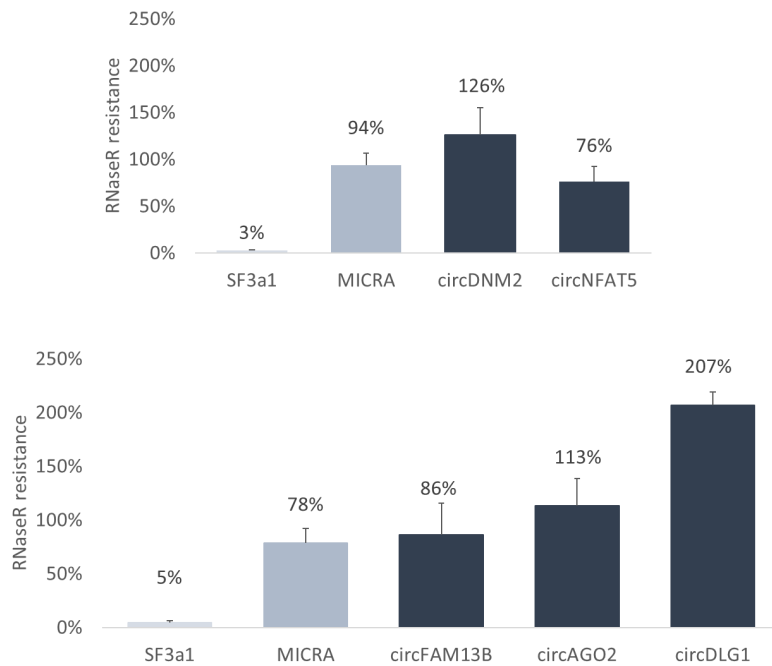


Figure 20. Bar graphs showing the confirmed circularity of 5 circRNAs identified in the RNA-seq data of the discovery cohort. Circularity was measured as the percentage of resistance to RNase R treatment. Linear transcript SF3a1 was used as the negative control of the experiment, and circRNA MICRA as the positive control. 500 ng of total RNA from whole blood PAXgene™ samples from 2 sets of 8 cardiac arrest patients (represented in 2 separate charts) were treated by RNase R prior reverse-transcription and qPCR.

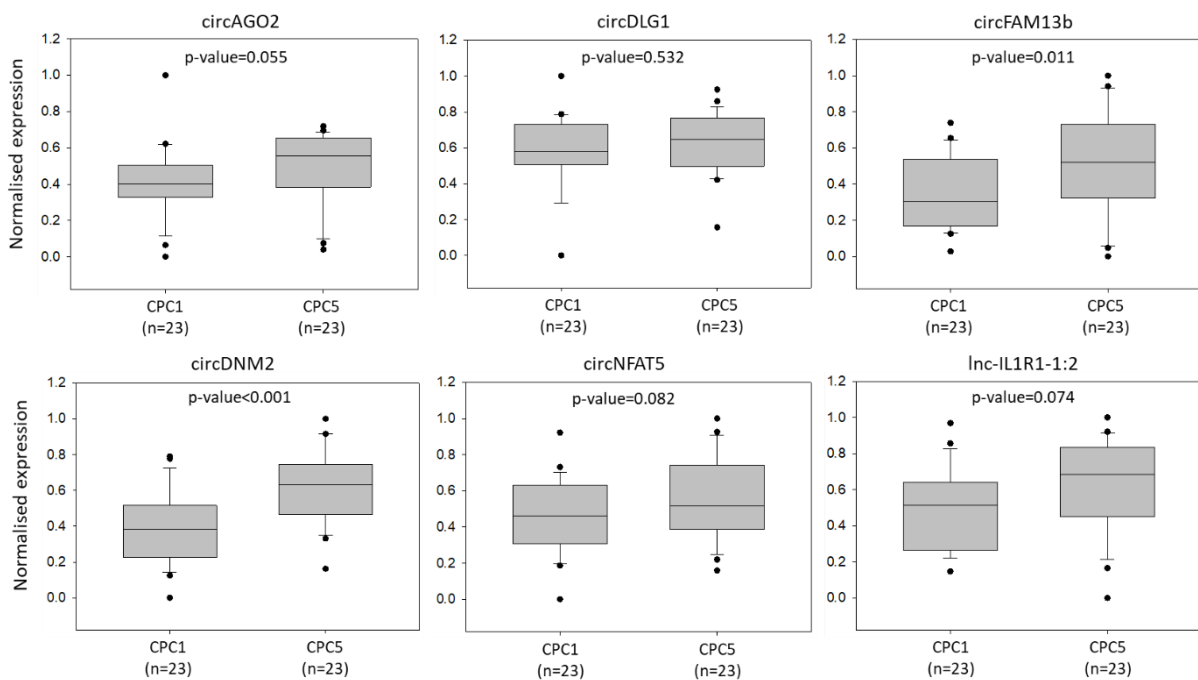


Figure 21. Box plots showing the differential expression of the 5 circRNAs and 1 lncRNA in the discovery cohort according to the neurological outcome of the patients (CPC1 or CPC5). Candidate expression levels were normalized, log2-transformed, and scaled. P-values were derived from the Mann-Whitney U test.

In addition, correlation analyses between the 6 candidates and established markers of cardiac arrest allowed the evaluation of potential relationships and thus potential dysfunction that these candidates might reflect in patients after cardiac arrest. In fact, the established biomarkers of cardiac arrest selected for correlation analyses are indicative of various dysfunctions, such as cerebral (NSE [49, 251, 454], S100 [266, 455]), renal (creatinine) [456, 457] and cardiovascular (BNP [458], copeptin [289, 459, 460] and TNT [286, 461]), as well as inflammation (CRP [462, 463], IL6 [291, 464] and PCT [290, 465, 466]).

All correlation analyses performed showed a correlation coefficient (r) of less than 0.5 (Table 10). Among the highest correlations found, a significant correlation was observed between circDNM2 and both brain damage biomarkers NSE and S100, with a correlation coefficient of 0.491 (p-value=0.001) and 0.449 (p-value=0.002), respectively. More moderate correlations were also observed between circFAM13b, circNFAT5 and lnc-IL1R1-1:2 with the same brain markers. CircDNM2 was also correlated with creatinine, a marker of renal damage (r=0.407; p-value=0.005) and BNP, a marker of cardiovascular dysfunction (r=0.422 p-value=0.004). Finally, among inflammatory markers, the highest correlation was observed between PCT and circDNM2 with r = 0.494 (p-value=0.001).

		Established cardiac arrest markers								
		Brain damage		Kidney damage	Cardiac dysfunction			Inflammation		
		NSE	S100	Creatinine	BNP	Copeptin	TNT	CRP	IL6	PCT
circRNAs	<i>circAGO2</i>	0.20	0.20	0.16	0.27	0.10	-0.19	-0.09	0.07	0.26
	<i>circDLG1</i>	0.09	0.19	-0.08	0.01	-0.06	-0.18	-0.07	-0.11	0.17
	<i>circFAM13b</i>	<b>0.35</b>	<b>0.30</b>	0.18	0.25	0.14	-0.11	0.05	0.08	0.25
	<i>circDNM2</i>	<b>0.49</b>	<b>0.45</b>	<b>0.41</b>	<b>0.42</b>	<b>0.34</b>	-0.05	0.11	0.26	<b>0.49</b>
	<i>circNFAT5</i>	<b>0.32</b>	<b>0.35</b>	0.09	0.16	0.18	-0.19	0.04	0.14	0.26
	<i>lncIL1R1-1 :2</i>	<b>0.36</b>	<b>0.33</b>	0.21	0.29	<b>0.33</b>	0.11	0.15	0.16	0.26

r values


Lowest (r=-0.19)  Highest (r=0.49)

Table 10. Spearman correlations between 5 circRNAs and 1 lncRNA with established prognostication markers of cardiac arrest. Spearman correlation coefficients (r) are shown in the table for each correlation performed. Statistically significant correlations (p-value < 0.05) are highlighted in bold. Abbreviations: NSE= neuron-specific enolase; S100= serum S100 protein; BNP= B-type natriuretic peptide; TNT= troponin T; CRP= C-reactive protein; IL6= interleukin-6; PCT= procalcitonin.

## 2.2. Biomarker potential assessment of the selected candidates in the whole TTM cohort

Validation of the 5 circRNAs and 1 lncRNA began with measurement by qPCR in the remaining 542 TTM patients not enrolled in the discovery phase. Of these patients, 241 were treated with targeted temperature at 33°C and 301 at 36°C. Patients were dichotomized using both CPC and mRS scores assessed 6 months after OHCA. The differences between the groups of patients divided according to CPC or mRS score were minimal. In fact, only 3 fewer patients had an unfavourable neurological outcome when considering mRS score (mRS 4-6, n=253) instead of CPC (CPC 4-5, n=256) (Figure 19).

The demographic and clinical characteristics of patients with good (CPC1-2 or mRS 0-3) or poor (CPC3-5 or mRS 4-6) neurological outcome are shown in Table 11. Similar to what was observed in the discovery cohort, in the entire TTM cohort, patients with poor outcome were older and presented with longer times from cardiac arrest to ROSC. In addition, these patients also more often had comorbidities, such as hypertension, diabetes mellitus, heart failure, and chronic obstructive pulmonary disease, higher lactate levels, and more frequently were in shock on admission (Table 11).

Characteristics	Neurological outcome		p-value	Neurological outcome		p-value
	CPC1-2 n=286	CPC3-5 n=256		mRS 0-3 n=289	mRS 4-6 n=253	
<b>Age, years</b>	60 (20-90)	68 (35-94)	<b>&lt;0.001</b>	60 (20-90)	68 (35-94)	<b>&lt;0.001</b>
<b>Sex</b>			0.405			0.464
Male	238 (83.2%)	205 (80.1%)		240 (83%)	203 (80.2%)	
Female	48 (16.8%)	51 (19.9%)		49 (17%)	50 (19.8%)	
<b>Co-morbidities</b>						
Hypertension	101 (35.3%)	124 (48.4%)	<b>0.003</b>	105 (36.3%)	120 (47.4%)	<b>0.032</b>
Diabetes mellitus	31 (10.8%)	44 (17.2%)	<b>0.044</b>	30 (10.4%)	45 (17.8%)	<b>0.044</b>
Known IHD	65 (22.7%)	74 (28.9%)	0.122	64 (22.1%)	75 (29.6%)	0.073
Previous MI	46 (16.1%)	57 (22.26)	0.085	45 (15.6%)	58 (22.9%)	<b>0.039</b>
Heart failure	7 (2.4%)	20 (7.8%)	<b>0.008</b>	7 (2.4%)	20 (7.9%)	<b>0.008</b>
COPD	18 (6.3%)	31 (12.1%)	<b>0.027</b>	19 (6.6%)	30 (11.9%)	<b>0.047</b>
Renal failure	1 (0.3%)	4 (1.6%)	0.306	1 (0.3%)	4 (1.6%)	0.294
Previous cerebral stroke	16 (5.6%)	24 (9.4%)	0.129	16 (5.5%)	24 (9.5%)	0.138
Alcohol abuse	7 (2.4%)	10 (3.9%)	0.468	7 (2.4%)	10 (4%)	0.333
<b>First monitored rhythm</b>			<b>&lt;0.001</b>			<b>&lt;0.001</b>
VF or non-perfusing VT	260 (90.9%)	170 (66.4%)		262 (90.7%)	168 (66.4%)	
Asystole or PEA	17 (5.9%)	77 (30.1%)		17 (5.9%)	77 (30.4%)	
ROSC after bystander	7 (2.4%)	1 (0.4%)		7 (2.4%)	1 (0.4%)	
unknown	2 (0.7%)	8 (3.1%)		3 (1%)	7 (2.8%)	
<b>Witnessed arrest</b>	262 (91.6%)	223 (87.1%)	0.118	265 (91.7%)	220 (87%)	0.098
<b>Bystander CPR</b>	229 (80.1%)	168 (65.6%)	<b>&lt;0.001</b>	234 (81%)	163 (64.4%)	<b>&lt;0.001</b>
<b>Time from CA to ROSC (mins)</b>	20 (0 - 160)	30 (0 - 170)	<b>&lt;0.001</b>	20 (0 - 160)	30 (0 - 170)	<b>&lt;0.001</b>
<b>Initial serum lactate (mmol/l)</b>	4.4 (0 - 20)	6.5 (0 - 21.3)	<b>&lt;0.001</b>	5 (1 - 20)	7 (1 - 21)	<b>&lt;0.001</b>
<b>Shock on admission</b>	23 (8%)	38 (14.8%)	<b>0.010</b>	25 (8.7%)	36 (14.2%)	0.056

Table 11. Demographic and clinical characteristics of 542 TTM patients (validation cohort). Patients were dichotomised using CPC and mRS scores. Continuous variables are reported as median (range) while categorical variables are reported as number (frequency). Abbreviations as in Table 8.

The differential expression levels of the selected candidates were evaluated according to the targeted temperature regimen used (Figure 22.a.), sex (Figure 22.b.) and neurological outcome (Figure 22.c.) of all patients or of patients separated according to the temperature treatment used. When dichotomizing patients according to the targeted temperature management, only circDNM2 showed significant differential expression, indicating that temperature could indeed influence the expression of this circRNA (Figure 22.a.). In contrast, no change was observed when separating patients according to their sex (Figure 22.b.). Therefore, none of the selected candidates appeared to exhibit sex specificity. Finally, higher levels of all selected candidates were observed in patients with unfavourable outcome compared with those with favourable outcome confirming the trends observed in RNA-seq and qPCR measurements in the discovery cohort, except for circDLG1 (Figure 22.c.). Indeed, in contrast to what was reported in RNA-seq and similar to what was obtained in qPCR measurements in the discovery cohort, circDLG1 showed increased expression in the group with unfavourable outcome in the entire TTM cohort as well.

Finally, similar results were also obtained when dichotomizing patients according to neurological outcome with the mRS score instead of the CPC score (Figure 22.c.).

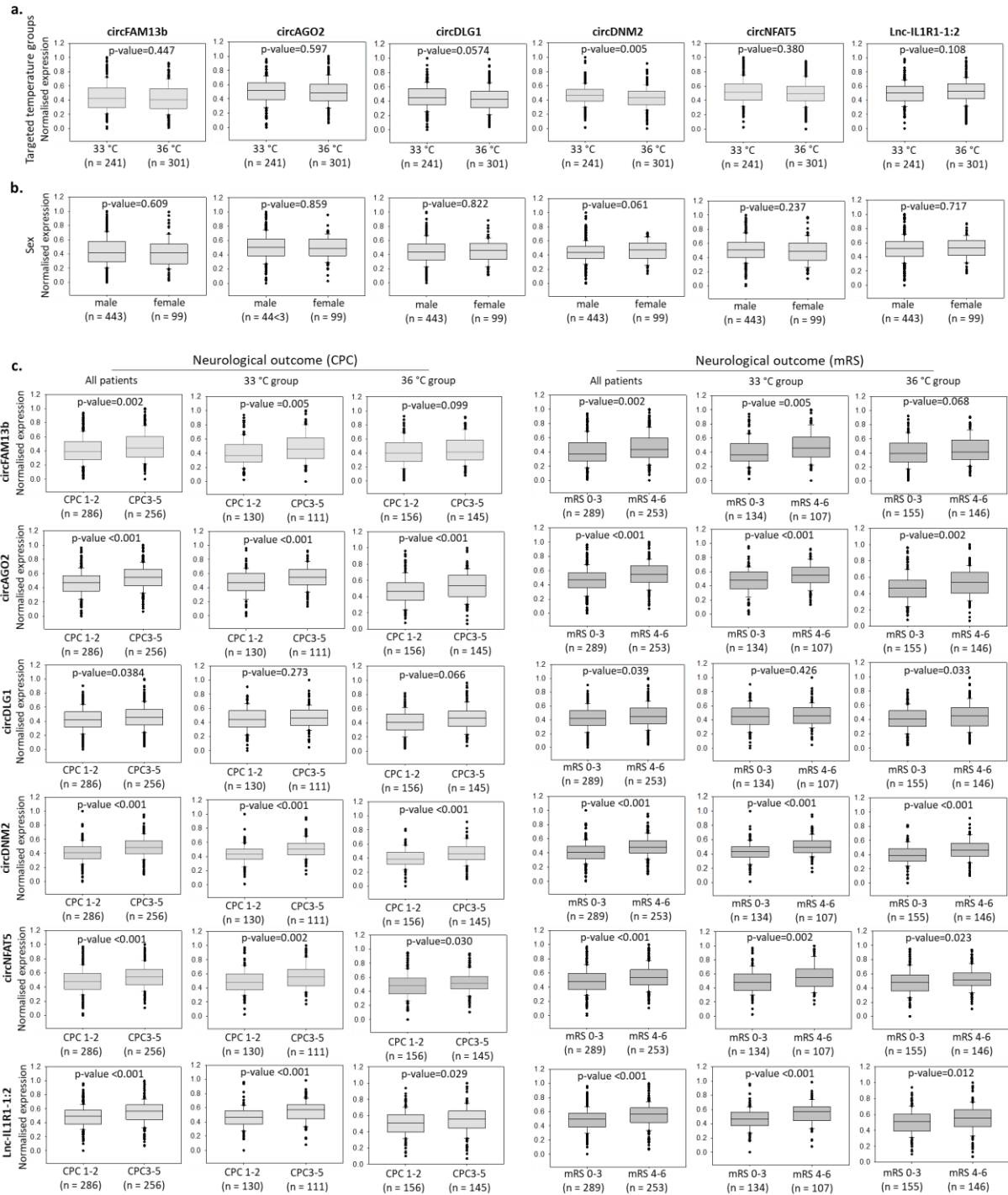


Figure 22. Differential expression levels of 5 circRNAs and 1 lncRNA in the 542 TTM patients of the validation cohort. Candidate expression levels were compared by temperature regime and independent of neurological outcome (a.), by patient sex (b.), by neurological outcome (c.) independent of temperature regime, and separately in patients treated at 36°C or 33°C. Patients were dichotomized according to neurological outcome using both CPC and mRS scores. Candidate expression levels were normalized, log<sub>2</sub>-transformed and scaled. P-values were derived from the Mann-Whitney U test.

### 2.2.1. Predicting 6-month neurological outcome in the TTM validation cohort

The potential of candidates in predicting neurological outcome at 6 months after OHCA was assessed by univariate and multivariable logistic regression analysis using both CPC and mRS scores to classify patients. The multivariable model included variables previously selected in past studies on this clinical trial, which were age, sex, first monitored rhythm, bystander CPR, circulatory shock on admission, targeted temperature regimen, time from cardiac arrest to ROSC, initial serum lactate levels and NSE levels. Analyses were performed considering both all patients and patients separated according to the temperature regimen used.

Regardless of the neurological outcome score used to classify patients, univariate analyses showed that all candidates were predictors of neurological outcome (Figure 23.a). For some candidates, such as circDLG1, circFAM13b and circNFAT5, the predictive potential was lost when only patients treated at 33°C or 36°C were considered (Figure 23.b.c.). However, after adjustment with clinical variables included the basal model for multivariable analysis, only circNFAT5 remained an independent predictor of neurological outcome at 6 months in TTM, with OR [95% CI; p-value]: 1.39 [1.07-1.83; 2.0E-02] when using the CPC score (Figure 24) and 1.40 [1.07-1.84; 0.016] when using the mRS score (Figure 25).

In addition, the candidate incremental value for predicting neurological outcome was determined using AIC. For the prediction of neurological outcome using the CPC as the classification score, the lowest AIC was observed when incorporating circNFAT5 into the basal model, both when considering all patients (LRT p-value= 0.015; Wald test p-value=4.23E-21) and only the 33°C group (LRT p-value= 0.003; Wald test p-value= 2.84E-08) (Table 12). This was associated with an AUC, NRI and IDI of 0.908, 0.272 and 0.05 respectively when considering all patients and 0.908, 0.494 and 0.021 when considering only the 33°C treated group (Table 12). However, when considering only the 36°C-treated group, the lowest AIC was observed when adding IncIL1R1-1:2 in the basal model (LRT p-value= 0.02; Wald test p-value=8.30E-11), with AUC of 0.926, NRI of 0.343 and IDI of 0.013 (Table 12). Similar results were obtained using the mRS score (Table 13).

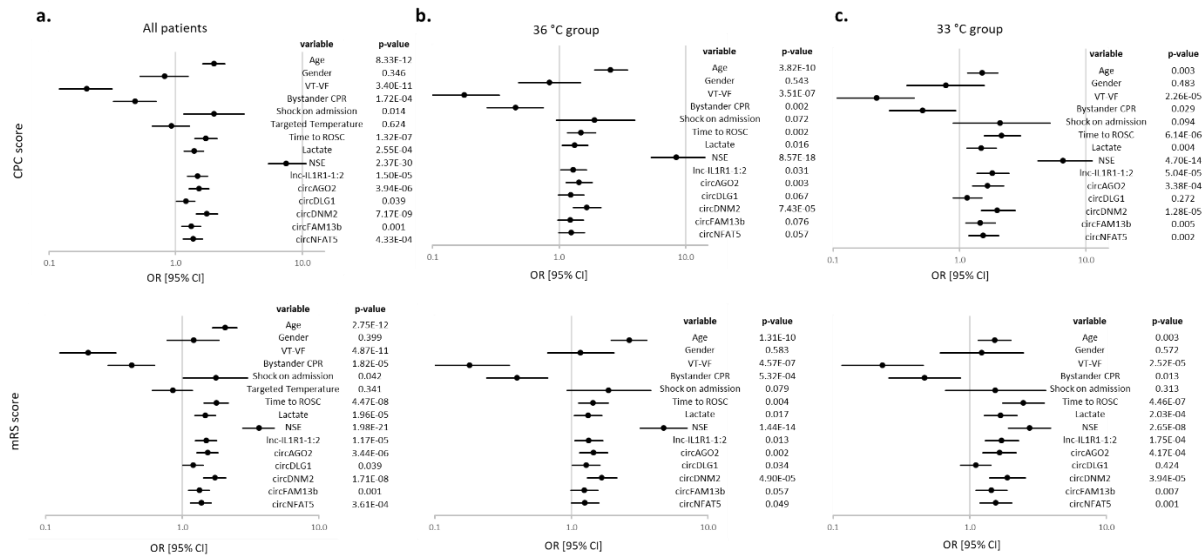


Figure 23. Univariate logistic regression analyses to predict 6-month neurological outcome in TTM validation cohort. Patients were dichotomised according to their neurological outcome using both CPC and mRS score. Analyses were performed using all patients (a.) patients treated with a targeted temperature regimen of 36°C (b.) or 33°C (c.). The forest plots show the odd ratio (OR) with  $\pm$  95% confidence interval [95% CI] and p-values are indicated for each variable. Abbreviations: VT-VF = ventricular tachycardia – ventricular fibrillation, CPR = cardiopulmonary resuscitation, ROSC = return of spontaneous circulation, NSE = neuron-specific enolase.

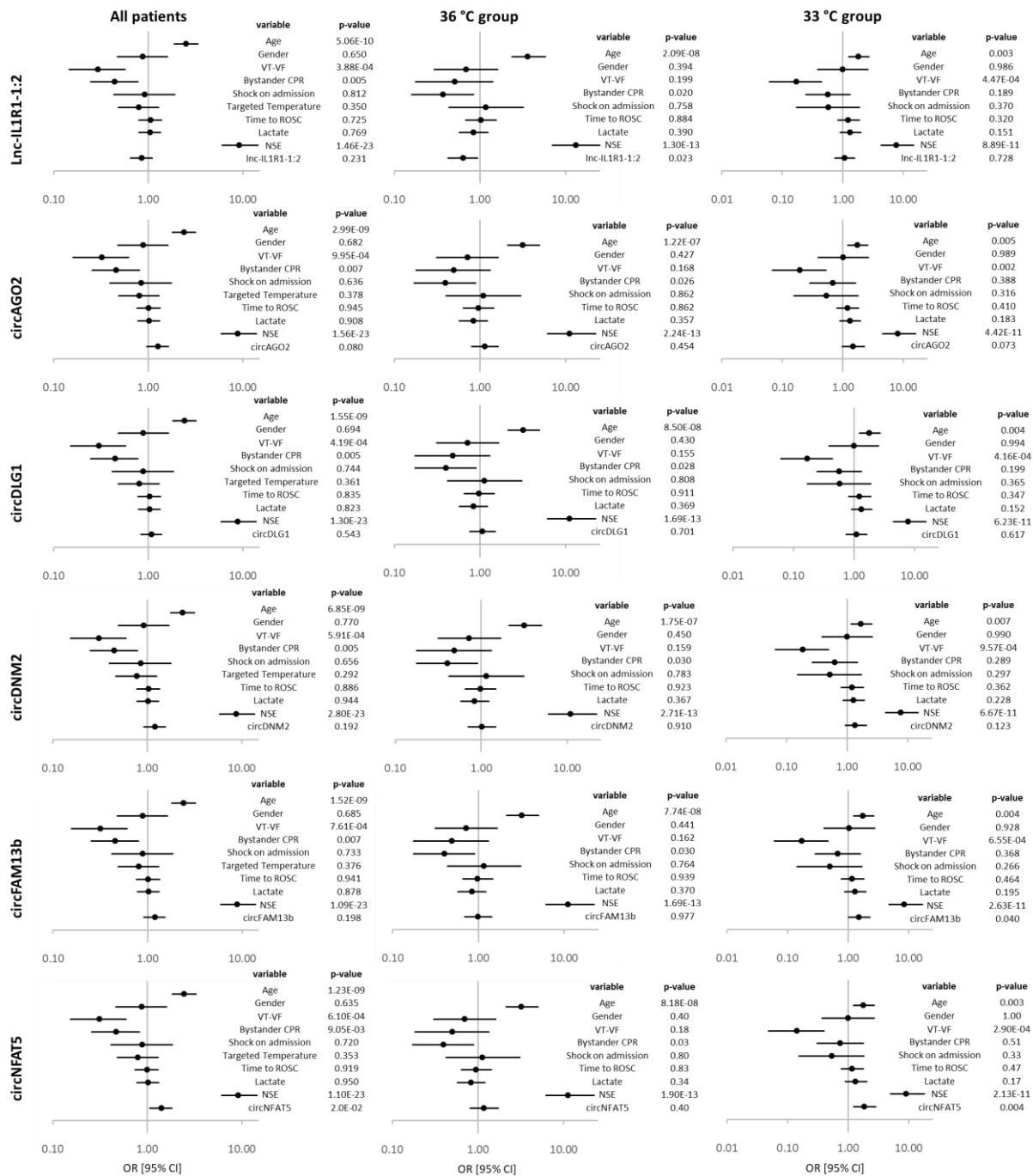
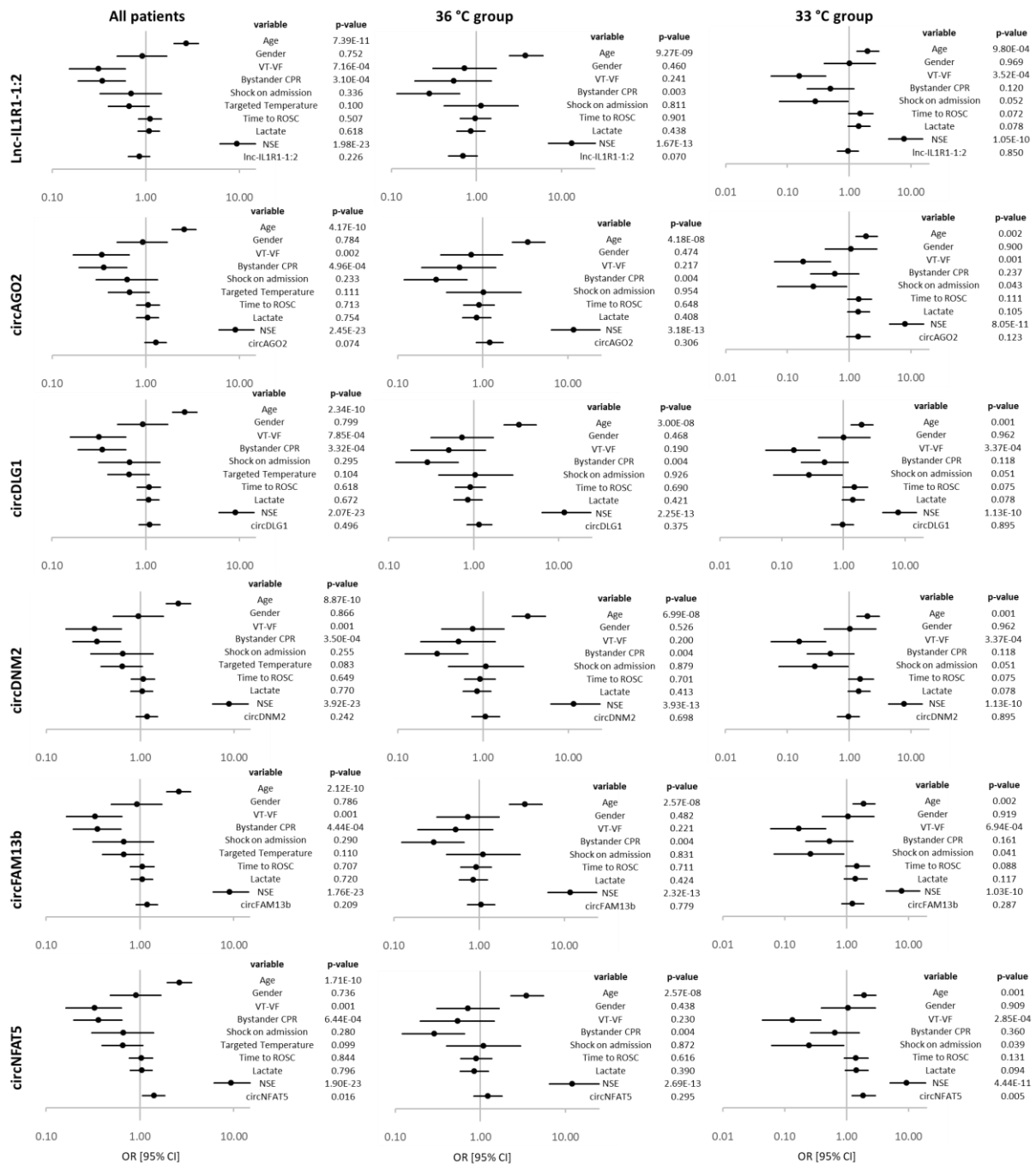


Figure 24. Multivariable logistic regression analyses using CPC score to predict 6-month neurological outcome in the TTM validation cohort. The forest plots show the odd ratio (OR) with  $\pm$  95% confidence interval [95% CI] and the p-values are indicated for each variable. Abbreviations are the same as presented in Figure 23.





		AIC	Wald_p	AUC	lr_p	NRI	NRI_p	IDI	IDI_p	
CPC score	All patients	basal model	433	1.14E-21	0.906	-	-	-	-	-
		basal model + lnc-IL1R1-1:2	434	3.81E-21	0.906	0.228	0.048	0.579	0.001	0.437
		basal model + circAGO2	432	4.02E-21	0.907	0.078	0.160	0.063	0.003	0.216
		basal model + circDLG1	435	4.50E-21	0.906	0.543	0.123	0.152	0.000	0.988
		basal model + circDNM2	433	4.14E-21	0.906	0.190	0.107	0.215	0.002	0.397
		basal model + circFAM13b	433	3.14E-21	0.906	0.196	0.065	0.448	0.001	0.578
		basal model + circNFAT5	429	4.23E-21	0.908	<b>0.015</b>	0.272	<b>0.001</b>	0.005	0.150
	36° group	basal model	229	2.59E-11	0.920	-	-	-	-	-
		basal model + lnc-IL1R1-1:2	226	8.30E-11	0.926	<b>0.020</b>	0.343	<b>0.002</b>	0.013	<b>0.050</b>
		basal model + circAGO2	231	8.29E-11	0.921	0.454	0.084	0.467	0.002	0.317
		basal model + circDLG1	231	7.62E-11	0.921	0.701	0.071	0.538	3.23E-04	0.773
		basal model + circDNM2	231	7.54E-11	0.920	0.910	-0.154	0.181	1.87E-05	0.952
		basal model + circFAM13b	231	7.55E-11	0.920	0.977	0.065	0.572	-2.68E-05	0.738
		basal model + circNFAT5	231	7.90E-11	0.921	0.399	0.175	0.128	0.002	0.309
	33° group	basal model	209	6.60E-09	0.899	-	-	-	-	-
		basal model + lnc-IL1R1-1:2	211	1.74E-08	0.900	0.728	0.258	<b>0.044</b>	0.001	0.531
		basal model + circAGO2	208	1.79E-08	0.903	0.068	0.215	0.094	0.010	0.131
		basal model + circDLG1	211	1.96E-08	0.900	0.617	0.299	<b>0.019</b>	1.92E-04	0.912
		basal model + circDNM2	209	1.84E-08	0.902	0.115	0.194	0.131	0.008	0.152
		basal model + circFAM13b	207	2.00E-08	0.904	<b>0.038</b>	0.291	<b>0.022</b>	0.009	0.217
		basal model + circNFAT5	203	2.84E-08	0.908	<b>0.003</b>	0.494	<b>7.72E-05</b>	0.021	<b>0.045</b>

Table 12. Candidate performance to predict 6-month neurological outcome in TTM validation cohort using CPC score. The basal model includes the following variables: age, sex, first monitored rhythm, bystander CPR, circulatory shock on admission, targeted temperature regimen, time from CA to ROSC, initial serum lactate levels and NSE levels at 48 h. Abbreviations: AIC = Akaike Information Criterion; AUC = Area Under the Curve; CPR = cardiopulmonary resuscitation; IDI = Integrated Discrimination Improvement; IDI\_p = Integrated Discrimination Improvement p-value; lr\_p = Likelihood Ratio Test p-value; NRI = Net Reclassification Improvement; NRI\_p = Net Reclassification Improvement p-value; Wald\_p = Wald test p-value.

		AIC	Wald_p	AUC	lr_p	NRI	NRI_p	IDI	IDI_p	
mRS score	All patients	basal model	424	1.11E-21	0.910					
		basal model + Inc-IL1R1-1:2	425	3.65E-21	0.910	0.224	0.033	0.701	0.001	0.447
		basal model + circAGO2	423	4.56E-21	0.912	0.072	0.159	0.064	0.004	0.187
		basal model + circDLG1	426	4.59E-21	0.910	0.495	0.130	0.130	4.26E-05	0.968
		basal model + circDNM2	425	4.47E-21	0.910	0.240	0.113	0.188	0.001	0.494
		basal model + circFAM13b	425	3.35E-21	0.910	0.207	0.085	0.324	0.001	0.598
		basal model + circNFAT5	420	5.18E-21	0.912	<b>0.015</b>	0.285	<b>0.001</b>	0.005	0.163
	36° group	basal model	225	3.21E-11	0.924	-	-	-	-	-
		basal model + Inc-IL1R1-1:2	224	8.53E-11	0.928	0.065	0.288	<b>0.012</b>	0.008	0.138
		basal model + circAGO2	226	1.15E-10	0.926	0.306	0.192	0.095	0.004	0.190
		basal model + circDLG1	226	9.37E-11	0.925	0.373	0.207	0.071	2.16E-03	0.404
		basal model + circDNM2	227	9.54E-11	0.924	0.698	-0.060	0.605	3.62E-04	0.735
basal model + circFAM13b		227	9.18E-11	0.924	0.779	0.030	0.795	4.41E-04	0.570	
basal model + circNFAT5		226	1.07E-10	0.925	0.295	0.216	0.059	0.003	0.252	
33° group	basal model	199	3.79E-09	0.910	-	-	-	-	-	
	basal model + Inc-IL1R1-1:2	201	1.01E-08	0.910	0.850	-0.189	0.144	0.000	0.946	
	basal model + circAGO2	199	1.01E-08	0.913	0.118	0.196	0.128	0.007	0.186	
	basal model + circDLG1	201	9.83E-09	0.910	0.895	-0.136	0.292	2.37E-04	0.598	
	basal model + circDNM2	200	1.10E-08	0.912	0.283	0.136	0.291	0.003	0.377	
	basal model + circFAM13b	198	1.39E-08	0.914	0.067	0.282	<b>0.027</b>	0.006	0.347	
	basal model + circNFAT5	193	2.22E-08	0.919	<b>0.004</b>	0.506	<b>5.42E-05</b>	0.019	0.056	

Table 13. Candidate performance to predict 6-month neurological outcome in TTM validation cohort using mRS score. Same variables of the basal model and abbreviations are the same as presented in Table 12.

### 2.2.2. Prediction 6-month survival in TTM validation cohort

The ability of candidates to predict 6-month survival was evaluated using Kaplan-Meier survival curves and Cox proportional hazards models. For each candidate, the Youden index was used to generate Kaplan-Meier survival curves. For all candidates, a significantly lower survival probability was observed in patients with candidate expression levels above the cut-off values (Figure 26).

In univariate Cox proportional hazards models, all candidates were predictors of survival at 6 months, except for circDLG1 when only the group of patients treated at 33 °C was considered (Figure 27). After adjustment with the same demographic and clinical variables previously used, among selected candidates and considering all TTM patients in the validation cohort, only circFAM13b and circNFAT5 remained independent predictors of 6-month survival with HR [95% CI; p-value] of 1.23 [1.07-1.42; 0.004] and 1.27 [1.10-1.46; 1.2E-03] respectively (Figure 28). While circNFAT5 continued to be an independent predictor of 6-month survival even when considering the separate TTM groups, circFAM13b was still an independent predictor only in the 33°C group (HR [95% CI; p-value] of 1.35 [1.08-1.68; 0.007]) but not in the 36°C group (Figure 28). In addition, circDNM2 was a 6-month survival independent predictor only in the 36°C group with a HR [95% CI; p-value] of 1.27 [1.04-1.55; 0.019] (Figure 28). Among all candidates, circNFAT5 showed the best performance in improving the survival model, with the lowest AIC (LRT p-value=3.91E-04; Wald test p-value=8.62E-74) associated with a C-index of 0.85 (Table 14).

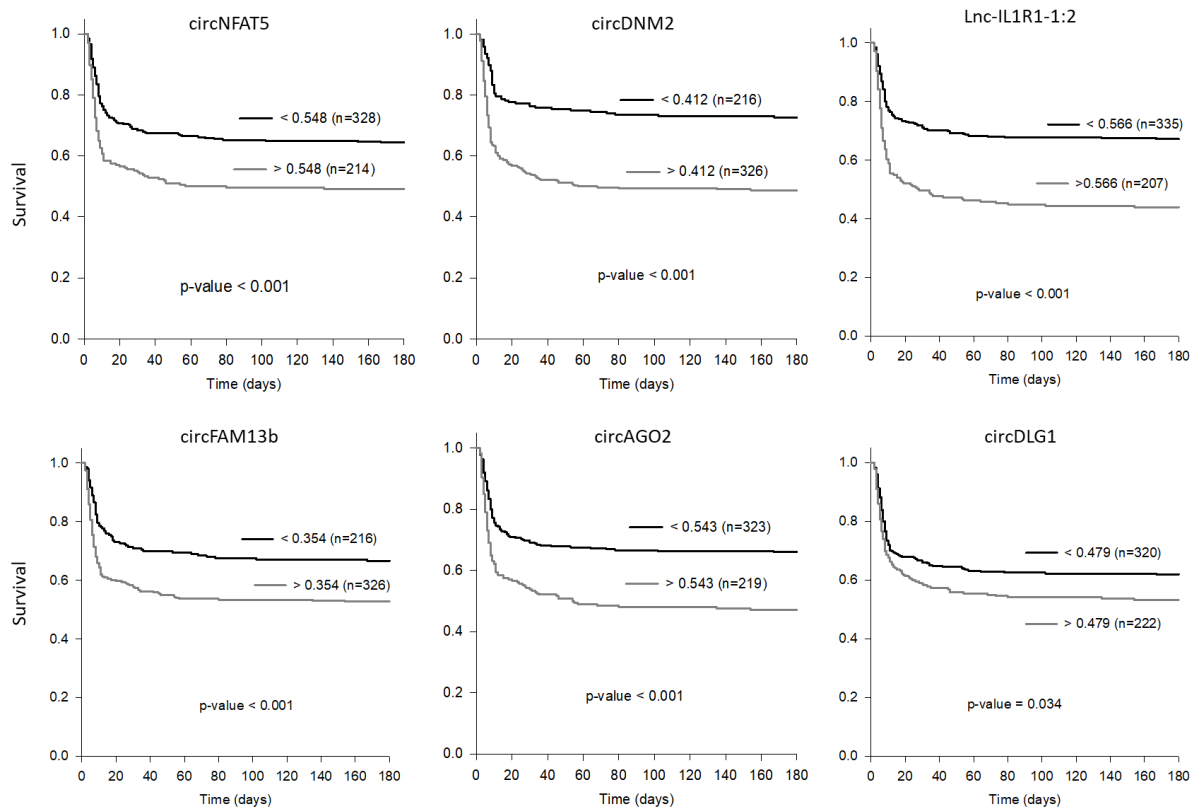


Figure 26. Kaplan-Meier curves in the TTM study at 6 months after CA, using Youden index as cut-off value. P-values are shown for each survival analysis. The number of patients with expression levels of each candidate above or below the cut-off is shown in parentheses.

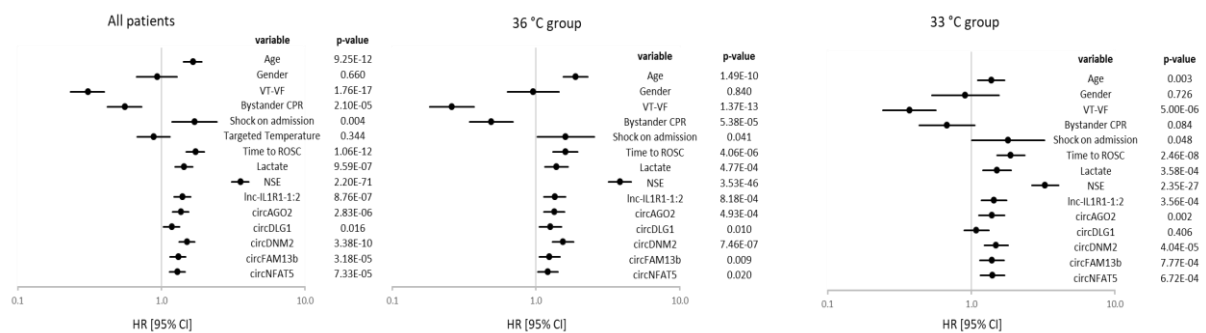


Figure 27. Univariate Cox proportional hazards for 9 independent variables plus selected candidates for survival prediction in the TTM validation cohort. Data in the forest plots are shown as hazard ratios (HR) with  $\pm$  95% confidence interval [95% CI], and p-values are given for each variable. Abbreviations as in Figure 23.

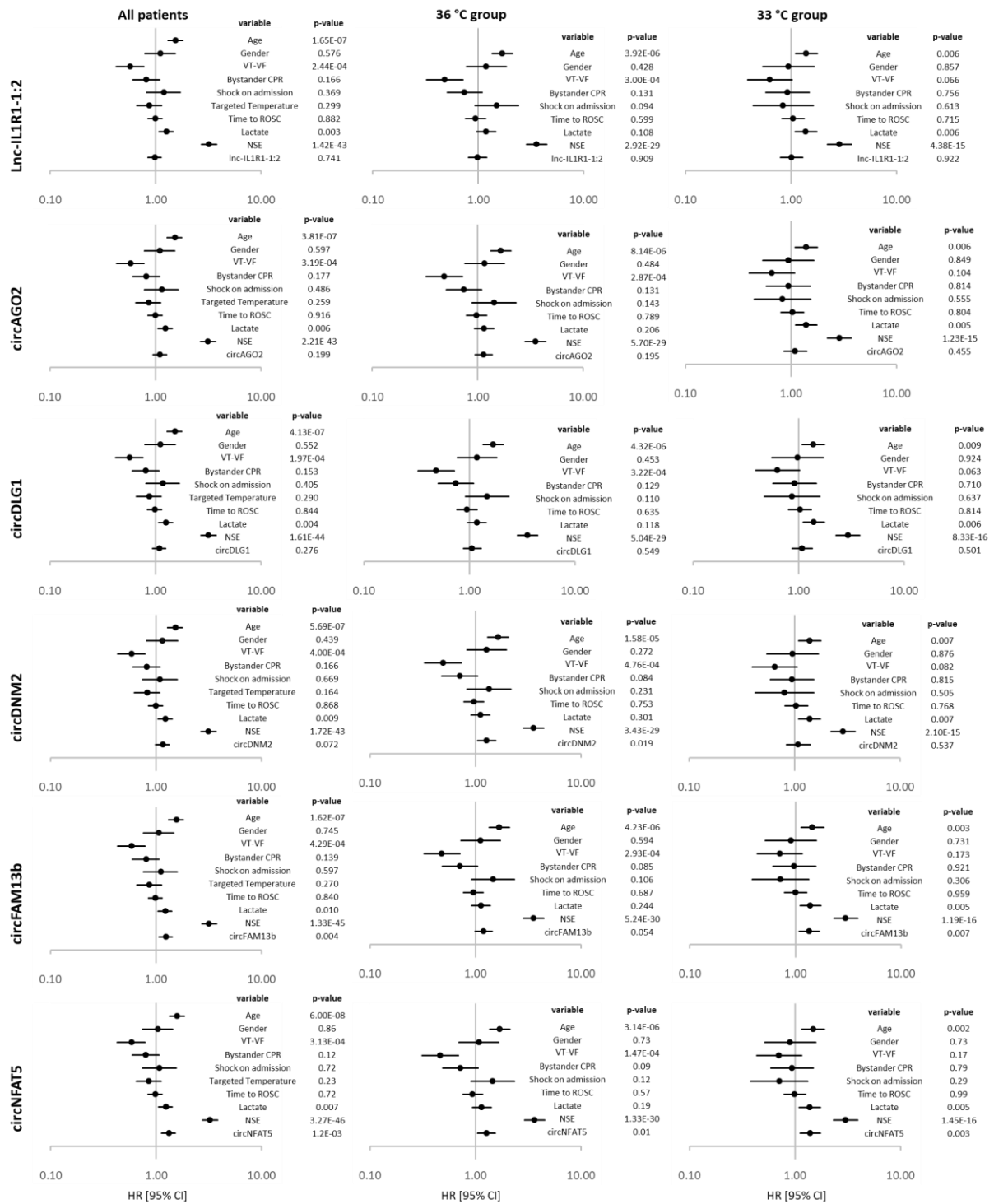


Figure 28. Multivariable Cox proportional hazards for predicting 6-month survival in TTM validation cohort. Forest plots as in Figure 27 and abbreviations as in Figure 23.

	AIC	Wald_p	C_idx	lr_p	
All patients	basal model	2373	2.35E-75	0.850	-
	basal model + lnc-IL1R1-1:2	2375	1.17E-74	0.851	0.741
	basal model + circAGO2	2373	3.44E-75	0.852	0.198
	basal model + circDLG1	2374	1.23E-74	0.851	0.277
	basal model + circDNM2	2372	2.68E-74	0.851	0.075
	basal model + circFAM13b	2367	1.04E-74	0.854	<b>0.004</b>
	basal model + circNFAT5	2362	8.62E-74	0.854	<b>3.91E-04</b>
36° group	basal model	1203	6.13E-44	0.865	-
	basal model + lnc-IL1R1-1:2	1205	3.29E-43	0.865	0.909
	basal model + circAGO2	1204	1.47E-43	0.865	0.195
	basal model + circDLG1	1205	2.83E-43	0.865	0.549
	basal model + circDNM2	1200	1.33E-42	0.864	<b>0.020</b>
	basal model + circFAM13b	1202	3.89E-43	0.865	0.057
	basal model + circNFAT5	1200	8.12E-43	0.865	<b>0.016</b>
33° group	basal model	866	5.67E-28	0.837	-
	basal model + lnc-IL1R1-1:2	868	2.80E-27	0.837	0.922
	basal model + circAGO2	867	2.22E-27	0.841	0.454
	basal model + circDLG1	867	2.40E-27	0.840	0.503
	basal model + circDNM2	867	3.25E-27	0.840	0.539
	basal model + circFAM13b	861	1.43E-27	0.846	<b>0.009</b>
	basal model + circNFAT5	859	4.51E-27	0.846	<b>0.004</b>

Table 14. Candidate performance to predict 6-month survival in TTM validation cohort. The basal model used the same variables as in Table 12. Abbreviations: AIC = Akaike Information Criterion; C\_idx = Harrell's C-index; lr\_p = Likelihood Ratio Test p-value; Wald\_p = Wald test p-value.

### 2.3. Molecular characterisation of circNFAT5

Among the candidates discovered in the TTM-trial, circNFAT5 emerged as the candidate with the most promising biomarker potential. Indeed, circNFAT5 was able to significantly predict neurological outcome and survival in TTM patients 6 months after cardiac arrest. Therefore, molecular studies were focused on this circRNA. At the time that this work was conducted, there was no information on circNFAT5 other than that it was a circular RNA composed of a single exon corresponding to the last exon of the NFAT5 linear transcript (as shown in Figure 15.a of the materials and methods section).

Although the role played by circNFAT5 in the context of cardiac arrest is still unclear, this work provided more information on the expression of circNFAT5 in blood cells and its intracellular localisation under basal conditions, treatments capable of modulating circNFAT5 expression levels *in-vitro*, the potential relationship of this circRNA with its linear counterpart and potential protein and miRNA interactors.

#### *2.3.1. Expression profiles of circNFAT5 in blood compartments and in in-vitro models*

Up until this point, circNFAT5 expression levels have been studied in PAXgene™ blood samples of cardiac arrest patients from the TTM-trial. RNA extracted from PAXgene™ samples is mainly from white blood cells. Therefore, to better understand in which blood compartment to focus molecular studies on circNFAT5, 65 blood cell markers were selected and correlated with circNFAT5 and the linear form of NFAT5 using RNA-seq data from the discovery cohort. The selection of these markers was made arbitrarily to encompass all different types of blood cells using several sources, including the BD biosciences human cluster of differentiation (CD) molecule manual ([https://www.bd.com/documents/bd-legacy/catalogue/biosciences/DS\\_Human-Mouse-CD-Maker-Biosciences\\_CT\\_DE.pdf](https://www.bd.com/documents/bd-legacy/catalogue/biosciences/DS_Human-Mouse-CD-Maker-Biosciences_CT_DE.pdf)) and <https://www.rndsystems.com/resources/cell-markers/immune-cells>.

From the 65 markers analysed, those with a correlation coefficient greater than 0.2 or -0.2 were reported in Tables 15 and 16 for circNFAT5 and linear NFAT5, respectively.

To better understand which cells are most likely to express circNFAT5, of greatest interest were the positive correlations ( $r > 0.2$ ) found between the markers studied and circNFAT5 (Table 15). Positive correlations with the host gene of circNFAT5 gene were also considered (Table 16). The results showed that the only blood cells in common among all the positively correlated markers with circNFAT5 and linear NFAT5 were monocytes. Thus, monocytes could express both circNFAT5 and its host gene (linear NFAT5) and consequently represent a good starting model for *in-vitro* studies on circNFAT5.

Marker	T cell	B cell	Dendritic cell	NK cell	Stem cell/precursor	Monocyte/macrophage	Granulocyte	Platelet	Erythrocyte	Gene locus	Correlation with circNFAT5 (r)	p-value
<b>CD11b</b>	+	+	+	+		+	+		-	16p 11.2	0.269	0.07
<b>CD138</b>	-	+		-	+	-	-	-	-	2p24.1	-0.248	0.10
CD161	+	-	-	+			-	-	-	12p13	-0.21	0.16
CD163	-	-	-			+	-	-	-	12p13.3	0.226	0.13
<b>CD25</b>	+	+	-	+	-	-	-	-	-	10p15-p14	-0.283	0.06
CD38	+	+		+	+	+	-			4p15	-0.216	0.15
CD4	+	-		-	-	+	+	-	-	12pter-p12	-0.209	0.16
<b>CD44</b>	+	+		+		+	+	-	+	11p13	0.29	0.05
<b>CD49b</b>	+	+		+	+	+	-	+	-	5q23-31	-0.304	0.04
<b>CD58</b>	+	+	+	+		+	+		+	1p13	0.225	0.13
<b>IFN<math>\gamma</math></b>	+			+						12q15	-0.192	0.20
<b>IL17</b>	+									6p12.2	-0.217	0.15
<b>IL23R</b>	+		+	+		+				1p31.3	-0.191	0.20
<b>IL4</b>	+					+	+			5 q31.1	-0.468	1.12E-03
<b>iNOS</b>	+		+			+				17 q11.2	-0.248	0.10

Table 15. Correlation between circNFAT5 and white blood cell markers in the RNA-seq data of the 46 TTM patients. Spearman correlation was used to correlate all white blood cell markers with circNFAT5. Markers with correlation coefficient (r) greater than 0.2 or -0.2 are represented in the table. For each correlation, the correlation coefficient and p-value are shown. White blood cells positive (+), positive upon activation (+) or negative (-) for each marker are shown along with the genomic location of the markers. The positive correlations ( $r > 0.2$ ) are highlighted in gray. In bold, common markers correlated with both circNFAT5 and linear NFAT5.

Marker	T cell	B cell	Dendritic cell	NK cell	Stem cell/precursor	Monocyte/macrophage	Granulocyte	Platelet	Erythrocyte	Gene locus	Correlation with NFAT5 (r)	p-value
CCR5	+	-		-		+	+	-	-	3p 21	-0.361	0.01
CCR6	+	+	+							6q 27	-0.507	3.58E-04
CD11a	+	+		+		+	+		-	16p 11.2	0.764	2.00E-07
<b>CD11b</b>	+	+	+	+		+	+		-	16p 11.2	0.732	2.00E-07
CD132	+	+		+		+	+	+	-	Xq 13.1	0.712	2.00E-07
<b>CD138</b>	-	+		-	+	-	-	-	-	2p24.1	-0.673	3.16E-09
CD14	-	-		-		+	+			5q 31.1	0.555	7.10E-05
CD15	-	-		-	-	+	+	-	-	11q21	0.297	0.05
CD16a	-	-		+	+	+	+	-	-	1q23	0.358	0.01
CD16b	+			+		+	+	-	-			
<b>CD25</b>	+	+	-	+	-	-	-	-	-	10p15-p14	-0.292	0.05
<b>CD44</b>	+	+		+		+	+	-	+	11p13	0.72	2.00E-07
CD45	+	+	+	+	+	+	+	-	-	1q31-q32	0.815	2.00E-07
<b>CD49b</b>	+	+		+	+	+	-	+	-	5q23-31	-0.306	0.04
CD56	+			+						11q23-q24	-0.544	1.06E-04
<b>CD58</b>	+	+	+	+		+	+		+	1p13	0.816	2.00E-07
CD69	+	+		+		+	+	+		12p13-p12	-0.335	0.02
CD80	+	+	+	-	-	+	-	-	-	3q13.3-q21	-0.522	2.25E-04
CXCR1	+	-		+	-	+	+	+		2q35	0.801	2.00E-07
CXCR2	+	-		+	-	+	+	+		2q35	0.738	2.00E-07
CXCR4	+	+	+			+				2q21	0.514	2.93E-04
<b>IFN<math>\gamma</math></b>	+			+						12q15	-0.583	2.43E-05
<b>IL17</b>	+									6p12.2	-0.62	4.37E-06
<b>IL23R</b>	+		+	+		+				1p31.3	-0.572	3.83E-05
<b>IL4</b>	+					+	+			5 q31.1	-0.637	1.64E-06
IL6	+					+				7 p15.3	-0.469	1.10E-03
<b>iNOS</b>	+		+			+				17 q11.2	-0.577	3.10E-05
IRF4	+	+	+			+				6 p25.3	-0.415	4.29E-03
PD1	+									2 q37.3	-0.739	2.00E-07
STAT3	+	+				+	+		+	17 q21.2	0.86	2.00E-07
STAT6	+	+				+	+		+	12 q13.3	0.822	2.00E-07
TGF $\beta$	+	+		+		+	+			19 q13.2	0.578	2.95E-05

Table 16. Correlation between linear NFAT5 and white blood cell markers in RNA-seq data of 46 TTM patients. Correlation analysis and table details as described in Table 15.

To further consolidate its blood origins, circNFAT5 levels were measured in primary white blood cells, plasma, and serum of three healthy volunteers. RNA samples extracted from different blood cell types



isolated from the three volunteers were available in the laboratory, and only qPCR measurements of circNFAT5 and SF3A1 (normaliser) were conducted in this study. The results confirmed the presence of circNFAT5 in the blood cell compartment (Figure 29.a.). Although monocytes still expressed circNFAT5 in the three healthy volunteers, higher levels of circNFAT5 were observed in peripheral blood mononuclear cells (PBMCs) and lymphocytes (Figure 29.a.). Blood-derived biofluids such as serum, plasma rich platelet (PRP), plasma pure platelet (PPP) and platelets (PQ) from three healthy volunteers were also available in the laboratory. Measurement of circNFAT5 in these samples further confirmed that circNFAT5 was not expressed or particularly lowly expressed ( $Ct > 37$ ) in the extracellular compartment of blood from healthy individuals (Figure 29.b). To confirm this finding also in patients after cardiac arrest, circNFAT5 levels were measured in 19 TTM serum samples from the discovery cohort. The results of these measurements, presented in Figure 30, resemble what was observed in the serum samples of the three healthy volunteers (Figure 29). In fact, very low expression levels of circNFAT5 ( $Ct > 34$ ) were observed in patients after cardiac arrest. Both results would suggest that circNFAT5 may not be freely circulating in the extracellular compartment of the blood.

In contrast, the measurements in primary white blood cells showed a good expression of circNFAT5 and therefore could be used as a model to study circNFAT5 *in-vitro*. For this purpose, jurkat and THP-1 cell lines, representing lymphocytic and monocytic lines respectively, were selected as *in-vitro* cell models. In addition, the expression levels of circNFAT5 were also measured in a neuronal cell line SH-SY5Y to test whether circNFAT5 could be expressed by neurone-like cells and thus to possibly study a potential relationship with the neurological damage that occurs after cardiac arrest. The normalised expression levels of circNFAT5 and linear NFAT5 presented in Figure 31 showed similar expression profiles in the three different cell lines, with slightly higher expression levels of circNFAT5 in THP1. Therefore, all three cell lines were used in this study as main models for the molecular characterization of circNFAT5.

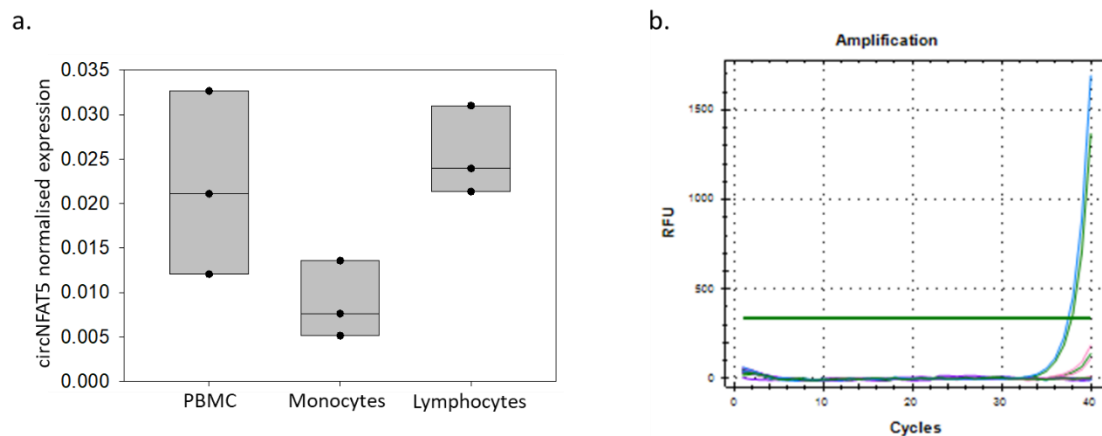


Figure 29. Expression profiles of circNFAT5 in blood compartments of three healthy volunteers. **a.** Expression profiles of circNFAT5 in white blood cells isolated from three healthy volunteers. 650 ng of RNA was retrotranscribed into cDNA. CircNFAT5 levels were normalized using 18s transcript with the gene study function of CFX maestro software version 1.1. Box plots generated using SigmaPlot software version 12.5. **b.** Amplification curves of circNFAT5 measured in serum (purple), platelet-rich plasma (PRP - pink), pure platelet plasma (PPP - green) and platelet (PQ - blue) samples from three healthy volunteers. Abbreviations: PBMC = peripheral blood mononuclear cells; RFU= Relative Fluorescence Unit.

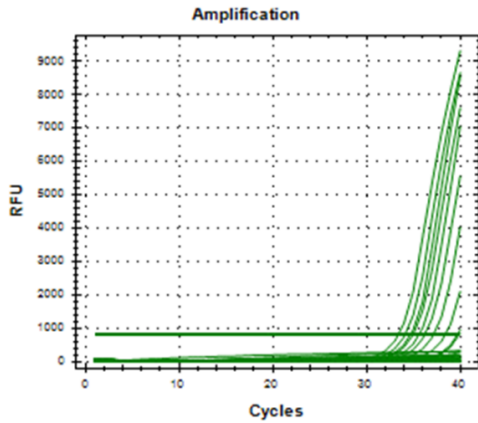


Figure 30. Amplification curves of circNFAT5 in serum samples from cardiac arrest patients. CircNFAT5 was measured in 19 TTM serum samples from the discovery cohort. Of these 19 patients, 9 had CPC1 and 10 had CPC5.

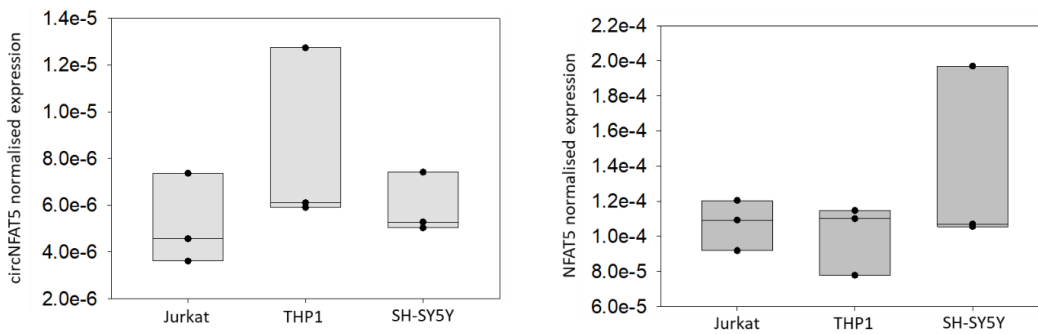


Figure 31. Expression levels of circNFAT5 and linear NFAT5 transcript in three different cell lines. Expression levels of circNFAT5 and linear NFAT5 were normalised using 18s transcript with CFX maestro software version 1.1. Data generated from 3 independent experiments.

### 2.3.2. Mimicking an ischaemic condition after cardiac arrest in-vitro

Hypoxic ischemic brain damage after cardiac arrest is the leading cause of mortality and neurological impairment in survivors [64]. Therefore, a first attempt was made to simulate an *in-vitro* hypoxic condition by incubating Jurkat, THP-1 and SH-SY5Y in a hypoxic chamber for 24 h and 48 h. Hypoxia is known to increase the transcriptional levels of the VEGF gene [467]. Therefore, VEGF was used as a positive control of successful hypoxic condition in this experiment. The results confirmed that the hypoxic condition worked in all cell lines with a significant increase in VEGF levels as early as 24 h in Jurkat and SH-SY5Y and at 48 h in THP-1 (Figure 32). Linear NFAT5 showed no significant modulation of expression levels, but a tendency to decrease under hypoxic conditions in Jurkat and THP1 and vice versa to increase in SH-SY5Y cell line 48 h after incubation in the hypoxia chamber (Figure 32). More interestingly, circNFAT5 levels do not appear to be affected by hypoxia in any of the cell lines studied, with the exception of Jurkat cells 48 h after the start of the experiment, where a significant decrease in circNFAT5 levels can be observed (Figure 32).

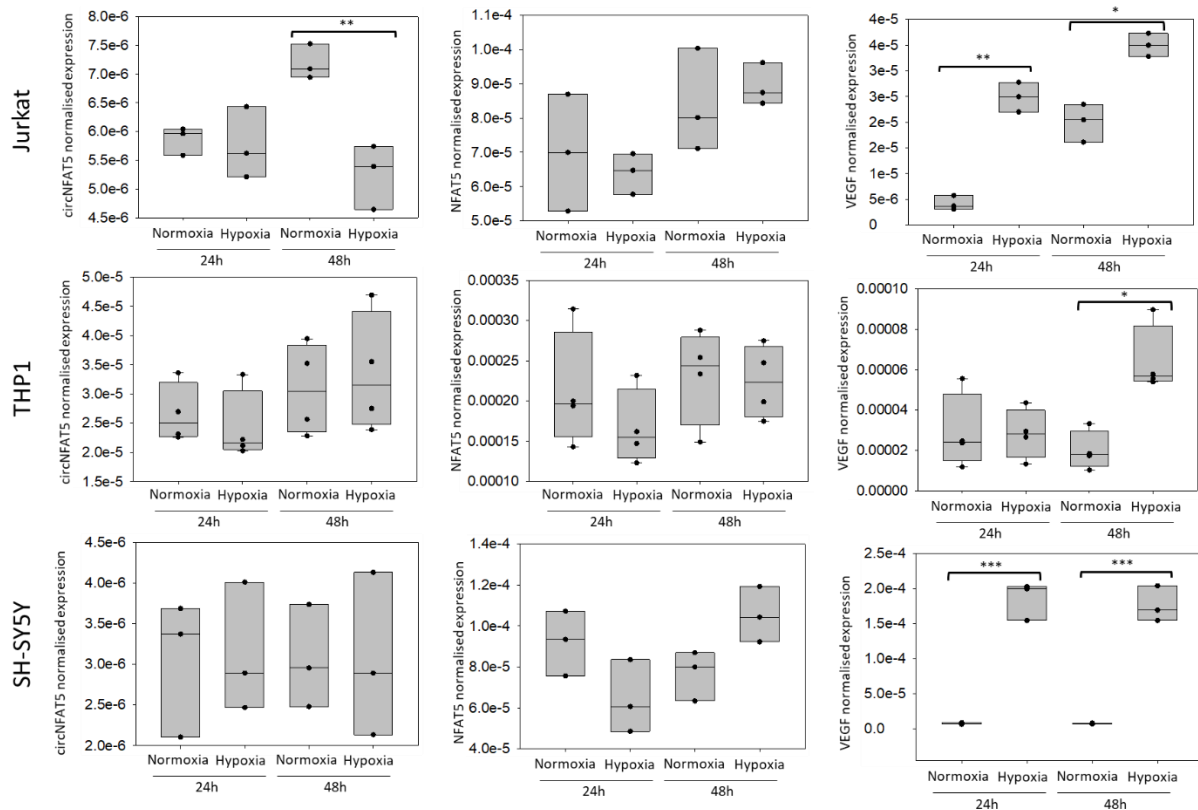


Figure 32. Modulation of circNFAT5 expression under normoxic and hypoxic conditions in different cell lines. Jurkat, THP-1 and SH-SY5Y cell lines were incubated in the hypoxic chamber (1% O<sub>2</sub>) or in a normal cell incubator (21% O<sub>2</sub>) for 24 h and 48 h, followed by total RNA extraction and retrotranscription. Boxplots show qPCR results obtained from three (jurkat and SH-SY5Y) or four (THP-1) independent experiments for circNFAT5, linear NFAT5 and VEGF, the latter used as a positive control of hypoxic treatment. The 18s transcript was used in this experiment as a normalizer. Paired t-test was used to indicate statistical significance (\*p<0.05, \*\*p<0.01, \*\*\*p<0.001).

A second attempt to mimic hypoxia was made using a chemical alternative, CoCl<sub>2</sub>. Indeed, CoCl<sub>2</sub> is a commonly used hypoxia-mimetic agent, which blocks degradation and this induces the accumulation of HIF-1α/2α transcription factors in a dose- and time-dependent manner, thereby activating the hypoxic response induced by these transcription factors [468].

For SH-SY5Y cells, CoCl<sub>2</sub> treatment had already been standardised in the laboratory in previous experiments. Therefore in this work, CoCl<sub>2</sub> was used at the concentration of 200 μM at 24 h and at 48 h in SH-SY5Y cells (Figure 33). While for jurkat and THP1, two different concentrations of CoCl<sub>2</sub> at 20 μM and 200 μM were used at the same time points as SH-SY5Y cells (Figure 33).

This experiment showed that circNFAT5 levels tended to decrease in jurkat and THP-1 in a dose- and time-dependent manner (Figure 33). While the opposite trend was observed in SH-SY5Y, although none of these changes were statistically significant (Figure 33). Furthermore, in jurkat cells VEGF did not increase under any of the conditions tested, indicating that this cell line may be more resistant to CoCl<sub>2</sub> treatment and that perhaps longer times or different CoCl<sub>2</sub> concentrations are needed to see an effect on these cells. THP1 cells also showed greater resistance to CoCl<sub>2</sub> treatment than SH-SY5Y cells, but an increase in VEGF 48 h after treatment could be observed. An explanation for the fact that VEGF does not increase significantly 48 h after treatment with CoCl<sub>2</sub> at 200 μM may be the high experimental variability.

In addition, no significant difference was also observed in linear NFAT5 in Jurkat and THP-1, while there was a tendency for NFAT5 to decrease after CoCl<sub>2</sub> treatment at both 24 h and 48 h in SH-SY5Y cells (Figure 33).

In conclusion, the results obtained from the two different hypoxic treatments did not show a clear change in circNFAT5 levels. Therefore, it could be speculated that other yet unknown conditions beyond hypoxia may influence the levels of this circRNA.

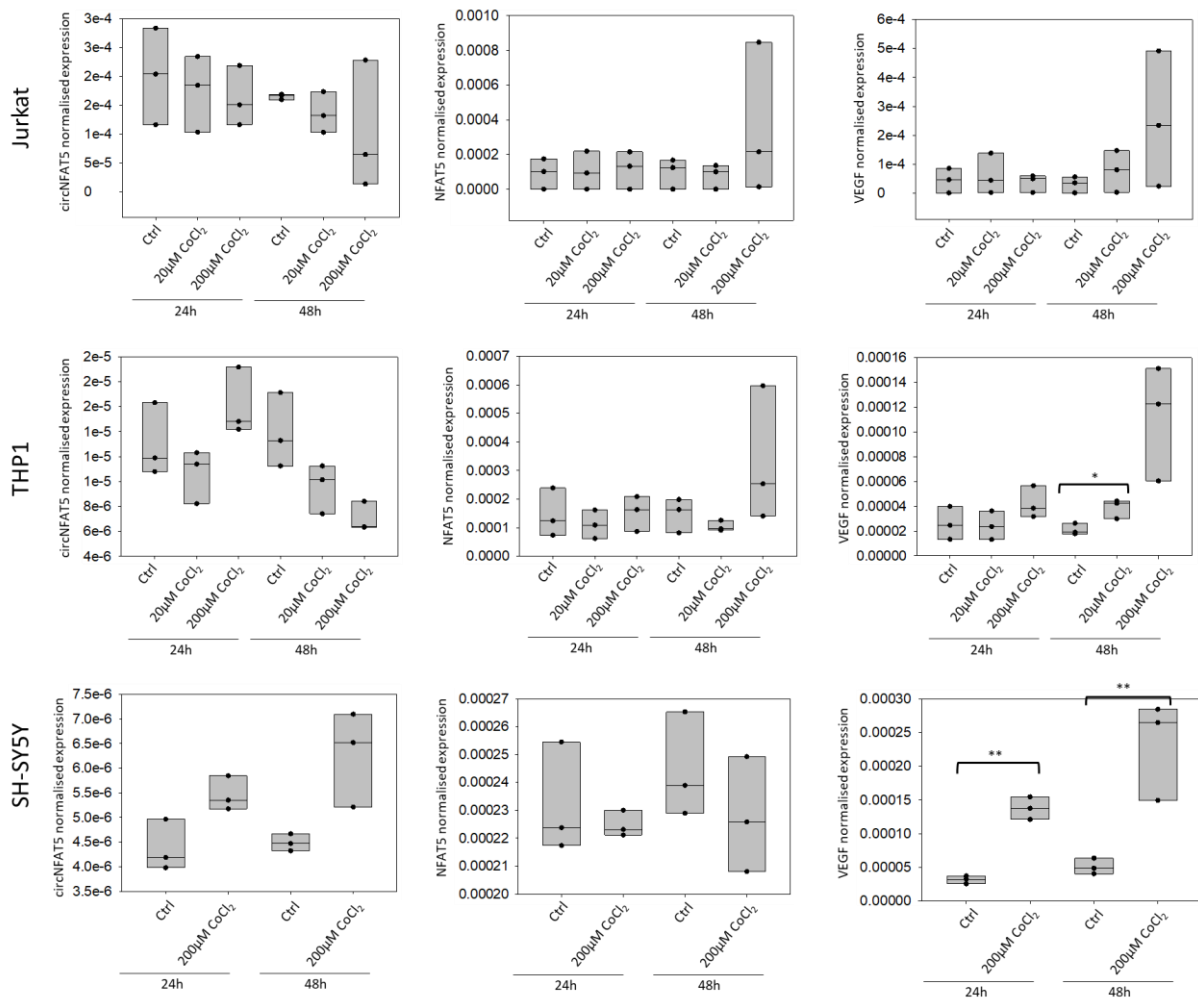


Figure 33. Modulation of circNFAT5 expression after CoCl<sub>2</sub> treatment in different cell lines. Jurkat and THP-1 cells were treated with 20 µM and 200 µM and SH-SY5Y with 200 µM of CoCl<sub>2</sub> for 24 h and 48 h, followed by total RNA extraction and retrotranscription. Boxplots show the qPCR results obtained in triplicate for circNFAT5, linear NFAT5 and VEGF, the latter used as a positive control of CoCl<sub>2</sub> treatment. Normalization and statistics as described in Figure 32.

### 2.3.3. Mimicking inflammation after cardiac arrest *in-vitro* through direct activation of monocytes or T cells

Inflammation is one of the mechanisms of ischemia/reperfusion injury after cardiac arrest. Indeed, after resuscitation, reoxygenation induces ROS production and the release of proinflammatory cytokines that trigger the migration of immune cells such as macrophages and T cells into the brain [65].

To understand whether the changes in circNFAT5 levels observed in the TTM samples could be due to the inflammatory process triggered after cardiac arrest, it was attempted to activate *in-vitro* immune blood cells represented by the THP-1 and Jurkat cell lines respectively, the monocytic cell and T-cell population.

A first attempt was made using lipopolysaccharide (LPS) to activate THP-1 cells. It is known that LPS activates monocytes through the Toll-like receptor 4 complex [469]. Therefore, THP-1 cells were incubated with 10ng/ml of LPS for 3 h, 6 h, 9 h, 24 h, 48 h as detailed in the materials and methods section. LPS induces the synthesis and secretion of several cytokines including TNF-alpha [469]. TNF-alpha is one of the best known pro-inflammatory cytokines produced by macrophages during inflammatory processes [470]. Therefore, TNF-alpha expression was used in this experiment as a positive control of the success of LPS treatment.

A notable increase in TNF-alpha production as early as 3 h after LPS treatment was indicative of the success of the experiment (Figure 34). Although a modulation of linear NFAT5 levels was observed after LPS treatment, with a peak in expression at 6h, no changes in circNFAT5 expression levels were observed (Figure 34). Since this first experiment did not show modulation of circNFAT5 levels after monocytes activation, at least in the *in-vitro* conditions used here, no further independent experiments were conducted.

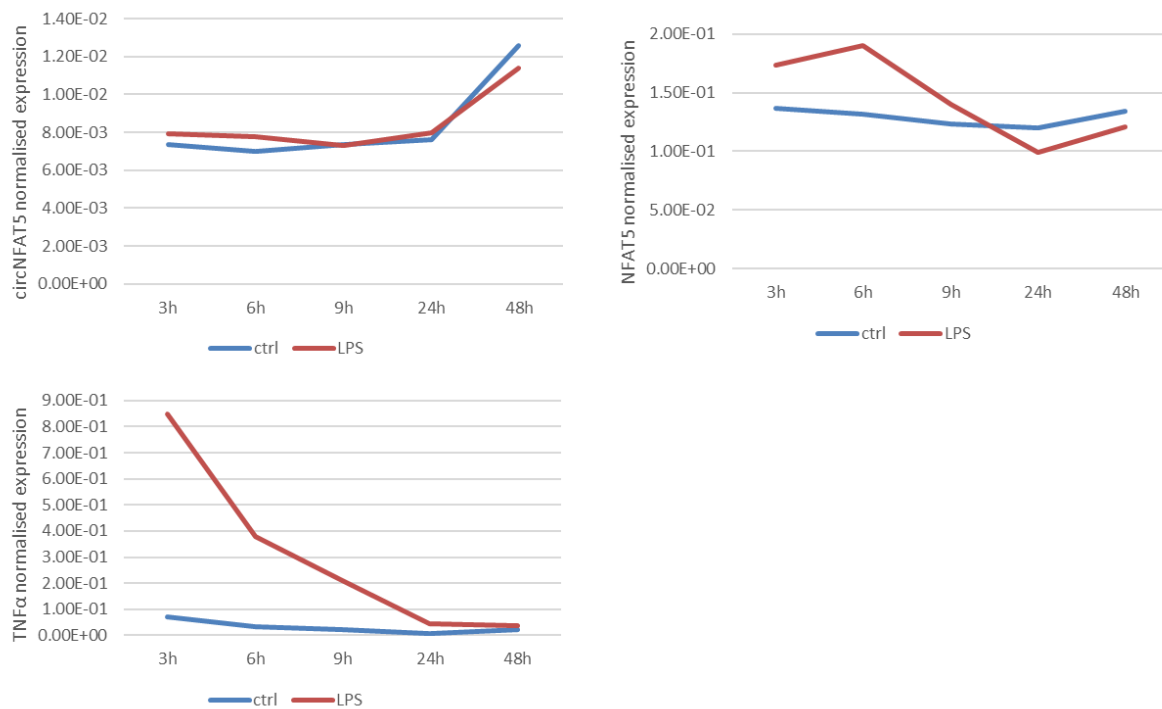


Figure 34. Expression profiles of circNFAT5 after treatment of THP-1 cells with LPS. THP-1 cells were treated with 10ng/ml of LPS for 3 h, 6 h, 9 h, 24 h, 48 h. Subsequently, cells were harvested, total RNA was extracted and retrotranscribed. The line graphs show the qPCR results for circNFAT5, linear NFAT5 and TNF-alpha after normalization with SF3a1 transcript. The experiment was performed once, thus no statistics were applied.

Therefore, the next step was to try to activate T cells *in-vitro* through the use of anti-CD3/CD28 antibodies. It is well known that T-cell activation requires two stimuli, CD3, which activates the TCR complex, and CD28, which is a co-stimulatory molecule required to initiate T-cell proliferation [66]. Thus, jurkat cells were stimulated *in-vitro* with a cocktail of antibodies anti-CD3/CD28 for 4 h, 24 h and 48 h as detailed in the materials and methods section. The success of the experiment shown in Figure 35 was confirmed by the significant overexpression of TNF-alpha as early as 4 h after the start of treatment. Indeed, TNF-alpha can also be produced by T cells [67] and was therefore used here as a positive control of the experiment. Furthermore, the levels of linear NFAT5 and circNFAT5 increased after treatment with anti-CD3/CD28, although at different time points. Indeed, like TNF-alpha, linear NFAT5 showed a peak of expression 4 h after treatment, while circNFAT5 expression levels started to increase at 24 h and showed highest expression levels at 48 h following treatment.

In conclusion, this experiment suggests that circNFAT5 might be involved in the inflammatory process triggered after cardiac arrest. However, further studies are required to confirm this hypothesis and to better understand which role circNFAT5 might play in the inflammatory process.

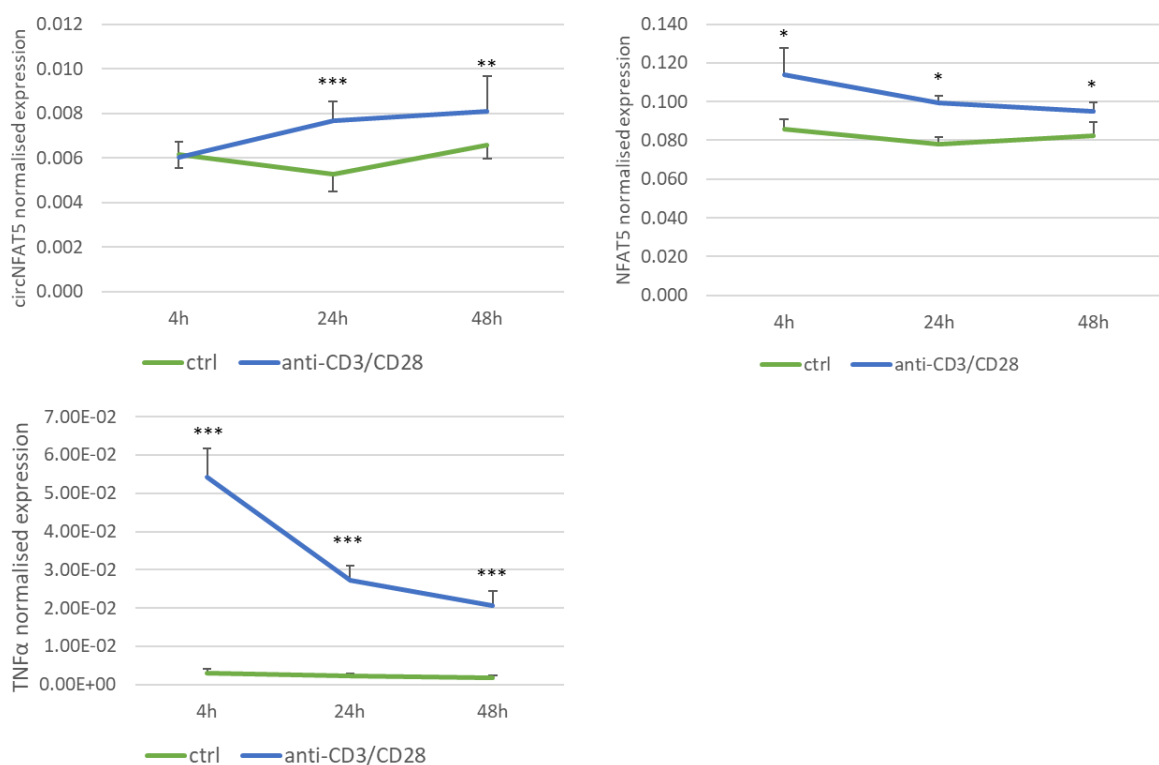


Figure 35. Expression profiles of circNFAT5 after treatment of jurkat cells with anti-CD3/CD28. Jurkat cells were treated with 25  $\mu$ L/ $1 \times 10^6$  cells of anti-CD3/CD28 for 4 h, 24 h and 48 h. At the end of treatment, the cells were harvested, and total RNA was extracted and retrotranscribed. Line graphs show the results of qPCRs for circNFAT5, linear NFAT5 and TNF-alpha after normalization with SF3a1. The experiment was performed 6 times. Statistical significance was determined by paired t-test using SigmaPlot software version 12.5 as described in Figure 32.

### 2.3.4. Relationship between linear and circular NFAT5 expression

In the previous chapter, it was observed that both linear and circular NFAT5 are modulated by T-cell activation. The expression pattern showed an initial increase in linear NFAT5 followed by an increase in the circular form in jurkat cells treated with anti-CD3/CD28 (Figure 35). This raised the question of whether circNFAT5 has a functional role or is simply a by-product of linear NFAT5 overexpression.

One way to better understand the relationship between linear NFAT5 and circNFAT5 is to block the expression of linear NFAT5 and use a system that can overexpress circNFAT5, such as activating jurkat cells with anti-CD3/CD28. In fact, in such a system, if in the absence of linear NFAT5, circNFAT5 levels increase in the same way as in the presence of linear NFAT5 following a stimulus, then the expression of linear NFAT5 and circNFAT5 are independent and thus circNFAT5 most likely has a function of its own (Figure 36). If, on the contrary, by blocking linear NFAT5 the levels of circNFAT5 do not change in the presence of a stimulus, then the expression of circNFAT5 would be dependent on linear NFAT5 and therefore most likely circNFAT5 would represent only a by-product of linear NFAT5 (Figure 36). To answer this question a number of preliminary experiments were necessary, so this chapter has been divided into further sub-chapters for ease of reading.

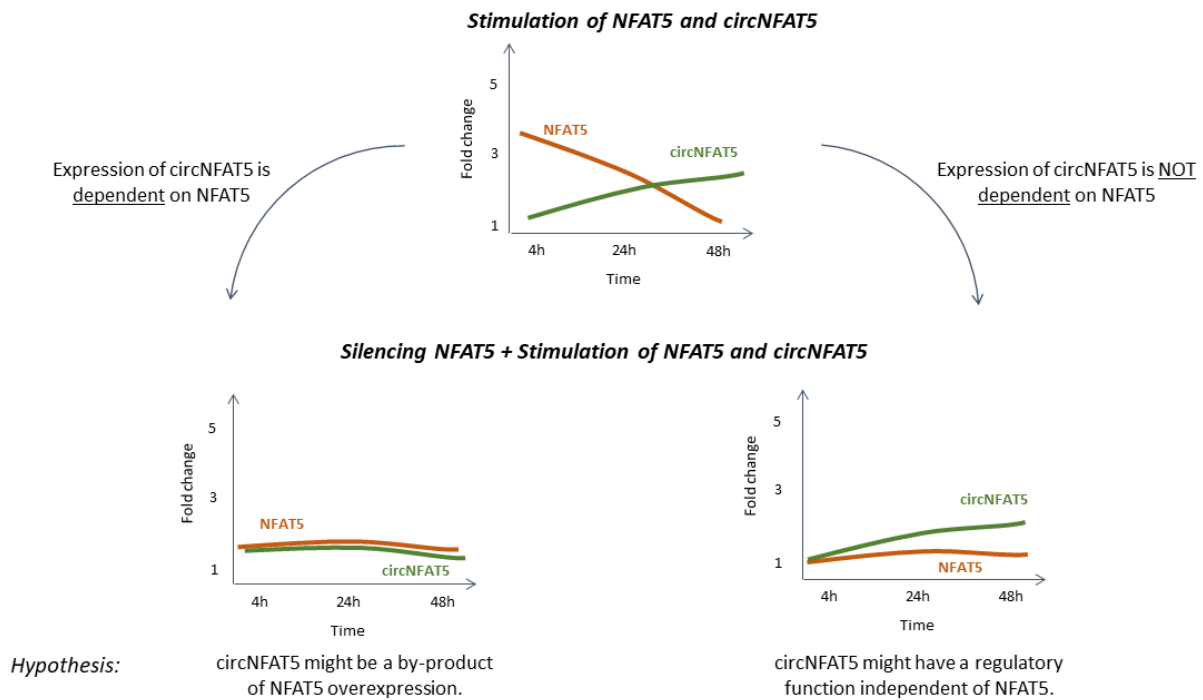
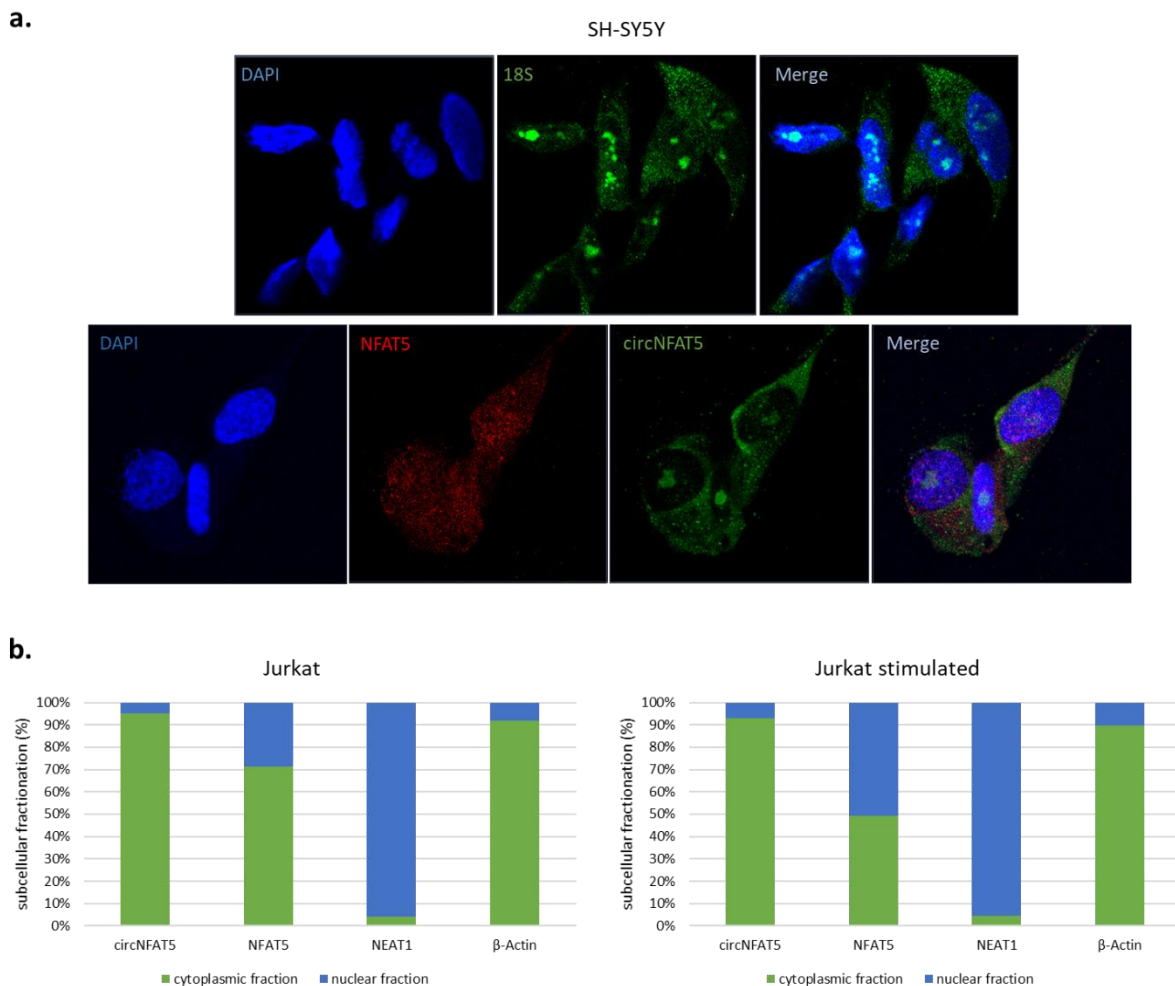


Figure 36. Schematic representation of the system used to study the hypothetical relationship between NFAT5 and circNFAT5.



### 2.3.4.1. Intracellular localisation of linear NFAT5 and circNFAT5

Before conducting such an experiment, the intracellular localisation of circNFAT5 was verified and the one of linear NFAT5 confirmed in two cell lines of interest (Figure 37). In SH-SY5Y cells a fluorescent in-situ hybridization (FISH) experiment using specific fluorescent DNA probes localized circNFAT5 predominantly in the cytoplasm of the cells and linear NFAT5 in both, nucleus and cytoplasm (Figure 37.a.). In addition, intracellular localisation of circNFAT5 and linear NFAT5 was also analysed in jurkat cells. However, unlike SH-SY5Y cells, jurkat cells are nonadherent cells, and the FISH protocol tested in SH-SY5Y cells was not optimal for accurate interpretation of results in this cell line. Therefore, a cytoplasm-nucleus fractionation experiment using the PARIS kit (Invitrogen) was chosen for jurkat cells. NEAT1 and  $\beta$ -actin are nuclear and cytoplasmic RNAs respectively and were used in the experiment as positive controls of successful fractionation. The results obtained in jurkat cells confirmed what was previously observed in SH-SY5Y cells; that circNFAT5 is predominantly localised in the cytoplasm, and that linear NFAT5 is equally distributed between cytoplasm and nucleus (Figure 37.b.).



**Figure 37. Intracellular localisation of circNFAT5 and linear NFAT5 in SHSY5Y and jurkat cells. a.** Fluorescence in situ hybridization (FISH) in SH-SY5Y cells. A specific probe on the junction was designed for circNFAT5. FISH probes were conjugated with FAM (green) or TAMRA (red) dyes for circNFAT5 and linear NFAT5, respectively. Images taken with the confocal microscope Zeiss LSM 880. **b.** Cytoplasmic-nucleus fractionation in jurkat cells. The fractionation was conducted using the manufacturer's protocol (PARIS kit, Invitrogen). Transcripts of interest were measured via qPCR after fractionation. Bar graphs show transcript expression as percent expression of nuclear and cytoplasmic fractions in three different experiments. NEAT1 and  $\beta$ -actin are nuclear and cytoplasmic enriched RNAs, respectively used as experimental controls. The experiment was conducted three times.



Since linear NFAT5 can be present in both the cytoplasm and the nucleus, the use of antisense LNA<sup>TM</sup> GapmeRs was chosen to silence this transcript. The antisense LNA<sup>TM</sup> GapmeR designed against linear NFAT5 was initially tested in jurkat cells. However, jurkat cells proved to be very difficult to transfect with antisense LNA<sup>TM</sup> GapmeRs. Consequently, it was not possible to continue to study the relationship between circNFAT5 and linear NFAT5 in this cell line.

#### 2.3.4.2. NaCl treatment as a system to modulate circNFAT5 levels in THP-1

Alternatively, the THP-1 cell line was chosen as an *in-vitro* model for this study. However, so far none of the stimuli tested in THP-1 cells induced significant modulation of circNFAT5. Since finding a stimulus that can modulate circNFAT5 is crucial to study the relationship between linear and circular form, an additional attempt was made to find such a stimulus.

It is known that NFAT5 is a major player involved in the response to hypertonic stimuli [68, 69]. However, it is not yet known whether hypertonic conditions can also increase circNFAT5 levels. Therefore, an *in-vitro* treatment using NaCl was attempted to induce a hypertonic condition in THP-1.

Simultaneously, prediction analyses in different databases were conducted to identify NFAT5 targets. A total of 83 proteins were in common across two databases used, hTFtarget (<http://bioinfo.life.hust.edu.cn/hTFtarget/#!/>) and the transcription factor target gene database (<http://tfbsdb.systemsbio.net/>). All those proteins were correlated with circNFAT5 and linear NFAT5 in the RNA-seq data of the 46 TTM patients used in the discovery cohort. Only significant correlations with coefficients above 0.5 or below -0.5 were selected. Among the 47 proteins matching these criteria, three proteins, S100A4, ZFP36L1 and SLC38A2, were also known to be involved in the hypertonic response [471-474] (Table 17). S100A4 and SLC38A2 are known targets of NFAT5 in hypertonic conditions [473, 475]. All the three proteins were highly correlated with linear NFAT5 but not with circNFAT5 in the RNA-seq data (Table 17). The identification of NFAT5-related proteins involved in NaCl stimulation allowed monitoring of potential downstream effects resulting from modulation of NFAT5 and, later in this work, also of circNFAT5 (Chapter 2.3.5.1); in addition, these proteins served as further positive controls of NaCl treatment. Therefore, these three proteins were measured in the hypertonic *in-vitro* model generated here.

To mimic a hypertonic condition in THP-1, different concentrations of NaCl (30 mM, 50 mM, 100 mM) were tested at 4 h, 8 h, 24 h and 48 h. As shown in Figure 38.a., NaCl appears to affect cell health in a dose- and time-dependent manner, however, the cytotoxicity assay performed did not show a significantly greater cytotoxic effect of NaCl in THP-1 at higher doses and times (Figure 38.b.). The overexpression of linear NFAT5 immediately after the NaCl treatment represented the positive control of the experiment (Figure 38.c.). Also S100A4, ZFP36L1 and SLC38A2 were significantly modulated in THP-1 treated with the highest concentration of NaCl, with overexpression of S100A4 and ZFP36L1 at later time and significant overexpression of SLC38A2 as early as 4 h after treatment with 50 mM NaCl (Figure 38.c.). Even more interesting, circNFAT5 levels started increasing significantly already 8 h after treatment with 50 mM and 100 mM NaCl (Figure 38.c.). Therefore, the expression patterns between linear and circular NFAT5 observed here resemble those previously observed in anti-CD3/CD28-stimulated jurkat cells with a delayed increase in circNFAT5 expression levels after linear NFAT5, making this experiment optimal for studying the relationship between circNFAT5 and linear NFAT5.

	CircNFAT5		Linear NFAT5		Complete protein name
	<i>r</i>	<i>p</i> -value	<i>r</i>	<i>p</i> -value	
<b>ZFP36L1</b>	0.0592	0.694	0.804	2.00E-07	mRNA decay activator protein ZFP36L1
<b>SLC38A2</b>	0.206	0.169	0.764	2.00E-07	Sodium-coupled neutral amino acid transporter 2
<b>S100A4</b>	-0.0368	0.807	0.527	1.89E-04	Protein S100-A4

Table 17. Spearman correlations between circNFAT5 or linear NFAT5 and the three proteins predicted to interact with linear NFAT5 and known to be involved in hypertonic responses. Correlations were performed using RNA-seq data from the discovery cohort (46 TTM patients). Spearman correlation coefficients (*r*) are shown for each correlation performed. Statistically significant correlations are considered with *p*-value < 0.05.

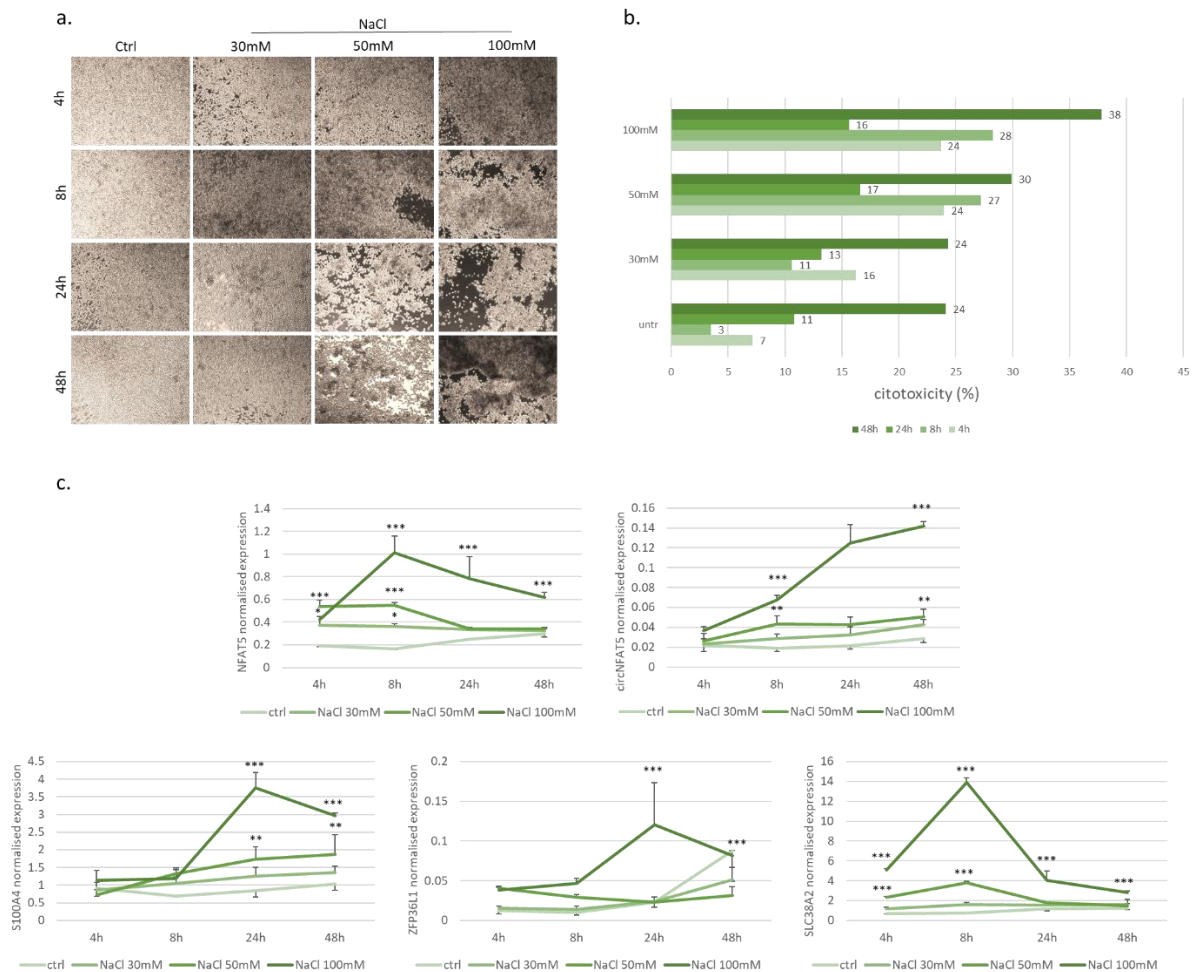


Figure 38. THP-1 cells treated with NaCl. Different concentrations of NaCl were tested, 30 mM, 50 mM and 100 mM at 4 h, 8 h, 24 h and 48 h. Data generated from 3 independent experiments. **a.** Images of cells at the end of treatment. Images taken with a LEICA DMIL microscope (camera DFC300FX) at a 10x magnification. **b.** LDH assay results represented in horizontal bar graphs as percent of cytotoxicity of different NaCl concentrations at different time points. **c.** qPCR measurement results for linear NFAT5, circNFAT5, S100A4, ZFP36L1 and SLC38A2 after normalisation with SF3a1. Statistical significance refers to treated condition vs control and was determined by paired t-test as described in Figure 32.

#### 2.3.4.3. Antisense LNA<sup>TM</sup> gapmeR as a system for silencing linear NFAT5 in THP1

Once a system able to modulate both linear NFAT5 and circNFAT5 levels in THP-1 was established, the next step was to test NFAT5 silencing in the same cell model. Therefore, the antisense LNA<sup>TM</sup> gapmeR against linear NFAT5 was tested in THP-1 at a concentration of 50 nM for 24 h, 48 h and 72 h (Figure 39). The levels of circNFAT5, S100A4, ZFP36L1 and SLC38A2 were also measured to see a potential effect of the antisense LNA<sup>TM</sup> gapmeR against linear NFAT5. The results showed a significant decrease of linear NFAT5 levels already 24 h after the transfection with the antisense LNA<sup>TM</sup> gapmeR (Figure 39). Among the other transcripts analysed, no modulation was observed in the levels of ZFP36L1 and SLC38A2 in presence of the antisense LNA<sup>TM</sup> gapmeR against linear NFAT5, unlike circNFAT5 and S100A4, which showed a tendency to decrease in its presence (Figure 39). Therefore, from this first experiment circNFAT5 expression levels appear to be dependent on linear NFAT5, but this could be more accurately determined by combining the antisense LNA<sup>TM</sup> gapmeR against linear NFAT5 with NaCl treatment, which can increase both circNFAT5 and linear NFAT5 levels. In fact, as mentioned earlier, if in the presence of the gapmeR and the stimulus circNFAT5 levels do not increase this would indicate a linear NFAT5 dependency of circNFAT5, and vice versa if, on the other hand, circNFAT5 levels increase in the same conditions.

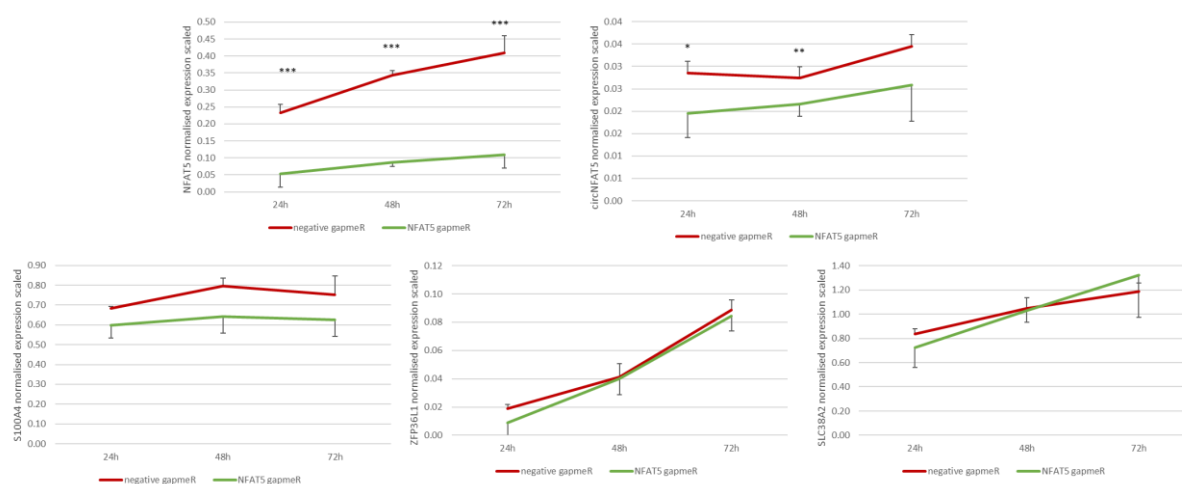


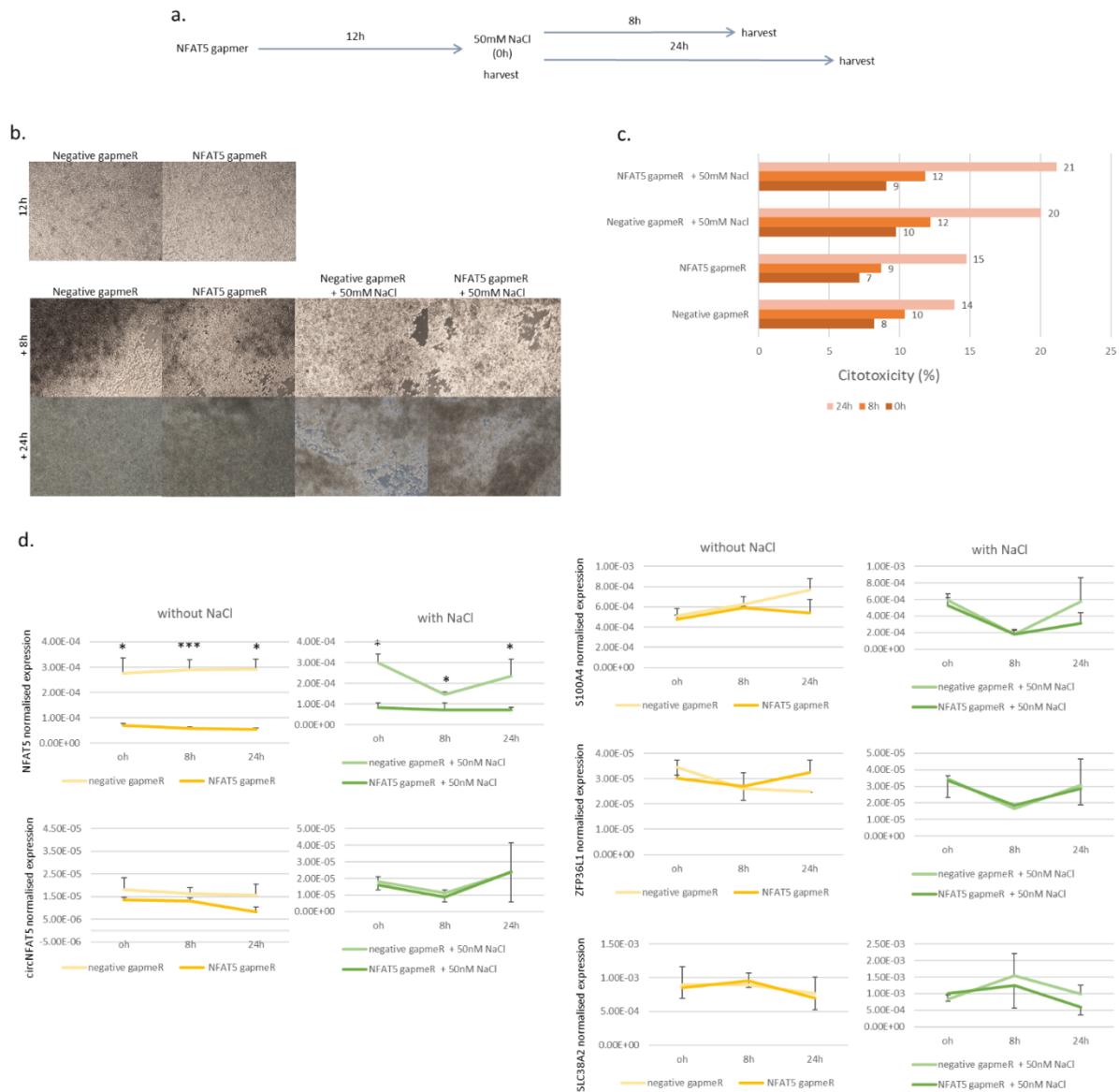
Figure 39. Expression levels of linear NFAT5, circNFAT5, S100A4, ZFP36L1 and SLC38A2 after silencing of linear NFAT5. Linear NFAT5 was silenced with 50 nM of antisense LNA<sup>TM</sup> gapmeR for 24 h, 48 h and 72 h. A negative control antisense LNA<sup>TM</sup> gapmeR was used as control condition of this experiment. Data generated from 3 independent experiments. The expression levels of the transcripts of interest were normalized with SF3a1. Statistical significance was determined by paired T-test, as described in Figure 32.

#### 2.3.4.4. Combining linear NFAT5 silencing with NaCl treatment in THP-1

Therefore, THP-1 cells were transfected for 12 h with 50 nM of linear NFAT5 antisense LNA<sup>TM</sup> gapmeR and subsequently treated with 50 mM of NaCl for 8 h and 24 h (Figure 40.a.). The concentration of 50 mM NaCl was selected in this experiment to minimize the toxic effect of NaCl on cells while maintaining the treatment effect on both circNFAT5 and linear NFAT5. Importantly, cell imaging and LDH assay did not show a major toxic effect on the cells derived from the combination of the antisense LNA<sup>TM</sup> gapmeR transfection and NaCl treatment (Figure 40.b.c.). The qPCR measurements confirmed that after transfection with the linear NFAT5 antisense LNA<sup>TM</sup> gapmeR even in the presence of NaCl there was a strong downregulation of linear NFAT5 (Figure 40.d.). Although the variability among the three experiments conducted was high when combining the antisense LNA<sup>TM</sup> gapmeR with NaCl treatment at 24 h, circNFAT5 levels did not appear to be affected by the linear NFAT5 antisense LNA<sup>TM</sup> gapmeR (Figure 40.d.). In fact, although a slight decrease in circNFAT5 levels was observed in presence of the linear NFAT5 antisense LNA<sup>TM</sup> gapmeR, when NaCl was added this tendency not only disappeared, but

in addition an initial increase in circNFAT5 levels was observed 24 h after NaCl treatment regardless the presence of the linear NFAT5 antisense LNA<sup>TM</sup> gapmeR (Figure 40.d.). None of the other transcripts measured showed a significant modulation in their expression patterns when combining the linear NFAT5 antisense LNA<sup>TM</sup> gapmeR with NaCl treatment.

In conclusion, under the conditions tested in this study it appears that modulation of circNFAT5 is independent of linear NFAT5, thus raising the possibility that circNFAT5 has its own regulatory function that has yet to be discovered.



**Figure 40. THP-1 cells treated with NaCl after silencing linear NFAT5. a.** Experimental design. THP-1 cells were first transfected with 50 nM gapmeR against linear NFAT5 or negative control for 12 h. Then 50 mM NaCl or equal volume of water for the control were added for 8 h and 24 h. Thereafter, cells were harvested, total RNA was extracted and retrotranscribed and the transcripts of interest measured by qPCR. **b.** Images of THP-1 cells with all the different conditions tested. Images taken with a LEICA DMIL microscope (camera DFC300FX) at a 10x magnification. **c.** LDH assay results reported as the percentage of cytotoxicity of the different conditions having gapmeRs or gapmeRs plus NaCl treatment. **d.** Results of qPCR measurements for linear NFAT5, circNFAT5, S100A4, ZFP36L1 and SLC38A2 after normalisation with SF3a1. Statistical analyses were measured between negative and linear NFAT5 gapmeRs in presence or absence of NaCl. Statistics were determined by paired t-test as described in Figure 32.

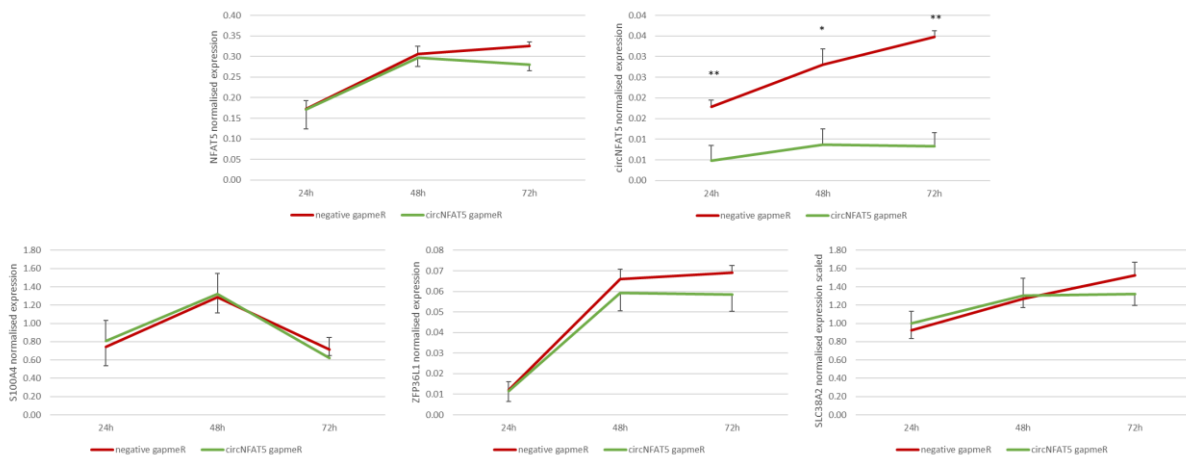
### 2.3.5. Exploring potential functions of circNFAT5

Earlier in the introduction of this manuscript, the various functions of circRNAs identified so far were described (Figure 11). Mainly, it has been described that circRNAs can regulate transcription of the parental gene, produce small proteins and therefore play the role of coding RNAs or sponge miRNAs and/or proteins (Figure 11). In this section, preliminary data were obtained to evaluate the potential functions that circNFAT5 might play. However, more in-depth studies are needed for each type of function and in different contexts to get a clear and precise idea of the potential functions that circNFAT5 could perform.

#### 2.3.5.1. *In-vitro* modulation of circNFAT5 expression

Beginning with the regulation of the parental gene, circNFAT5 silencing and overexpression experiments were conducted to see how these might affect NFAT5.

As done previously for linear NFAT5, an antisense LNA<sup>TM</sup> gapmeR was designed to silence circNFAT5. The circNFAT5 antisense LNA<sup>TM</sup> gapmeR was specifically designed at the junction point to selectively target only the circular form of the transcript. Therefore, 30 nM of circNFAT5 antisense LNA<sup>TM</sup> gapmeR were tested on THP-1 cells for 24 h, 48 h and 72 h. The results showed a significant downregulation of the levels of circNFAT5 already 24 h after the addition of the antisense LNA<sup>TM</sup> gapmeR (Figure 41). However, no modulation of linear NFAT5 expression levels or other measured transcripts, such as S100A4, ZFP36L1 and SLC38A2 was observed in the presence of circNFAT5 antisense LNA<sup>TM</sup> gapmeR (Figure 41).



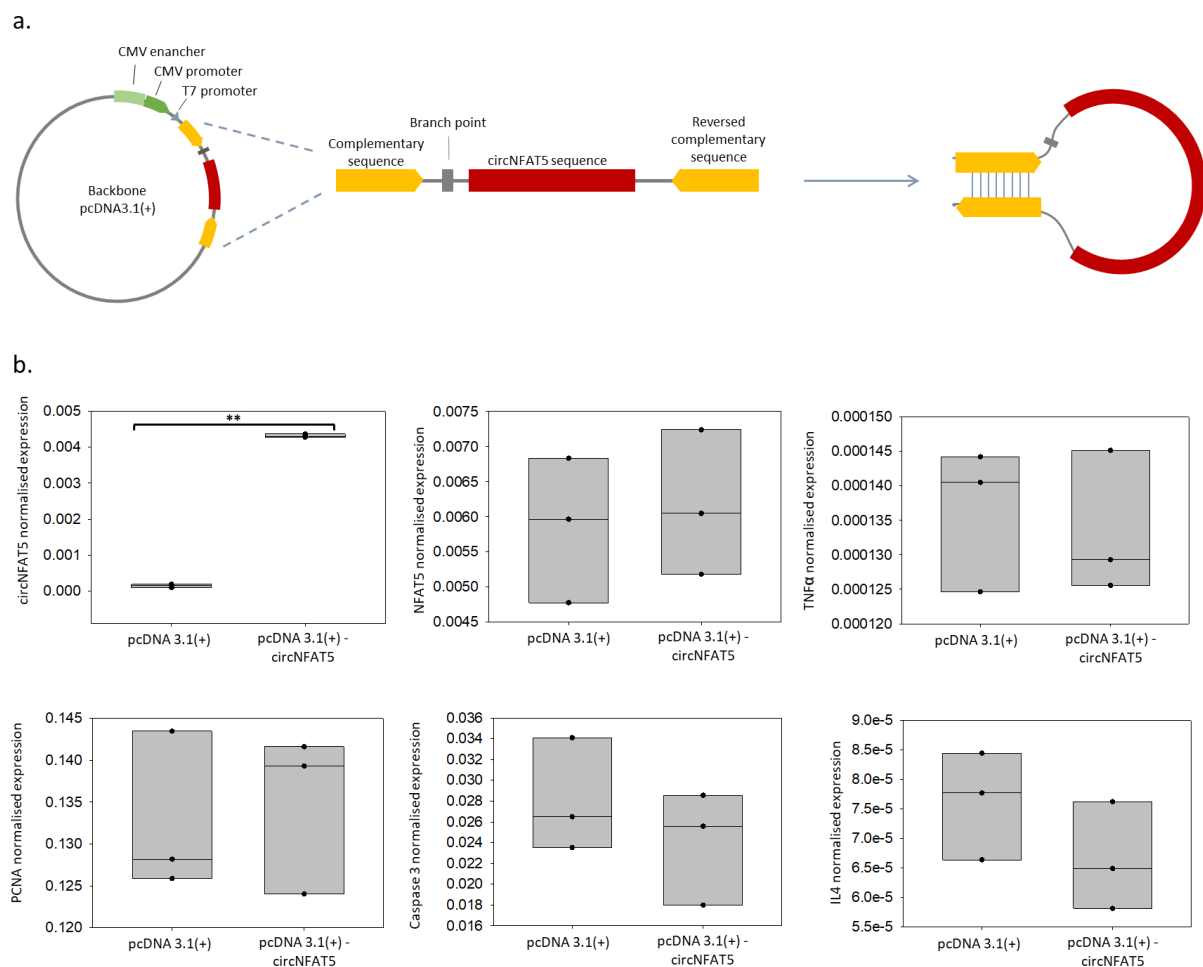
**Figure 41.** Expression levels of linear NFAT5, circNFAT5, S100A4, ZFP36L1 and SLC38A2 after silencing of circNFAT5 with antisense LNA<sup>TM</sup> gapmeR in THP-1 cells. CircNFAT5 was silenced using 30 nM of antisense LNA<sup>TM</sup> gapmeR for 24 h, 48 h and 72 h. A negative control antisense LNA<sup>TM</sup> gapmeR was used as control condition to confirm that the modulation in expression levels of the transcripts was due to the specific antisense LNA<sup>TM</sup> gapmeR used and not because of the transfection. The experiment was conducted in triplicate and the expression levels of the transcripts were normalised with SF3a1 as previously described. Statistical analyses as in Figure 32.

Regarding overexpression experiments, circNFAT5 RNA sequence was cloned into pcDNA3.1(+) vector. As better described in the materials and methods section, two complementary sequences were added to the ends of the circNFAT5 sequence to facilitate the circularization process in cells (Figure 42.a.).

THP-1 cells were particularly difficult to electroporate with the pcDNA 3.1(+)-circNFAT5 vector even following the manufacturer's protocol specific to this cell line. Therefore, an attempt was made in jurkat cells. The results of nucleofection in jurkat cells are presented in Figure 42.b.

CircNFAT5 is found to be significantly over-expressed following nucleofection with the pcDNA 3.1(+)-circNFAT5 vector compared to the mock vector (figure 42.b.). However, no change in linear NFAT5 expression levels was observed following circNFAT5 overexpression. In addition, genes implicated in cell proliferation (PCNA) [476], apoptosis (caspase 3) [477], and inflammation (TNF-alpha and IL4) [478, 479] were measured via qPCR to identify potential downstream effects triggered by circNFAT5. IL4 transcript was also selected because from a previous correlation analysis in the RNA-seq data of the 46 TTM patients it was significantly correlated with circNFAT5 with a negative correlation coefficient of -0.468 (Table 15). Although, IL4 levels tended to decrease upon overexpression of circNFAT5 this modulation was not significant after three independent experiments.

Therefore, these experiments suggest that circNFAT5 has no effect on its parental gene, nor on cell proliferation, apoptosis, and inflammation, at least under the conditions studied here.



**Figure 42. Overexpressing circNFAT5 in jurkat cells. a.** Schematic representation of the cloning strategy used to clone circNFAT5 into the pcDNA3.1(+) backbone vector. **b.** Expression levels of circNFAT5, linear NFAT5, PCNA, caspase 3, TNF-alpha and IL4 after electroporating jurkat cells with the pcDNA3.1(+)-circNFAT5 vector. Jurkat cells were electroporated with 2  $\mu$ g of plasmid and harvested after 24 h. The experiment was conducted in triplicate, and the measured transcripts expression levels were normalized with GAPDH. Statistical significance was determined by paired t-test, as described previously in Figure 32.

#### 2.3.5.2. CircNFAT5 protein-coding potential

Although circRNAs are classified as ncRNAs, it has recently emerged that some circRNAs can code for proteins in a 5'cap-independent manner. In fact, the presence of ORFs, IRES elements and m6A modifications are indications of the high protein-coding potential of a circRNA [71].

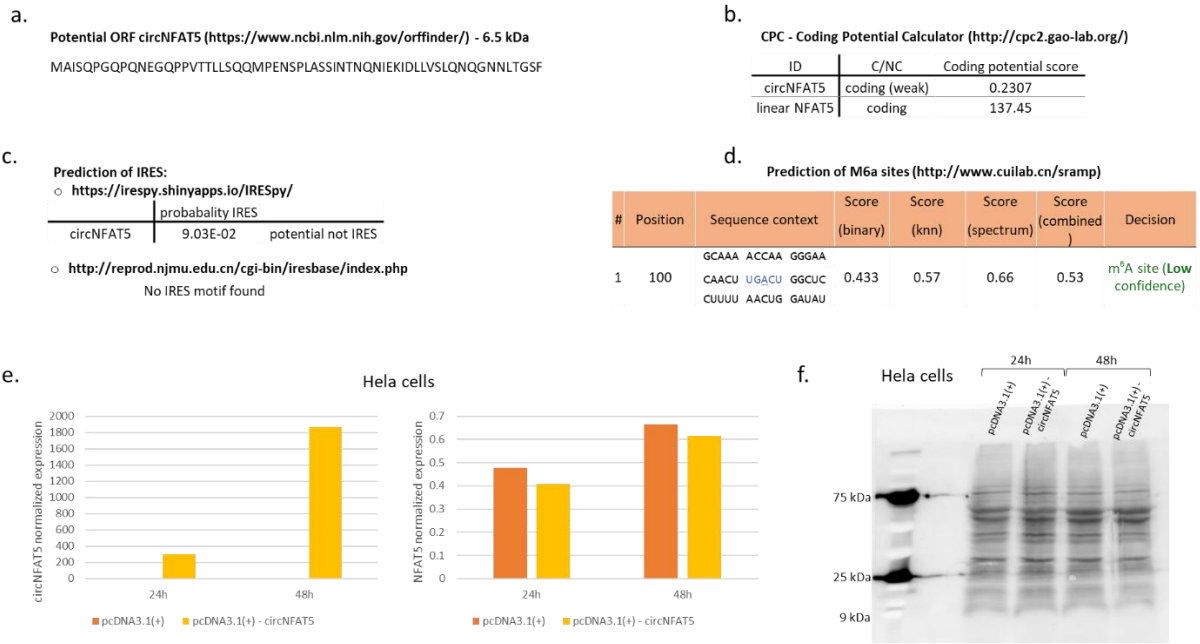
Therefore, to find out whether circNFAT5 could have protein-coding potential, the presence of an ORF was first searched using the database <https://www.ncbi.nlm.nih.gov/orffinder/>. As shown in Figure 43.a., circNFAT5 has an ORF that could potentially produce a protein of about 6.5 kDa. Thus, the coding potential of circNFAT5 was calculated by the tool <http://cpc2.gao-lab.org/> for which the higher the coding score, the more reliable the prediction. According to these prediction tools, RNAs with coding scores between -1 and 1 are considered to have weak coding potential [480]. As such, the results showed a weak coding potential for circNFAT5, with a coding score of 0.23, in contrast to linear NFAT5, which had a coding score of 137.45 (Figure 43.b.).

Next, the presence of IRES motifs or m6A methylation sites were searched (Figure 43.c.d.). Regarding IRES motifs, both databases used, *irespy* (<https://irespy.shinyapps.io/IRESpy/>) and *iresbase* (<http://reprod.njmu.edu.cn/cgi-bin/iresbase/index.php>), did not identify any IRES motifs (Figure 43.c.). For m6A on the other hand, only one m6A methylation site was identified in the circNFAT5 sequence but with a low level of prediction confidence using the *sramp* tool (<http://www.cuilab.cn/sramp>).

Consequently, the analyses conducted up to this point have suggested that circNFAT5 does not code for any protein. However, an attempt was made to verify this prediction with an *in-vitro* experiment conducted on HeLa cells. Indeed, HeLa cells were transfected with the pcDNA3.1(+)-circNFAT5 vector to overexpress circNFAT5 for 24 h and 48 h. Both total RNA and protein were extracted from the experiment. The bar graphs in Figure 43.e. confirmed that circNFAT5 overexpression worked and that again circNFAT5 overexpression did not affect linear NFAT5 levels. In addition, western blot analysis was performed to identify the potential presence of a circNFAT5 protein (Figure 43.f.). The western blot was modified for the detection of very small proteins, as described in the materials and methods section. In addition, because there is no antibody that recognises a potential circNFAT5 protein, the No-Stain™ Protein Labelling Reagent (Invitrogen) was used to check for the presence of a 6.5-kDa molecular weight band. The results showed no signal at the expected level of circNFAT5 protein in both circNFAT5-overexpressing and non-overexpressing cells (Figure 43.f.).

Therefore, these experiments suggested that circNFAT5 do not code for a protein.





**Figure 43. Protein-coding potential of circNFAT5. a.** Identification of potential ORFs in the sequence of circNFAT5 using <https://www.ncbi.nlm.nih.gov/orffinder/>. **b.** Evaluation of protein-coding potential of circNFAT5 and linear NFAT5 using the tool <http://cpc2.gao-lab.org/>. **c.** Identification of IRES elements using two databases, <https://irespy.shinyapps.io/IRESpy/> and <http://reprod.njmu.edu.cn/cgi-bin/iresbase/index.php>. **d.** Prediction of m6A methylation sites in circNFAT5 using the tool <http://www.cuilab.cn/sramp>. **e.** qPCR measurements of circNFAT5 and linear NFAT5 after overexpression of circNFAT5 in HeLa cells for 24 h and 48 h using the pcDNA3.1(+)-circNFAT5 vector. Transfection with the original pcDNA3.1(+) vector was used as mock control. The experiment was conducted once, and the measured transcripts were normalized with SF3a1. **f.** Western blot analysis results showing all proteins revealed through chemiluminescence with the No-Stain™ Protein Labeling Reagent.



### 2.3.5.3. miRNA sponging

Among the various functions of identified circRNAs, miRNAs sponging is the most extensively studied [481].

To explore the potential of circNFAT5 in miRNA sponging, a prediction analysis of miRNAs binding sites on the sequence of circNFAT5 was performed using the mirDB database (<http://www.mirdb.org/>). Of the 19 miRNAs predicted to bind circNFAT5, one (miR-145-5p) recognised a region just adjacent to the junction point, and two (miR-144-3p and miR-139-5p) were potentially binding on the junction point and thus were able to recognise only circNFAT5 and not its linear form (Table 18).

Rank	Score	miRNA name	Binding site - starting nucleotide	Number binding sites
1	90	hsa-miR-106a-3p	74	1
2	82	hsa-miR-5195-3p	113	1
<b>3</b>	<b>82</b>	<b>hsa-miR-145-5p</b>	<b>113</b>	<b>1</b>
4	76	hsa-miR-12122	219	1
5	70	hsa-miR-7152-3p	146	1
6	69	hsa-miR-623	85	1
<b>7</b>	<b>67</b>	<b>hsa-miR-144-3p</b>	<b>121</b>	<b>1</b>
8	65	hsa-miR-4742-5p	158	1
9	64	hsa-miR-450b-5p	76	1
10	62	hsa-miR-4772-5p	161	1
11	61	hsa-miR-4529-5p	172	1
12	54	hsa-miR-29b-1-5p	40	1
13	53	hsa-miR-19b-2-5p	78	1
14	53	hsa-miR-19b-1-5p	78	1
15	53	hsa-miR-19a-5p	78	1
16	52	hsa-miR-6755-3p	222	1
17	52	hsa-miR-655-5p	138	1
<b>18</b>	<b>52</b>	<b>hsa-miR-139-5p</b>	<b>123</b>	<b>1</b>
19	51	hsa-miR-642b-5p	87	1

Table 18. Predicted miRNAs with binding sites on circNFAT5. Custom prediction with mirDB database using the sequence of circNFAT5 with junction point in the middle.

Of the 50 TTM patients who underwent small RNA-seq and the 46 TTM patients who underwent whole RNA-seq, 23 miRNAs were in common. The data of these 23 patients from the two RNA-seq were then combined to perform correlation analyses between circNFAT5 or linear NFAT5 and the previously identified miRNAs. The purpose of these correlations was to select miRNAs on which circNFAT5 could have had a potential sponging effect. Indeed, in the event that a circRNA sponges a miRNA, a negative correlation between the circRNA and the miRNA in question would be expected.

Among the correlation analyses conducted, miR-144-3p was found to be the only miRNA significantly correlated with circNFAT5 with a negative correlation coefficient of -0.52 (Table 19). On the contrary, there appeared to be no correlation between miR-144-3p and linear NFAT5 ( $r = -0.3$ ;  $p$ -value = 0.16), consistent with the fact that this miRNA can only bind circNFAT5 on the junction point, and thus has no binding site for linear NFAT5.

The relationship between miR-144-3p and circNFAT5 or linear NFAT5, can be seen a little more thoroughly in the scatter plots presented in Figure 44, where correlation lines were drawn considering all patients analysed or patients dichotomized according to favourable (CPC1, n=12) or unfavourable (CPC5, n=11) neurological outcome. Indeed, further corroborating the hypothesis of a sponging effect of circNFAT5 on miR-144-3p is the fact that the negative correlation between the two was significant only in the group with CPC5, i.e., the group in which circNFAT5 levels increase significantly (Table 19).

	circNFAT5		NFAT5	
	r	p-value	r	p-value
hsa-miR-145-5p	-0.116	0.592	0.0615	0.778
<b>hsa-miR-144-3p</b>	<b>-0.52</b>	<b>0.011</b>	-0.3	0.161
hsa-miR-139-5p	0.0588	0.785	0.0405	0.851
hsa-miR-29b-1-5p	--	--	--	--
hsa-miR-106a-3p	--	--	--	--
hsa-miR-5195-3p	--	--	--	--
hsa-miR-7152-3p	--	--	--	--
hsa-miR-623	--	--	--	--
hsa-miR-4742-5p	-0.13	0.551	0.161	0.458
hsa-miR-450b-5p	-0.207	0.34	-0.132	0.542
hsa-miR-4772-5p	0.031	0.887	0.231	0.284
hsa-miR-4529-5p	--	--	--	--
hsa-miR-19b-2-5p	--	--	--	--
hsa-miR-19b-1-5p	--	--	--	--
hsa-miR-19a-5p	--	--	--	--
hsa-miR-6755-3p	--	--	--	--
hsa-miR-655-5p	--	--	--	--
hsa-miR-642b-5p	--	--	--	--

*Table 19. Spearman correlations between circNFAT5 or linear NFAT5 and the predicted miRNAs binding circNFAT5 in the 23 TTM patients common to the two RNA-seq datasets. Spearman correlation coefficients (r) are shown for each correlation performed. Statistically significant correlations are considered with p-value < 0.05.*

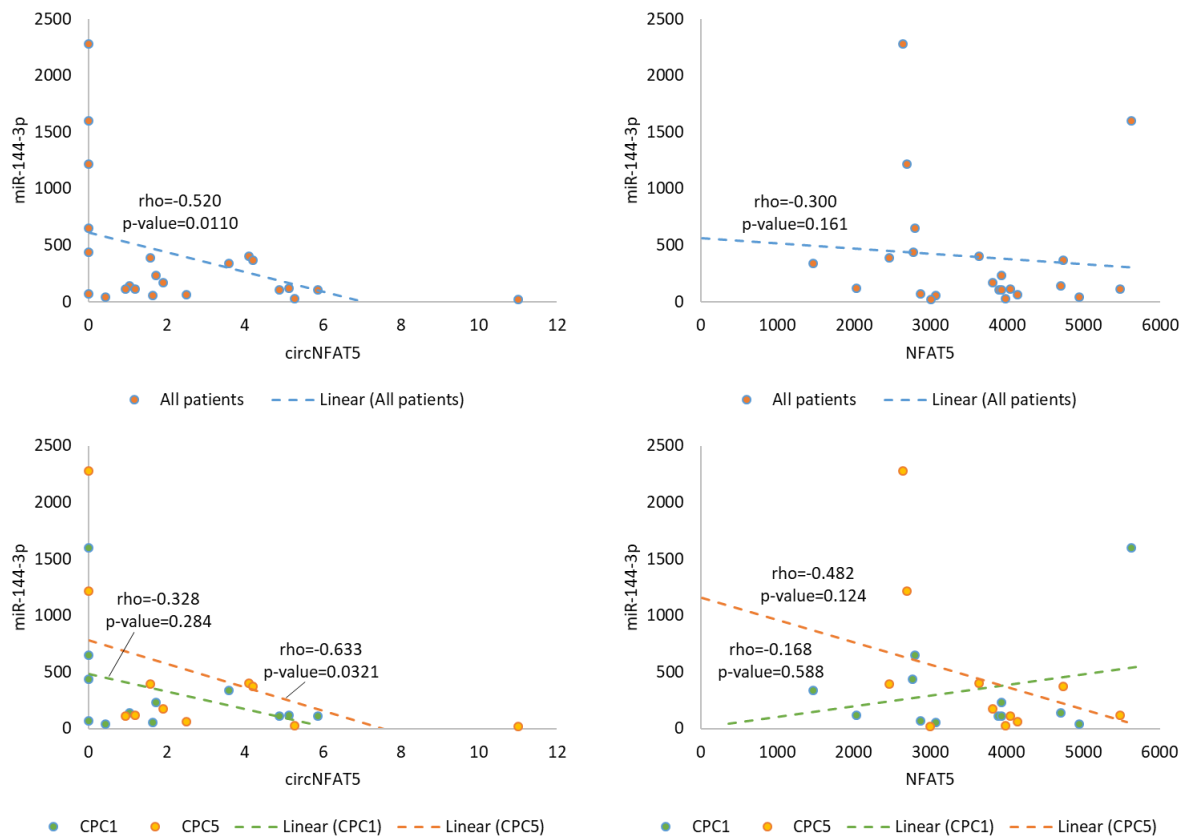


Figure 44. Scatter plots showing the correlation between circNFAT5 or linear NFAT5 and miR-144-3p. The correlations were performed considering all 23 TTM patients (a.) or the patients dichotomized according to their CPC score (b.).

To study the binding between miR-144-3p and circNFAT5 *in-vitro*, a luciferase assay was conducted using the Genecopoeia Dual luminescence assay kit pEZX-MT05 system in HEK293 cells. As the word implies this dual luminescence system consists of two reporters located on the vector upstream and downstream, respectively, of the target gene to be tested (Figure 45.a.). The downstream reporter, alkaline phosphatase (AP), represents the internal control of the system. Indeed, regardless of whether the miRNA under study, here miR-144-3p, binds to the target gene or not, AP should never change. Instead, the upstream reporter, Gaussia luciferase, is the reporter that should provide the information about whether the miRNA under study binds to the target gene. In fact, if miR-144-3p binds to the target gene, the luciferase protein will not be produced and therefore there will be no luminescence emission; on the contrary, in the absence of binding, luminescence will be emitted (Figure 45.a.).

In this study, the target genes were first cloned into the pEZX-MT05 vector (Figure 45.a.). Then, HEK293 cells were transfected with 120 µg of the vector containing the target gene sequence to be analysed in combination with 30 ng of pre-miR-144-3p (Applied Biosystems) or scramble microRNA for 48 h. Finally, secreted luciferase and alkaline phosphatase activity was measured in the cell supernatant.

MYB was identified as target of miR-144-3p in TargetScan database ([https://www.targetscan.org/vert\\_80/](https://www.targetscan.org/vert_80/)) and then used as positive control of the experiment (Figure 45.b.), while the empty vector pEZX-MT05 was used as negative control. MYB was confirmed as a target of miR-144-3p by the significant decrease in the luciferase/AP ratio (Figure 45.c.). More interestingly, miR-144-3p appears to be able to bind circNFAT5 but not linear NFAT5; in fact, while for circNFAT5



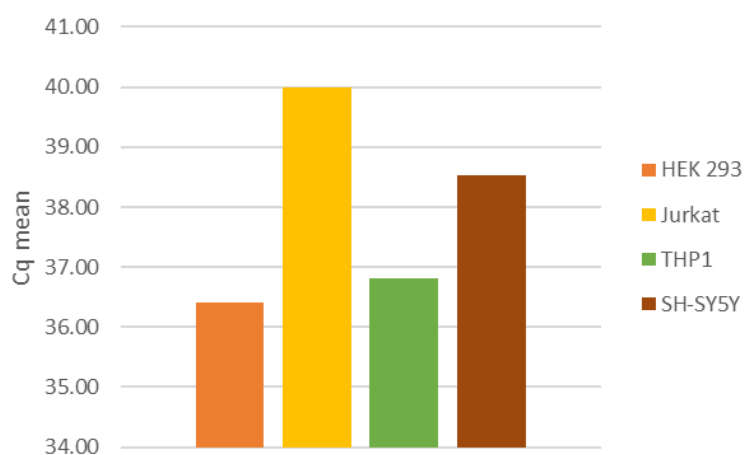


Figure 46. Bar graphs representing qPCR measurements of miR-144-3p in HEK293, jurkat, THP-1 and SH-SY5Y cell lines. The miR-144-3p measurements are shown as mean values of the quantification cycle (Cq).

#### 2.3.5.4. Prediction of potential binding proteins

The last function investigated here is the potential sponging effect of circNFAT5 on proteins.

To see whether circNFAT5 was able to bind RBPs, a prediction analysis was performed using the RBPmap database (<http://rbpmap.technion.ac.il/>). Among the proteins identified to have a binding site on circNFAT5, ZNF326, RC3H1, and KHDRBS2 appeared to have a binding site at the junction point and thus be specific only to the circular form of NFAT5. The details on the binding site, the motif, the sequence and the prediction power are presented in Table 20.

Protein	Binding Position	Motif	Occurrence	Z-score	p-value
ZNF326	119	cuauaa	Aacuugacuggcuccuuuuuacugga <u>uauac</u> ugua gucagcuuuuuaaccucuggac	2.321	0.010
RC3H1	120	uauauua	Acuugacuggcuccuuuuuacugga <u>uauac</u> uguagu cagcuuuuuaaccucuggacca	1.859	0.032
	118	uauauua	Caacuugacuggcuccuuuuuacugga <u>uauac</u> ugu agucagcuuuuuaaccucuggac	1.817	0.035
KHDRBS2	118	aauaaa	Caacuugacuggcuccuuuuuacugga <u>uauac</u> ugu agucagcuuuuuaaccucugga	1.759	0.039

Table 20. RBPs predicted by RBPmap database to bind circNFAT5 at the junction point.

As highlighted in Table 20, three RBPs were correlated with circNFAT5 and linear NFAT5 in the whole RNA-seq data of the 46 TTM patients. Interestingly, none of the identified proteins correlated with circNFAT5, either considering all patients or dichotomizing them according to their CPC score (Figure 47.a.). This indicates that a potential binding of circNFAT5 to these proteins would not affect their transcript expression levels. In contrast, a strong correlation was identified between RC3H1 and linear NFAT5 in all patients and regardless of their CPC score (Figure 47.b.). In addition, a weaker but significant correlation was also observed between linear NFAT5 and KHDRBS2 in the group with CPC1 (Figure 47.b.). Unfortunately, no further *in-vitro* experiments were performed to confirm the predicted binding between the three proteins and circNFAT5. Instead, to also identify potential indirect interactions between RBPs and circNFAT5, 403 RBPs, identified in Homo Sapiens in the RBPDB

database (<http://rbpdb.cbr.utoronto.ca/>), were correlated with circNFAT5 and linear NFAT5 in the whole RNA-seq data. Among all proteins examined, YTHDC2 was significantly correlated with circNFAT5 in the CPC5 group ( $r = 0.637$ ;  $p\text{-value} = 0.001$ ) but not with linear NFAT5 (Figure 48). However, the type of relationship between circNFAT5 and YTHDC2 has not been further investigated.

Therefore, these preliminary studies have provided the basis on which future experiments could be initiated in order to shed light on the possible interactions that circNFAT5 may have with RBPs and thus better understand what kind of pathways this circRNA may be involved in.



**Figure 47.** Scatter plots showing the correlation between circNFAT5 (a.) or linear NFAT5 (b.) and RBPs predicted to bind circNFAT5 at the junction point in the RNA-seq data of TTM. Analyses were performed considering all 46 patients or patients dichotomized according to their CPC score. Spearman correlation coefficient indicated as  $r$  and statistically significant  $p$ -value considered as  $<0.05$ .

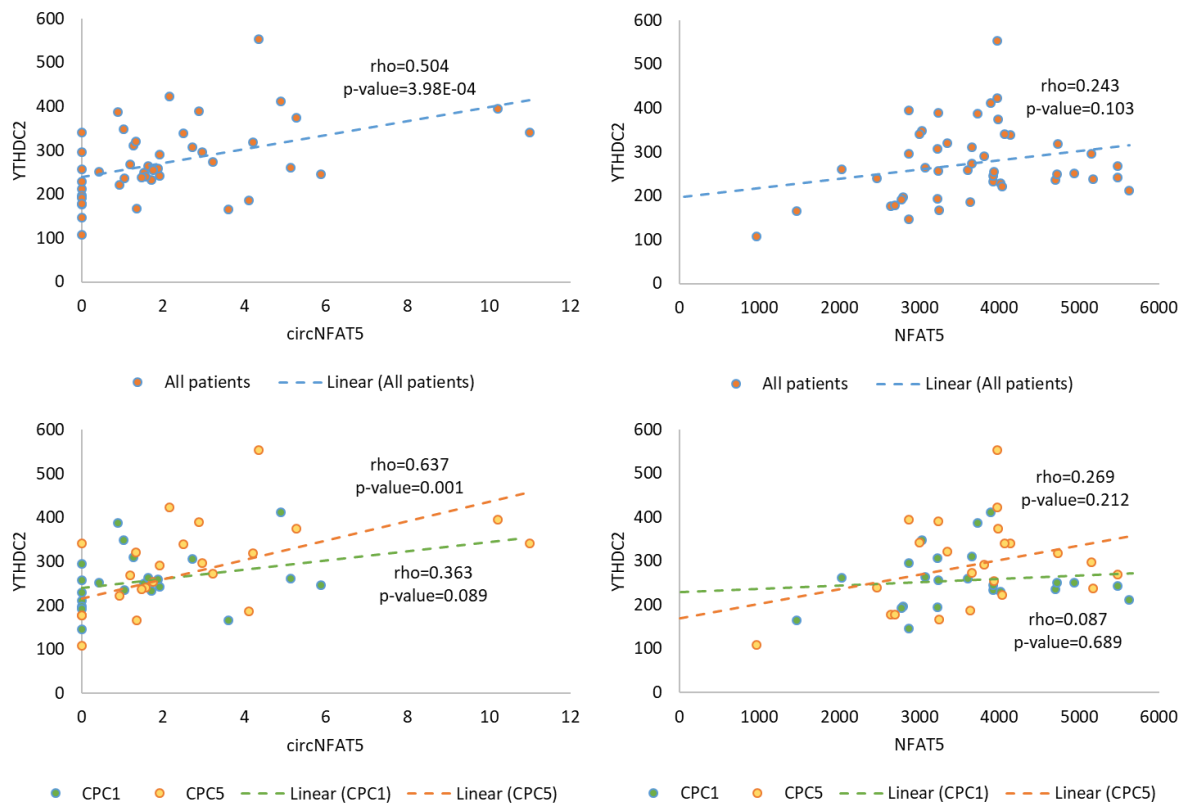


Figure 48. Scatter plots showing the correlation between circNFAT5 or linear NFAT5 and YTHDC2 in the RNA-seq data of TTM. Correlation analyses were conducted for all 46 TTM patients and for patients dichotomized according to their CPC score. For each correlation performed, the correlation coefficient was reported ( $r$ ) and a significant  $p$  value was considered as  $< 0.05$ .

#### 2.4. Validation of the biomarker potential of 3 circRNAs in TTM2-trial

Based on what was previously observed in TTM, the potential for predicting 6 months neurological outcome and survival of circNFAT5, circFAM13b and circDNM2 was further validated in 674 patients in the TTM2-trial for whom RNA samples were available 48 h after ROSC (Figure 49). The neurological outcome of these patients was assessed by mRS score only and counted 369 patients with good outcome (mRS 0-3) and 305 with poor outcome (mRS 4-6) (Figure 49). Of the 674 patients who participated in this study, 339 received targeted hypothermia treatment at 33 °C, and the remaining 335 received targeted normothermia with early treatment of fever (considered  $> 37.8$  °C).

The demographic and clinical characteristics of the TTM2 study were similar to those of the patients in the TTM study, with the exception of the significantly higher number of males in the group with good neurological outcome compared with the group with poor neurological outcome in the TTM2 study (Table 21).

As observed in the TTM study, circDNM2 also showed significantly different expression levels in the different targeted temperature regimens used, with higher expression levels in patients treated with lower temperatures (Figure 50.a.). In addition, in TTM2, circFAM13b also showed significantly higher levels in the hypothermic group than in the normothermic group (Figure 50.a.). A significant difference in circDNM2 expression levels was also observed between male and female patients, with higher levels of circDNM2 in males (Figure 50.b.). In contrast to circFAM13b and circDNM2 and similar to what was observed in TTM, no significant changes in circNFAT5 expression levels were observed when patients

were dichotomized according to the temperature regimen used or their sex in the TTM2 study (Figure 50.a.b.). Conversely, patients in the normothermia group of the TTM2 study with unfavourable neurological outcome had significantly higher levels of circNFAT5 than patients with good neurological outcome (Figure 50.c.). However, circNFAT5 levels were comparable between patients with poor and good neurological outcome when considering all patients or patients in the hypothermia group (Figure 50.c.). CircDNM2 and circFAM13b, on the other hand, showed similar expression patterns, with significantly higher expression levels when considering all patients or patients treated with a normothermic regimen but not in the hypothermic condition (Figure 50.c.).

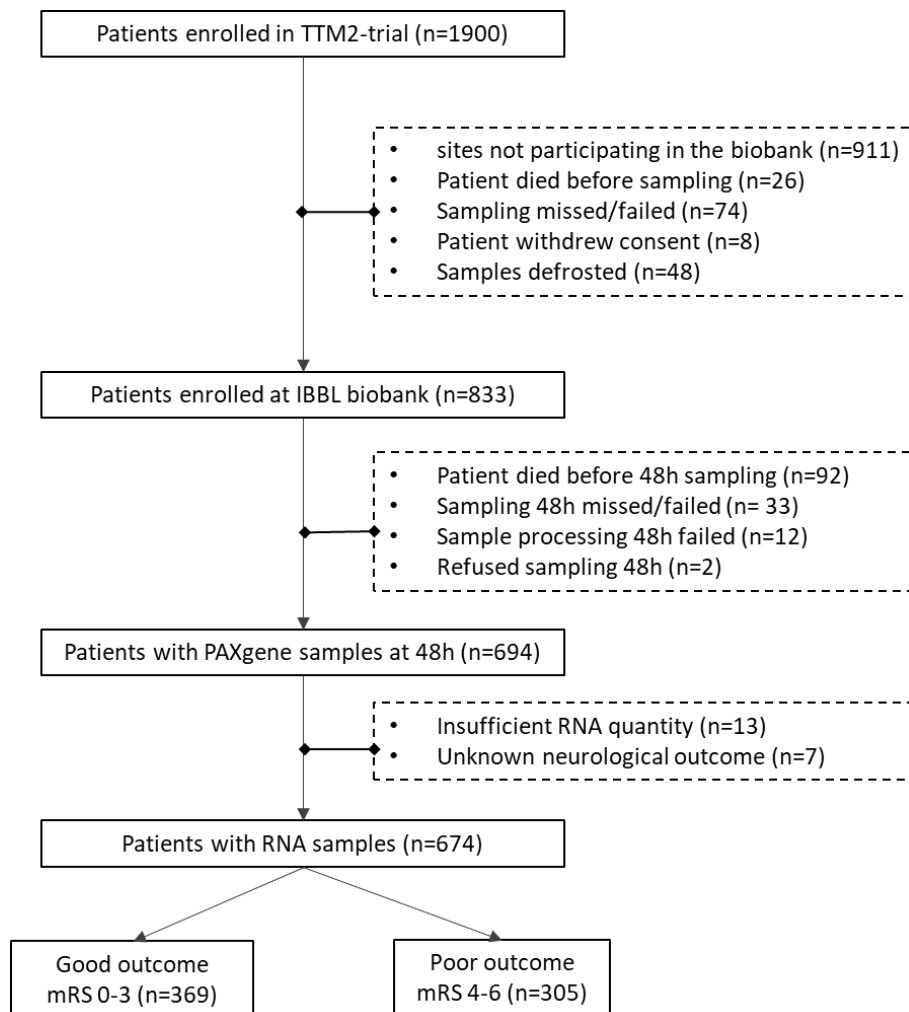


Figure 49. Study flow chart TTM2-trial. Abbreviations: IBBL = International biobank of Luxembourg; mRS = modified Rankin Scale.



Characteristics	Neurological outcome		p-value
	mRS 0-3	mRS 4-6	
	n=369	n=305	
<b>Age, years</b>	61 (19-87)	69 (33-89)	<b>&lt;0.001</b>
<b>Sex</b>			<b>0.037</b>
Male	311 (84.3%)	237 (77.7%)	
Female	58 (15.7%)	68 (22.3%)	
<b>Co-morbidities</b>			
Hypertension	106 (28.7%)	109 (35.7%)	<b>0.004</b>
Diabetes mellitus	49 (13.3%)	71 (23.3%)	<b>0.001</b>
Heart failure	12 (3.3%)	33 (10.8%)	<b>&lt;0.001</b>
COPD	15 (4.1%)	42 (13.8%)	<b>&lt;0.001</b>
<b>First monitored rhythm</b>			<b>0.001</b>
VF or non-perfusing VT	284 (77.0%)	170 (55.7%)	
Asystole or PEA	27 (7.3%)	111 (36.4%)	
ROSC after bystander defibrillation	26 (7.0%)	5 (1.6%)	
unknown	32 (8.7%)	19 (6.2%)	
<b>Witnessed arrest</b>	348 (94.3%)	281 (92.1%)	0.33
<b>Bystander CPR</b>	317 (85.9%)	242 (79.3%)	<b>0.031</b>
<b>Time from CA to ROSC (mins)</b>	20 (2 - 135)	29 (2 - 91)	<b>&lt;0.001</b>
<b>Initial serum lactate (mmol/l)</b>	3 (1 - 20)	5 (0 - 15)	<b>&lt;0.001</b>
<b>Shock on admission</b>	54 (14.6%)	77 (25.2%)	<b>&lt;0.001</b>

Table 21. Demographic and clinical characteristics of 674 TTM2 patients. The patients were dichotomised according to their neurological outcome determined by mRS score. Median (range) indicates continuous variables, and number (frequency) categorical variables. Abbreviations: COPD = chronic obstructive pulmonary disease; VF = ventricular fibrillation; VT = ventricular tachycardia; PEA = pulseless electrical activity; ROSC = return of spontaneous circulation; CPR = cardiopulmonary resuscitation; CA = cardiac arrest.

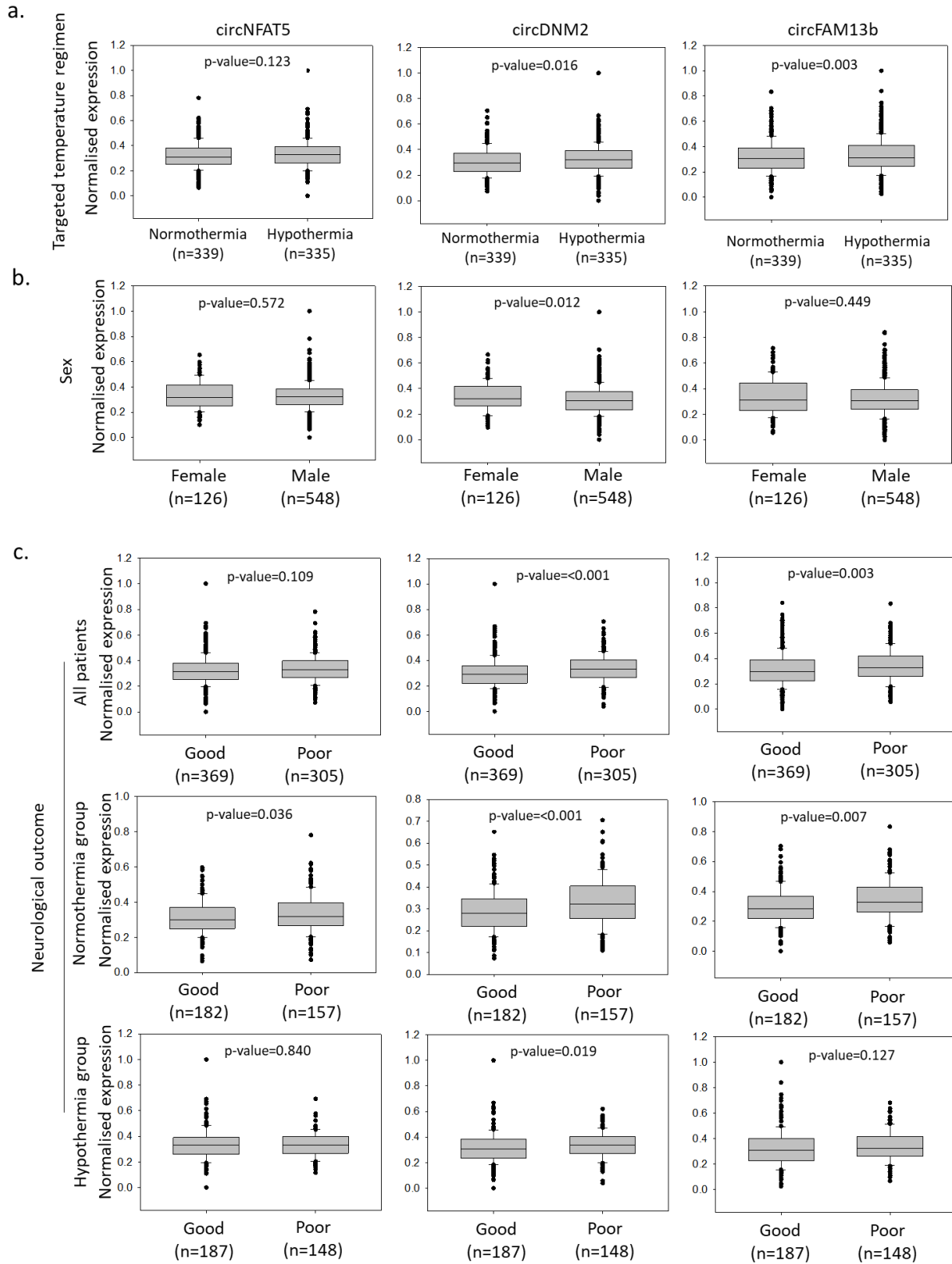


Figure 50. Differential expression levels of 3 selected circRNAs in 674 TTM2 patients. Candidate expression levels were compared according to the temperature regime used in the trial (a.), patient sex (b.) and neurological outcome (c.) considering all patients or patients dichotomized according to temperature regimen. Candidate expression levels were normalized, log2-transformed and scaled. P-values were derived from the Mann-Whitney U test.

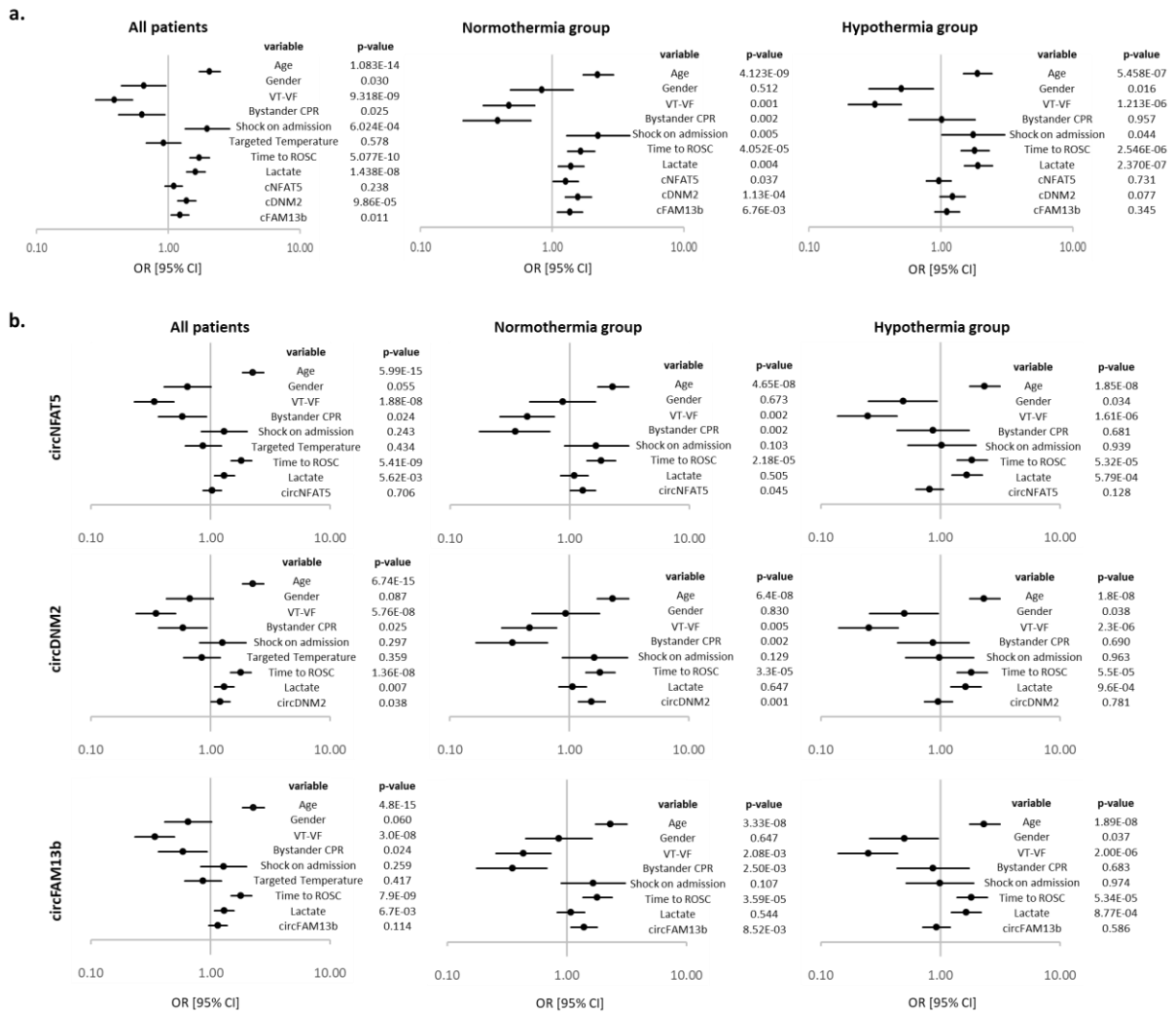
#### 2.4.1. Prediction 6-month neurological outcome in TTM2-trial

The predictive ability of the 3 circRNAs was confirmed in univariate logistic regression analyses in the normothermia group of TTM2, but not in the hypothermia group (Figure 51.a.). Considering all patients, only circFAM13b and circDNM2 remained predictors of neurological outcome (Figure 51.a.).

Although multivariable logistic regression analyses were performed using the same clinical variables used previously for TTM, measurements of NSE in TTM2 at the time this study was conducted were not available and therefore were not included in the basal model. After adjustment with clinical variables, all circRNAs were confirmed as predictors of neurological outcome at 6 months in the normothermia group with ORs [95% CI; p-value] of 1.29 [1.00-1.65; 0.045], 1.53[1.19-2.00; 0.001] and 1.39[1.09-1.79; 8.52E-03] for circNFAT5, circDNM2 and circFAM13b respectively (Figure 51.b.). However, this predictive ability was lost in all candidates when considering only patients treated with hypothermia and for circNFAT5 and circFAM13b even when considering all patients regardless of the temperature regimen used in the study (Figure 51.b.).

The incremental predictive value of each candidate in the normothermia group was confirmed by a decrease in AIC compared with the basal model (Table 22). Among them, circDNM2 performed best in the normothermia group with an AIC of 387 (LRT p-value= 0.001; Wald test p-value=3.13E-10) associated with an NRI of 0.403 and IDI of 0.030 (Table 22).

In conclusion, the selected candidates showed potential in predicting neurological outcome only in the normothermic patient group. Moreover, among the three candidates, circDNM2 performed better in predicting the neurological outcome of TTM2 patients.



All patients	AIC	Wald_p	AUC	lr_p	NRI	NRI_p	IDI	IDI_p
<i>basal model</i>	765	4.69E-21	0.779	-	-	-	-	-
<i>basal model + circNFAT5</i>	767	1.77E-20	0.779	0.706	0.056	0.471	1.55E-04	0.764
<i>basal model + circDNM2</i>	763	7.25E-21	0.783	<b>0.036</b>	0.179	<b>0.020</b>	5.68E-03	<b>0.049</b>
<i>basal model + circFAM13b</i>	764	1.11E-20	0.781	0.113	0.144	0.060	3.40E-03	0.116
<b>Normothermia group</b>								
<i>basal model</i>	396	9.11E-10	0.771	-	-	-	-	-
<i>basal model + circNFAT5</i>	394	1.53E-09	0.780	<b>0.043</b>	0.263	<b>0.015</b>	0.012	<b>0.039</b>
<i>basal model + circDNM2</i>	387	3.13E-10	0.790	<b>0.001</b>	0.403	<b>1.47E-04</b>	0.030	<b>0.001</b>
<i>basal model + circFAM13b</i>	391	7.82E-10	0.786	<b>0.008</b>	0.252	<b>0.019</b>	0.020	<b>0.008</b>
<b>Hypothermia group</b>								
<i>basal model</i>	370	3.89E-11	0.809	-	-	-	-	-
<i>basal model + circNFAT5</i>	370	9.86E-11	0.810	0.126	0.081	0.462	0.006	0.162
<i>basal model + circDNM2</i>	372	1.21E-10	0.808	0.781	-0.003	0.982	8.56E-05	0.908
<i>basal model + circFAM13b</i>	372	1.21E-10	0.808	0.586	0.063	0.566	0.001	0.706

Table 22. Candidate performance to predict 6-month neurological outcome in TTM2 patients. Patients were dichotomised using the mRS score. Basal model includes the following 8 variables: age, sex, first rhythm monitored, CPR by bystanders, circulatory shock on admission, targeted temperature regimen, time from CA to ROSC, initial serum lactate levels. Abbreviations as given in Figure 12.

#### 2.4.2. Prediction 6-month survival in TTM2-trial

In survival analyses, Kaplan-Meier curves were generated as previously generated for TTM, using the Youden index to identify the cut-off to be used for each candidate. The Kaplan-Meier curves showed that patients with circNFAT5 levels > 0.28, circDNM2 > 0.36 and circFAM13b > 0.25 had a significantly higher risk of death (Figure 52).

Cox proportional hazards models confirmed that circNFAT5, circDNM2 and circFAM13b were independent predictors of survival in the normothermia group with HRs [95% CI; p-value] of 1.24[1.05-1.47; p-value=0.013], 1.34[1.14-1.59; p-value=5.11E-04] and 1.29[1.09-1.53; p-value=3.09E-03] respectively (Figure 53). However, all candidates lost the ability to predict 6-month survival after OHCA when considering all patients or only those that underwent hypothermia treatment (Figure 53).

Finally, the quality of the prediction models generated for each circRNA was confirmed in the normothermia group with an AIC of 1464 (LRT p-value= 0.014; Wald test p-value=2.43E-13), 1458 (LRT p-value= 0.001; Wald test p-value=1.89E-14) and 1462 (LRT p-value= 0.004; Wald test p-value=1.85E-13) for circNFAT5, circDNM2 and circFAM13b respectively (Table 23).

In conclusion, even with regard to survival analysis, the candidates studied showed predictive potential only in the normothermic TTM2 group. CircDNM2 was identified as the best candidate for improving the survival model.

Finally, Figure 54 shows a summary of the best predictors of neurological outcome and survival identified by the various analyses in both the TTM-trial and the TTM2-trial.

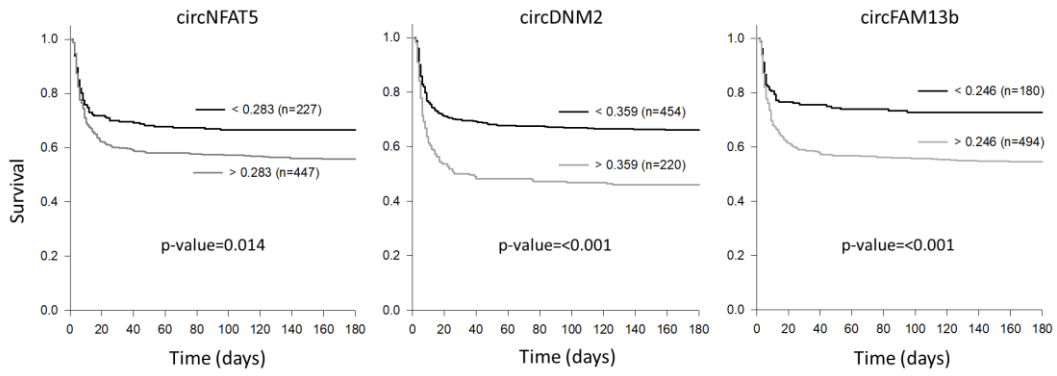


Figure 52. Kaplan-Meier curves to predict 6-month survival in TTM2 patients. Youden index was used to determine the cut-off value for each circRNA tested. P-values are given for each survival analysis. The number of patients with expression levels of each candidate above or below the cut-off is indicated in parentheses.

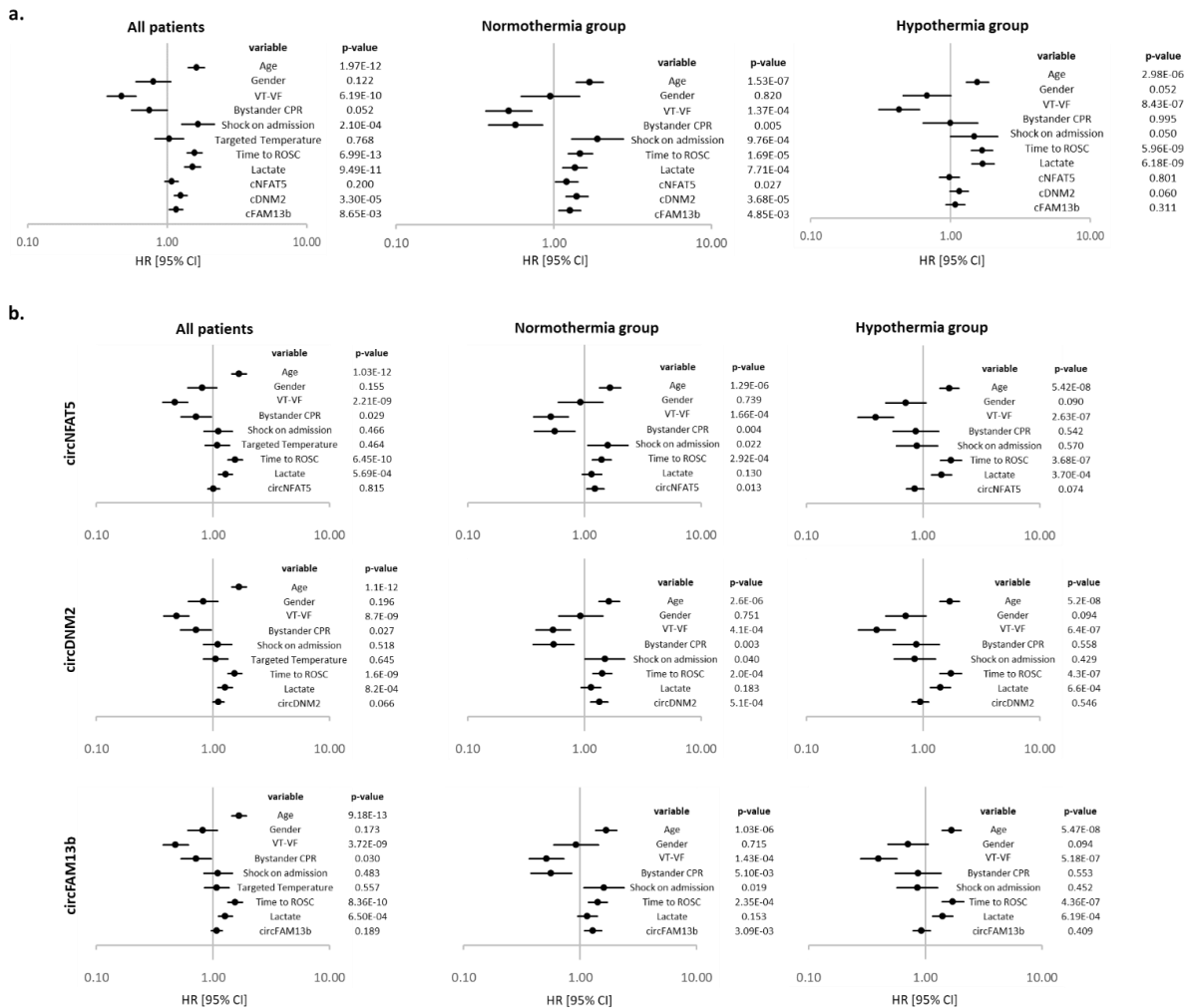


Figure 53. Univariate (a.) and multivariable (b.) Cox proportional hazards for 8 independent variables and 3 candidate circRNAs for predicting 6-month survival in the TTM2-trial. Data in forest plots are shown as hazard ratios (HRs) with  $\pm$  95% confidence interval [95% CI], and p-values are shown for each variable. Abbreviations as reported in Figure 23.

<b>All patients</b>	<i>AIC</i>	<i>Wald_p</i>	<i>C_idx</i>	<i>lr_p</i>
<i>basal model</i>	3265	3.01E-31	0.730	-
<i>basal model + circNFAT5</i>	3267	1.38E-30	0.730	0.816
<i>basal model + circDNM2</i>	3264	3.50E-31	0.733	0.072
<i>basal model + circFAM13b</i>	3266	9.00E-31	0.732	0.193
<b>Normothermia group</b>				
<i>basal model</i>	1468	8.29E-13	0.711	-
<i>basal model + circNFAT5</i>	1464	2.43E-13	0.715	<b>0.014</b>
<i>basal model + circDNM2</i>	1458	1.89E-14	0.724	<b>0.001</b>
<i>basal model + circFAM13b</i>	1461	1.85E-13	0.720	<b>0.004</b>
<b>Hypothermia group</b>				
<i>basal model</i>	1420	2.41E-19	0.761	-
<i>basal model + circNFAT5</i>	1419	3.03E-19	0.763	0.064
<i>basal model + circDNM2</i>	1422	9.29E-19	0.760	0.542
<i>basal model + circFAM13b</i>	1422	6.96E-19	0.760	0.402

Table 23. Candidate performance to predict 6-month survival in 674 TTM2 patients. Basal model includes the same variables as shown in Table 22. Abbreviations as in Table 14.




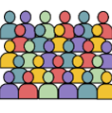


	TTM-trial			TTM2-trial		
	All  n=542	36°C  n=301	33°C  n=241	All  n=674	Normothermia  n=339	Hypothermia  n=335
<b>Differential expression</b>	circFAM13b circAGO2 circDLG1 circDNM2 circNFAT5 lncL1R1-1:2	circFAM13b circAGO2 circDNM2 circNFAT5 lncL1R1-1:2	circAGO2 circDLG1 (mRS) circDNM2 circNFAT5 lncL1R1-1:2	circFAM13b circDNM2	circFAM13b circDNM2 circNFAT5	circDNM2
<b>Binary outcome classification</b>	circNFAT5	circFAM13b (CPC) circNFAT5	lncL1R1-1:2 (CPC)	circDNM2	circFAM13b circDNM2 circNFAT5	
<b>Survival analysis with time-to-event data</b>	circFAM13b circNFAT5	circFAM13b circNFAT5	circDNM2 circNFAT5		circFAM13b circDNM2 circNFAT5	

Figure 54. Best predictors identified in TTM-trial and TTM2-trial. The Figure shows the names of the selected circRNAs or lncRNAs that performed well in the different types of analysis. Since both CPC and mRS scores were used in the TTM-trial to dichotomise patients with good and bad neurological outcome, the results obtained from both types of scores are summarised here and those obtained from only one of the scores (CPC or mRS) are shown in brackets.

# *Discussion*



This research project aimed to deepen the knowledge of the potential role played by ncRNAs as prognostic biomarkers after OHCA. Indeed, OHCA represents a major cause of death worldwide, and the outcome prognostication of patients with OHCA must be accurate with the lowest possible false-positive rate to avoid WLST in patients with still a chance of survival [129]. As the main reason for non-recovery in these patients is severe neurological damage, most predictors of outcome of patients with OHCA assess the level of neurological damage [9]. However, because even the most reliable predictors are not 100% accurate, the use of a multimodal approach is recommended to obtain a more accurate prognosis [9]. Indeed, this multimodal approach involves clinical examinations, neuroimaging, biomarker measurements and electrophysiological investigations [9].

Although currently used biomarkers are protein-derived markers measured in the bloodstream to predominantly detect levels of neuronal damage [244], more and more studies are reporting the biomarker potential of ncRNAs. In fact, RNA markers, similar to protein markers, can provide a dynamic view of the cellular state, but they have the advantage of being more sensitive and specific yet less costly than protein markers [482]. In fact, while protein markers require specific antibodies to be detected, RNA markers are easily measured by PCR, requiring simply a primer pair to be detected and measured specifically with high sensitivity [482]. The ncRNAs most studied as biomarkers in cardiovascular disease are miRNAs [416, 417, 420]. Previously in the same laboratory where this research was conducted, miR-21, miR-122-5p and miR-124-3p were identified as potential prognostic biomarkers after OHCA in plasma samples of TTM-trial [36, 37, 422]. However, it is still not entirely clear whether circulating miRNAs after OHCA can reflect levels of brain injury. Therefore, the first study in this thesis project aimed to investigate the possible correlation of miRNAs found in the plasma of TTM-trial patients with NSE, the gold standard biomarker used in the clinic to assess the neurological outcome of patients after cardiac arrest. The results of this study reported a strong correlation between miR9-3p, miR124-3p and miR129-5p, which are all brain-enriched miRNAs, and NSE. Moreover, when dichotomizing patients according to neurological outcome, this correlation was maintained only in the group with unfavourable outcome, thus strengthening the hypothesis that miR9-3p, miR124-3p and miR129-5p may reflect the extent of brain damage. Even further, miR-124-3p and miR-129-5p showed a significant correlation with the time from cardiac arrest to ROSC in the CPC5 group while no correlations were found between the 3 miRNAs and the comorbidities presented in table 7. Logistic regression analyses also reported an association between the three miRNAs and 6-month neurological outcome after OHCA. The predictive model containing the three miRNAs and NSE or time from cardiac arrest to ROSC remained significant but with reduced predictive ability. This was consistent with the previously observed correlation between the three miRNAs and NSE and time from cardiac arrest to ROSC. Thus, suggesting that miR9-3p, miR124-3p and miR129-5p might aid in the outcome prognostication of OHCA. As these 3 miRNAs are involved in brain development, differentiation, and plasticity [45-48] among other physiological processes, their presence in the bloodstream after OHCA most probably derives from the disruption of the blood brain barrier and cellular death from the brain.

Whilst this first study showed that 3 circulating brain-enriched miRNAs might contribute to the prognostication of patients after OHCA, there are limitations most notably with the sample size. Indeed, all the analyses performed have been done using plasma samples of 50 TTM patients used for short RNA sequencing. Due to the very short number of patients used in the study it was not possible in the multivariable analyses to adjust the model using all relevant demographics and clinical parameters simultaneously. Another limitation is that miRNAs were measured in plasma while NSE was measured in serum, even though these patients showed comparable levels of miRNAs in plasma and serum. Furthermore, the correlation between brain damage and miRNA levels in circulation was assessed only at 48 h after ROSC, considering that NSE levels reach a peak at this time point presenting

the highest prognostic value [49]. However, this does not exclude that patients with co-morbidities died for other causes other than brain damage with an impact on the correlation between miRNAs and NSE.

Although brain damage is a major determinant in predicting outcome and survival of patients with OHCA, other factors contribute to PCAS. Among these factors, systemic inflammation after ischemia/reperfusion represents another key element of PCAS [56-58]. Indeed, PCAS is considered a syndrome similar to sepsis, as the early inflammatory response induces an exacerbation of the immune-inflammatory profile that is associated with the clinical outcome of these patients [58, 100, 483]. Therefore, the study of regulatory ncRNAs in the context of the inflammatory response in patients after OHCA was particularly interesting. In this context, an increasing number of studies have turned to other classes of ncRNAs, other than miRNAs, for which potential clinical use as biomarkers after OHCA has already been established. Indeed, lncRNAs and circRNAs modulate gene expression at different levels [50] and have already been recognised to play key roles in physiological conditions and in diseases related to cardiac arrest [22, 34, 50, 55, 440]. However, the prognostic potential of lncRNAs and circRNAs after OHCA has not yet been studied.

Therefore, the focus of this thesis project was directed to study the modulation of lncRNAs and circRNAs in the immunoinflammatory response after OHCA. For this purpose, whole transcriptome sequencing conducted on 46 patients of the TTM-trial identified 41 lncRNAs and 28 circRNAs with significant differential expression levels among patients with good or poor neurological outcome in a discovery phase. Primer's standardisation and correct product amplification allowed the selection of one lncRNA, lnc-IL1R1-1:2 and 5 circRNAs, named circAGO2, circDLG1, circDNM2, circFAM13b, and circNFAT5 respectively, for further qPCR measurements. In the RNA-seq data, all selected candidates showed increased expression levels in patients with poor outcome 6 months after cardiac arrest, with the exception of circDLG1, which instead showed an opposite trend. If it is thought that these RNA molecules may somehow be involved in the inflammatory process triggered after cardiac arrest then it is not surprising that most of them exhibit the same tendency to increase in expression levels in patients with unfavourable outcomes and for whom inflammatory levels are found to be more severe. Downstream qPCR analyses performed on the same TTM samples confirmed the trends observed in the RNA-seq data, although statistical significance was reached only for circFAM13b and circDNM2, probably due to small sample size (46 patients). CircDLG1 was the only candidate for which differential expression was not confirmed by qPCR.

To obtain more reliable results on the differential expression of the 6 selected candidates, their expression levels were measured in the remaining TTM samples (n=542). The results confirmed what was observed in the qPCR measurements of the discovery cohort, regardless of the score used for the patient classification (CPC or mRS). In addition, no differential expression was observed in any of the selected candidates when dichotomizing patients according to sex or target temperature, with the exception of circDNM2, which was shown to be significantly higher in patients treated with 33 °C. A similar result was observed later in this study in the hypothermic group of the TTM2-trial. However, the reason why circDNM2 may be more expressed in lower body temperature conditions and how this may be associated with an unfavourable neurological outcome remains unclear. Although more in-depth studies on this circRNA need to be conducted, a recent study reported an overexpression of circDNM2 in pulmonary tuberculosis [484], a chronic infectious disease, thereby strengthening the hypothesis of the involvement of this circRNA in immune-inflammatory responses.

After adjustment with 9 different demographic and clinical parameters, including NSE, in the baseline model, circNFAT5 was identified among various candidates as the only independent predictor of neurological outcome in the TTM cohort. Further statistical analysis determined the incremental

predictive value of candidates for neurological outcome and confirmed the strong performance of circNFAT5 in TTM.

Similarly, survival analyses performed at 6 months after cardiac arrest showed 2 circRNAs, circFAM13b and circNFAT5, as independent predictors of survival after adjustment with the same clinical parameters previously used. Again, circNFAT5 performed better in improving the survival model, with the lowest AIC and best c-index among the various candidates.

One of the advantages of this first part of the study is that it was a predefined sub-study of a large multicentre clinical trial of patients with OHCA. Another advantage is that the collection, storage, and processing of TTM blood samples were done in a homogeneous manner according to protocols validated by the central biobank. In addition, to improve the robustness of the results and eliminate interlaboratory variability of measured candidates, all measurements were conducted in the same laboratory. However, several limitations are also present at this early stage of the study. In fact, the predictive value of single lncRNAs and circRNAs was measured, but not the combination of multiple lncRNAs and circRNAs that might provide better prediction. Another limitation is that all candidates were measured in TTM blood samples collected 48 h after ROSC, but it is not known whether these selected candidates could be detected at earlier stages after ROSC and what their prognostic value might be at earlier stages. Despite these limitations, this was the first study to identify potential lncRNAs and circRNAs as prognostic biomarkers of outcome after OHCA.

Although the mechanisms of action of the best-performing circRNAs identified in the TTM-trial need to be elucidated, recent studies have demonstrated the involvement of circFAM13b for instance in cancer development and its potential role as a diagnostic or prognostic biomarker [485, 486]. It has been shown that circFAM13b can promote the proliferation of hepatocellular carcinoma cells by sponging miR-212 [485]. Further studies closer to cardiovascular disease, have found dysregulated circFAM13b levels in exosomes of serum samples from patients with proliferative diabetic retinopathy [487]. Despite little current knowledge about the biological functions performed by circFAM13b, it appears that this circRNA may play important roles in pathological conditions. Therefore, future research might shed light on the biological functions played by circFAM13b in cardiac arrest.

As for circNFAT5, at the time this study was conducted, nothing was known about its functions in physiological and pathological conditions. CircNFAT5 is located in the last exon of the transcription factor NFAT5, which is expressed in various tissues, including skeletal muscle, heart, brain, and peripheral blood leukocytes [488-491]. In this research project, circNFAT5 was shown to be the candidate with the best potential as a prognostic biomarker in the TTM-trial, and therefore it was selected for further functional studies. Although the role played by circNFAT5 in the context of cardiac arrest is still unclear, this study provided initial insight into the potential functions of this circRNA.

Among the treatments used to simulate a postcardiac arrest condition in selected cellular models, a significant increase in circNFAT5 levels was observed after stimulation of jurkat cells with anti-CD3/CD28 antibodies. The fact that circNFAT5 levels changed significantly after activation of a T cell-like model suggests a potential involvement of this circRNA in immune processes such as those activated after cardiac arrest. However, this remains to be determined in future studies as this experiment raised a more relevant question that needed to be investigated. Indeed, following treatment with anti-CD3/CD28, a delayed modulation of circNFAT5 compared with its linear counterpart was observed, raising the suspicion that circNFAT5 simply represents a by-product of linear NFAT5 overexpression instead of performing a regulatory function.

The study of its parental gene could also help uncover some elements of the function of circNFAT5. Indeed, several studies have already reported the key role played by NFAT5 in inflammatory responses

in pathologies associated with cardiovascular diseases like hypertension, atherosclerosis and diabetes mellitus [492-495].

Unfortunately, loss-of-function studies in jurkat cells had proven very difficult to perform, thus the focus shifted to studying the relationship between linear NFAT5 and circNFAT5 in THP-1 cells.

NaCl treatment was chosen as the best condition to study this relationship since NFAT5 is known to be an important player in triggering the osmotic stress response [496, 497]. Therefore, it could be hypothesized that if circNFAT5 followed NFAT5 overexpression, an increase in circNFAT5 expression should have been observed after NaCl treatment, whereas no modulation should have been observed in the presence of this stimulus in conjunction with NFAT5 silencing. In contrast, if the expression of circNFAT5 did not follow that of linear NFAT5, then circNFAT5 levels should have shown modulation even after NFAT5 silencing. The results of this study showed a clear increase in circNFAT5 expression levels after NaCl treatment; moreover, circNFAT5 levels did not appear to be significantly affected by NFAT5 silencing in the presence of NaCl. Therefore, these preliminary data suggested that the expression of circNFAT5 is independent on linear NFAT5. Consequently, circNFAT5 might have a functional regulatory role independent of its parental gene and thus not represent a simple by-product of linear NFAT5. However, it should be noted that the experiments conducted showed high variability limiting the robustness of these conclusions. Therefore, further experiments will be required to confirm what was observed here.

The next step was to obtain an overview of the potential regulatory roles that circNFAT5 might play under physiological conditions. Therefore, preliminary data were generated on the four types of functions defined so far for circRNAs. Indeed, circRNAs can regulate transcription of their parental genes, encode proteins, or sponge miRNAs and/or proteins. Although it was not possible to fully analyse each of these functions, several possible functions were investigated in general in this research project to get an initial overview of the possible functions performed by circNFAT5.

Starting from the potential modulation of its parental gene, silencing and overexpression experiments of circNFAT5 were conducted in THP-1 and jurkat cells, respectively. Despite technical issues with the cellular models used in this work, both silencing and overexpression of circNFAT5 did not appear to affect linear NFAT5 levels at all, thus indicating the absence of modulation of the parental gene.

Subsequently, a potential ORF on circNFAT5 that could produce a protein of approximately 6.5 kDa was identified. The protein-coding potential of circNFAT5 was then evaluated. At first, prediction analyses were conducted to check for the presence of IRES motifs and m6A modifications, known to drive cap-independent protein translation of circRNAs. Subsequently, an *in-vitro* assay performed by over-expressing circNFAT5 in HeLa cells and western blot analysis for the detection of small proteins allowed to investigate the potential presence of a circNFAT5-encoded protein. The low predicted protein-coding potential for circNFAT5, together with the absence of IRES elements and the low confidence predicted m6A modification, led to the assumption that circNFAT5 has little or no protein-coding potential. This assumption was later confirmed by the western blot, which saw the presence of no protein following circNFAT5 overexpression. Therefore, these analyses led to the conclusion that circNFAT5 does not produce any protein.

The functional studies of circNFAT5 continued with the evaluation of its potential sponging effect, one of the most widely studied functions in circRNAs. To assess the potential of circNFAT5 in sponging miRNAs first, a prediction analysis was conducted on the potential miRNAs that could bind circNFAT5 at the junction site. The identified miRNAs were then correlated with circNFAT5 and linear NFAT5 in 23 common TTM patients between short and whole RNA-seq data. MiR-144-3p was the only miRNA predicted to bind on the junction point and presented a significant negative correlation with

circNFAT5. Moreover, by dichotomizing the patients with CPC1 and CPC5, it was seen that the negative correlation remained significant only in the group of 11 patients with CPC5, further corroborating the potential sponging effect in those patients having higher circNFAT5 levels. To further validate what was observed in the prediction and correlation analyses, a luciferase assay was performed in HEK293 cells using a dual luminescence system. The results obtained in this system appear to indicate that indeed circNFAT5 could bind miR-144-3p. However, the expression levels of miR-144-3p were very low in the cell models studied here. Therefore, even if future studies confirm this binding, it may not necessarily represent the main mechanism by which circNFAT5 performs its regulatory functions in the cellular models analysed. Therefore, future studies should focus on confirming the data obtained here and the context in which this potential binding might occur. Furthermore, it should be kept in mind that for the sponging effect to be meaningful in the cell, several binding sites should be present on the sequence of the circRNA in question. Ultimately, this work focused on the potential interaction between circNFAT5 and miR-144-3p, but it cannot be excluded the possibility of circNFAT5 binding other miRNAs as well.

Lastly, prediction analyses generated preliminary data on the potential of circNFAT5 to sponge proteins. Of the three proteins predicted to bind circNFAT5 at the junction site, none showed a correlation with circNFAT5 in the whole RNA-seq data, indicating that potential binding to these proteins would not affect their transcripts. In addition, further correlation analyses were conducted between circNFAT5 and all RBPs identified in Homo Sapiens (n=403). Of all correlations conducted, YTHDC2 was the only protein significantly correlated with circNFAT5 in the CPC5 group but not with linear NFAT5. Although a direct link between YTHDC2 and circNFAT5 is unlikely, as no binding site was identified for YTHDC2 on circNFAT5, it might be interesting to further investigate a potential indirect link between the two. However, these were only prediction and correlation analyses and no *in-vitro* experiments were conducted to confirm a potential interaction with the identified proteins. Therefore, further *in-vitro* studies are required to better understand the protein sponging potential of circNFAT5.

Although the role played by circNFAT5 in the context of cardiac arrest has not been clarified in this work, preliminary data have provided more insight into the regulation of circNFAT5 levels in blood cells under basal conditions and following different stimuli, the potential relationship of this circRNA with its linear counterpart, and its possible mechanisms of action.

Finally, in the last part of this study, the 3 best-performing circRNAs identified in the TTM-trial, circNFAT5, circDNM2, and circFAM13b, were further validated in 674 TTM2-trial patients collected 48 h after ROSC.

Differential expression measurements according to the targeted temperature regimen used in the study showed significantly higher expression of circDNM2 and circFAM13b in the hypothermic treatment group than in the normothermic one. In addition, circDNM2 was significantly upregulated in males compared with females. However, these results may have been influenced by a significantly higher presence of males (n=548) than females (n=126) in the TTM2 cohort. Therefore, further independent validations in other cardiac arrest cohorts should assess the robustness of what was observed here. In addition, circNFAT5 did not show significant differential expression in relation to the target temperature regimen used or the sex of the patient, highlighting the potential use of this circRNA in more heterogeneous populations of cardiac arrest patients. Whereas, in contrast, circFAM13b and circDNM2 could represent potential markers of more specific sub-populations of cardiac arrest patients.

Regarding the assessment of the neurological outcome of TTM2 patients, unlike the TTM-trial, only the mRS score was used in TTM2-trial, as it was considered to be more accurate than the CPC score in

the evaluation of neuronal functions [143]. Therefore, patients were dichotomized as having good neurological outcome (mRS 0-3) and poor neurological outcome (mRS 4-6), and the differential expression patterns observed in TTM patients were confirmed only for circDNM2 and circFAM13b. While no significant differential expression was observed in the expression levels of circNFAT5 according to neurological outcome when considering the whole TTM2 population. CircNFAT5 levels were only found significantly higher in the subgroup of normothermic patients with unfavourable neurological outcome.

In addition, unlike TTM, the multivariable regression analyses performed in TTM2 contained all the parameters previously used for TTM, with the exception of NSE for which measurements had not been completed at the time this work was performed. Therefore, it was not possible at this time to compare the results obtained in the TTM-trial with those of the TTM2-trial. With these assumptions, multivariable logistic regression analyses conducted in TTM2 confirmed all three candidates as predictors of neurological outcome 6 months after cardiac arrest in the normothermic group. However, this ability was lost in all candidates, except circDNM2, when considering all TTM2 patients and in all candidates when considering only the hypothermic group of patients. Among the three candidates, circDNM2 presented the best performance in improving the prediction model of the normothermic group. Similarly, multivariable survival analyses confirmed the improved survival model when one of the three candidates was integrated only in the normothermic group, with circDNM2 as the best predictor of survival. In fact, even in multivariable survival analyses the predictive ability of the candidates was lost when all patients or only those in the hypothermic group were considered. In the future it would be appropriate to conduct multivariable regression analyses again in TTM2 by including NSE in the basal model and then compare the results of each model obtained from the addition of the single candidates studied in the TTM and TTM2 cohorts.

The last part of this study had the advantage of being a predefined sub-study of the TTM2-trial, one of the largest multicentre trials of cardiac arrest patients. In addition, as seen for TTM, sample collection, storage, and processing followed biobank validated protocols for TTM2, and ncRNA measurements were performed in the same laboratory to avoid interlaboratory variability. However, as mentioned above, the absence of NSE measurements prevented the results obtained in TTM2 from being compared with those obtained in TTM. Combination analyses with different candidates were also not performed in TTM2. Finally, candidate ncRNAs were measured 48 h after ROSC, and no measurements were made at earlier time points, therefore, it is not possible to know whether these candidates could be detected earlier after ROSC and their predictive values at earlier time points.

This research work presented the basis for the use of lncRNAs and circRNAs as biomarkers to aid in the prognostication of patients after OHCA. However, this represents an initial study, and further research is needed before translating these findings into clinically useful tools. Similarly, the functional studies that have been conducted here need to be further investigated to better understand the roles played by the identified candidates and whether they may indeed be specific biomarkers for the disease under study.

# *Conclusions and future perspectives*

Advances in the field of transcriptomics have made it possible to discover new RNA molecules and identify those that are poorly expressed. In addition, high throughput technologies allow to obtain a complete picture of the transcriptome under specific conditions, whether physiological or pathological. Although the potential of transcriptomic biomarkers is now well recognised not many have reached the clinic. Therefore, more studies are required to identify transcripts with biomarker value in conditions like OHCA.

Body fluids, including the blood compartment, represent an easy and relatively non-invasive source to study potential transcript biomarkers with clinical value. Therefore, in an initial study of this research project, 3 circulating miRNAs, miR9-3p, miR124-3p and miR129-5p were found to be strongly associated with NSE in plasma samples of patients after OHCA. Furthermore, the 3 miRNAs were associated with neurological outcome and survival 6 months after OHCA, supporting the ability of brain-enriched miRNAs to contribute to the prognostication of patients after OHCA. However, their ability to determine brain damage and their biological functions in OHCA require future explorations. In a second study, the focus shifted to studying the prognostic biomarker potential of lncRNAs and circRNAs in the blood cell compartment in patients after OHCA to include other components of PCAS other than neurological damage, such as severe systemic inflammation. For practical reasons this second study was divided into four parts. The first part consisted of identification of potential lncRNA and circRNA candidates with differential expression profiles in a subset of TTM-trial patients with favourable or unfavourable outcome after OHCA, followed by validation of the selected candidates in the remaining cohort of TTM-trial patients. In fact, 5 circRNAs and 1 lncRNA were identified and validated in the entire TTM. Prediction analyses after adjustment with 9 clinical variables, including the gold standard biomarker NSE, showed circNFAT5, among other candidates, as the best independent predictor of neurological outcome and survival at 6 months after OHCA. Therefore, in the third part of this study, circNFAT5 was selected for preliminary *in-vitro* functional studies. These studies identified *in-vitro* treatments that can significantly increase circNFAT5 levels in a manner similar to that observed in whole blood samples of TTM, such as activating jurkat cells with anti-CD3/CD28 and simulating hypertonic conditions in THP-1 with NaCl. An initial investigation of the relationship between circNFAT5 and its parental gene appeared to indicate an independent expression pattern of circNFAT5 from its linear counterpart. However, this experiment represents only the tip of the iceberg, and further examination is needed to better understand the relationship between circNFAT5 and linear NFAT5. Preliminary experiments of gain and loss of function of circNFAT5 have not yet shown a downstream effect between the evaluated pathways, but further examination in this regard is also needed before drawing any conclusion. Several experiments have been conducted to gain insights into the possible mechanisms of action of circNFAT5, although none have been identified to date. Therefore, the functional characterisation of circNFAT5 conducted here represents a starting point for future studies to individually investigate the various hypotheses raised. The fourth and final part of this study consisted of independent validation in the TTM2-trial of the 3 best-performing candidates identified in the TTM-trial, circDNM2, circFAM13b, and circNFAT5. The independent ability to predict neurological outcome and survival was confirmed for all 3 candidates only in the normothermia group of TTM2. In fact, when considering only the hypothermia group or all patients in the cohort, only circDNM2 remained an independent predictor of neurological outcome but not of patient survival. Moreover, among the candidates, circDNM2 presented the best predictive performance. However, due to the absence of NSE in the prediction models, a comparison with the results obtained in TTM was not possible.



Future studies should reanalyse what was observed in TTM2 by including NSE in the basal model, so that the results obtained in the TTM2 cohort can be compared with the TTM cohort. In addition, the combination of the different candidates in the multivariable analyses should be evaluated to assess the potential improvement of models for predicting neurological outcome and survival. Then, the further biomarker potential of these candidates should be validated in independent cohorts of OHCA patients.

Furthermore, as the prognostic ability of a transcriptional biomarker changes over time, the timing of candidate measurement is of paramount importance. Thus, analysis of the expression patterns of the candidates identified here prior to 48 h after ROSC could provide additional relevant information about their biomarker potency as well as contribute to their potential clinical utility. In addition, identifying the cellular origin of the candidates by isolating the different blood compartments could provide further insight into the processes in which these ncRNAs are involved after OHCA. In line with this, further in-depth functional studies on selected candidates could shed light on the specific biological functions performed after cardiac arrest and thus determine whether their association with disease is specific. This will further help determine the therapeutic potential of the studied ncRNAs after OHCA. Finally, the identification of specific biomarkers for certain categories of patients, such as sex-specific biomarkers, may further aid in the progression toward precision medicine.

## References

1. Grasner, J.T., et al., *Survival after out-of-hospital cardiac arrest in Europe - Results of the EuReCa TWO study*. Resuscitation, 2020. **148**: p. 218-226.
2. Andersen, L.W., et al., *In-Hospital Cardiac Arrest: A Review*. JAMA, 2019. **321**(12): p. 1200-1210.
3. Kiguchi, T., et al., *Out-of-hospital cardiac arrest across the World: First report from the International Liaison Committee on Resuscitation (ILCOR)*. Resuscitation, 2020. **152**: p. 39-49.
4. Kuriachan, V.P., G.L. Sumner, and L.B. Mitchell, *Sudden cardiac death*. Curr Probl Cardiol, 2015. **40**(4): p. 133-200.
5. Grasner, J.T., et al., *European Resuscitation Council Guidelines 2021: Epidemiology of cardiac arrest in Europe*. Resuscitation, 2021. **161**: p. 61-79.
6. Lybeck, A., et al., *Time to awakening after cardiac arrest and the association with target temperature management*. Resuscitation, 2018. **126**: p. 166-171.
7. Neumar, R.W., et al., *Post-cardiac arrest syndrome: epidemiology, pathophysiology, treatment, and prognostication. A consensus statement from the International Liaison Committee on Resuscitation (American Heart Association, Australian and New Zealand Council on Resuscitation, European Resuscitation Council, Heart and Stroke Foundation of Canada, InterAmerican Heart Foundation, Resuscitation Council of Asia, and the Resuscitation Council of Southern Africa); the American Heart Association Emergency Cardiovascular Care Committee; the Council on Cardiovascular Surgery and Anesthesia; the Council on Cardiopulmonary, Perioperative, and Critical Care; the Council on Clinical Cardiology; and the Stroke Council*. Circulation, 2008. **118**(23): p. 2452-83.
8. Perkins, G.D., et al., *Brain injury after cardiac arrest*. Lancet, 2021. **398**(10307): p. 1269-1278.
9. Nolan, J.P., et al., *European Resuscitation Council and European Society of Intensive Care Medicine guidelines 2021: post-resuscitation care*. Intensive Care Med, 2021. **47**(4): p. 369-421.
10. Drury, P.P., et al., *Mechanisms of hypothermic neuroprotection*. Clin Perinatol, 2014. **41**(1): p. 161-75.
11. Nielsen, N., et al., *Targeted temperature management at 33 degrees C versus 36 degrees C after cardiac arrest*. N Engl J Med, 2013. **369**(23): p. 2197-206.
12. Dankiewicz, J., et al., *Hypothermia versus Normothermia after Out-of-Hospital Cardiac Arrest*. N Engl J Med, 2021. **384**(24): p. 2283-2294.
13. Grossestreuer, A.V., et al., *Inter-rater reliability of post-arrest cerebral performance category (CPC) scores*. Resuscitation, 2016. **109**: p. 21-24.
14. *A randomized clinical study of cardiopulmonary-cerebral resuscitation: design, methods, and patient characteristics*. Brain Resuscitation Clinical Trial I Study Group. Am J Emerg Med, 1986. **4**(1): p. 72-86.
15. Banks, J.L. and C.A. Marotta, *Outcomes validity and reliability of the modified Rankin scale: implications for stroke clinical trials: a literature review and synthesis*. Stroke, 2007. **38**(3): p. 1091-6.
16. Raina, K.D., et al., *Neurological and functional status following cardiac arrest: method and tool utility*. Resuscitation, 2008. **79**(2): p. 249-56.
17. Salgado-Somoza, A., et al., *Non-Coding RNAs to Aid in Neurological Prognosis after Cardiac Arrest*. Noncoding RNA, 2018. **4**(4).
18. Hoiland, R.L., et al., *Neurologic Prognostication After Cardiac Arrest Using Brain Biomarkers: A Systematic Review and Meta-analysis*. JAMA Neurol, 2022. **79**(4): p. 390-398.
19. Olivier, M., et al., *The Need for Multi-Omics Biomarker Signatures in Precision Medicine*. Int J Mol Sci, 2019. **20**(19).

20. McColl, E.R., et al., *The Age of Omics-Driven Precision Medicine*. Clin Pharmacol Ther, 2019. **106**(3): p. 477-481.
21. Riedmaier, I. and M.W. Pfaffl, *Transcriptional biomarkers--high throughput screening, quantitative verification, and bioinformatical validation methods*. Methods, 2013. **59**(1): p. 3-9.
22. Beermann, J., et al., *Non-coding RNAs in Development and Disease: Background, Mechanisms, and Therapeutic Approaches*. Physiol Rev, 2016. **96**(4): p. 1297-325.
23. Boon, R.A., et al., *Long Noncoding RNAs: From Clinical Genetics to Therapeutic Targets?* J Am Coll Cardiol, 2016. **67**(10): p. 1214-1226.
24. Zhang, P., et al., *Non-Coding RNAs and their Integrated Networks*. J Integr Bioinform, 2019. **16**(3).
25. Cech, T.R. and J.A. Steitz, *The noncoding RNA revolution--trashing old rules to forge new ones*. Cell, 2014. **157**(1): p. 77-94.
26. Peschansky, V.J. and C. Wahlestedt, *Non-coding RNAs as direct and indirect modulators of epigenetic regulation*. Epigenetics, 2014. **9**(1): p. 3-12.
27. Gomes, C.P.C., et al., *Regulatory RNAs in Heart Failure*. Circulation, 2020. **141**(4): p. 313-328.
28. Mercer, T.R., M.E. Dinger, and J.S. Mattick, *Long non-coding RNAs: insights into functions*. Nat Rev Genet, 2009. **10**(3): p. 155-9.
29. Harrington, C.A., et al., *RNA-Seq of human whole blood: Evaluation of globin RNA depletion on Ribo-Zero library method*. Sci Rep, 2020. **10**(1): p. 6271.
30. Etheridge, A., et al., *The complexity, function and applications of RNA in circulation*. Front Genet, 2013. **4**: p. 115.
31. Valadi, H., et al., *Exosome-mediated transfer of mRNAs and microRNAs is a novel mechanism of genetic exchange between cells*. Nat Cell Biol, 2007. **9**(6): p. 654-9.
32. Weber, J.A., et al., *The microRNA spectrum in 12 body fluids*. Clin Chem, 2010. **56**(11): p. 1733-41.
33. Devaux, Y., *Transcriptome of blood cells as a reservoir of cardiovascular biomarkers*. Biochim Biophys Acta Mol Cell Res, 2017. **1864**(1): p. 209-216.
34. E, S., et al., *The circulating non-coding RNA landscape for biomarker research: lessons and prospects from cardiovascular diseases*. Acta Pharmacol Sin, 2018. **39**(7): p. 1085-1099.
35. Videira, R.F., P.A. da Costa Martins, and I. Falcao-Pires, *Non-Coding RNAs as Blood-Based Biomarkers in Cardiovascular Disease*. Int J Mol Sci, 2020. **21**(23).
36. Stammet, P., et al., *Circulating microRNAs after cardiac arrest*. Crit Care Med, 2012. **40**(12): p. 3209-14.
37. Devaux, Y., et al., *Association of Circulating MicroRNA-124-3p Levels With Outcomes After Out-of-Hospital Cardiac Arrest: A Substudy of a Randomized Clinical Trial*. JAMA Cardiol, 2016. **1**(3): p. 305-13.
38. Enuka, Y., et al., *Circular RNAs are long-lived and display only minimal early alterations in response to a growth factor*. Nucleic Acids Res, 2016. **44**(3): p. 1370-83.
39. Memczak, S., et al., *Circular RNAs are a large class of animal RNAs with regulatory potency*. Nature, 2013. **495**(7441): p. 333-8.
40. Jeck, W.R., et al., *Circular RNAs are abundant, conserved, and associated with ALU repeats*. RNA, 2013. **19**(2): p. 141-57.
41. Devaux, Y., et al., *Circular RNAs in heart failure*. Eur J Heart Fail, 2017. **19**(6): p. 701-709.
42. Elia, L., M. Quintavalle, and G. Condorelli, *Circular RNAs and heart failure: new players for an old disease*. Cardiovasc Res, 2017. **113**(3): p. 254-255.
43. Zhao, C., et al., *Identification of Regulatory circRNAs Involved in the Pathogenesis of Acute Myocardial Infarction*. Front Genet, 2020. **11**: p. 626492.
44. Stefanizzi, F.M., et al., *Circulating Levels of Brain-Enriched MicroRNAs Correlate with Neuron Specific Enolase after Cardiac Arrest-A Substudy of the Target Temperature Management Trial*. Int J Mol Sci, 2020. **21**(12).

45. Ma, Q., L. Zhang, and W.J. Pearce, *MicroRNAs in brain development and cerebrovascular pathophysiology*. *Am J Physiol Cell Physiol*, 2019. **317**(1): p. C3-C19.
46. Sim, S.E., et al., *The Brain-Enriched MicroRNA miR-9-3p Regulates Synaptic Plasticity and Memory*. *J Neurosci*, 2016. **36**(33): p. 8641-52.
47. Rajman, M., et al., *A microRNA-129-5p/Rbfox crosstalk coordinates homeostatic downscaling of excitatory synapses*. *EMBO J*, 2017. **36**(12): p. 1770-1787.
48. Wu, C., et al., *MicroRNA-129 modulates neuronal migration by targeting Fmr1 in the developing mouse cortex*. *Cell Death Dis*, 2019. **10**(4): p. 287.
49. Stammet, P., et al., *Neuron-Specific Enolase as a Predictor of Death or Poor Neurological Outcome After Out-of-Hospital Cardiac Arrest and Targeted Temperature Management at 33 degrees C and 36 degrees C*. *J Am Coll Cardiol*, 2015. **65**(19): p. 2104-14.
50. Devaux, Y., et al., *Long noncoding RNAs in cardiac development and ageing*. *Nat Rev Cardiol*, 2015. **12**(7): p. 415-25.
51. Dahariya, S., et al., *Long non-coding RNA: Classification, biogenesis and functions in blood cells*. *Mol Immunol*, 2019. **112**: p. 82-92.
52. Wu, Z., et al., *Regulation of lncRNA expression*. *Cell Mol Biol Lett*, 2014. **19**(4): p. 561-75.
53. Derrien, T., et al., *The GENCODE v7 catalog of human long noncoding RNAs: analysis of their gene structure, evolution, and expression*. *Genome Res*, 2012. **22**(9): p. 1775-89.
54. Nisar, S., et al., *Insights Into the Role of CircRNAs: Biogenesis, Characterization, Functional, and Clinical Impact in Human Malignancies*. *Front Cell Dev Biol*, 2021. **9**: p. 617281.
55. Gomes, C.P.C., et al., *The Function and Therapeutic Potential of Long Non-coding RNAs in Cardiovascular Development and Disease*. *Mol Ther Nucleic Acids*, 2017. **8**: p. 494-507.
56. Tsivilika, M., et al., *The adaptive immune response in cardiac arrest resuscitation induced ischemia reperfusion renal injury*. *J Biol Res (Thessalon)*, 2020. **27**: p. 15.
57. Beurskens, C.J., et al., *Cardiac arrest patients have an impaired immune response, which is not influenced by induced hypothermia*. *Crit Care*, 2014. **18**(4): p. R162.
58. Langeland, H., et al., *The inflammatory response is related to circulatory failure after out-of-hospital cardiac arrest: A prospective cohort study*. *Resuscitation*, 2022. **170**: p. 115-125.
59. Contreras, J. and D.S. Rao, *MicroRNAs in inflammation and immune responses*. *Leukemia*, 2012. **26**(3): p. 404-13.
60. Dai, R. and S.A. Ahmed, *MicroRNA, a new paradigm for understanding immunoregulation, inflammation, and autoimmune diseases*. *Transl Res*, 2011. **157**(4): p. 163-79.
61. O'Connell, R.M., D.S. Rao, and D. Baltimore, *microRNA regulation of inflammatory responses*. *Annu Rev Immunol*, 2012. **30**: p. 295-312.
62. O'Neill, L.A., F.J. Sheedy, and C.E. McCoy, *MicroRNAs: the fine-tuners of Toll-like receptor signalling*. *Nat Rev Immunol*, 2011. **11**(3): p. 163-75.
63. Walther, K. and L.N. Schulte, *The role of lncRNAs in innate immunity and inflammation*. *RNA Biol*, 2021. **18**(5): p. 587-603.
64. Sekhon, M.S., P.N. Ainslie, and D.E. Griesdale, *Clinical pathophysiology of hypoxic ischemic brain injury after cardiac arrest: a "two-hit" model*. *Crit Care*, 2017. **21**(1): p. 90.
65. Xiang, Y., et al., *Inflammatory mechanisms involved in brain injury following cardiac arrest and cardiopulmonary resuscitation*. *Biomed Rep*, 2016. **5**(1): p. 11-17.
66. Frauwirth, K.A. and C.B. Thompson, *Activation and inhibition of lymphocytes by costimulation*. *J Clin Invest*, 2002. **109**(3): p. 295-9.
67. Mehta, A.K., D.T. Gracias, and M. Croft, *TNF activity and T cells*. *Cytokine*, 2018. **101**: p. 14-18.
68. Cheung, C.Y. and B.C. Ko, *NFAT5 in cellular adaptation to hypertonic stress - regulations and functional significance*. *J Mol Signal*, 2013. **8**(1): p. 5.
69. Lee, N., D. Kim, and W.U. Kim, *Role of NFAT5 in the Immune System and Pathogenesis of Autoimmune Diseases*. *Front Immunol*, 2019. **10**: p. 270.
70. Zhang, Z., T. Yang, and J. Xiao, *Circular RNAs: Promising Biomarkers for Human Diseases*. *EBioMedicine*, 2018. **34**: p. 267-274.

71. Sinha, T., et al., *Circular RNA translation, a path to hidden proteome*. Wiley Interdiscip Rev RNA, 2022. **13**(1): p. e1685.
72. Patel, K. and J.E. Hipskind, *Cardiac Arrest*, in *StatPearls*. 2022: Treasure Island (FL).
73. Lacerte, M., A. Hays Shapshak, and F.B. Mesfin, *Hypoxic Brain Injury*, in *StatPearls*. 2022: Treasure Island (FL).
74. Rea, T.D., et al., *Predicting survival after out-of-hospital cardiac arrest: role of the Utstein data elements*. Ann Emerg Med, 2010. **55**(3): p. 249-57.
75. Merchant, R.M., et al., *Hospital variation in survival after in-hospital cardiac arrest*. J Am Heart Assoc, 2014. **3**(1): p. e000400.
76. Centers for Disease, C. and Prevention, *State-specific mortality from sudden cardiac death--United States, 1999*. MMWR Morb Mortal Wkly Rep, 2002. **51**(6): p. 123-6.
77. Porzer, M., et al., *Out-of-hospital cardiac arrest*. Biomed Pap Med Fac Univ Palacky Olomouc Czech Repub, 2017. **161**(4): p. 348-353.
78. Adabag, A.S., et al., *Sudden cardiac death: epidemiology and risk factors*. Nat Rev Cardiol, 2010. **7**(4): p. 216-25.
79. Chugh, S.S., et al., *Current burden of sudden cardiac death: multiple source surveillance versus retrospective death certificate-based review in a large U.S. community*. J Am Coll Cardiol, 2004. **44**(6): p. 1268-75.
80. Kannel, W.B., et al., *Sudden coronary death in women*. Am Heart J, 1998. **136**(2): p. 205-12.
81. Mazzanti, A., et al., *The usual suspects in sudden cardiac death of the young: a focus on inherited arrhythmogenic diseases*. Expert Rev Cardiovasc Ther, 2014. **12**(4): p. 499-519.
82. Cummins, R.O., et al., *Improving survival from sudden cardiac arrest: the "chain of survival" concept. A statement for health professionals from the Advanced Cardiac Life Support Subcommittee and the Emergency Cardiac Care Committee, American Heart Association*. Circulation, 1991. **83**(5): p. 1832-47.
83. Morrison, L.J., et al., *Strategies for improving survival after in-hospital cardiac arrest in the United States: 2013 consensus recommendations: a consensus statement from the American Heart Association*. Circulation, 2013. **127**(14): p. 1538-63.
84. *Part 3: adult basic life support. European Resuscitation Council*. Resuscitation, 2000. **46**(1-3): p. 29-71.
85. Muller, D., R. Agrawal, and H.R. Arntz, *How sudden is sudden cardiac death?* Circulation, 2006. **114**(11): p. 1146-50.
86. Gullo, A., *Cardiac arrest, chain of survival and Utstein style*. Eur J Anaesthesiol, 2002. **19**(9): p. 624-33.
87. Panchal, A.R., et al., *Part 3: Adult Basic and Advanced Life Support: 2020 American Heart Association Guidelines for Cardiopulmonary Resuscitation and Emergency Cardiovascular Care*. Circulation, 2020. **142**(16\_suppl\_2): p. S366-S468.
88. Berg, R.A., et al., *Part 5: adult basic life support: 2010 American Heart Association Guidelines for Cardiopulmonary Resuscitation and Emergency Cardiovascular Care*. Circulation, 2010. **122**(18 Suppl 3): p. S685-705.
89. Travers, A.H., et al., *Part 4: CPR overview: 2010 American Heart Association Guidelines for Cardiopulmonary Resuscitation and Emergency Cardiovascular Care*. Circulation, 2010. **122**(18 Suppl 3): p. S676-84.
90. Edelson, D.P., et al., *Improving in-hospital cardiac arrest process and outcomes with performance debriefing*. Arch Intern Med, 2008. **168**(10): p. 1063-9.
91. Edelson, D.P., et al., *Effects of compression depth and pre-shock pauses predict defibrillation failure during cardiac arrest*. Resuscitation, 2006. **71**(2): p. 137-45.
92. Meaney, P.A., et al., *Cardiopulmonary resuscitation quality: [corrected] improving cardiac resuscitation outcomes both inside and outside the hospital: a consensus statement from the American Heart Association*. Circulation, 2013. **128**(4): p. 417-35.
93. Larsen, M.P., et al., *Predicting survival from out-of-hospital cardiac arrest: a graphic model*. Ann Emerg Med, 1993. **22**(11): p. 1652-8.

94. Swor, R.A., et al., *Bystander CPR, ventricular fibrillation, and survival in witnessed, unmonitored out-of-hospital cardiac arrest*. *Ann Emerg Med*, 1995. **25**(6): p. 780-4.
95. *Part 4: the automated external defibrillator: key link in the chain of survival*. *European Resuscitation Council*. *Resuscitation*, 2000. **46**(1-3): p. 73-91.
96. Cummins, R.O., et al., *Automatic external defibrillators used by emergency medical technicians. A controlled clinical trial*. *JAMA*, 1987. **257**(12): p. 1605-10.
97. Stults, K.R., D.D. Brown, and R.E. Kerber, *Efficacy of an automated external defibrillator in the management of out-of-hospital cardiac arrest: validation of the diagnostic algorithm and initial clinical experience in a rural environment*. *Circulation*, 1986. **73**(4): p. 701-9.
98. Marengo, J.P., et al., *Improving survival from sudden cardiac arrest: the role of the automated external defibrillator*. *JAMA*, 2001. **285**(9): p. 1193-200.
99. Mullie, A., R. Van Hoeyweghen, and A. Quets, *Influence of time intervals on outcome of CPR. The Cerebral Resuscitation Study Group*. *Resuscitation*, 1989. **17 Suppl**: p. S23-33; discussion S199-206.
100. Adrie, C., et al., *Successful cardiopulmonary resuscitation after cardiac arrest as a "sepsis-like" syndrome*. *Circulation*, 2002. **106**(5): p. 562-8.
101. Sugita, A., et al., *Systemic impact on secondary brain aggravation due to ischemia/reperfusion injury in post-cardiac arrest syndrome: a prospective observational study using high-mobility group box 1 protein*. *Crit Care*, 2017. **21**(1): p. 247.
102. Kawata, M., et al., *Erythropoietin protects the central nervous system during prolonged hypothermic circulatory arrest: an experimental study in a canine model*. *J Thorac Cardiovasc Surg*, 2006. **131**(6): p. 1331-7.
103. Vereczki, V., et al., *Normoxic resuscitation after cardiac arrest protects against hippocampal oxidative stress, metabolic dysfunction, and neuronal death*. *J Cereb Blood Flow Metab*, 2006. **26**(6): p. 821-35.
104. Takasu, A., et al., *Hyperthermia: is it an ominous sign after cardiac arrest?* *Resuscitation*, 2001. **49**(3): p. 273-7.
105. Zeiner, A., et al., *Hyperthermia after cardiac arrest is associated with an unfavorable neurologic outcome*. *Arch Intern Med*, 2001. **161**(16): p. 2007-12.
106. Langhelle, A., et al., *In-hospital factors associated with improved outcome after out-of-hospital cardiac arrest. A comparison between four regions in Norway*. *Resuscitation*, 2003. **56**(3): p. 247-63.
107. Longstreth, W.T., Jr. and T.S. Inui, *High blood glucose level on hospital admission and poor neurological recovery after cardiac arrest*. *Ann Neurol*, 1984. **15**(1): p. 59-63.
108. Calle, P.A., W.A. Buylaert, and O.A. Vanhaute, *Glycemia in the post-resuscitation period. The Cerebral Resuscitation Study Group*. *Resuscitation*, 1989. **17 Suppl**: p. S181-8; discussion S199-206.
109. Lybeck, A., et al., *Prognostic significance of clinical seizures after cardiac arrest and target temperature management*. *Resuscitation*, 2017. **114**: p. 146-151.
110. Jentzer, J.C., M.D. Chonde, and C. Dezfulian, *Myocardial Dysfunction and Shock after Cardiac Arrest*. *Biomed Res Int*, 2015. **2015**: p. 314796.
111. Kern, K.B., et al., *Myocardial dysfunction after resuscitation from cardiac arrest: an example of global myocardial stunning*. *J Am Coll Cardiol*, 1996. **28**(1): p. 232-40.
112. Laurent, I., et al., *Reversible myocardial dysfunction in survivors of out-of-hospital cardiac arrest*. *J Am Coll Cardiol*, 2002. **40**(12): p. 2110-6.
113. Ruiz-Bailen, M., et al., *Reversible myocardial dysfunction after cardiopulmonary resuscitation*. *Resuscitation*, 2005. **66**(2): p. 175-81.
114. Kern, K.B., et al., *Postresuscitation left ventricular systolic and diastolic dysfunction. Treatment with dobutamine*. *Circulation*, 1997. **95**(12): p. 2610-3.
115. Huang, L., et al., *Comparison between dobutamine and levosimendan for management of postresuscitation myocardial dysfunction*. *Crit Care Med*, 2005. **33**(3): p. 487-91.

116. Karimova, A. and D.J. Pinsky, *The endothelial response to oxygen deprivation: biology and clinical implications*. Intensive Care Med, 2001. **27**(1): p. 19-31.
117. Naito, H., et al., *Therapeutic strategies for ischemia reperfusion injury in emergency medicine*. Acute Med Surg, 2020. **7**(1): p. e501.
118. Shoemaker, W.C., P.L. Appel, and H.B. Kram, *Role of oxygen debt in the development of organ failure sepsis, and death in high-risk surgical patients*. Chest, 1992. **102**(1): p. 208-15.
119. Shoemaker, W.C., P.L. Appel, and H.B. Kram, *Tissue oxygen debt as a determinant of lethal and nonlethal postoperative organ failure*. Crit Care Med, 1988. **16**(11): p. 1117-20.
120. Engdahl, J., et al., *Is hospital care of major importance for outcome after out-of-hospital cardiac arrest? Experience acquired from patients with out-of-hospital cardiac arrest resuscitated by the same Emergency Medical Service and admitted to one of two hospitals over a 16-year period in the municipality of Goteborg*. Resuscitation, 2000. **43**(3): p. 201-11.
121. Bulut, S., et al., *Successful out-of-hospital cardiopulmonary resuscitation: what is the optimal in-hospital treatment strategy?* Resuscitation, 2000. **47**(2): p. 155-61.
122. Nolan, J.P., et al., *Post-cardiac arrest syndrome: epidemiology, pathophysiology, treatment, and prognostication. A Scientific Statement from the International Liaison Committee on Resuscitation; the American Heart Association Emergency Cardiovascular Care Committee; the Council on Cardiovascular Surgery and Anesthesia; the Council on Cardiopulmonary, Perioperative, and Critical Care; the Council on Clinical Cardiology; the Council on Stroke*. Resuscitation, 2008. **79**(3): p. 350-79.
123. Wilder Schaaf, K.P., et al., *Anxiety, depression, and PTSD following cardiac arrest: a systematic review of the literature*. Resuscitation, 2013. **84**(7): p. 873-7.
124. Moulart, V.R., et al., *Cognitive impairments in survivors of out-of-hospital cardiac arrest: a systematic review*. Resuscitation, 2009. **80**(3): p. 297-305.
125. Lilja, G., et al., *Cognitive function in survivors of out-of-hospital cardiac arrest after target temperature management at 33 degrees C versus 36 degrees C*. Circulation, 2015. **131**(15): p. 1340-9.
126. Elmer, J., et al., *Association of early withdrawal of life-sustaining therapy for perceived neurological prognosis with mortality after cardiac arrest*. Resuscitation, 2016. **102**: p. 127-35.
127. Cour, M., et al., *Risk factors for progression toward brain death after out-of-hospital cardiac arrest*. Ann Intensive Care, 2019. **9**(1): p. 45.
128. Yan, S., et al., *The global survival rate among adult out-of-hospital cardiac arrest patients who received cardiopulmonary resuscitation: a systematic review and meta-analysis*. Crit Care, 2020. **24**(1): p. 61.
129. Witten, L., et al., *Reasons for death in patients successfully resuscitated from out-of-hospital and in-hospital cardiac arrest*. Resuscitation, 2019. **136**: p. 93-99.
130. Mark, N.M., et al., *Global variability in withholding and withdrawal of life-sustaining treatment in the intensive care unit: a systematic review*. Intensive Care Med, 2015. **41**(9): p. 1572-85.
131. Sprung, C.L., et al., *Seeking worldwide professional consensus on the principles of end-of-life care for the critically ill. The Consensus for Worldwide End-of-Life Practice for Patients in Intensive Care Units (WELPICUS) study*. Am J Respir Crit Care Med, 2014. **190**(8): p. 855-66.
132. Sandroni, C., et al., *The rate of brain death and organ donation in patients resuscitated from cardiac arrest: a systematic review and meta-analysis*. Intensive Care Med, 2016. **42**(11): p. 1661-1671.
133. Olasveengen, T.M., et al., *Adult Basic Life Support: International Consensus on Cardiopulmonary Resuscitation and Emergency Cardiovascular Care Science With Treatment Recommendations*. Resuscitation, 2020. **156**: p. A35-A79.
134. Song, J., et al., *The effect of bystander cardiopulmonary resuscitation on the survival of out-of-hospital cardiac arrests: a systematic review and meta-analysis*. Scand J Trauma Resusc Emerg Med, 2018. **26**(1): p. 86.

135. Hollenberg, J., et al., *Improved survival after out-of-hospital cardiac arrest is associated with an increase in proportion of emergency crew--witnessed cases and bystander cardiopulmonary resuscitation*. *Circulation*, 2008. **118**(4): p. 389-96.
136. Nordberg, P., et al., *Aspects on the increase in bystander CPR in Sweden and its association with outcome*. *Resuscitation*, 2009. **80**(3): p. 329-33.
137. Geocadin, R.G., et al., *Standards for Studies of Neurological Prognostication in Comatose Survivors of Cardiac Arrest: A Scientific Statement From the American Heart Association*. *Circulation*, 2019. **140**(9): p. e517-e542.
138. Huybrechts, K.F., et al., *The prognostic value of the modified Rankin Scale score for long-term survival after first-ever stroke. Results from the Athens Stroke Registry*. *Cerebrovasc Dis*, 2008. **26**(4): p. 381-7.
139. Jennett, B. and M. Bond, *Assessment of outcome after severe brain damage*. *Lancet*, 1975. **1**(7905): p. 480-4.
140. Perkins, G.D., et al., *Cardiac arrest and cardiopulmonary resuscitation outcome reports: update of the Utstein Resuscitation Registry Templates for Out-of-Hospital Cardiac Arrest: a statement for healthcare professionals from a task force of the International Liaison Committee on Resuscitation (American Heart Association, European Resuscitation Council, Australian and New Zealand Council on Resuscitation, Heart and Stroke Foundation of Canada, InterAmerican Heart Foundation, Resuscitation Council of Southern Africa, Resuscitation Council of Asia); and the American Heart Association Emergency Cardiovascular Care Committee and the Council on Cardiopulmonary, Critical Care, Perioperative and Resuscitation*. *Circulation*, 2015. **132**(13): p. 1286-300.
141. Arrich, J., et al., *Factors associated with a change in functional outcome between one month and six months after cardiac arrest: a retrospective cohort study*. *Resuscitation*, 2009. **80**(8): p. 876-80.
142. Tong, J.T., et al., *Functional Neurologic Outcomes Change Over the First 6 Months After Cardiac Arrest*. *Crit Care Med*, 2016. **44**(12): p. e1202-e1207.
143. Haywood, K., et al., *COSCA (Core Outcome Set for Cardiac Arrest) in Adults: An Advisory Statement From the International Liaison Committee on Resuscitation*. *Circulation*, 2018. **137**(22): p. e783-e801.
144. Abe, T., Y. Tokuda, and E.F. Cook, *Time-based partitioning model for predicting neurologically favorable outcome among adults with witnessed bystander out-of-hospital CPA*. *PLoS One*, 2011. **6**(12): p. e28581.
145. Matsuyama, T., et al., *Impact of cardiopulmonary resuscitation duration on neurologically favourable outcome after out-of-hospital cardiac arrest: A population-based study in Japan*. *Resuscitation*, 2017. **113**: p. 1-7.
146. Oh, S.H., et al., *The impact of sex and age on neurological outcomes in out-of-hospital cardiac arrest patients with targeted temperature management*. *Crit Care*, 2017. **21**(1): p. 272.
147. Hiemstra, B., et al., *Long-term outcome of elderly out-of-hospital cardiac arrest survivors as compared with their younger counterparts and the general population*. *Ther Adv Cardiovasc Dis*, 2018. **12**(12): p. 341-349.
148. Mody, P., et al., *Gender-Based Differences in Outcomes Among Resuscitated Patients With Out-of-Hospital Cardiac Arrest*. *Circulation*, 2021. **143**(7): p. 641-649.
149. Grunau, B., et al., *Comparing the prognosis of those with initial shockable and non-shockable rhythms with increasing durations of CPR: Informing minimum durations of resuscitation*. *Resuscitation*, 2016. **101**: p. 50-6.
150. Wee, J.H., et al., *Outcomes of asphyxial cardiac arrest patients who were treated with therapeutic hypothermia: a multicentre retrospective cohort study*. *Resuscitation*, 2015. **89**: p. 81-5.
151. Tamura, T., et al., *Early outcome prediction with quantitative pupillary response parameters after out-of-hospital cardiac arrest: A multicenter prospective observational study*. *PLoS One*, 2020. **15**(3): p. e0228224.



152. Solari, D., et al., *Early prediction of coma recovery after cardiac arrest with blinded pupillometry*. *Ann Neurol*, 2017. **81**(6): p. 804-810.
153. Martinell, L., et al., *Early predictors of poor outcome after out-of-hospital cardiac arrest*. *Crit Care*, 2017. **21**(1): p. 96.
154. Longstreth, W.T., Jr., P. Diehr, and T.S. Inui, *Prediction of awakening after out-of-hospital cardiac arrest*. *N Engl J Med*, 1983. **308**(23): p. 1378-82.
155. Levy, D.E., et al., *Predicting outcome from hypoxic-ischemic coma*. *JAMA*, 1985. **253**(10): p. 1420-6.
156. Jorgensen, E.O. and A.M. Malchow-Moller, *Cerebral prognostic signs during cardiopulmonary resuscitation*. *Resuscitation*, 1978. **6**(4): p. 217-25.
157. Seder, D.B., et al., *Neurologic outcomes and postresuscitation care of patients with myoclonus following cardiac arrest*. *Crit Care Med*, 2015. **43**(5): p. 965-72.
158. Sandroni, C., et al., *Prediction of poor neurological outcome in comatose survivors of cardiac arrest: a systematic review*. *Intensive Care Med*, 2020. **46**(10): p. 1803-1851.
159. Torbey, M.T., et al., *Quantitative analysis of the loss of distinction between gray and white matter in comatose patients after cardiac arrest*. *Stroke*, 2000. **31**(9): p. 2163-7.
160. Kjos, B.O., M. Brant-Zawadzki, and R.G. Young, *Early CT findings of global central nervous system hypoperfusion*. *AJR Am J Roentgenol*, 1983. **141**(6): p. 1227-32.
161. Sandroni, C., S. D'Arrigo, and J.P. Nolan, *Prognostication after cardiac arrest*. *Crit Care*, 2018. **22**(1): p. 150.
162. Greer, D.M., et al., *Hippocampal magnetic resonance imaging abnormalities in cardiac arrest are associated with poor outcome*. *J Stroke Cerebrovasc Dis*, 2013. **22**(7): p. 899-905.
163. Ryoo, S.M., et al., *Predicting Outcome With Diffusion-Weighted Imaging in Cardiac Arrest Patients Receiving Hypothermia Therapy: Multicenter Retrospective Cohort Study*. *Crit Care Med*, 2015. **43**(11): p. 2370-7.
164. Jeon, C.H., et al., *Comparison of brain computed tomography and diffusion-weighted magnetic resonance imaging to predict early neurologic outcome before target temperature management comatose cardiac arrest survivors*. *Resuscitation*, 2017. **118**: p. 21-26.
165. Wijdicks, E.F., et al., *Practice parameter: prediction of outcome in comatose survivors after cardiopulmonary resuscitation (an evidence-based review): report of the Quality Standards Subcommittee of the American Academy of Neurology*. *Neurology*, 2006. **67**(2): p. 203-10.
166. Sondag, L., et al., *Early EEG for outcome prediction of postanoxic coma: prospective cohort study with cost-minimization analysis*. *Crit Care*, 2017. **21**(1): p. 111.
167. Westhall, E., et al., *Standardized EEG interpretation accurately predicts prognosis after cardiac arrest*. *Neurology*, 2016. **86**(16): p. 1482-90.
168. Amorim, E., et al., *Malignant EEG patterns in cardiac arrest patients treated with targeted temperature management who survive to hospital discharge*. *Resuscitation*, 2015. **90**: p. 127-32.
169. Elmer, J., et al., *Clinically distinct electroencephalographic phenotypes of early myoclonus after cardiac arrest*. *Ann Neurol*, 2016. **80**(2): p. 175-84.
170. Dragancea, I., et al., *Neurological prognostication after cardiac arrest and targeted temperature management 33 degrees C versus 36 degrees C: Results from a randomised controlled clinical trial*. *Resuscitation*, 2015. **93**: p. 164-70.
171. Zhou, S.E., et al., *Distinct predictive values of current neuroprognostic guidelines in post-cardiac arrest patients*. *Resuscitation*, 2019. **139**: p. 343-350.
172. Oddo, M., et al., *Quantitative versus standard pupillary light reflex for early prognostication in comatose cardiac arrest patients: an international prospective multicenter double-blinded study*. *Intensive Care Med*, 2018. **44**(12): p. 2102-2111.
173. Choi, S.P., et al., *Can somatosensory and visual evoked potentials predict neurological outcome during targeted temperature management in post cardiac arrest patients?* *Resuscitation*, 2017. **119**: p. 70-75.

174. Kim, S.W., et al., *Short-Latency Positive Peak Following N20 Somatosensory Evoked Potential Is Superior to N20 in Predicting Neurologic Outcome After Out-of-Hospital Cardiac Arrest*. Crit Care Med, 2018. **46**(6): p. e545-e551.
175. Sandroni, C., et al., *Predictors of poor neurological outcome in adult comatose survivors of cardiac arrest: a systematic review and meta-analysis. Part 2: Patients treated with therapeutic hypothermia*. Resuscitation, 2013. **84**(10): p. 1324-38.
176. Horn, J. and M.C. Tjepkema-Cloostermans, *Somatosensory Evoked Potentials in Patients with Hypoxic-Ischemic Brain Injury*. Semin Neurol, 2017. **37**(1): p. 60-65.
177. Pfeifer, R., et al., *Investigation of the inter-observer variability effect on the prognostic value of somatosensory evoked potentials of the median nerve (SSEP) in cardiac arrest survivors using an SSEP classification*. Resuscitation, 2013. **84**(10): p. 1375-81.
178. Madhok, J., et al., *Hypothermia amplifies somatosensory-evoked potentials in uninjured rats*. J Neurosurg Anesthesiol, 2012. **24**(3): p. 197-202.
179. Bouwes, A., et al., *Prognosis of coma after therapeutic hypothermia: a prospective cohort study*. Ann Neurol, 2012. **71**(2): p. 206-12.
180. Bouwes, A., et al., *Hypothermia after CPR prolongs conduction times of somatosensory evoked potentials*. Neurocrit Care, 2013. **19**(1): p. 25-30.
181. Peberdy, M.A., et al., *Part 9: post-cardiac arrest care: 2010 American Heart Association Guidelines for Cardiopulmonary Resuscitation and Emergency Cardiovascular Care*. Circulation, 2010. **122**(18 Suppl 3): p. S768-86.
182. Amorim, E., et al., *Estimating the False Positive Rate of Absent Somatosensory Evoked Potentials in Cardiac Arrest Prognostication*. Crit Care Med, 2018. **46**(12): p. e1213-e1221.
183. Hypothermia after Cardiac Arrest Study, G., *Mild therapeutic hypothermia to improve the neurologic outcome after cardiac arrest*. N Engl J Med, 2002. **346**(8): p. 549-56.
184. Bernard, S.A., et al., *Treatment of comatose survivors of out-of-hospital cardiac arrest with induced hypothermia*. N Engl J Med, 2002. **346**(8): p. 557-63.
185. Holzer, M., et al., *Hypothermia for neuroprotection after cardiac arrest: systematic review and individual patient data meta-analysis*. Crit Care Med, 2005. **33**(2): p. 414-8.
186. Oksanen, T., et al., *Postresuscitation hemodynamics during therapeutic hypothermia after out-of-hospital cardiac arrest with ventricular fibrillation: a retrospective study*. Resuscitation, 2014. **85**(8): p. 1018-24.
187. Chalkias, A. and T. Xanthos, *Pathophysiology and pathogenesis of post-resuscitation myocardial stunning*. Heart Fail Rev, 2012. **17**(1): p. 117-28.
188. Russo, J.J., et al., *Optimal mean arterial pressure in comatose survivors of out-of-hospital cardiac arrest: An analysis of area below blood pressure thresholds*. Resuscitation, 2018. **128**: p. 175-180.
189. Chiu, Y.K., C.T. Lui, and K.L. Tsui, *Impact of hypotension after return of spontaneous circulation on survival in patients of out-of-hospital cardiac arrest*. Am J Emerg Med, 2018. **36**(1): p. 79-83.
190. Trzeciak, S., et al., *Significance of arterial hypotension after resuscitation from cardiac arrest*. Crit Care Med, 2009. **37**(11): p. 2895-903; quiz 2904.
191. Shin, J., et al., *Impact of early coronary angiography on the survival to discharge after out-of-hospital cardiac arrest*. Clin Exp Emerg Med, 2017. **4**(2): p. 65-72.
192. Spaulding, C.M., et al., *Immediate coronary angiography in survivors of out-of-hospital cardiac arrest*. N Engl J Med, 1997. **336**(23): p. 1629-33.
193. Bougouin, W., et al., *Should We Perform an Immediate Coronary Angiogram in All Patients After Cardiac Arrest?: Insights From a Large French Registry*. JACC Cardiovasc Interv, 2018. **11**(3): p. 249-256.
194. Hamel, M.B., et al., *Cost effectiveness of aggressive care for patients with nontraumatic coma*. Crit Care Med, 2002. **30**(6): p. 1191-6.
195. Burke, D.T., et al., *Rehabilitation outcomes of cardiac and non-cardiac anoxic brain injury: a single institution experience*. Brain Inj, 2005. **19**(9): p. 675-80.

196. Geocadin, R.G., et al., *Intensive care for brain injury after cardiac arrest: therapeutic hypothermia and related neuroprotective strategies*. Crit Care Clin, 2006. **22**(4): p. 619-36; abstract viii.
197. Kragholm, K., et al., *Return to Work in Out-of-Hospital Cardiac Arrest Survivors: A Nationwide Register-Based Follow-Up Study*. Circulation, 2015. **131**(19): p. 1682-90.
198. Kragholm, K., et al., *Employment status 1 year after out-of-hospital cardiac arrest in comatose patients treated with therapeutic hypothermia*. Acta Anaesthesiol Scand, 2013. **57**(7): p. 936-43.
199. Fugate, J.E., et al., *Cognitive outcomes of patients undergoing therapeutic hypothermia after cardiac arrest*. Neurology, 2013. **81**(1): p. 40-5.
200. Hofgren, C., et al., *Two years after cardiac arrest; cognitive status, ADL function and living situation*. Brain Inj, 2008. **22**(12): p. 972-8.
201. Biomarkers Definitions Working, G., *Biomarkers and surrogate endpoints: preferred definitions and conceptual framework*. Clin Pharmacol Ther, 2001. **69**(3): p. 89-95.
202. Group., F.D.A.-N.I.H.B.W., *BEST (Biomarkers, EndpointS, and other Tools) Resource [Internet]*, in *BEST (Biomarkers, EndpointS, and other Tools) Resource*. 2016, Silver Spring (MD): Food and Drug Administration (US): Silver Spring (MD).
203. Huss, R., *Biomarkers*, in *Translational Regenerative Medicine*, J.G.A. Anthony Atala, Editor. 2015, Elsevier Inc. p. 235-241.
204. Broza, Y.Y., et al., *Disease Detection with Molecular Biomarkers: From Chemistry of Body Fluids to Nature-Inspired Chemical Sensors*. Chem Rev, 2019. **119**(22): p. 11761-11817.
205. Mayeux, R., *Biomarkers: potential uses and limitations*. NeuroRx, 2004. **1**(2): p. 182-8.
206. Tezak, Z., M.V. Kondratovich, and E. Mansfield, *US FDA and personalized medicine: in vitro diagnostic regulatory perspective*. Per Med, 2010. **7**(5): p. 517-530.
207. Byrnes, S.A. and B.H. Weigl, *Selecting analytical biomarkers for diagnostic applications: a first principles approach*. Expert Rev Mol Diagn, 2018. **18**(1): p. 19-26.
208. Abeel, T., et al., *Robust biomarker identification for cancer diagnosis with ensemble feature selection methods*. Bioinformatics, 2010. **26**(3): p. 392-8.
209. Ray, C.A., *Biomarker accuracy: exploring the truth*. Bioanalysis, 2014. **6**(3): p. 269-71.
210. Ray, P., et al., *Statistical evaluation of a biomarker*. Anesthesiology, 2010. **112**(4): p. 1023-40.
211. Scherer, A., *Reproducibility in biomarker research and clinical development: a global challenge*. Biomark Med, 2017. **11**(4): p. 309-312.
212. Gonzalez, L.A., M.F. Ugarte-Gil, and G.S. Alarcon, *Systemic lupus erythematosus: The search for the ideal biomarker*. Lupus, 2021. **30**(2): p. 181-203.
213. Wang, Z., M. Gerstein, and M. Snyder, *RNA-Seq: a revolutionary tool for transcriptomics*. Nat Rev Genet, 2009. **10**(1): p. 57-63.
214. Hung, J.H. and Z. Weng, *Analysis of Microarray and RNA-seq Expression Profiling Data*. Cold Spring Harb Protoc, 2017. **2017**(3).
215. Lockey, C., E. Otto, and Z. Long, *Real-time fluorescence detection of a single DNA molecule*. Biotechniques, 1998. **24**(5): p. 744-6.
216. Livak, K.J. and T.D. Schmittgen, *Analysis of relative gene expression data using real-time quantitative PCR and the 2(-Delta Delta C(T)) Method*. Methods, 2001. **25**(4): p. 402-8.
217. Higuchi, R., et al., *Simultaneous amplification and detection of specific DNA sequences*. Biotechnology (N Y), 1992. **10**(4): p. 413-7.
218. Yan, S.K., et al., *"Omics" in pharmaceutical research: overview, applications, challenges, and future perspectives*. Chin J Nat Med, 2015. **13**(1): p. 3-21.
219. Rainen, L., et al., *Stabilization of mRNA expression in whole blood samples*. Clin Chem, 2002. **48**(11): p. 1883-90.
220. Shen, Y., et al., *Impact of RNA integrity and blood sample storage conditions on the gene expression analysis*. Onco Targets Ther, 2018. **11**: p. 3573-3581.

221. Nouvel, A., et al., *Optimization of RNA extraction methods from human metabolic tissue samples of the COMET biobank*. Sci Rep, 2021. **11**(1): p. 20975.
222. Stevenson, H.S., et al., *Long-term stability of total RNA in RNAsstable(R) as evaluated by expression microarray*. Biopreserv Biobank, 2015. **13**(2): p. 114-22.
223. Mohr, S. and C.C. Liew, *The peripheral-blood transcriptome: new insights into disease and risk assessment*. Trends Mol Med, 2007. **13**(10): p. 422-32.
224. Slikker, W., Jr., *Biomarkers and their impact on precision medicine*. Exp Biol Med (Maywood), 2018. **243**(3): p. 211-212.
225. Schrohl, A.S., et al., *Banking of biological fluids for studies of disease-associated protein biomarkers*. Mol Cell Proteomics, 2008. **7**(10): p. 2061-6.
226. Unal, I., *Defining an Optimal Cut-Point Value in ROC Analysis: An Alternative Approach*. Comput Math Methods Med, 2017. **2017**: p. 3762651.
227. Ruopp, M.D., et al., *Youden Index and optimal cut-point estimated from observations affected by a lower limit of detection*. Biom J, 2008. **50**(3): p. 419-30.
228. Grant, S.W., G.L. Hickey, and S.J. Head, *Statistical primer: multivariable regression considerations and pitfalls*. Eur J Cardiothorac Surg, 2019. **55**(2): p. 179-185.
229. Giannini, H.I.B.a.E.H., *TRIAL DESIGN, MEASUREMENT, AND ANALYSIS OF CLINICAL INVESTIGATIONS*, in *Textbook of Pediatric Rheumatology*. 2011. p. 127–156.
230. Schober, P., S.M. Bossers, and L.A. Schwarte, *Statistical Significance Versus Clinical Importance of Observed Effect Sizes: What Do P Values and Confidence Intervals Really Represent?* Anesth Analg, 2018. **126**(3): p. 1068-1072.
231. Spruance, S.L., et al., *Hazard ratio in clinical trials*. Antimicrob Agents Chemother, 2004. **48**(8): p. 2787-92.
232. Rich, J.T., et al., *A practical guide to understanding Kaplan-Meier curves*. Otolaryngol Head Neck Surg, 2010. **143**(3): p. 331-6.
233. Goel, M.K., P. Khanna, and J. Kishore, *Understanding survival analysis: Kaplan-Meier estimate*. Int J Ayurveda Res, 2010. **1**(4): p. 274-8.
234. Bewick, V., L. Cheek, and J. Ball, *Statistics review 12: survival analysis*. Crit Care, 2004. **8**(5): p. 389-94.
235. Reznick, R.K. and C.B. Guest, *Survival analysis: a practical approach*. Dis Colon Rectum, 1989. **32**(10): p. 898-902.
236. Bland, J.M. and D.G. Altman, *Survival probabilities (the Kaplan-Meier method)*. BMJ, 1998. **317**(7172): p. 1572.
237. Bland, J.M. and D.G. Altman, *The logrank test*. BMJ, 2004. **328**(7447): p. 1073.
238. Cook, N.R., *Quantifying the added value of new biomarkers: how and how not*. Diagn Progn Res, 2018. **2**: p. 14.
239. Profillidis, V.A. and G.N. Botzoris, *Statistical Methods for Transport Demand Modeling*. Modeling of Transport Demand, 2019.
240. Chen, W., et al., *On the assessment of the added value of new predictive biomarkers*. BMC Med Res Methodol, 2013. **13**: p. 98.
241. Pencina, M.J., et al., *Evaluating the added predictive ability of a new marker: from area under the ROC curve to reclassification and beyond*. Stat Med, 2008. **27**(2): p. 157-72; discussion 207-12.
242. Kerr, K.F., et al., *Evaluating the incremental value of new biomarkers with integrated discrimination improvement*. Am J Epidemiol, 2011. **174**(3): p. 364-74.
243. Pencina, M.J., J.P. Fine, and R.B. D'Agostino, Sr., *Discrimination slope and integrated discrimination improvement - properties, relationships and impact of calibration*. Stat Med, 2017. **36**(28): p. 4482-4490.
244. Andersson, P., et al., *Predicting neurological outcome after out-of-hospital cardiac arrest with cumulative information; development and internal validation of an artificial neural network algorithm*. Crit Care, 2021. **25**(1): p. 83.

245. Scolletta, S., et al., *Biomarkers as predictors of outcome after cardiac arrest*. *Expert Rev Clin Pharmacol*, 2012. **5**(6): p. 687-99.
246. Vondrakova, D., et al., *Association of neuron-specific enolase values with outcomes in cardiac arrest survivors is dependent on the time of sample collection*. *Crit Care*, 2017. **21**(1): p. 172.
247. Tiainen, M., et al., *Serum neuron-specific enolase and S-100B protein in cardiac arrest patients treated with hypothermia*. *Stroke*, 2003. **34**(12): p. 2881-6.
248. Chung-Esaki, H.M., et al., *The neuron specific enolase (NSE) ratio offers benefits over absolute value thresholds in post-cardiac arrest coma prognosis*. *J Clin Neurosci*, 2018. **57**: p. 99-104.
249. Isgro, M.A., P. Bottoni, and R. Scatena, *Neuron-Specific Enolase as a Biomarker: Biochemical and Clinical Aspects*. *Adv Exp Med Biol*, 2015. **867**: p. 125-43.
250. Oddo, M. and A.O. Rossetti, *Early multimodal outcome prediction after cardiac arrest in patients treated with hypothermia*. *Crit Care Med*, 2014. **42**(6): p. 1340-7.
251. Streitberger, K.J., et al., *Neuron-Specific Enolase Predicts Poor Outcome After Cardiac Arrest and Targeted Temperature Management: A Multicenter Study on 1,053 Patients*. *Crit Care Med*, 2017. **45**(7): p. 1145-1151.
252. Pfeifer, R., M. Franz, and H.R. Figulla, *Hypothermia after cardiac arrest does not affect serum levels of neuron-specific enolase and protein S-100b*. *Acta Anaesthesiol Scand*, 2014. **58**(9): p. 1093-100.
253. Soar, J., et al., *Adult Advanced Life Support: 2020 International Consensus on Cardiopulmonary Resuscitation and Emergency Cardiovascular Care Science with Treatment Recommendations*. *Resuscitation*, 2020. **156**: p. A80-A119.
254. Marangos, P.J., et al., *Blood platelets contain a neuron-specific enolase subunit*. *J Neurochem*, 1980. **34**(5): p. 1254-8.
255. Ramont, L., et al., *Effects of hemolysis and storage condition on neuron-specific enolase (NSE) in cerebrospinal fluid and serum: implications in clinical practice*. *Clin Chem Lab Med*, 2005. **43**(11): p. 1215-7.
256. Rundgren, M., et al., *Serum neuron specific enolase - impact of storage and measuring method*. *BMC Res Notes*, 2014. **7**: p. 726.
257. Stammet, P., et al., *Modeling serum level of s100beta and bispectral index to predict outcome after cardiac arrest*. *J Am Coll Cardiol*, 2013. **62**(9): p. 851-8.
258. Duez, C.H.V., et al., *Neuron-specific enolase and S-100b in prolonged targeted temperature management after cardiac arrest: A randomised study*. *Resuscitation*, 2018. **122**: p. 79-86.
259. Jang, J.H., et al., *Combination of S100B and procalcitonin improves prognostic performance compared to either alone in patients with cardiac arrest: A prospective observational study*. *Medicine (Baltimore)*, 2019. **98**(6): p. e14496.
260. Jonsson, H., et al., *Elimination of S100B and renal function after cardiac surgery*. *J Cardiothorac Vasc Anesth*, 2000. **14**(6): p. 698-701.
261. Riuzzi, F., et al., *Levels of S100B protein drive the reparative process in acute muscle injury and muscular dystrophy*. *Sci Rep*, 2017. **7**(1): p. 12537.
262. Bloomfield, S.M., et al., *Reliability of S100B in predicting severity of central nervous system injury*. *Neurocrit Care*, 2007. **6**(2): p. 121-38.
263. Hidaka, H., et al., *Purification and characterization of adipose tissue S-100b protein*. *J Biol Chem*, 1983. **258**(4): p. 2705-9.
264. Stefansson, K., R. Wollmann, and M. Jerkovic, *S-100 protein in soft-tissue tumors derived from Schwann cells and melanocytes*. *Am J Pathol*, 1982. **106**(2): p. 261-8.
265. Stefansson, K., et al., *S-100 protein in human chondrocytes*. *Nature*, 1982. **295**(5844): p. 63-4.
266. Stammet, P., et al., *Protein S100 as outcome predictor after out-of-hospital cardiac arrest and targeted temperature management at 33 degrees C and 36 degrees C*. *Crit Care*, 2017. **21**(1): p. 153.
267. Mattsson, N., et al., *Serum tau and neurological outcome in cardiac arrest*. *Ann Neurol*, 2017. **82**(5): p. 665-675.

268. Humaloja, J., et al., *GFAP and tau protein as predictors of neurological outcome after out-of-hospital cardiac arrest: A post hoc analysis of the COMACARE trial*. Resuscitation, 2022. **170**: p. 141-149.
269. Ebner, F., et al., *Serum GFAP and UCH-L1 for the prediction of neurological outcome in comatose cardiac arrest patients*. Resuscitation, 2020. **154**: p. 61-68.
270. Helwig, K., et al., *Elevated Serum Glial Fibrillary Acidic Protein (GFAP) is Associated with Poor Functional Outcome After Cardiopulmonary Resuscitation*. Neurocrit Care, 2017. **27**(1): p. 68-74.
271. Rana, O.R., et al., *Neurofilament light chain as an early and sensitive predictor of long-term neurological outcome in patients after cardiac arrest*. Int J Cardiol, 2013. **168**(2): p. 1322-7.
272. Moseby-Knappe, M., et al., *Serum Neurofilament Light Chain for Prognosis of Outcome After Cardiac Arrest*. JAMA Neurol, 2019. **76**(1): p. 64-71.
273. Hunziker, S., et al., *Serum neurofilament measurement improves clinical risk scores for outcome prediction after cardiac arrest: results of a prospective study*. Crit Care, 2021. **25**(1): p. 32.
274. Kirschen, M.P., et al., *Circulating Neurofilament Light Chain Is Associated With Survival After Pediatric Cardiac Arrest*. Pediatr Crit Care Med, 2020. **21**(7): p. 656-661.
275. Abe, A., et al., *Neurofilament light chain polypeptide gene mutations in Charcot-Marie-Tooth disease: nonsense mutation probably causes a recessive phenotype*. J Hum Genet, 2009. **54**(2): p. 94-7.
276. Khalil, M., et al., *Serum neurofilament light levels in normal aging and their association with morphologic brain changes*. Nat Commun, 2020. **11**(1): p. 812.
277. Hansson, O., et al., *Blood-based NfL: A biomarker for differential diagnosis of parkinsonian disorder*. Neurology, 2017. **88**(10): p. 930-937.
278. Mattsson, N., et al., *Association Between Longitudinal Plasma Neurofilament Light and Neurodegeneration in Patients With Alzheimer Disease*. JAMA Neurol, 2019. **76**(7): p. 791-799.
279. De Marchis, G.M., et al., *Serum neurofilament light chain in patients with acute cerebrovascular events*. Eur J Neurol, 2018. **25**(3): p. 562-568.
280. Feneberg, E., et al., *Multicenter evaluation of neurofilaments in early symptom onset amyotrophic lateral sclerosis*. Neurology, 2018. **90**(1): p. e22-e30.
281. Shahim, P., et al., *Serum neurofilament light protein predicts clinical outcome in traumatic brain injury*. Sci Rep, 2016. **6**: p. 36791.
282. Tiedt, S., et al., *Serum neurofilament light: A biomarker of neuroaxonal injury after ischemic stroke*. Neurology, 2018. **91**(14): p. e1338-e1347.
283. Rosen, C., et al., *Cerebrospinal fluid biomarkers in cardiac arrest survivors*. Resuscitation, 2014. **85**(2): p. 227-32.
284. Wihersaari, L., et al., *Neurofilament light as an outcome predictor after cardiac arrest: a post hoc analysis of the COMACARE trial*. Intensive Care Med, 2021. **47**(1): p. 39-48.
285. Moseby-Knappe, M., et al., *Serum markers of brain injury can predict good neurological outcome after out-of-hospital cardiac arrest*. Intensive Care Med, 2021. **47**(9): p. 984-994.
286. Rosjo, H., et al., *Prognostic value of high-sensitivity troponin T levels in patients with ventricular arrhythmias and out-of-hospital cardiac arrest: data from the prospective FINNRESUSCI study*. Crit Care, 2014. **18**(6): p. 605.
287. Myhre, P.L., et al., *NT-proBNP in patients with out-of-hospital cardiac arrest: Results from the FINNRESUSCI Study*. Resuscitation, 2016. **104**: p. 12-8.
288. Frydland, M., et al., *Usefulness of Serum B-Type Natriuretic Peptide Levels in Comatose Patients Resuscitated from Out-of-Hospital Cardiac Arrest to Predict Outcome*. Am J Cardiol, 2016. **118**(7): p. 998-1005.
289. During, J., et al., *Copeptin as a marker of outcome after cardiac arrest: a sub-study of the TTM trial*. Crit Care, 2020. **24**(1): p. 185.

290. Annborn, M., et al., *Procalcitonin after cardiac arrest - an indicator of severity of illness, ischemia-reperfusion injury and outcome*. Resuscitation, 2013. **84**(6): p. 782-7.
291. Bro-Jeppesen, J., et al., *Predictive value of interleukin-6 in post-cardiac arrest patients treated with targeted temperature management at 33 degrees C or 36 degrees C*. Resuscitation, 2016. **98**: p. 1-8.
292. Crick, F.H., *On protein synthesis*. Symp Soc Exp Biol, 1958. **12**: p. 138-63.
293. Trapnell, C., et al., *Transcript assembly and quantification by RNA-Seq reveals unannotated transcripts and isoform switching during cell differentiation*. Nat Biotechnol, 2010. **28**(5): p. 511-5.
294. Pan, Q., et al., *Deep surveying of alternative splicing complexity in the human transcriptome by high-throughput sequencing*. Nat Genet, 2008. **40**(12): p. 1413-5.
295. Martinez, O. and M.H. Reyes-Valdes, *Defining diversity, specialization, and gene specificity in transcriptomes through information theory*. Proc Natl Acad Sci U S A, 2008. **105**(28): p. 9709-14.
296. Wang, E.T., et al., *Alternative isoform regulation in human tissue transcriptomes*. Nature, 2008. **456**(7221): p. 470-6.
297. Frith, M.C., M. Pheasant, and J.S. Mattick, *The amazing complexity of the human transcriptome*. Eur J Hum Genet, 2005. **13**(8): p. 894-7.
298. Uchida, S. and S. Dimmeler, *Long noncoding RNAs in cardiovascular diseases*. Circ Res, 2015. **116**(4): p. 737-50.
299. Liu, G., J.S. Mattick, and R.J. Taft, *A meta-analysis of the genomic and transcriptomic composition of complex life*. Cell Cycle, 2013. **12**(13): p. 2061-72.
300. Hube, F. and C. Francastel, *Coding and Non-coding RNAs, the Frontier Has Never Been So Blurred*. Front Genet, 2018. **9**: p. 140.
301. Uzman, A., *Molecular biology of the cell (4th ed.): Alberts, B., Johnson, A., Lewis, J., Raff, M., Roberts, K., and Walter, P.* Biochemistry and Molecular Biology Education, 2003. **31**(4): p. 212-214.
302. Kutter, C. and P. Svoboda, *miRNA, siRNA, piRNA: Knowns of the unknown*. RNA Biol, 2008. **5**(4): p. 181-8.
303. Siomi, M.C., et al., *PIWI-interacting small RNAs: the vanguard of genome defence*. Nat Rev Mol Cell Biol, 2011. **12**(4): p. 246-58.
304. O'Brien, J., et al., *Overview of MicroRNA Biogenesis, Mechanisms of Actions, and Circulation*. Front Endocrinol (Lausanne), 2018. **9**: p. 402.
305. Bartel, D.P., *MicroRNAs: genomics, biogenesis, mechanism, and function*. Cell, 2004. **116**(2): p. 281-97.
306. Liang, H., et al., *Nuclear microRNAs and their unconventional role in regulating non-coding RNAs*. Protein Cell, 2013. **4**(5): p. 325-30.
307. Roberts, T.C., *The MicroRNA Biology of the Mammalian Nucleus*. Mol Ther Nucleic Acids, 2014. **3**: p. e188.
308. Vasudevan, S., Y. Tong, and J.A. Steitz, *Switching from repression to activation: microRNAs can up-regulate translation*. Science, 2007. **318**(5858): p. 1931-4.
309. Axtell, M.J., J.O. Westholm, and E.C. Lai, *Vive la difference: biogenesis and evolution of microRNAs in plants and animals*. Genome Biol, 2011. **12**(4): p. 221.
310. Dexheimer, P.J. and L. Cochella, *MicroRNAs: From Mechanism to Organism*. Front Cell Dev Biol, 2020. **8**: p. 409.
311. Friedman, R.C., et al., *Most mammalian mRNAs are conserved targets of microRNAs*. Genome Res, 2009. **19**(1): p. 92-105.
312. Lee, C.T., T. Risom, and W.M. Strauss, *Evolutionary conservation of microRNA regulatory circuits: an examination of microRNA gene complexity and conserved microRNA-target interactions through metazoan phylogeny*. DNA Cell Biol, 2007. **26**(4): p. 209-18.
313. Xiong, P., et al., *Conservation and novelty in the microRNA genomic landscape of hyperdiverse cichlid fishes*. Sci Rep, 2019. **9**(1): p. 13848.

314. Liu, N., et al., *The evolution and functional diversification of animal microRNA genes*. Cell Res, 2008. **18**(10): p. 985-96.
315. Zhu, Y., et al., *Evolutionary relationships between miRNA genes and their activity*. BMC Genomics, 2012. **13**: p. 718.
316. Lee, Y., et al., *MicroRNA maturation: stepwise processing and subcellular localization*. EMBO J, 2002. **21**(17): p. 4663-70.
317. Kabekkodu, S.P., et al., *Clustered miRNAs and their role in biological functions and diseases*. Biol Rev Camb Philos Soc, 2018. **93**(4): p. 1955-1986.
318. Wang, Y., et al., *microRNAs in the Same Clusters Evolve to Coordinately Regulate Functionally Related Genes*. Mol Biol Evol, 2016. **33**(9): p. 2232-47.
319. Ventura, A., et al., *Targeted deletion reveals essential and overlapping functions of the miR-17 through 92 family of miRNA clusters*. Cell, 2008. **132**(5): p. 875-86.
320. Yuan, X., et al., *Clustered microRNAs' coordination in regulating protein-protein interaction network*. BMC Syst Biol, 2009. **3**: p. 65.
321. Borchert, G.M., W. Lanier, and B.L. Davidson, *RNA polymerase III transcribes human microRNAs*. Nat Struct Mol Biol, 2006. **13**(12): p. 1097-101.
322. Cullen, B.R., *Transcription and processing of human microRNA precursors*. Mol Cell, 2004. **16**(6): p. 861-5.
323. Lee, Y., et al., *The nuclear RNase III Drosha initiates microRNA processing*. Nature, 2003. **425**(6956): p. 415-9.
324. Denli, A.M., et al., *Processing of primary microRNAs by the Microprocessor complex*. Nature, 2004. **432**(7014): p. 231-5.
325. Feng, Y., et al., *A comprehensive analysis of precursor microRNA cleavage by human Dicer*. RNA, 2012. **18**(11): p. 2083-92.
326. Yoda, M., et al., *ATP-dependent human RISC assembly pathways*. Nat Struct Mol Biol, 2010. **17**(1): p. 17-23.
327. Okamura, K., N. Liu, and E.C. Lai, *Distinct mechanisms for microRNA strand selection by Drosophila Argonautes*. Mol Cell, 2009. **36**(3): p. 431-44.
328. Hartford, C.C.R. and A. Lal, *When Long Noncoding Becomes Protein Coding*. Mol Cell Biol, 2020. **40**(6).
329. Li, J. and C. Liu, *Coding or Noncoding, the Converging Concepts of RNAs*. Front Genet, 2019. **10**: p. 496.
330. Anderson, D.M., et al., *A micropeptide encoded by a putative long noncoding RNA regulates muscle performance*. Cell, 2015. **160**(4): p. 595-606.
331. Nam, J.W., S.W. Choi, and B.H. You, *Incredible RNA: Dual Functions of Coding and Noncoding*. Mol Cells, 2016. **39**(5): p. 367-74.
332. Dinger, M.E., D.K. Gascoigne, and J.S. Mattick, *The evolution of RNAs with multiple functions*. Biochimie, 2011. **93**(11): p. 2013-8.
333. Camilleri-Robles, C., et al., *Genomic and functional conservation of lncRNAs: lessons from flies*. Mamm Genome, 2022. **33**(2): p. 328-342.
334. Jalali, S., et al., *Systematic transcriptome wide analysis of lncRNA-miRNA interactions*. PLoS One, 2013. **8**(2): p. e53823.
335. Bhartiya, D. and V. Scaria, *Genomic variations in non-coding RNAs: Structure, function and regulation*. Genomics, 2016. **107**(2-3): p. 59-68.
336. Johnsson, P., et al., *Evolutionary conservation of long non-coding RNAs; sequence, structure, function*. Biochim Biophys Acta, 2014. **1840**(3): p. 1063-71.
337. Amaral, P.P., et al., *Genomic positional conservation identifies topological anchor point RNAs linked to developmental loci*. Genome Biol, 2018. **19**(1): p. 32.
338. Ramirez-Colmenero, A., K. Oktaba, and S.L. Fernandez-Valverde, *Evolution of Genome-Organizing Long Non-coding RNAs in Metazoans*. Front Genet, 2020. **11**: p. 589697.
339. Pegueroles, C. and T. Gabaldon, *Secondary structure impacts patterns of selection in human lncRNAs*. BMC Biol, 2016. **14**: p. 60.



340. Fernandes, J.C.R., et al., *Long Non-Coding RNAs in the Regulation of Gene Expression: Physiology and Disease*. Noncoding RNA, 2019. **5**(1).
341. Huo, X., et al., *Dysregulated long noncoding RNAs (lncRNAs) in hepatocellular carcinoma: implications for tumorigenesis, disease progression, and liver cancer stem cells*. Mol Cancer, 2017. **16**(1): p. 165.
342. Greco, S., et al., *Long noncoding RNA dysregulation in ischemic heart failure*. J Transl Med, 2016. **14**(1): p. 183.
343. Asadi, M.R., et al., *The Perspective of Dysregulated lncRNAs in Alzheimer's Disease: A Systematic Scoping Review*. Front Aging Neurosci, 2021. **13**: p. 709568.
344. Kristensen, L.S., et al., *The biogenesis, biology and characterization of circular RNAs*. Nat Rev Genet, 2019. **20**(11): p. 675-691.
345. Wang, M., et al., *Circular RNAs: A novel type of non-coding RNA and their potential implications in antiviral immunity*. Int J Biol Sci, 2017. **13**(12): p. 1497-1506.
346. Zhang, Y., et al., *The Biogenesis of Nascent Circular RNAs*. Cell Rep, 2016. **15**(3): p. 611-624.
347. Ivanov, A., et al., *Analysis of intron sequences reveals hallmarks of circular RNA biogenesis in animals*. Cell Rep, 2015. **10**(2): p. 170-7.
348. Kramer, M.C., et al., *Combinatorial control of Drosophila circular RNA expression by intronic repeats, hnRNPs, and SR proteins*. Genes Dev, 2015. **29**(20): p. 2168-82.
349. Wu, J., et al., *Emerging Epigenetic Regulation of Circular RNAs in Human Cancer*. Mol Ther Nucleic Acids, 2019. **16**: p. 589-596.
350. Zhao, X., Y. Cai, and J. Xu, *Circular RNAs: Biogenesis, Mechanism, and Function in Human Cancers*. Int J Mol Sci, 2019. **20**(16).
351. Schwanhausser, B., et al., *Global quantification of mammalian gene expression control*. Nature, 2011. **473**(7347): p. 337-42.
352. Liu, C.X., et al., *Structure and Degradation of Circular RNAs Regulate PKR Activation in Innate Immunity*. Cell, 2019. **177**(4): p. 865-880 e21.
353. Park, O.H., et al., *Endoribonucleolytic Cleavage of m(6)A-Containing RNAs by RNase P/MRP Complex*. Mol Cell, 2019. **74**(3): p. 494-507 e8.
354. He, X., et al., *Circular RNAs: Their Role in the Pathogenesis and Orchestration of Breast Cancer*. Front Cell Dev Biol, 2021. **9**: p. 647736.
355. Bie, F., et al., *The potential roles of circular RNAs as modulators in traumatic spinal cord injury*. Biomed Pharmacother, 2021. **141**: p. 111826.
356. Doxakis, E., *Insights into the multifaceted role of circular RNAs: implications for Parkinson's disease pathogenesis and diagnosis*. NPJ Parkinsons Dis, 2022. **8**(1): p. 7.
357. Li, M., et al., *Biogenesis of circular RNAs and their roles in cardiovascular development and pathology*. FEBS J, 2018. **285**(2): p. 220-232.
358. Liu, W. and G. Yan, *The Emerging Role of Circular RNAs in Cerebral Vascular Disorders*. Eur Neurol, 2021. **84**(4): p. 230-236.
359. Meng, S., et al., *CircRNA: functions and properties of a novel potential biomarker for cancer*. Mol Cancer, 2017. **16**(1): p. 94.
360. Hansen, T.B., et al., *Natural RNA circles function as efficient microRNA sponges*. Nature, 2013. **495**(7441): p. 384-8.
361. Geng, X., et al., *Circular RNA: biogenesis, degradation, functions and potential roles in mediating resistance to anticarcinogens*. Epigenomics, 2020. **12**(3): p. 267-283.
362. Jiang, C., et al., *The Emerging Picture of the Roles of CircRNA-CDR1as in Cancer*. Front Cell Dev Biol, 2020. **8**: p. 590478.
363. Geng, H.H., et al., *The Circular RNA Cdr1as Promotes Myocardial Infarction by Mediating the Regulation of miR-7a on Its Target Genes Expression*. PLoS One, 2016. **11**(3): p. e0151753.
364. Mester-Tonczar, J., et al., *Association between Circular RNA CDR1as and Post-Infarction Cardiac Function in Pig Ischemic Heart Failure: Influence of the Anti-Fibrotic Natural Compounds Bufalin and Lycorine*. Biomolecules, 2020. **10**(8).

365. Du, W.W., et al., *Foxo3 circular RNA promotes cardiac senescence by modulating multiple factors associated with stress and senescence responses*. Eur Heart J, 2017. **38**(18): p. 1402-1412.
366. Du, W.W., et al., *Foxo3 circular RNA retards cell cycle progression via forming ternary complexes with p21 and CDK2*. Nucleic Acids Res, 2016. **44**(6): p. 2846-58.
367. Rao, D., et al., *The Emerging Roles of circFOXO3 in Cancer*. Front Cell Dev Biol, 2021. **9**: p. 659417.
368. Li, Z., et al., *Corrigendum: Exon-intron circular RNAs regulate transcription in the nucleus*. Nat Struct Mol Biol, 2017. **24**(2): p. 194.
369. Shao, T., Y.H. Pan, and X.D. Xiong, *Circular RNA: an important player with multiple facets to regulate its parental gene expression*. Mol Ther Nucleic Acids, 2021. **23**: p. 369-376.
370. Yang, F., et al., *Circ-HuR suppresses HuR expression and gastric cancer progression by inhibiting CNBP transactivation*. Mol Cancer, 2019. **18**(1): p. 158.
371. Yang, Y., et al., *Extensive translation of circular RNAs driven by N(6)-methyladenosine*. Cell Res, 2017. **27**(5): p. 626-641.
372. Pamudurti, N.R., et al., *Translation of CircRNAs*. Mol Cell, 2017. **66**(1): p. 9-21 e7.
373. Legnini, I., et al., *Circ-ZNF609 Is a Circular RNA that Can Be Translated and Functions in Myogenesis*. Mol Cell, 2017. **66**(1): p. 22-37 e9.
374. Dvorak, P., S. Leupen, and P. Soucek, *Circulating and circular RNAs and the need for rationalization and synthesis of the research spiral*. Adv Clin Exp Med, 2019. **28**(6): p. 833-838.
375. Pardini, B. and G.A. Calin, *MicroRNAs and Long Non-Coding RNAs and Their Hormone-Like Activities in Cancer*. Cancers (Basel), 2019. **11**(3).
376. Huang, X., et al., *Characterization of human plasma-derived exosomal RNAs by deep sequencing*. BMC Genomics, 2013. **14**: p. 319.
377. Fritz, J.V., et al., *Sources and Functions of Extracellular Small RNAs in Human Circulation*. Annu Rev Nutr, 2016. **36**: p. 301-36.
378. Arroyo, J.D., et al., *Argonaute2 complexes carry a population of circulating microRNAs independent of vesicles in human plasma*. Proc Natl Acad Sci U S A, 2011. **108**(12): p. 5003-8.
379. Turchinovich, A., et al., *Characterization of extracellular circulating microRNA*. Nucleic Acids Res, 2011. **39**(16): p. 7223-33.
380. Wang, K., et al., *Export of microRNAs and microRNA-protective protein by mammalian cells*. Nucleic Acids Res, 2010. **38**(20): p. 7248-59.
381. Vickers, K.C., et al., *MicroRNAs are transported in plasma and delivered to recipient cells by high-density lipoproteins*. Nat Cell Biol, 2011. **13**(4): p. 423-33.
382. Wagner, J., et al., *Characterization of levels and cellular transfer of circulating lipoprotein-bound microRNAs*. Arterioscler Thromb Vasc Biol, 2013. **33**(6): p. 1392-400.
383. Lotvall, J. and H. Valadi, *Cell to cell signalling via exosomes through esRNA*. Cell Adh Migr, 2007. **1**(3): p. 156-8.
384. Ying, W., et al., *Adipose Tissue Macrophage-Derived Exosomal miRNAs Can Modulate In Vivo and In Vitro Insulin Sensitivity*. Cell, 2017. **171**(2): p. 372-384 e12.
385. Fabbri, M., *MicroRNAs and miReceptors: a new mechanism of action for intercellular communication*. Philos Trans R Soc Lond B Biol Sci, 2018. **373**(1737).
386. Dragomir, M., B. Chen, and G.A. Calin, *Exosomal lncRNAs as new players in cell-to-cell communication*. Transl Cancer Res, 2018. **7**(Suppl 2): p. S243-S252.
387. Lasda, E. and R. Parker, *Circular RNAs Co-Precipitate with Extracellular Vesicles: A Possible Mechanism for circRNA Clearance*. PLoS One, 2016. **11**(2): p. e0148407.
388. Turchinovich, A., L. Weiz, and B. Burwinkel, *Extracellular miRNAs: the mystery of their origin and function*. Trends Biochem Sci, 2012. **37**(11): p. 460-5.
389. Heil, B. and W.H. Tang, *Biomarkers: Their potential in the diagnosis and treatment of heart failure*. Cleve Clin J Med, 2015. **82**(12 Suppl 2): p. S28-35.

390. Viereck, J. and T. Thum, *Circulating Noncoding RNAs as Biomarkers of Cardiovascular Disease and Injury*. *Circ Res*, 2017. **120**(2): p. 381-399.
391. Previdi, M.C., et al., *Noncoding RNAs as novel biomarkers in pancreatic cancer: what do we know?* *Future Oncol*, 2017. **13**(5): p. 443-453.
392. Frieler, R.A. and R.M. Mortensen, *Immune cell and other noncardiomyocyte regulation of cardiac hypertrophy and remodeling*. *Circulation*, 2015. **131**(11): p. 1019-30.
393. Dutta, P. and M. Nahrendorf, *Monocytes in myocardial infarction*. *Arterioscler Thromb Vasc Biol*, 2015. **35**(5): p. 1066-70.
394. Fitzgerald, K.A. and D.R. Caffrey, *Long noncoding RNAs in innate and adaptive immunity*. *Curr Opin Immunol*, 2014. **26**: p. 140-6.
395. Zhang, L., X. Xu, and X. Su, *Noncoding RNAs in cancer immunity: functions, regulatory mechanisms, and clinical application*. *Mol Cancer*, 2020. **19**(1): p. 48.
396. O'Connell, R.M., et al., *Inositol phosphatase SHIP1 is a primary target of miR-155*. *Proc Natl Acad Sci U S A*, 2009. **106**(17): p. 7113-8.
397. Androulidaki, A., et al., *The kinase Akt1 controls macrophage response to lipopolysaccharide by regulating microRNAs*. *Immunity*, 2009. **31**(2): p. 220-31.
398. Alivernini, S., et al., *MicroRNA-155-at the Critical Interface of Innate and Adaptive Immunity in Arthritis*. *Front Immunol*, 2017. **8**: p. 1932.
399. Kurowska-Stolarska, M., et al., *MicroRNA-155 as a proinflammatory regulator in clinical and experimental arthritis*. *Proc Natl Acad Sci U S A*, 2011. **108**(27): p. 11193-8.
400. Murugaiyan, G., et al., *Silencing microRNA-155 ameliorates experimental autoimmune encephalomyelitis*. *J Immunol*, 2011. **187**(5): p. 2213-21.
401. O'Connell, R.M., et al., *MicroRNA-155 promotes autoimmune inflammation by enhancing inflammatory T cell development*. *Immunity*, 2010. **33**(4): p. 607-19.
402. Satpathy, A.T. and H.Y. Chang, *Long noncoding RNA in hematopoiesis and immunity*. *Immunity*, 2015. **42**(5): p. 792-804.
403. Xie, N. and G. Liu, *ncRNA-regulated immune response and its role in inflammatory lung diseases*. *Am J Physiol Lung Cell Mol Physiol*, 2015. **309**(10): p. L1076-87.
404. Carpenter, S., et al., *A long noncoding RNA mediates both activation and repression of immune response genes*. *Science*, 2013. **341**(6147): p. 789-92.
405. Li, Z., et al., *The long noncoding RNA THRIL regulates TNFalpha expression through its interaction with hnRNPL*. *Proc Natl Acad Sci U S A*, 2014. **111**(3): p. 1002-7.
406. Imamura, K., et al., *Long noncoding RNA NEAT1-dependent SFPQ relocation from promoter region to paraspeckle mediates IL8 expression upon immune stimuli*. *Mol Cell*, 2014. **53**(3): p. 393-406.
407. Chew, C.L., et al., *Noncoding RNAs: Master Regulators of Inflammatory Signaling*. *Trends Mol Med*, 2018. **24**(1): p. 66-84.
408. Zhou, Z., et al., *Roles of circular RNAs in immune regulation and autoimmune diseases*. *Cell Death Dis*, 2019. **10**(7): p. 503.
409. Chai, V., et al., *Optimization of the PAXgene blood RNA extraction system for gene expression analysis of clinical samples*. *J Clin Lab Anal*, 2005. **19**(5): p. 182-8.
410. He, D., et al., *Whole blood vs PBMC: compartmental differences in gene expression profiling exemplified in asthma*. *Allergy Asthma Clin Immunol*, 2019. **15**: p. 67.
411. Barwari, T., A. Joshi, and M. Mayr, *MicroRNAs in Cardiovascular Disease*. *J Am Coll Cardiol*, 2016. **68**(23): p. 2577-2584.
412. Matkovich, S.J., et al., *Reciprocal regulation of myocardial microRNAs and messenger RNA in human cardiomyopathy and reversal of the microRNA signature by biomechanical support*. *Circulation*, 2009. **119**(9): p. 1263-71.
413. van Rooij, E., et al., *A signature pattern of stress-responsive microRNAs that can evoke cardiac hypertrophy and heart failure*. *Proc Natl Acad Sci U S A*, 2006. **103**(48): p. 18255-60.
414. Fang, Y., et al., *Recent advances on the roles of LncRNAs in cardiovascular disease*. *J Cell Mol Med*, 2020. **24**(21): p. 12246-12257.

415. Das, S., et al., *Noncoding RNAs in Cardiovascular Disease: Current Knowledge, Tools and Technologies for Investigation, and Future Directions: A Scientific Statement From the American Heart Association*. *Circ Genom Precis Med*, 2020. **13**(4): p. e000062.
416. Zhou, S.S., et al., *miRNAs in cardiovascular diseases: potential biomarkers, therapeutic targets and challenges*. *Acta Pharmacol Sin*, 2018. **39**(7): p. 1073-1084.
417. Colpaert, R.M.W. and M. Calore, *MicroRNAs in Cardiac Diseases*. *Cells*, 2019. **8**(7).
418. Yeh, C.F., et al., *Expedition to the missing link: Long noncoding RNAs in cardiovascular diseases*. *J Biomed Sci*, 2020. **27**(1): p. 48.
419. Hobuss, L., C. Bar, and T. Thum, *Long Non-coding RNAs: At the Heart of Cardiac Dysfunction?* *Front Physiol*, 2019. **10**: p. 30.
420. Peters, L.J.F., et al., *Small Things Matter: Relevance of MicroRNAs in Cardiovascular Disease*. *Front Physiol*, 2020. **11**: p. 793.
421. Elbaz, M., et al., *MiR-223 and MiR-186 Are Associated with Long-Term Mortality after Myocardial Infarction*. *Biomolecules*, 2022. **12**(9).
422. Gilje, P., et al., *The brain-enriched microRNA miR-124 in plasma predicts neurological outcome after cardiac arrest*. *Crit Care*, 2014. **18**(2): p. R40.
423. Devaux, Y., et al., *Incremental Value of Circulating MiR-122-5p to Predict Outcome after Out of Hospital Cardiac Arrest*. *Theranostics*, 2017. **7**(10): p. 2555-2564.
424. Kumarswamy, R., et al., *Circulating long noncoding RNA, LIPCAR, predicts survival in patients with heart failure*. *Circ Res*, 2014. **114**(10): p. 1569-75.
425. Meessen, J., et al., *LIPCAR Is Increased in Chronic Symptomatic HF Patients. A Sub-Study of the GISSI-HF Trial*. *Clin Chem*, 2021. **67**(12): p. 1721-1731.
426. Vausort, M., D.R. Wagner, and Y. Devaux, *Long noncoding RNAs in patients with acute myocardial infarction*. *Circ Res*, 2014. **115**(7): p. 668-77.
427. Chen, Y. and J. Zhou, *LncRNAs: macromolecules with big roles in neurobiology and neurological diseases*. *Metab Brain Dis*, 2017. **32**(2): p. 281-291.
428. Li, L., et al., *Long Non-coding RNA in Neuronal Development and Neurological Disorders*. *Front Genet*, 2018. **9**: p. 744.
429. Antoniou, D., A. Stergiopoulos, and P.K. Politis, *Recent advances in the involvement of long non-coding RNAs in neural stem cell biology and brain pathophysiology*. *Front Physiol*, 2014. **5**: p. 155.
430. Qureshi, I.A. and M.F. Mehler, *Long non-coding RNAs: novel targets for nervous system disease diagnosis and therapy*. *Neurotherapeutics*, 2013. **10**(4): p. 632-46.
431. Liu, R., et al., *Expression profiles of long noncoding RNAs and mRNAs in post-cardiac arrest rat brains*. *Mol Med Rep*, 2018. **17**(5): p. 6413-6424.
432. Zhong, J., et al., *Altered expression of long non-coding RNA and mRNA in mouse cortex after traumatic brain injury*. *Brain Res*, 2016. **1646**: p. 589-600.
433. Wang, C.F., et al., *Alteration in Long Non-Coding RNA Expression after Traumatic Brain Injury in Rats*. *J Neurotrauma*, 2017. **34**(13): p. 2100-2108.
434. Vausort, M., et al., *Myocardial Infarction-Associated Circular RNA Predicting Left Ventricular Dysfunction*. *J Am Coll Cardiol*, 2016. **68**(11): p. 1247-1248.
435. Salgado-Somoza, A., et al., *The circular RNA MICRA for risk stratification after myocardial infarction*. *Int J Cardiol Heart Vasc*, 2017. **17**: p. 33-36.
436. Zhang, Z.H., et al., *Circ-camk4 involved in cerebral ischemia/reperfusion induced neuronal injury*. *Sci Rep*, 2020. **10**(1): p. 7012.
437. Zuo, L., et al., *Down-regulation of circular RNA CDC14A peripherally ameliorates brain injury in acute phase of ischemic stroke*. *J Neuroinflammation*, 2021. **18**(1): p. 283.
438. Chen, W., et al., *Overexpression of circRNA circUCK2 Attenuates Cell Apoptosis in Cerebral Ischemia-Reperfusion Injury via miR-125b-5p/GDF11 Signaling*. *Mol Ther Nucleic Acids*, 2020. **22**: p. 673-683.
439. Mehta, S.L., G. Pandi, and R. Vemuganti, *Circular RNA Expression Profiles Alter Significantly in Mouse Brain After Transient Focal Ischemia*. *Stroke*, 2017. **48**(9): p. 2541-2548.

440. Tian, M., Z. Cao, and H. Pang, *Circular RNAs in Sudden Cardiac Death Related Diseases: Novel Biomarker for Clinical and Forensic Diagnosis*. *Molecules*, 2021. **26**(4).
441. Bei, Y., et al., *Circular RNAs as Potential Theranostics in the Cardiovascular System*. *Mol Ther Nucleic Acids*, 2018. **13**: p. 407-418.
442. Nielsen, N., et al., *Target Temperature Management after out-of-hospital cardiac arrest--a randomized, parallel-group, assessor-blinded clinical trial--rationale and design*. *Am Heart J*, 2012. **163**(4): p. 541-8.
443. Dankiewicz, J., et al., *Targeted hypothermia versus targeted Normothermia after out-of-hospital cardiac arrest (TTM2): A randomized clinical trial-Rationale and design*. *Am Heart J*, 2019. **217**: p. 23-31.
444. Ryu, A.H., et al., *Use antibiotics in cell culture with caution: genome-wide identification of antibiotic-induced changes in gene expression and regulation*. *Sci Rep*, 2017. **7**(1): p. 7533.
445. Singh, R., L. Sripada, and R. Singh, *Side effects of antibiotics during bacterial infection: mitochondria, the main target in host cell*. *Mitochondrion*, 2014. **16**: p. 50-4.
446. Dobin, A., et al., *STAR: ultrafast universal RNA-seq aligner*. *Bioinformatics*, 2013. **29**(1): p. 15-21.
447. Trapnell, C., et al., *Differential analysis of gene regulation at transcript resolution with RNA-seq*. *Nat Biotechnol*, 2013. **31**(1): p. 46-53.
448. Volders, P.J., et al., *LNCipedia 5: towards a reference set of human long non-coding RNAs*. *Nucleic Acids Res*, 2019. **47**(D1): p. D135-D139.
449. Cheng, J., F. Metge, and C. Dieterich, *Specific identification and quantification of circular RNAs from sequencing data*. *Bioinformatics*, 2016. **32**(7): p. 1094-6.
450. Love, M.I., W. Huber, and S. Anders, *Moderated estimation of fold change and dispersion for RNA-seq data with DESeq2*. *Genome Biol*, 2014. **15**(12): p. 550.
451. Stekhoven, D.J. and P. Bühlmann, *MissForest--non-parametric missing value imputation for mixed-type data*. *Bioinformatics*, 2012. **28**(1): p. 112-8.
452. Condrat, C.E., et al., *miRNAs as Biomarkers in Disease: Latest Findings Regarding Their Role in Diagnosis and Prognosis*. *Cells*, 2020. **9**(2).
453. Park, J.S., et al., *Study on the timing of severe blood-brain barrier disruption using cerebrospinal fluid-serum albumin quotient in post cardiac arrest patients treated with targeted temperature management*. *Resuscitation*, 2019. **135**: p. 118-123.
454. Luescher, T., et al., *Neuron-specific enolase (NSE) improves clinical risk scores for prediction of neurological outcome and death in cardiac arrest patients: Results from a prospective trial*. *Resuscitation*, 2019. **142**: p. 50-60.
455. Kleissner, M., et al., *Serum S100 Protein Is a Reliable Predictor of Brain Injury After Out-of-Hospital Cardiac Arrest: A Cohort Study*. *Front Cardiovasc Med*, 2021. **8**: p. 624825.
456. Domanovits, H., et al., *Impairment of renal function in patients resuscitated from cardiac arrest: frequency, determinants and impact on outcome*. *Wien Klin Wochenschr*, 2000. **112**(4): p. 157-61.
457. Hasper, D., et al., *Changes in serum creatinine in the first 24 hours after cardiac arrest indicate prognosis: an observational cohort study*. *Crit Care*, 2009. **13**(5): p. R168.
458. Kashiwagi, Y., et al., *Therapeutic hypothermia after cardiac arrest increases the plasma level of B-type natriuretic peptide*. *Sci Rep*, 2020. **10**(1): p. 15545.
459. Cakmak, S., et al., *Serum Copeptin Levels Predict the Return of Spontaneous Circulation and the Short-Term Prognosis of Patients with Out-of-Hospital Cardiac Arrest: A Randomized Control Study*. *Prehosp Disaster Med*, 2020. **35**(2): p. 120-127.
460. Paramanathan, S., et al., *Copeptin as a Prognostic Marker in Prolonged Targeted Temperature Management After Out-of-Hospital Cardiac Arrest*. *Ther Hypothermia Temp Manag*, 2021. **11**(4): p. 216-222.
461. Gilje, P., et al., *High-sensitivity troponin-T as a prognostic marker after out-of-hospital cardiac arrest - A targeted temperature management (TTM) trial substudy*. *Resuscitation*, 2016. **107**: p. 156-61.

462. Dell'anna, A.M., et al., *C-reactive protein levels after cardiac arrest in patients treated with therapeutic hypothermia*. Resuscitation, 2014. **85**(7): p. 932-8.
463. Schriefl, C., et al., *Admission C-reactive protein concentrations are associated with unfavourable neurological outcome after out-of-hospital cardiac arrest*. Sci Rep, 2021. **11**(1): p. 10279.
464. Chong, J.Y., et al., *Interleukin-6 as a Potential Predictor of Neurologic Outcomes in Cardiac Arrest Survivors Who Underwent Target Temperature Management*. J Emerg Med, 2020. **59**(6): p. 828-835.
465. Stammel, P., et al., *Assessment of procalcitonin to predict outcome in hypothermia-treated patients after cardiac arrest*. Crit Care Res Pract, 2011. **2011**: p. 631062.
466. Fries, M., et al., *Procalcitonin serum levels after out-of-hospital cardiac arrest*. Resuscitation, 2003. **59**(1): p. 105-9.
467. Liu, Y., et al., *Hypoxia regulates vascular endothelial growth factor gene expression in endothelial cells. Identification of a 5' enhancer*. Circ Res, 1995. **77**(3): p. 638-43.
468. Munoz-Sanchez, J. and M.E. Chanez-Cardenas, *The use of cobalt chloride as a chemical hypoxia model*. J Appl Toxicol, 2019. **39**(4): p. 556-570.
469. Plevin, R.E., et al., *The Role of Lipopolysaccharide Structure in Monocyte Activation and Cytokine Secretion*. Shock, 2016. **45**(1): p. 22-7.
470. Idriss, H.T. and J.H. Naismith, *TNF alpha and the TNF receptor superfamily: structure-function relationship(s)*. Microsc Res Tech, 2000. **50**(3): p. 184-95.
471. Rivard, C.J., et al., *Expression of the calcium-binding protein S100A4 is markedly up-regulated by osmotic stress and is involved in the renal osmoadaptive response*. J Biol Chem, 2007. **282**(9): p. 6644-52.
472. Viengchareun, S., et al., *Hypertonicity compromises renal mineralocorticoid receptor signaling through Tis11b-mediated post-transcriptional control*. J Am Soc Nephrol, 2014. **25**(10): p. 2213-21.
473. Trama, J., W.Y. Go, and S.N. Ho, *The osmoprotective function of the NFAT5 transcription factor in T cell development and activation*. J Immunol, 2002. **169**(10): p. 5477-88.
474. Maallem, S., et al., *Selective tonicity-induced expression of the neutral amino-acid transporter SNAT2 in oligodendrocytes in rat brain following systemic hypertonicity*. Neuroscience, 2008. **153**(1): p. 95-107.
475. Kuper, C., F.X. Beck, and W. Neuhofer, *NFAT5-mediated expression of S100A4 contributes to proliferation and migration of renal carcinoma cells*. Front Physiol, 2014. **5**: p. 293.
476. Strzalka, W. and A. Ziemienowicz, *Proliferating cell nuclear antigen (PCNA): a key factor in DNA replication and cell cycle regulation*. Ann Bot, 2011. **107**(7): p. 1127-40.
477. Porter, A.G. and R.U. Janicke, *Emerging roles of caspase-3 in apoptosis*. Cell Death Differ, 1999. **6**(2): p. 99-104.
478. Popa, C., et al., *The role of TNF-alpha in chronic inflammatory conditions, intermediary metabolism, and cardiovascular risk*. J Lipid Res, 2007. **48**(4): p. 751-62.
479. Luzina, I.G., et al., *Regulation of inflammation by interleukin-4: a review of "alternatives"*. J Leukoc Biol, 2012. **92**(4): p. 753-64.
480. Kong, L., et al., *CPC: assess the protein-coding potential of transcripts using sequence features and support vector machine*. Nucleic Acids Res, 2007. **35**(Web Server issue): p. W345-9.
481. Panda, A.C., *Circular RNAs Act as miRNA Sponges*. Adv Exp Med Biol, 2018. **1087**: p. 67-79.
482. Xi, X., et al., *RNA Biomarkers: Frontier of Precision Medicine for Cancer*. Noncoding RNA, 2017. **3**(1).
483. Geppert, A., et al., *Soluble selectins and the systemic inflammatory response syndrome after successful cardiopulmonary resuscitation*. Crit Care Med, 2000. **28**(7): p. 2360-5.
484. Yuan, Q., et al., *Identification of Key CircRNAs Related to Pulmonary Tuberculosis Based on Bioinformatics Analysis*. Biomed Res Int, 2022. **2022**: p. 1717784.

485. Xie, Y., et al., *CircFAM13B promotes the proliferation of hepatocellular carcinoma by sponging miR-212, upregulating E2F5 expression and activating the P53 pathway*. *Cancer Cell Int*, 2021. **21**(1): p. 410.
486. Ning, L., et al., *Circular RNA profiling reveals circEXOC6B and circN4BP2L2 as novel prognostic biomarkers in epithelial ovarian cancer*. *Int J Oncol*, 2018. **53**(6): p. 2637-2646.
487. Li, X., et al., *Serum Exosomal Circular RNA Expression Profile and Regulative Role in Proliferative Diabetic Retinopathy*. *Front Genet*, 2021. **12**: p. 719312.
488. O'Connor, R.S., et al., *A combinatorial role for NFAT5 in both myoblast migration and differentiation during skeletal muscle myogenesis*. *J Cell Sci*, 2007. **120**(Pt 1): p. 149-59.
489. Adachi, A., et al., *NFAT5 regulates the canonical Wnt pathway and is required for cardiomyogenic differentiation*. *Biochem Biophys Res Commun*, 2012. **426**(3): p. 317-23.
490. Loyher, M.L., et al., *Transcription factor tonicity-responsive enhancer-binding protein (TonEBP) which transactivates osmoprotective genes is expressed and upregulated following acute systemic hypertonicity in neurons in brain*. *Neuroscience*, 2004. **124**(1): p. 89-104.
491. Trama, J., et al., *The NFAT-related protein NFATL1 (TonEBP/NFAT5) is induced upon T cell activation in a calcineurin-dependent manner*. *J Immunol*, 2000. **165**(9): p. 4884-94.
492. Machnik, A., et al., *Macrophages regulate salt-dependent volume and blood pressure by a vascular endothelial growth factor-C-dependent buffering mechanism*. *Nat Med*, 2009. **15**(5): p. 545-52.
493. Ma, P., et al., *NFAT5 mediates hypertonic stress-induced atherosclerosis via activating NLRP3 inflammasome in endothelium*. *Cell Commun Signal*, 2019. **17**(1): p. 102.
494. Neuhofer, W., *Role of NFAT5 in inflammatory disorders associated with osmotic stress*. *Curr Genomics*, 2010. **11**(8): p. 584-90.
495. Cen, L., et al., *Potential Role of Gene Regulator NFAT5 in the Pathogenesis of Diabetes Mellitus*. *J Diabetes Res*, 2020. **2020**: p. 6927429.
496. Go, W.Y., et al., *NFAT5/TonEBP mutant mice define osmotic stress as a critical feature of the lymphoid microenvironment*. *Proc Natl Acad Sci U S A*, 2004. **101**(29): p. 10673-8.
497. Kumar, R., et al., *NFAT5, which protects against hypertonicity, is activated by that stress via structuring of its intrinsically disordered domain*. *Proc Natl Acad Sci U S A*, 2020. **117**(33): p. 20292-20297.

# Appendix I





# Non-Coding RNAs to Aid in Neurological Prognosis after Cardiac Arrest

Antonio Salgado-Somoza <sup>1,†</sup>, Francesca Maria Stefanizzi <sup>1,†</sup> , Pascal Stammet <sup>2,†</sup>, David Erlinge <sup>3,†</sup>, Hans Friberg <sup>4,†</sup>, Niklas Nielsen <sup>5,†</sup> and Yvan Devaux <sup>1,†,\*</sup>

<sup>1</sup> Cardiovascular Research Unit, Department of Population Health, Luxembourg Institute of Health, L-1445 Strassen, Luxembourg; antonio.salgadosomoza@lih.lu (A.S.-S.); francescamaria.stefanizzi@lih.lu (F.M.S.)

<sup>2</sup> Medical and Health Department, Luxembourg Fire and Rescue Corps, L-2557 Luxembourg, Luxembourg; Pascal.Stammet@secours.etat.lu

<sup>3</sup> Department of Cardiology, Clinical Sciences, Lund University, 221 85 Lund, Sweden; david.erlinge@gmail.com

<sup>4</sup> Skane University Hospital, Lund University, 221 85 Malmö, Sweden; hans.a.friberg@gmail.com

<sup>5</sup> Helsingborg Hospital, Lund University, 25187 Helsingborg, Sweden; niklas.nielsen@telia.com

\* Correspondence: yvan.devoux@lih.lu; Tel.: +352-26970-300 † On behalf of the Cardiolic™ network.



Received: 8 November 2018; Accepted: 12 December 2018; Published: 18 December 2018

**Abstract:** Cardiovascular disease in general, and sudden cardiac death in particular, have an enormous socio-economic burden worldwide. Despite significant efforts to improve cardiopulmonary resuscitation, survival rates remain low. Moreover, patients who survive to hospital discharge have a high risk of developing severe physical or neurological symptoms. Being able to predict outcomes after resuscitation from cardiac arrest would make it possible to tailor healthcare approaches, thereby maximising efforts for those who would mostly benefit from aggressive therapy. However, the identification of patients at risk of poor recovery after cardiac arrest is still a challenging task which could be facilitated by novel biomarkers. Recent investigations have

## 1. Background

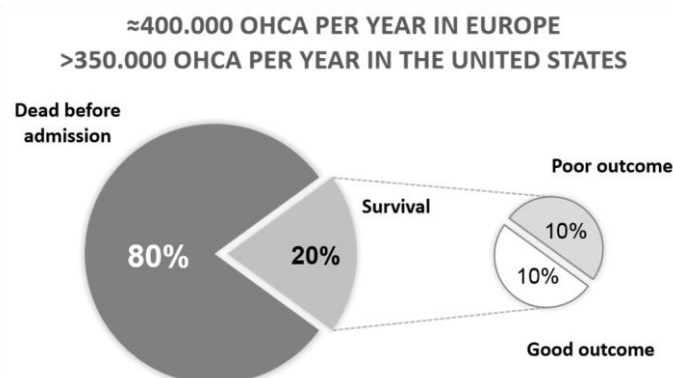
Despite joint efforts from the clinical and research communities in the field, cardiovascular disease remains the leading cause of mortality in the modern world, accounting for 45% of all deaths in Europe [1]. A high percentage of these deaths is attributed to sudden death or cardiac arrest (CA). According to the Declaration of the European Parliament of 14 June 2012, some 400,000 people suffer a sudden out-of-hospital CA each year in Europe. Similar numbers can be found in the United States, where cardiac arrest affects more than 350,000 people per year [2].

## 2. Outcome after Cardiac Arrest

Outcome is extremely poor following CA, as more than half of the people who suffer an arrest will die before reaching the hospital. Overall, less than 10% of patients who receive cardiopulmonary resuscitation survive after out-of-hospital CA (Figure 1). The survival rate slightly ameliorates when CA occurs inside the hospital [3,4]. The expectancy of survival depends on both extrinsic (management shortly after the event or in the hospital) and intrinsic factors (gender, age . . .).

recognised the potential of non-coding RNAs to aid in outcome prediction after cardiac arrest. In this review, we summarize recent discoveries and propose a handful of novel perspectives for the use of non-coding RNAs to predict outcome after cardiac arrest, discussing their use for precision medicine.

**Keywords:** cardiac arrest; biomarkers; non-coding RNAs



**Figure 1.** Graphic representation of the patient survival (showed as percentage) after Out-of-Hospital Cardiac Arrest (OHCA).

An important variable affecting the outcome after out-of-hospital CA (OHCA) is the application of proper and rapid cardiopulmonary resuscitation by bystanders [5,6]. The improvement of cardiopulmonary resuscitation techniques and the increased presence of automated external defibrillators in public areas are at least partly responsible for the tendency towards the better outcomes and survival rates observed in the past decades [4,7,8]. In addition, targeted temperature management at 33–36 °C has been implemented in clinical practice to protect the brain from ischemia-induced injury, but many questions about the ideal target temperature management remain unsolved [9]. As such, there is a need for new strategies to improve survival after OHCA.

Among patients who reach the hospital alive, approximately 50% survive in good condition (i.e., without major neurological sequelae [10]), whilst the other half suffer severe and irreversible neurological damage often leading to death [11], despite the use of modern, invasive, and intensive care treatment including targeted temperature management. In fact, in addition to hypothermia and early coronary reperfusion, patients in critical conditions need close monitoring of several parameters such as electrolytes and blood glucose. Mechanical ventilator supports are required to avoid hyperoxia and to ensure adequate ventilation. Pharmacological hemodynamic supports and devices are also needed in case of cardiogenic shock, mainly to improve arterial pressure and renal function. Lastly, a series of specific treatments are involved in case of other organ complications.

As mentioned above, several intrinsic factors affect the outcome after CA. For example, females are more prone to a worse outcome, which may be explained by differences in arrest circumstances, comorbidities, and in-hospital management [12]. In a large registry, men had a higher survival rate and a better neurological outcome at hospital discharge than women [13]. As for other cardiovascular diseases, survival expectancy after CA might be higher in obese patients and smokers (often called obesity and smoking paradoxes) [14–16], even though these are known risk factors triggering this cardiovascular complication. The delay between cardiac arrest and return of spontaneous circulation (ROSC), as well as the subsequent extent of brain damage, are both strongly associated with a poor outcome [17].

### 3. Prediction of Neurological Outcome after Cardiac Arrest

Being able to predict the outcome after CA would represent a breakthrough towards personalized/precision medicine. Extensive and costly treatments could be maximized to patients who are likely to survive without major neurological sequelae, and long futile care could be avoided in patients with severe and irreversible brain damage. The withdrawal of life-sustaining therapies could be adjudicated for patients with a certain poor prognosis. Importantly, patient relatives, who often experience a long and painful waiting period before being

reliably informed of the prognosis, could be guided at an early stage [18]. As stated in the 2010 European Resuscitation Guidelines for Resuscitation,

3 of 16

“a means of predicting neurological outcome that can be applied to individual patients immediately after ROSC is required” [19].

Current guidelines to predict outcome after CA recommend the combined use of neurophysiological tests, reflecting brain function, and brain-derived biomarkers released in the bloodstream after disruption of the blood-brain-barrier induced by cerebral ischemia, and hence, reflecting the extent of brain injury [20]. Clinical examination of the patient is of paramount importance for outcome prediction. The absence of normal ocular reflexes or response to pain and the presence of myoclonus during the first days after ROSC are indicators of poor prognosis. However, these markers can be attenuated or masked by sedation, making their interpretation difficult and unreliable. The absence of pupillary light and corneal reflexes on day 3 after CA has been reported to reliably predict poor outcome, with a false positive rate of 0% [21]. However, neurophysiological tests are limited by the need for specific expertise and training.

**Box 1. Main Protein biomarkers for CA prognosis: strengths and limitations.**

• **Neuron specific enolase (NSE):**

Strengths: Recognized as prognostic biomarker for CA in the guidelines of the American Heart Association [22]. Blood levels are predictors of neurological outcome in a timeline going from 24 h to 72 h after ROSC [23–26].

Limitations: Increased levels are found in other disorders, leading to patient misclassification [27–29].

Haemolysis can increase serum levels of NSE. Outcome prediction earlier than 48 h shows lack of accuracy.

• **S100 calcium-binding protein B (S100B):**

Strengths: Predicts the ongoing of cerebral injury at a very early stage after CA [30,31].

Limitations: Lacks specificity and does not add value to the current prognostication models [26].

• **TAU protein:**

Strengths: High serum levels reveal axonal dysfunction. Increased circulating levels of the protein can be detected in patients after CA with a poor neurological outcome.

Limitations: Peaks of TAU are reached at 48h and 96h after ROSC [32,33]. Few data supporting its utility as marker of severity of acute brain injury after CA [32,33].

• **Plasma neurofilament light chain (NfL)**

Strengths: Sensitive marker of long-term outcome in patients after CA, its blood levels increase significantly and remain stable for 7 days after CA [34].

Limitations: Supporting evidence comes only from small single-centre patient cohorts.

• **Procalcitonin (PCT)**

Strengths: Its circulating levels increase significantly, within 2 h, during bacterial infections. Various small-cohort studies showed the PCT potential to predict poor outcome in CA patients with high accuracy [35–37]. Limitations: Confirmed biomarker for detection of acute infections and sepsis, which can act as confounding factors [38]. Larger studies needed to support its potential value as biomarker.

Neuron-specific enolase (NSE), the only biomarker so far recommended in the guidelines [20], needs serial assessment and high values in order to optimally predict poor outcomes [17,39]. In addition, there is no consensus on the threshold to be used as a definition of a high value, with suggestions ranging between 25–85 mg L<sup>-1</sup> measured at different time points among studies [18,40]. Recently, Chung-Esaki and colleagues proposed the NSE ratio, instead of its absolute value, to track the protein changes over time after CA; however no threshold value has been identified, and future studies on larger cohorts need to be performed to validate the advantages of this method [41]. S100B is an acidic Ca<sup>2+</sup>-binding protein predominantly expressed in astroglial cells which is detected in the blood after CA and which has been reported as a potential biomarker of outcome [42,43]. Its use is limited by fluctuating levels due to peripheral injuries and to a short half-life of 25 min followed by renal

clearance [44,45]. Inflammatory and cardiac markers such as interleukin-6 [46], procalcitonin [47], brain natriuretic peptides [48] and troponins [49] are also associated with outcome, but they are limited in accuracy (See Box 1). Lactate levels are increased in patients with poor outcome [50], and secretoneurin, a small peptide with a potential role in cardiomyocyte calcium homeostasis, improved the prediction of mortality and brain injury by NSE [51]. Yet, apart from NSE, only few of these markers are applied in clinical practice to help outcome prediction.

In summary, to date, no method securely predicts outcome after CA. To be clinically useful, a prognostication method requires a very low false positive rate (5% or lower), since it is undesirable to use a method which could predict a poor outcome in a patient who would eventually recover. Therefore, novel methods or biomarkers are needed to improve prediction of outcome after CA.

## 4. Non-Coding RNAs

Here, we focus on studies reporting potential benefits of non-coding RNA biomarkers on outcome prediction after CA (Tables 1–3). The explosion of RNA knowledge in recent years has provided the tools and opportunity to explore the potential of RNA molecules as biomarkers. Much attention has been brought to RNA molecules lacking protein-coding potential following the discovery that, although 80% of human genes are effectively transcribed into RNA molecules, only less than 2% of these molecules encode proteins [52]. These so-called non-coding RNAs are a subclass of the RNA family which contains multiple types of RNAs, classified according to their sub-cellular location, function, size and protein-coding potential.

### 4.1. MicroRNAs

MicroRNAs (miRNAs) are 20–22 nucleotides-long non-coding RNA molecules involved in gene regulation. Their role in heart development and disease as well as their biomarker potential to advance personalized medicine have been extensively studied [53]. However, the study of their role in CA is still in its infancy (Table 1). In a small proof-of-concept study including 28 patients after resuscitated CA, circulating levels of miR-122-5p and miR-21 were elevated in patients with poor outcome and were associated with neurological outcome and survival [54]. It is noteworthy that miR-21 was elevated in a murine model of traumatic brain injury [55], and plasma levels of miR-122-5p were increased in a porcine cardiogenic shock model and attenuated by hypothermia [56]. Those observations in animal models supported the results of the human small scale study. Lately, 23 microRNAs involved in neurologic, circulatory, metabolic, or vascular processes were studied in 45 patients and 15 controls from the Cardiac Arrest Blood Study. The vast majority of them were upregulated in sudden cardiac arrest when compared with age-, sex- and race-matched controls [57]. Among them, miR-122-5p presented higher expression values in successfully resuscitated patients compared to dead ones [57]. It has to be taken into account that miR-122-5p expression levels (as well as other miRNAs) could be influenced by other pathologies. Thus, a study involving 239 patients who suffered sudden cardiac death (SCD) showed lower hepatic expression of miR-122-5p and higher expression of miR-34a-5p in patients whose SCD was related to coronary artery disease ( $n = 68$ ) compared with those with non coronary artery disease-related SCD ( $n = 27$ ) [58]. When patients were stratified according to the level of liver damage, miR-122-5p presented the lowest expression values in patients with necroinflammatory statohepatitis, pointing at a deficit of this miRNA in the liver if this organ is subjected to an insult [58].

In another small-scale study, circulating levels of miR-124-3p, a brain-enriched miRNA, were elevated in patients with poor outcomes compared to patients with favourable outcomes [59]. Similarly to miR-21, miR-124-3p was previously described as a biomarker for ischemic brain injury, as demonstrated in an experimental model of cerebral stroke in rats [60]. It is known that circulating miRNAs can reflect brain damage, since dying neurons release microparticles carrying miRNAs in the cerebrospinal fluid [61]. As such, miR-124-3p arises as a perfect candidate to be measured in the bloodstream because its plasma levels are elevated in a rat model with a cerebral artery occlusion despite its neuron-specific origin [62]. Indeed, some miRNAs appear to be able to cross the blood brain barrier, which is disrupted following cerebral ischemia [63], and to accumulate in the blood.

**Table 1.** Current knowledge of microRNAs in cardiac arrest or related brain disease.

ID	Specie	Disease	Experimental Model	Observation	Ref.
miR-21	Human	OHCA	—	Elevated plasma levels in patients with poor neurological outcome	[54]
	Rat	TBI	Fluid percussion injury	Elevated serum levels in rats with poor outcome	[55]
miR-34a	Human	SCD	Coronary artery and non-alcoholic fatty liver disease	Higher hepatic levels in coronary artery disease-related SCD	[58]
miR-122	Human	OHCA	—	Elevated serum levels in patients with poor neurological outcome	[54,65]
		SCA	Ventricular tachycardia-derived cardiac arrest	Elevated in plasma from patients compared to controls. Elevated in successfully resuscitated or discharged alive only versus patients died in the field.	[57]
	SCD	Coronary artery and non-alcoholic fatty liver disease	Lower hepatic levels in coronary artery disease-related SCD	[58]	
	Pig	Cardiogenic shock	LAD artery occlusion	Elevated plasma levels after injury. Attenuation by hypothermia.	[56]
miR-124	Human	OHCA	—	Elevated serum and plasma levels in patients with poor neurological outcome	[59,64]
	Rat	Ischemic brain damage	MCAO	Plasma biomarker of ischemic brain damage	[60,62]
miR-466l-3p	Mouse	Mechanical injury	Primary astrocytes	Inhibited <i>Tnfa</i> expression after stretch injury and interacted with lncRNA <i>Gm4419</i>	[66]
Other	Human	SCA	Ventricular tachycardia-derived cardiac arrest	Expression levels of plasmatic miRs were higher (n = 17) or lower (n = 3) in CA patients compared to controls. Mir-122 and miR-205 were elevated in patients successfully resuscitated versus death in the field. Lower levels of cardiac enriched microRNAs were observed in patients discharged alive versus the ones who died in the field.	[57]

CA: Cardiac Arrest; LAD: left anterior descending; MCAO: middle cerebral artery occlusion; OHCA: out-of-hospital cardiac arrest; SCA: Sudden Cardiac Arrest; SCD: Sudden Cardiac Death; TBI: traumatic brain injury.

Encouraging results from these small-scale studies motivated the testing of the association between circulating miRNAs and outcome after CA in larger cohorts. Consortium members of the Target Temperature Management (TTM)—trial (NCT01020916 [9]) investigated this association in plasma samples harvested 48h after CA from almost 600 CA patients. Using small RNA sequencing on 50 patients of the TTM cohort, miRNAs associated with neurological outcome, as assessed by the cerebral performance category score, were identified [64]. A follow-up validation study in the entire cohort revealed that among miRNA candidates, miR-124-3p was the most strongly associated with outcome. Together with demographic and clinical parameters, it was able to accurately predict neurological outcome (odds ratio of 1.62 with a 95% confidence interval of 1.13–2.32) and survival (hazard ratio of 1.63 with a 95% confidence interval of 1.37–1.93) [64]. Using the same TTM—trial cohort, miR-122-5p was able to provide an incremental predictive value to a model containing both clinical parameters and miR-124-3p, showing that combining multiple explanatory variables may increase the predictive value of miRNAs [65].

#### 4.2. Long Non-Coding RNAs

Long non-coding RNAs (lncRNAs) are defined as RNA molecules longer than 200 nucleotides and lacking protein-coding potential [67,68]. The spreading of the use of deep RNA sequencing techniques has made possible the discovery and annotation of more than 146,000 lncRNAs in human (LNCipedia 4.1 [69]). Only a minority of these lncRNAs have known roles in pathophysiology, and even fewer have been shown to regulate cardiac development and disease [70–73]. This might be due in part to the relatively low conservation of lncRNAs between species which hinders mechanistic studies in animal models. While different mechanisms of action of lncRNAs have been proposed [70,72,73], much remains to be discovered regarding their regulation and function in cardiac disease. One interesting property of lncRNAs is their ability to bind and sequester miRNAs, acting as a sponge, and thereby inhibiting the action of miRNAs on gene expression.

There are some indications pointing at the potential of lncRNAs as biomarkers of cardiovascular disease [70,72,73]. Since lncRNA expression profiles in blood cells have been shown to be associated with outcome after acute myocardial infarction [74], and considering that the aetiology of CA is often a prior acute myocardial infarction, it can be expected that lncRNAs may also be associated with outcome after CA (Table 2).

lncRNAs are expressed in the brain and are involved in neurological disease development [75], thereby constituting candidate targets for future research. As an example, it has been shown that downregulation of the lncRNA Meg3 after 2 h of occlusion of the middle cerebral artery in rats reduced the lesion volume and improved neurological outcome through the stimulation of angiogenesis mediated by the Notch signalling pathway [76]. Silencing Meg3 in a human endothelial cell line induced an activation of pro-angiogenic properties of the cells, such as cell migration, sprouting and tube formation [76]. In hypertensive rats following 1h of occlusion, upregulation of FosDT modulates brain damage via an indirect modulation of downstream genes of repressor element-1 silencing transcription factor [77]. One of the downstream pathways of this transcription factor involves nuclear factor kappa B (NFκB) which is also associated with the lncRNAs C2dat1 and Gm4419. Indeed, C2dat1 regulates calmodulin kinase to promote neuronal survival after ischemia reperfusion in mice [78], while Gm4419 contributes to NFκB activation in rat microglial cells [79]. Furthermore, Gm4419 expression levels are upregulated in injured mouse astrocytes, and scavenge miR-4661-3p, which induces tumour necrosis factor alpha (TNFα) production and apoptosis [66]. The later study revealed an interaction of three different members of the RNA family (one lncRNA, one miRNA and one lncRNA), which shows the complex regulation networks taking place in the affected brain.

**Table 2.** Current knowledge of lncRNAs in CA-related brain disease models.

ID	Specie	Disease	Experimental Model	Observation	Ref.
C2dat1	Mouse	Ischemic brain damage	MCAO	Upregulated after transient focal ischemia	[78]
FosDT	Rat	Ischemic brain damage	MCAO in spontaneous hypertensive rats	Increased after ischemic brain injury. Potentially regulated brain damage by association with key elements of the <i>Rest</i> complex, upstream of <i>NFκB</i>	[77]
Gm4419	Rat	Ischemia	OGD/R in primary microglial cells	Controlled inflammatory response through <i>NFκB</i> signaling pathway	[79]
	Mouse	Mechanical injury	Primary astrocytes	Induced after stretch injury. Upregulates <i>Tnfa</i> expression by sponging miR-4661-3p	[66]
Meg3	Human	—	HMEC-1	Downregulation of MEG3 increased angiogenesis	[76]
	Rat	Ischemic brain damage	MCAO	Downregulated after ischemic stroke. Silencing of <i>Meg3</i> improved neurological outcome.	[76]
Neat1	Mouse	TBI	Controlled cortical impact	Upregulated after injury. Absence of <i>Neat1</i> increases apoptosis around the impacted area.	[81,82]
	Mouse	Ischemia	OGD in primary new-born neurons, HT22, and BV2 lines	Upregulated under bexatorene treatment or OGD. Promoted axonal extension in primary neurons. Anti-inflammatory effect via <i>Pidd1</i> .	[81]
Other		CA-ROSC	Electrically-induced ventricular tachycardia followed by manual chest compression	Dysregulation of 58 lncRNAs and 258 mRNAs in brain cortex of rats.	[80]
	Rat	TBI	Fluid percussion injury	Upregulation of 271 lncRNAs in the hippocampus assessed by microarray, including 4 lncRNAs validated by PCR ( <i>Zfas1</i> , <i>Bsr</i> , <i>Gas5</i> , and <i>Snhg6</i> )	[83]
		Stroke	Subarachnoid haemorrhage	Microarray analysis showed 64 upregulated and 144 downregulated lncRNAs between control and haemorrhagic animals.	[84]
		TBI	Controlled cortical impact	Alteration of the expression levels of 823 lncRNAs assessed by RNA-Seq 24 h after injury.	[82]
	Mouse	Stroke	Subarachnoid haemorrhage	RNA-Seq analysis identified 103 upregulated and 514 downregulated lncRNAs between injured and control mice.	[85]

BV2: microglial cell line. CA-ROSC: Cardiac Arrest-Return to Spontaneous Circulation; HMEC-1: human microvascular endothelial cells; HT22: hippocampal neuron line MCAO: middle cerebral artery occlusion; OGD/R: oxygen and glucose deprivation/reoxygenation; PCR: Polymerase Chain Reaction; TBI: traumatic brain injury.



Maybe the best indication about the regulation of lncRNAs after CA arose from a rat model, where ventricular fibrillation was induced by alternating current. This study showed the upregulation of 37 lncRNAs and the downregulation of 21 lncRNAs in post-CA brain samples. [80]. Results from another study showed an upregulation of the lncRNA Neat1 after treatment with bexarotene (an agonist of the retinoid X receptor used in some types of cancer), thereby reducing inflammation and apoptosis [81]. This observation suggested that lncRNAs may be involved in a patient's response to treatment. However, the study was carried out in different cellular and animal models whose relevance for humans needs further exploration. In addition, other attempts using animal models aimed to reflect how brain damage can alter the transcription of lncRNAs. In traumatic brain injury models in rodents, several lncRNAs, including the well-known Neat1 and Malat1, were regulated and considered as potential players in brain injury [82,83]. In a subarachnoid haemorrhage murine model, microarrays and deep RNA sequencing allowed researchers to identify more than 200 and 600 differentially-expressed lncRNAs, respectively [84,85]. Confirmation by PCR was achieved for several lncRNAs which were found to be either upregulated (MRuc008hvl and BC0092207) or downregulated after haemorrhage (XR\_006756, MRAK017168, and MRAK038897) [84]. However, there is a lack of mechanistic studies following the discovery of the dysregulated RNAs by high throughput analysis. So, whether these lncRNAs actively contribute to brain injury or are mere bystanders remains to be determined.

In order to become useful biomarkers, lncRNAs would need to be measurable in the blood. As previously mentioned for miRNAs, the accumulation of lncRNAs in the blood will rely on their ability to cross the blood brain barrier. Whether lncRNAs have this capacity remains to be demonstrated.

### 4.3. Circular RNAs

A subclass of lncRNAs called circular RNAs (circRNAs), which are formed by a back-splicing event, showed a higher stability in body fluids compared to their linear counterparts [86,87]. Indeed, this circular form protects them from degradation by exoribonucleases, thus providing them with an interesting biomarker potential [88]. Although circRNAs have been proposed as candidate biomarkers of cardiovascular disease including heart failure [87], their presence in the blood has only been shown in blood cells [89], and whether they are able to cross the blood brain barrier remains to be determined. So far, there is no study directly linking the regulation of circRNAs with the prognosis after CA (Table 3).

Again, studies performed with animal models suggest a possible involvement of circRNAs in the underlying mechanisms of brain injury, be it ischemic or traumatic. Using a mouse model of stroke induced by occlusion of the middle cerebral artery, two microarray approaches using RNase R treated RNA identified modified circRNAs patterns in the brain. Thus, after 45 min of ischemia and 48h of reperfusion, 1027 circRNAs were differentially expressed (914 upregulated and 113 downregulated) [90]. Among the differentially expressed RNAs, circRNA\_40001, circRNA\_013120, circRNA\_25329 (upregulated), and circRNA\_40806 (downregulated) were confirmed by PCR. When the mice were submitted to 90 min of ischemia followed by 6, 21 or 24 h of reperfusion, 283 circRNAs were altered in at least one time point, and 16 of them were common to all three time-points [91]. The top three upregulated (circ\_008018, circ\_015350, and circ\_016128) and downregulated (circ\_011137, circ\_001729, and circ\_006696) circRNAs were confirmed by PCR [91].

A microarray analysis revealed 98 upregulated and 94 downregulated circRNAs in a traumatic brain injury model [92], where four of them were confirmed by PCR (circ\_006508 and circ\_010705 were up-regulated whilst circ\_001167 and circ\_001168 were down-regulated). CircRNA dysregulation was studied in exosomes from brain explants of mouse with traumatic brain injury [93]. Next generation sequencing followed by a specific bioinformatics pipeline for the analysis of circRNAs identified 155 up- and 76 down-regulated circRNAs [93]. Therefore, the circular RNA reservoir might constitute another source of interesting biomarkers of outcome after CA.



**Table 3.** Current knowledge of circRNAs in brain disease animal models.

<b>Specie</b>	<b>Disease</b>	<b>Model</b>	<b>Observation</b>	<b>Ref.</b>
Mouse	Ischemic brain damage	MCAO	Microarray analysis after RNase R treatment	[90]
			Microarray analysis after RNase R treatment	[91]
	TBI	Fluid percussion injury	RNA sequencing analysis from brain exosomes.	[93]
Rat	TBI	Fluid percussion injury	Microarray analysis using RNA from ipsilateral hippocampus after RNase R treatment	[92]

MCAO: middle cerebral artery occlusion; PCR: Polymerase Chain Reaction; TBI: traumatic brain injury.

## 5. Future Directions and Conclusions

The following points could be considered in future studies on the biomarker potential of non-coding RNAs after CA.

- Further deep RNA sequencing experiments are needed to identify the best candidates for prediction among the currently-identified 2500 human mature miRNAs, 146,000 human annotated lncRNAs and 32,000 predicted circRNAs.
- Independent validation of candidates in large patient cohorts will be the key to discovering robust and clinically-applicable biomarkers.
- Address gender specificities.
- Test the incremental predictive value of panels of non-coding RNAs using suitable correction strategies to avoid model overfitting.
- Assess the evolution of circulating levels of non-coding RNAs within the few hours/days after CA.
- Assess the influence of co-variables, such as age and target temperature, on circulating levels of non-coding RNAs.
- Define optimized protocols for blood sample collection, handling, storage and processing for RNA biomarkers assessment.
- Design molecular diagnostic assays for RNA assessment at the bedside that will allow clinically-applicable decision support systems combining biomarker assessment, neurophysiology, clinical examination, statistical analysis and risk stratification models.

Recent studies support the use of circulating miRNAs as predictors of outcome after CA. The potential of lncRNAs and circRNAs to aid in outcome prediction after CA needs to be further investigated. Using circulating, non-coding RNAs to risk stratify patients after CA would allow us to tailor healthcare to the individual patient, maximising efforts to those who would mostly benefit from aggressive therapy while avoiding therapeutic obstinacy in patients with poor prognoses. This would represent a major step forward towards precision medicine.

**Author Contributions:** A.S.-S., F.M.S. and Y.D. wrote the manuscript. P.S., H.F., D.E. and N.N. provided critical review and clinical guidance. All authors read and approved the final manuscript. All the authors are members of the Cardioline™ network ([www.cardiolinc.org/](http://www.cardiolinc.org/)).

**Funding:** This work was funded by the National Research Fund (grants # C14/BM/8225223 and C17/BM/11613033), the Ministry of Higher Education and Research, the Society for Research on Cardiovascular Diseases of Luxembourg, the Swedish Research Council and the Swedish governmental funding within the ALF-system.

**Acknowledgments:** The authors thank A.I. Lumley for proof reading the manuscript.

**Conflicts of Interest:** The authors declare no conflict of interest.

## Abbreviations

CA	Cardiac arrest
circRNAs	Circular RNAs
HUVEC	Human umbilical vein endothelial cells
LAD	Left anterior descending
lncRNA	Long non-coding RNA
MCAO	Middle cerebral artery occlusion
miRNA	MicroRNA
NFκB	Nuclear Factor kappa B
NSE	Neuron Specific Enolase
OGD/R	Oxygen and glucose deprivation/reoxygenation
OHCA	Out-of-hospital cardiac arrest
RNA	Ribonucleic acid
RNase	Ribonuclease

ROSC	Return Of Spontaneous Circulation
TBI	Traumatic brain injury
TNF	Tumor Necrosis Factor
TTM	Target Temperature Management

## References

1. Townsend, N.; Wilson, L.; Bhatnagar, P.; Wickramasinghe, K.; Rayner, M.; Nichols, M. Cardiovascular disease in Europe: Epidemiological update 2016. *Eur. Heart J.* **2016**, *37*, 3232–3245. [[CrossRef](#)] [[PubMed](#)]
2. Benjamin, E.J.; Blaha, M.J.; Chiuve, S.E.; Cushman, M.; Das, S.R.; Deo, R.; de Ferranti, S.D.; Floyd, J.; Fornage, M.; Gillespie, C.; et al. Heart Disease and Stroke Statistics-2017 Update: A Report From the American Heart Association. *Circulation* **2017**, *135*, e146–e603. [[CrossRef](#)] [[PubMed](#)]
3. Sandroni, C.; Nolan, J.; Cavallaro, F.; Antonelli, M. In-hospital cardiac arrest: Incidence, prognosis and possible measures to improve survival. *Intens. Care Med.* **2007**, *33*, 237–245. [[CrossRef](#)] [[PubMed](#)]
4. Wissenberg, M.; Lippert, F.K.; Folke, F.; Weeke, P.; Hansen, C.M.; Christensen, E.F.; Jans, H.; Hansen, P.A.; Lang-Jensen, T.; Olesen, J.B.; et al. Association of national initiatives to improve cardiac arrest management with rates of bystander intervention and patient survival after out-of-hospital cardiac arrest. *JAMA* **2013**, *310*, 1377–1384. [[CrossRef](#)] [[PubMed](#)]
5. Hasselqvist-Ax, I.; Riva, G.; Herlitz, J.; Rosenqvist, M.; Hollenberg, J.; Nordberg, P.; Ringh, M.; Jonsson, M.; Axelsson, C.; Lindqvist, J.; et al. Early cardiopulmonary resuscitation in out-of-hospital cardiac arrest. *N. Engl. J. Med.* **2015**, *372*, 2307–2315. [[CrossRef](#)] [[PubMed](#)]
6. Perkins, G.D.; Handley, A.J.; Koster, R.W.; Castren, M.; Smyth, M.A.; Olasveengen, T.; Monsieurs, K.G.; Raffay, V.; Grasner, J.T.; Wenzel, V.; et al. European Resuscitation Council Guidelines for Resuscitation 2015: Section 2. Adult basic life support and automated external defibrillation. *Resuscitation* **2015**, *95*, 81–99. [[CrossRef](#)] [[PubMed](#)]
7. Fordyce, C.B.; Hansen, C.M.; Kragholm, K.; Dupre, M.E.; Jollis, J.G.; Roettig, M.L.; Becker, L.B.; Hansen, S.M.; Hinohara, T.T.; Corbett, C.C.; et al. Association of Public Health Initiatives with Outcomes for Out-of-Hospital Cardiac Arrest at Home and in Public Locations. *JAMA Cardiol.* **2017**, *2*, 1226–1235. [[CrossRef](#)] [[PubMed](#)]
8. Larribau, R.; Deham, H.; Niquille, M.; Sarasin, F.P. Improvement of out-of-hospital cardiac arrest survival rate after implementation of the 2010 resuscitation guidelines. *PLoS ONE* **2018**, *13*, e0204169. [[CrossRef](#)] [[PubMed](#)]
9. Nielsen, N.; Wetterslev, J.; Cronberg, T.; Erlinge, D.; Gasche, Y.; Hassager, C.; Horn, J.; Hovdenes, J.; Kjaergaard, J.; Kuiper, M.; et al. Targeted temperature management at 33 °C versus 36 °C after cardiac arrest. *N. Engl. J. Med.* **2013**, *369*, 2197–2206. [[CrossRef](#)] [[PubMed](#)]
10. Moolaert, V.R.; Verbunt, J.A.; van Heugten, C.M.; Wade, D.T. Cognitive impairments in survivors of out-of-hospital cardiac arrest: A systematic review. *Resuscitation* **2009**, *80*, 297–305. [[CrossRef](#)] [[PubMed](#)]
11. Dragancea, I.; Horn, J.; Kuiper, M.; Friberg, H.; Ullen, S.; Wetterslev, J.; Cranshaw, J.; Hassager, C.; Nielsen, N.; Cronberg, T.; et al. Neurological prognostication after cardiac arrest and targeted temperature management 33 °C versus 36 °C: Results from a randomised controlled clinical trial. *Resuscitation* **2015**, *93*, 164–170. [[CrossRef](#)] [[PubMed](#)]
12. Winther-Jensen, M.; Pellis, T.; Kuiper, M.; Koopmans, M.; Hassager, C.; Nielsen, N.; Wetterslev, J.; Cronberg, T.; Erlinge, D.; Friberg, H.; et al. Mortality and neurological outcome in the elderly after target temperature management for out-of-hospital cardiac arrest. *Resuscitation* **2015**, *91*, 92–98. [[CrossRef](#)] [[PubMed](#)]
13. Karlsson, V.; Dankiewicz, J.; Nielsen, N.; Kern, K.B.; Mooney, M.R.; Riker, R.R.; Rubertsson, S.; Seder, D.B.; Stammet, P.; Sunde, K.; et al. Association of gender to outcome after out-of-hospital cardiac arrest—A report from the International Cardiac Arrest Registry. *Crit. Care* **2015**, *19*, 182. [[CrossRef](#)] [[PubMed](#)]
14. Gupta, T.; Kolte, D.; Khera, S.; Aronow, W.S.; Palaniswamy, C.; Mujib, M.; Jain, D.; Sule, S.; Ahmed, A.; Iwai, S.; et al. Relation of smoking status to outcomes after cardiopulmonary resuscitation for in-hospital cardiac arrest. *Am. J. Cardiol.* **2014**, *114*, 169–174. [[CrossRef](#)] [[PubMed](#)]
15. Gupta, T.; Kolte, D.; Mohanane, D.; Khera, S.; Goel, K.; Mondal, P.; Aronow, W.S.; Jain, D.; Cooper, H.A.; Iwai, S.; et al. Relation of Obesity to Survival After In-Hospital Cardiac Arrest. *Am. J. Cardiol.* **2016**, *118*, 662–667. [[CrossRef](#)] [[PubMed](#)]
16. Matinrazm, S.; Ladejobi, A.; Pasupula, D.K.; Javed, A.; Durrani, A.; Ahmad, S.; Munir, M.B.; Adelstein, E.; Jain, S.K.; Saba, S. Effect of body mass index on survival after sudden cardiac arrest. *Clin. Cardiol.* **2018**, *41*, 46–50. [[CrossRef](#)] [[PubMed](#)]

17. Stammet, P.; Collignon, O.; Hassager, C.; Wise, M.P.; Hovdenes, J.; Aneman, A.; Horn, J.; Devaux, Y.; Erlinge, D.; Kjaergaard, J.; et al. Neuron-Specific Enolase as a Predictor of Death or Poor Neurological Outcome After Out-of-Hospital Cardiac Arrest and Targeted Temperature Management at 33 °C and 36 °C. *J. Am. Coll. Cardiol.* **2015**, *65*, 2104–2114. [[CrossRef](#)] [[PubMed](#)]
18. Devaux, Y.; Stammet, P.; Friberg, H.; Hassager, C.; Kuiper, M.A.; Wise, M.P.; Nielsen, N.; Biomarker subcommittee of TTM trial (Target Temperature Management After Cardiac Arrest, NCT01020916). MicroRNAs: New biomarkers and therapeutic targets after cardiac arrest? *Crit. Care* **2015**, *19*, 54. [[CrossRef](#)] [[PubMed](#)]
19. Deakin, C.D.; Nolan, J.P.; Soar, J.; Sunde, K.; Koster, R.W.; Smith, G.B.; Perkins, G.D. European Resuscitation Council Guidelines for Resuscitation 2010 Section 4. Adult advanced life support. *Resuscitation* **2010**, *81*, 1305–1352. [[CrossRef](#)] [[PubMed](#)]
20. Nolan, J.P.; Soar, J.; Cariou, A.; Cronberg, T.; Moulaert, V.R.; Deakin, C.D.; Bottiger, B.W.; Friberg, H.; Sunde, K.; Sandroni, C.; et al. European Resuscitation Council and European Society of Intensive Care Medicine 2015 guidelines for post-resuscitation care. *Intens. Care Med.* **2015**, *41*, 2039–2056. [[CrossRef](#)] [[PubMed](#)]
21. Zandbergen, E.G.; Hijdra, A.; Koelman, J.H.; Hart, A.A.; Vos, P.E.; Verbeek, M.M.; de Haan, R.J.; Group, P.S. Prediction of poor outcome within the first 3 days of postanoxic coma. *Neurology* **2006**, *66*, 62–68. [[CrossRef](#)] [[PubMed](#)]
22. Nolan, J.P.; Soar, J.; Cariou, A.; Cronberg, T.; Moulaert, V.R.; Deakin, C.D.; Bottiger, B.W.; Friberg, H.; Sunde, K.; Sandroni, C. European Resuscitation Council and European Society of Intensive Care Medicine Guidelines for Post-resuscitation Care 2015: Section 5 of the European Resuscitation Council Guidelines for Resuscitation 2015. *Resuscitation* **2015**, *95*, 202–222. [[CrossRef](#)] [[PubMed](#)]
23. Storm, C.; Nee, J.; Jorres, A.; Leithner, C.; Hasper, D.; Ploner, C.J. Serial measurement of neuron specific enolase improves prognostication in cardiac arrest patients treated with hypothermia: A prospective study. *Scand. J. Trauma Resusc. Emerg. Med.* **2012**, *20*, 6. [[CrossRef](#)] [[PubMed](#)]
24. Schoerkhuber, W.; Kittler, H.; Sterz, F.; Behringer, W.; Holzer, M.; Frossard, M.; Spitzauer, S.; Laggner, A.N. Time course of serum neuron-specific enolase. A predictor of neurological outcome in patients resuscitated from cardiac arrest. *Stroke* **1999**, *30*, 1598–1603. [[CrossRef](#)] [[PubMed](#)]
25. Rech, T.H.; Vieira, S.R.; Nagel, F.; Brauner, J.S.; Scalco, R. Serum neuron-specific enolase as early predictor of outcome after in-hospital cardiac arrest: A cohort study. *Crit. Care* **2006**, *10*, R133. [[CrossRef](#)] [[PubMed](#)]
26. Rundgren, M.; Karlsson, T.; Nielsen, N.; Cronberg, T.; Johnsson, P.; Friberg, H. Neuron specific enolase and S-100B as predictors of outcome after cardiac arrest and induced hypothermia. *Resuscitation* **2009**, *80*, 784–789. [[CrossRef](#)] [[PubMed](#)]
27. Burghuber, O.C.; Worofka, B.; Scherthaner, G.; Vetter, N.; Neumann, M.; Dudczak, R.; Kuzmits, R. Serum neuron-specific enolase is a useful tumor marker for small cell lung cancer. *Cancer* **1990**, *65*, 1386–1390. [[CrossRef](#)]
28. DeGiorgio, C.M.; Gott, P.S.; Rabinowicz, A.L.; Heck, C.N.; Smith, T.D.; Correale, J.D. Neuron-specific enolase, a marker of acute neuronal injury, is increased in complex partial status epilepticus. *Epilepsia* **1996**, *37*, 606–609. [[CrossRef](#)] [[PubMed](#)]
29. Pelinka, L.E.; Jafarmadar, M.; Redl, H.; Bahrami, S. Neuron-specific-enolase is increased in plasma after hemorrhagic shock and after bilateral femur fracture without traumatic brain injury in the rat. *Shock* **2004**, *22*, 88–91. [[CrossRef](#)] [[PubMed](#)]
30. Choi, S.; Park, K.; Ryu, S.; Kang, T.; Kim, H.; Cho, S.; Oh, S. Use of S-100B, NSE, CRP and ESR to predict neurological outcomes in patients with return of spontaneous circulation and treated with hypothermia. *Emerg. Med. J.* **2016**, *33*, 690–695. [[CrossRef](#)] [[PubMed](#)]
31. Mussack, T.; Biberthaler, P.; Kanz, K.G.; Wiedemann, E.; Gippner-Steppert, C.; Mutschler, W.; Jochum, M. Serum S-100B and interleukin-8 as predictive markers for comparative neurologic outcome analysis of patients after cardiac arrest and severe traumatic brain injury. *Crit. Care Med.* **2002**, *30*, 2669–2674. [[CrossRef](#)] [[PubMed](#)]
32. Randall, J.; Mortberg, E.; Provuncher, G.K.; Fournier, D.R.; Duffy, D.C.; Rubertsson, S.; Blennow, K.; Zetterberg, H.; Wilson, D.H. Tau proteins in serum predict neurological outcome after hypoxic brain injury from cardiac arrest: Results of a pilot study. *Resuscitation* **2013**, *84*, 351–356. [[CrossRef](#)] [[PubMed](#)]
33. Mortberg, E.; Zetterberg, H.; Nordmark, J.; Blennow, K.; Catry, C.; Decraemer, H.; Vanmechelen, E.; Rubertsson, S. Plasma tau protein in comatose patients after cardiac arrest treated with therapeutic hypothermia. *Acta Anaesthesiol. Scand.* **2011**, *55*, 1132–1138. [[CrossRef](#)] [[PubMed](#)]

34. Rana, O.R.; Schroder, J.W.; Baukloh, J.K.; Saygili, E.; Mischke, K.; Schiefer, J.; Weis, J.; Marx, N.; Rassaf, T.; Kelm, M.; et al. Neurofilament light chain as an early and sensitive predictor of long-term neurological outcome in patients after cardiac arrest. *Int. J. Cardiol.* **2013**, *168*, 1322–1327. [[CrossRef](#)] [[PubMed](#)]
35. Fries, M.; Kunz, D.; Gressner, A.M.; Rossaint, R.; Kuhlen, R. Procalcitonin serum levels after out-of-hospital cardiac arrest. *Resuscitation* **2003**, *59*, 105–109. [[CrossRef](#)]
36. Stammet, P.; Devaux, Y.; Azuaje, F.; Werer, C.; Lorang, C.; Gilson, G.; Max, M. Assessment of procalcitonin to predict outcome in hypothermia-treated patients after cardiac arrest. *Crit. Care Res. Pract.* **2011**, *2011*, 631062. [[CrossRef](#)] [[PubMed](#)]
37. Hayashida, H.; Kaneko, T.; Kasaoka, S.; Oshima, C.; Miyauchi, T.; Fujita, M.; Oda, Y.; Tsuruta, R.; Maekawa, T. Comparison of the predictability of neurological outcome by serum procalcitonin and glial fibrillary acidic protein in postcardiac-arrest patients. *Neurocrit. Care* **2010**, *12*, 252–257. [[CrossRef](#)] [[PubMed](#)]
38. Assicot, M.; Gendrel, D.; Carsin, H.; Raymond, J.; Guilbaud, J.; Bohuon, C. High serum procalcitonin concentrations in patients with sepsis and infection. *Lancet* **1993**, *341*, 515–518. [[CrossRef](#)]
39. Wiberg, S.; Hassager, C.; Stammet, P.; Winther-Jensen, M.; Thomsen, J.H.; Erlinge, D.; Wanscher, M.; Nielsen, N.; Pellis, T.; Aneman, A.; et al. Single versus Serial Measurements of Neuron-Specific Enolase and Prediction of Poor Neurological Outcome in Persistently Unconscious Patients after Out-Of-Hospital Cardiac Arrest—A TTM-Trial Substudy. *PLoS ONE* **2017**, *12*, e0168894. [[CrossRef](#)] [[PubMed](#)]
40. Sandroni, C.; Cariou, A.; Cavallaro, F.; Cronberg, T.; Friberg, H.; Hoedemaekers, C.; Horn, J.; Nolan, J.P.; Rossetti, A.O.; Soar, J. Prognostication in comatose survivors of cardiac arrest: An advisory statement from the European Resuscitation Council and the European Society of Intensive Care Medicine. *Resuscitation* **2014**, *85*, 1779–1789. [[CrossRef](#)] [[PubMed](#)]
41. Chung-Esaki, H.M.; Mui, G.; Mlynash, M.; Eyngorn, I.; Catabay, K.; Hirsch, K.G. The neuron specific enolase (NSE) ratio offers benefits over absolute value thresholds in post-cardiac arrest coma prognosis. *J. Clin. Neurosci.* **2018**, *57*, 99–104. [[CrossRef](#)] [[PubMed](#)]
42. Stammet, P.; Wagner, D.R.; Gilson, G.; Devaux, Y. Modeling serum level of s100beta and bispectral index to predict outcome after cardiac arrest. *J. Am. Coll. Cardiol.* **2013**, *62*, 851–858. [[CrossRef](#)] [[PubMed](#)]
43. Stammet, P.; Dankiewicz, J.; Nielsen, N.; Fays, F.; Collignon, O.; Hassager, C.; Wanscher, M.; Uden, J.; Wetterslev, J.; Pellis, T.; et al. Protein S100 as outcome predictor after out-of-hospital cardiac arrest and targeted temperature management at 33 °C and 36 °C. *Crit. Care* **2017**, *21*, 153. [[CrossRef](#)] [[PubMed](#)]
44. Jonsson, H.; Johnsson, P.; Hoglund, P.; Alling, C.; Blomquist, S. Elimination of S100B and renal function after cardiac surgery. *J. Cardiothorac. Vasc. Anesth.* **2000**, *14*, 698–701. [[CrossRef](#)] [[PubMed](#)]
45. Bloomfield, S.M.; McKinney, J.; Smith, L.; Brisman, J. Reliability of S100B in predicting severity of central nervous system injury. *Neurocrit. Care* **2007**, *6*, 121–138. [[CrossRef](#)] [[PubMed](#)]
46. Bro-Jeppesen, J.; Kjaergaard, J.; Stammet, P.; Wise, M.P.; Hovdenes, J.; Aneman, A.; Horn, J.; Devaux, Y.; Erlinge, D.; Gasche, Y.; et al. Predictive value of interleukin-6 in post-cardiac arrest patients treated with targeted temperature management at 33 °C or 36 °C. *Resuscitation* **2016**, *98*, 1–8. [[CrossRef](#)] [[PubMed](#)]
47. Dankiewicz, J.; Nielsen, N.; Linder, A.; Kuiper, M.; Wise, M.P.; Cronberg, T.; Erlinge, D.; Gasche, Y.; Harmon, M.B.; Hassager, C.; et al. Infectious complications after out-of-hospital cardiac arrest—A comparison between two target temperatures. *Resuscitation* **2017**, *113*, 70–76. [[CrossRef](#)] [[PubMed](#)]
48. Frydland, M.; Kjaergaard, J.; Erlinge, D.; Stammet, P.; Nielsen, N.; Wanscher, M.; Pellis, T.; Friberg, H.; Hovdenes, J.; Horn, J.; et al. Usefulness of Serum B-Type Natriuretic Peptide Levels in Comatose Patients Resuscitated from Out-of-Hospital Cardiac Arrest to Predict Outcome. *Am. J. Cardiol.* **2016**, *118*, 998–1005. [[CrossRef](#)] [[PubMed](#)]
49. Gilje, P.; Koul, S.; Thomsen, J.H.; Devaux, Y.; Friberg, H.; Kuiper, M.; Horn, J.; Nielsen, N.; Pellis, T.; Stammet, P.; et al. High-sensitivity troponin-T as a prognostic marker after out-of-hospital cardiac arrest—A targeted temperature management (TTM) trial substudy. *Resuscitation* **2016**, *107*, 156–161. [[CrossRef](#)] [[PubMed](#)]
50. Frydland, M.; Kjaergaard, J.; Erlinge, D.; Wanscher, M.; Nielsen, N.; Pellis, T.; Aneman, A.; Friberg, H.; Hovdenes, J.; Horn, J.; et al. Target temperature management of 33 °C and 36 °C in patients with out-of-hospital cardiac arrest with initial non-shockable rhythm—A TTM sub-study. *Resuscitation* **2015**, *89*, 142–148. [[CrossRef](#)] [[PubMed](#)]
51. Hasslacher, J.; Lehner, G.F.; Harler, U.; Beer, R.; Ulmer, H.; Kirchmair, R.; Fischer-Colbrie, R.; Bellmann, R.; Duzendorfer, S.; Joannidis, M. Secretoneurin as a marker for hypoxic brain injury after cardiopulmonary resuscitation. *Intens. Care Med.* **2014**, *40*, 1518–1527. [[CrossRef](#)] [[PubMed](#)]

52. Consortium, E.P. An integrated encyclopedia of DNA elements in the human genome. *Nature* **2012**, *489*, 57–74. [[CrossRef](#)] [[PubMed](#)]
53. Goretti, E.; Wagner, D.R.; Devaux, Y. miRNAs as biomarkers of myocardial infarction: A step forward towards personalized medicine? *Trends Mol. Med.* **2014**, *20*, 716–725. [[CrossRef](#)] [[PubMed](#)]
54. Stammet, P.; Goretti, E.; Vausort, M.; Zhang, L.; Wagner, D.R.; Devaux, Y. Circulating microRNAs after cardiac arrest. *Crit. Care Med.* **2012**, *40*, 3209–3214. [[CrossRef](#)] [[PubMed](#)]
55. Lei, P.; Li, Y.; Chen, X.; Yang, S.; Zhang, J. Microarray based analysis of microRNA expression in rat cerebral cortex after traumatic brain injury. *Brain Res.* **2009**, *1284*, 191–201. [[CrossRef](#)] [[PubMed](#)]
56. Andersson, P.; Gidlof, O.; Braun, O.O.; Gotberg, M.; van der Pals, J.; Olde, B.; Erlinge, D. Plasma levels of liver-specific miR-122 is massively increased in a porcine cardiogenic shock model and attenuated by hypothermia. *Shock* **2012**, *37*, 234–238. [[CrossRef](#)] [[PubMed](#)]
57. Wander, P.L.; Enquobahrie, D.A.; Pritchard, C.C.; McKnight, B.; Rice, K.; Christiansen, M.; Lemaitre, R.N.; Rea, T.; Siscovick, D.; Sotoodehnia, N. Circulating microRNAs and sudden cardiac arrest outcomes. *Resuscitation* **2016**, *106*, 96–101. [[CrossRef](#)] [[PubMed](#)]
58. Braza-Boils, A.; Mari-Alexandre, J.; Molina, P.; Arnau, M.A.; Barcelo-Molina, M.; Domingo, D.; Girbes, J.; Giner, J.; Martinez-Dolz, L.; Zorio, E. Deregulated hepatic microRNAs underlie the association between non-alcoholic fatty liver disease and coronary artery disease. *Liver Int.* **2016**, *36*, 1221–1229. [[CrossRef](#)] [[PubMed](#)]
59. Gilje, P.; Gidlof, O.; Rundgren, M.; Cronberg, T.; Al-Mashat, M.; Olde, B.; Friberg, H.; Erlinge, D. The brain-enriched microRNA miR-124 in plasma predicts neurological outcome after cardiac arrest. *Crit. Care* **2014**, *18*, R40. [[CrossRef](#)] [[PubMed](#)]
60. Laterza, O.F.; Lim, L.; Garrett-Engele, P.W.; Vlasakova, K.; Muniappa, N.; Tanaka, W.K.; Johnson, J.M.; Sina, J.F.; Fare, T.L.; Sistare, F.D.; et al. Plasma MicroRNAs as sensitive and specific biomarkers of tissue injury. *Clin. Chem.* **2009**, *55*, 1977–1983. [[CrossRef](#)] [[PubMed](#)]
61. Patz, S.; Trattnig, C.; Grunbacher, G.; Ebner, B.; Gully, C.; Novak, A.; Rinner, B.; Leitinger, G.; Absenger, M.; Tomescu, O.A.; et al. More than cell dust: Microparticles isolated from cerebrospinal fluid of brain injured patients are messengers carrying mRNAs, miRNAs, and proteins. *J. Neurotrauma* **2013**, *30*, 1232–1242. [[CrossRef](#)] [[PubMed](#)]
62. Weng, H.; Shen, C.; Hirokawa, G.; Ji, X.; Takahashi, R.; Shimada, K.; Kishimoto, C.; Iwai, N. Plasma miR-124 as a biomarker for cerebral infarction. *Biomed. Res.* **2011**, *32*, 135–141. [[CrossRef](#)] [[PubMed](#)]
63. Rink, C.; Khanna, S. MicroRNA in ischemic stroke etiology and pathology. *Physiol. Genom.* **2011**, *43*, 521–528. [[CrossRef](#)] [[PubMed](#)]
64. Devaux, Y.; Dankiewicz, J.; Salgado-Somoza, A.; Stammet, P.; Collignon, O.; Gilje, P.; Gidlof, O.; Zhang, L.; Vausort, M.; Hassager, C.; et al. Association of Circulating MicroRNA-124-3p Levels With Outcomes After Out-of-Hospital Cardiac Arrest: A Substudy of a Randomized Clinical Trial. *JAMA Cardiol.* **2016**, *1*, 305–313. [[CrossRef](#)] [[PubMed](#)]
65. Devaux, Y.; Salgado-Somoza, A.; Dankiewicz, J.; Boileau, A.; Stammet, P.; Schritz, A.; Zhang, L.; Vausort, M.; Gilje, P.; Erlinge, D.; et al. Incremental Value of Circulating MiR-122-5p to Predict Outcome after Out of Hospital Cardiac Arrest. *Theranostics* **2017**, *7*, 2555–2564. [[CrossRef](#)] [[PubMed](#)]
66. Yu, Y.; Cao, F.; Ran, Q.; Wang, F. Long non-coding RNA Gm4419 promotes trauma-induced astrocyte apoptosis by targeting tumor necrosis factor alpha. *Biochem. Biophys. Res. Commun.* **2017**, *491*, 478–485. [[CrossRef](#)] [[PubMed](#)]
67. Mercer, T.R.; Dinger, M.E.; Mattick, J.S. Long non-coding RNAs: Insights into functions. *Nat. Rev. Genet.* **2009**, *10*, 155–159. [[CrossRef](#)] [[PubMed](#)]
68. Ponting, C.P.; Oliver, P.L.; Reik, W. Evolution and functions of long noncoding RNAs. *Cell* **2009**, *136*, 629–641. [[CrossRef](#)] [[PubMed](#)]
69. Volders, P.J.; Verheggen, K.; Menschaert, G.; Vandepoele, K.; Martens, L.; Vandesompele, J.; Mestdagh, P. An update on LNCipedia: A database for annotated human lncRNA sequences. *Nucleic Acids Res.* **2015**, *43*, D174–D180. [[CrossRef](#)] [[PubMed](#)]
70. Devaux, Y.; Zangrando, J.; Schroen, B.; Creemers, E.E.; Pedrazzini, T.; Chang, C.P.; Dorn, G.W., 2nd; Thum, T.; Heymans, S.; Cardioline, N. Long noncoding RNAs in cardiac development and ageing. *Nat. Rev. Cardiol.* **2015**, *12*, 415–425. [[CrossRef](#)] [[PubMed](#)]



71. Beermann, J.; Piccoli, M.T.; Viereck, J.; Thum, T. Non-coding RNAs in Development and Disease: Background, Mechanisms, and Therapeutic Approaches. *Physiol. Rev.* **2016**, *96*, 1297–1325. [[CrossRef](#)] [[PubMed](#)]
72. Gomes, C.P.C.; Spencer, H.; Ford, K.L.; Michel, L.Y.M.; Baker, A.H.; Emanuelli, C.; Balligand, J.L.; Devaux, Y.; Cardiolinc, N. The Function and Therapeutic Potential of Long Non-coding RNAs in Cardiovascular Development and Disease. *Mol. Therapy Nucleic Acids* **2017**, *8*, 494–507. [[CrossRef](#)] [[PubMed](#)]
73. Greco, S.; Salgado Somoza, A.; Devaux, Y.; Martelli, F. Long Noncoding RNAs and Cardiac Disease. *Antioxid. Redox Signal.* **2017**. [[CrossRef](#)] [[PubMed](#)]
74. Vausort, M.; Wagner, D.R.; Devaux, Y. Long noncoding RNAs in patients with acute myocardial infarction. *Circul. Res.* **2014**, *115*, 668–677. [[CrossRef](#)] [[PubMed](#)]
75. Chen, Y.; Zhou, J. LncRNAs: Macromolecules with big roles in neurobiology and neurological diseases. *Metab. Brain Dis.* **2017**, *32*, 281–291. [[CrossRef](#)] [[PubMed](#)]
76. Liu, J.; Li, Q.; Zhang, K.S.; Hu, B.; Niu, X.; Zhou, S.M.; Li, S.G.; Luo, Y.P.; Wang, Y.; Deng, Z.F. Downregulation of the Long Non-Coding RNA Meg3 Promotes Angiogenesis After Ischemic Brain Injury by Activating Notch Signaling. *Mol. Neurobiol.* **2017**, *54*, 8179–8190. [[CrossRef](#)] [[PubMed](#)]
77. Mehta, S.L.; Kim, T.; Vemuganti, R. Long Noncoding RNA FosDT Promotes Ischemic Brain Injury by Interacting with REST-Associated Chromatin-Modifying Proteins. *J. Neurosci.* **2015**, *35*, 16443–16449. [[CrossRef](#)] [[PubMed](#)]
78. Xu, Q.; Deng, F.; Xing, Z.; Wu, Z.; Cen, B.; Xu, S.; Zhao, Z.; Nepomuceno, R.; Bhuiyan, M.I.; Sun, D.; et al. Long non-coding RNA C2dat1 regulates CaMKII $\delta$  expression to promote neuronal survival through the NF $\kappa$ B signaling pathway following cerebral ischemia. *Cell Death Dis.* **2016**, *7*, e2173. [[CrossRef](#)] [[PubMed](#)]
79. Wen, Y.; Yu, Y.; Fu, X. LncRNA Gm4419 contributes to OGD/R injury of cerebral microglial cells via I $\kappa$ B phosphorylation and NF $\kappa$ B activation. *Biochem. Biophys. Res. Commun.* **2017**, *487*, 923–929. [[CrossRef](#)] [[PubMed](#)]
80. Liu, R.; Liao, X.; Li, X.; Wei, H.; Liang, Q.; Zhang, Z.; Yin, M.; Zeng, X.; Liang, Z.; Hu, C. Expression profiles of long noncoding RNAs and mRNAs in post-cardiac arrest rat brains. *Mol. Med. Rep.* **2018**, *17*, 6413–6424. [[CrossRef](#)] [[PubMed](#)]
81. Zhong, J.; Jiang, L.; Huang, Z.; Zhang, H.; Cheng, C.; Liu, H.; He, J.; Wu, J.; Darwazeh, R.; Wu, Y.; et al. The long non-coding RNA Neat1 is an important mediator of the therapeutic effect of bexarotene on traumatic brain injury in mice. *Brain Behav. Immun.* **2017**, *65*, 183–194. [[CrossRef](#)] [[PubMed](#)]
82. Zhong, J.; Jiang, L.; Cheng, C.; Huang, Z.; Zhang, H.; Liu, H.; He, J.; Cao, F.; Peng, J.; Jiang, Y.; et al. Altered expression of long non-coding RNA and mRNA in mouse cortex after traumatic brain injury. *Brain Res.* **2016**, *1646*, 589–600. [[CrossRef](#)] [[PubMed](#)]
83. Wang, C.F.; Zhao, C.C.; Weng, W.J.; Lei, J.; Lin, Y.; Mao, Q.; Gao, G.Y.; Feng, J.F.; Jiang, J.Y. Alteration in Long Non-Coding RNA Expression after Traumatic Brain Injury in Rats. *J. Neurotrauma* **2017**, *34*, 2100–2108. [[CrossRef](#)] [[PubMed](#)]
84. Zheng, B.; Liu, H.; Wang, R.; Xu, S.; Liu, Y.; Wang, K.; Hou, X.; Shen, C.; Wu, J.; Chen, X.; et al. Expression signatures of long non-coding RNAs in early brain injury following experimental subarachnoid hemorrhage. *Mol. Med. Rep.* **2015**, *12*, 967–973. [[CrossRef](#)] [[PubMed](#)]
85. Peng, J.; Wu, Y.; Tian, X.; Pang, J.; Kuai, L.; Cao, F.; Qin, X.; Zhong, J.; Li, X.; Li, Y.; et al. High-Throughput Sequencing and Co-Expression Network Analysis of lncRNAs and mRNAs in Early Brain Injury Following Experimental Subarachnoid Haemorrhage. *Sci. Rep.* **2017**, *7*, 46577. [[CrossRef](#)] [[PubMed](#)]
86. Memczak, S.; Papavasileiou, P.; Peters, O.; Rajewsky, N. Identification and Characterization of Circular RNAs As a New Class of Putative Biomarkers in Human Blood. *PLoS ONE* **2015**, *10*, e0141214. [[CrossRef](#)] [[PubMed](#)]
87. Devaux, Y.; Creemers, E.E.; Boon, R.A.; Werfel, S.; Thum, T.; Engelhardt, S.; Dimmeler, S.; Squire, I.; Cardiolinc, n. Circular RNAs in heart failure. *Eur. J. Heart Fail.* **2017**, *19*, 701–709. [[CrossRef](#)] [[PubMed](#)]
88. Suzuki, H.; Zuo, Y.; Wang, J.; Zhang, M.Q.; Malhotra, A.; Mayeda, A. Characterization of RNase R-digested cellular RNA source that consists of lariat and circular RNAs from pre-mRNA splicing. *Nucleic Acids Res.* **2006**, *34*, e63. [[CrossRef](#)] [[PubMed](#)]
89. Vausort, M.; Salgado-Somoza, A.; Zhang, L.; Leszek, P.; Scholz, M.; Teren, A.; Burkhardt, R.; Thiery, J.; Wagner, D.R.; Devaux, Y. Myocardial Infarction-Associated Circular RNA Predicting Left Ventricular Dysfunction. *J. Am. Coll. Cardiol.* **2016**, *68*, 1247–1248. [[CrossRef](#)] [[PubMed](#)]
90. Liu, C.; Zhang, C.; Yang, J.; Geng, X.; Du, H.; Ji, X.; Zhao, H. Screening circular RNA expression patterns following focal cerebral ischemia in mice. *Oncotarget* **2017**, *8*, 86535–86547. [[CrossRef](#)] [[PubMed](#)]

91. Mehta, S.L.; Pandi, G.; Vemuganti, R. Circular RNA Expression Profiles Alter Significantly in Mouse Brain After Transient Focal Ischemia. *Stroke* **2017**, *48*, 2541–2548. [[CrossRef](#)] [[PubMed](#)]
92. Xie, B.; Wang, Y.; Lin, Y.; Zhao, C.C.; Mao, Q.; Feng, J.F.; Cao, J.; Gao, G.Y.; Jiang, J. Circular RNA Expression Profiles Alter Significantly After Traumatic Brain Injury in Rats. *J. Neurotrauma* **2018**. [[CrossRef](#)] [[PubMed](#)]
93. Zhao, R.; Zhou, J.; Dong, X.; Bi, C.; Jiang, R.; Dong, J.; Tian, Y.; Yuan, H.; Zhang, J.N. Circular RNA expression alteration in exosomes from the brain extracellular space after traumatic brain injury in mice. *J. Neurotrauma* **2018**. [[CrossRef](#)] [[PubMed](#)]



© 2018 by the authors. Licensee MDPI, Basel, Switzerland. This article is an open access article distributed under the terms and conditions of the Creative Commons Attribution (CC BY) license (<http://creativecommons.org/licenses/by/4.0/>).



# Appendix II



Article

## Circulating Levels of Brain-Enriched MicroRNAs Correlate with Neuron Specific Enolase after Cardiac Arrest—A Substudy of the Target Temperature Management Trial

†

Francesca Maria Stefanizzi <sup>1</sup>, Niklas Nielsen <sup>2</sup>, Lu Zhang <sup>1</sup>, Josef Dankiewicz <sup>3</sup>, Pascal Stammet <sup>4</sup>, Patrik Gilje <sup>3</sup>, David Erlinge <sup>3</sup>, Christian Hassager <sup>5</sup>, Matthew P. Wise <sup>6</sup>, Michael Kuiper <sup>7</sup>, Hans Friberg <sup>8</sup>, Yvan Devaux <sup>1,\*</sup> and Antonio Salgado-Somoza <sup>1</sup>

<sup>1</sup> Cardiovascular Research Unit, Department of Population Health, Luxembourg Institute of Health, L-1445 Strassen, Luxembourg; francescamaria.stefanizzi@lih.lu (F.M.S.); lu.zhang@lih.lu (L.Z.); antonio.salgadosomoza@lih.lu (A.S.-S.)

<sup>2</sup> Department of Anesthesia and Intensive Care, Clinical Sciences, Lund University and Helsingborg Hospital, SE-25187 Lund, Sweden; niklas.nielsen@med.lu.se

<sup>3</sup> Department of Cardiology, Clinical Sciences, Lund University and Skane University Hospital, SE-221 85 Lund, Sweden; josef.dankiewicz@gmail.com (J.D.); patrik.gilje@med.lu.se (P.G.); david.erlinge@gmail.com (D.E.)

<sup>4</sup> Medical and Health Department, National Fire and Rescue Corps, L-2557 Luxembourg, Luxembourg; pascal.stammet@secours.etat.lu

<sup>5</sup> Department of Cardiology B, The Heart Centre, Rigshospitalet University Hospital, 2100 Copenhagen, Denmark; christian.hassager@regionh.dk

<sup>6</sup> Department of Intensive Care, University Hospital of Wales, Cardiff CF144XW, UK; mattwise@doctors.org.uk

<sup>7</sup> Department of Intensive Care, Leeuwarden Medical Centrum, 8934 Leeuwarden, The Netherlands; mi.kuiper@wxs.nl

<sup>8</sup> Department of Anesthesia and Intensive Care, Clinical Sciences, Lund University and Skane University Hospital, SE-221 85 Lund, Sweden; hans.a.friberg@gmail.com

\* Correspondence: yvan.devaux@lih.lu; Tel.: +352-26970300

† TTM-trial investigators and on behalf of the EU-CardioRNA COST Action CA174129.



Received: 14 May 2020; Accepted: 17 June 2020; Published: 19 June 2020

**Abstract:** Outcome prognostication after cardiac arrest (CA) is challenging. Current multimodal prediction approaches would benefit from new biomarkers. MicroRNAs constitute a novel class of disease markers and circulating levels of brain-enriched ones have been associated with outcome after CA. To determine whether these levels reflect the extent of brain damage in CA patients, we assessed their correlation with neuron-specific enolase (NSE), a marker of brain damage. Blood samples taken 48 h after return of spontaneous circulation from two groups of patients from the Targeted Temperature Management trial were used. Patients were grouped depending on their neurological outcome at six months. Circulating levels of microRNAs were assessed by sequencing. NSE was measured at the same time-point. Among the 673 microRNAs detected, brain-enriched miR9-3p, miR124-3p and miR129-5p positively correlated with NSE levels (all  $p < 0.001$ ). Interestingly, these correlations were absent when only the good outcome group was analyzed ( $p > 0.5$ ). Moreover, these correlations were unaffected by demographic and clinical characteristics. All three microRNAs predicted neurological outcome at 6 months. Circulating levels of brain-enriched microRNAs are correlated with NSE levels and hence can reflect the extent of brain injury in patients after CA. This observation strengthens the potential of brain-enriched microRNAs to aid in outcome prognostication after CA.

**Keywords:** microRNAs; biomarker; prognostic; cardiac arrest; neurological function

---

## 1. Introduction

Cardiac arrest (CA) is the third leading cause of death in industrialised countries. Prediction of neurological outcome of comatose patients after CA is fundamental for optimal treatment for each patient. Currently, multimodal approaches are recommended to prognosticate outcome in these patients [1]. These strategies and their associated predictive models include several tests such as brain computed tomography, electroencephalogram, somatosensory-evoked potentials, pupil light reflex and the measurement of serum neuron-specific enolase (NSE) [2].

NSE has been widely studied as a prognostic biomarker after CA [3], as it is easily detectable and independent from the effect of sedatives [4]. However, the use of this protein biomarker has a number of limitations. First, it is accepted as marker of other non-brain diseases such as small cell lung cancer, renal cell carcinoma and several other syndromes [5], thus, increasing the risk of false positives results. Second, the lack of standardised protocol for assaying NSE levels [6,7] prevents the use of a single threshold for outcome prediction. Third, since this protein is released from the brain into the bloodstream after injury, the permeability of the brain blood barrier—variable across a spectrum of brain injury—affects the circulating levels of NSE reflecting the extent of brain damage [8], resulting in a lower sensitivity of NSE. Therefore, there is a need to discover new biomarkers to be combined with existing prognostication strategies [9].

MicroRNAs (miRNAs—short single stranded non coding RNAs) are increasingly recognised as potential disease markers. They can be found in different body fluids circulating either freely, bound to proteins, or packaged into microvesicles where they are protected against RNase degradation [10,11]. It is noteworthy, miRNAs can be released at an earlier stage than proteins during a pathological process and their expression levels are easily detectable using different techniques such as quantitative PCR, microarrays and high-throughput sequencing, with high specificity and sensitivity [12]. We and others have reported the potential of miRNAs, such as brain-enriched miR-124-3p, to aid in outcome prognostication after out of hospital cardiac arrest [13,14]. Combined approaches using several miRNAs appeared to provide an incremental predictive value [15]. Although it has been reported that the brain blood barrier is disrupted within the first 24 h after return of spontaneous circulation after cardiac arrest [16], allowing the release of miRNAs from the brain into the blood, it is still unclear whether circulating levels of miRNAs reflect the extent of brain damage. This is a prerequisite to the value of miRNAs as prognostic biomarkers after cardiac arrest.

To address this, we tested a potential correlation circulating levels of miRNAs and NSE measured 48 h after return of spontaneous circulation (ROSC).

## 2. Results

Two groups of 25 cardiac arrest patients with either a good (CPC 1) or a poor (CPC 5) neurological outcome at 6 months were enrolled in this study. Each group had an equal percentage of males and females (84% and 16%, respectively). Patients with a poor neurological outcome were older, had more frequent arrhythmias, a longer time from cardiac arrest to ROSC, higher levels of brain natriuretic peptide, creatinine, procalcitonin, S100 and NSE (Table 1).

Small RNA sequencing was performed in plasma samples drawn 48 h after ROSC. An average of 18.5 million reads per sample was obtained. Data are available at the Gene Expression Omnibus under the reference GSE74198. After filtering out miRNAs expressed with less than five counts in less than 12 samples of at least one of the two groups of patients, a total of 673 miRNAs remained and were considered for subsequent analysis. We investigated the correlations between these miRNAs and demographic and clinical variables including age and sex, comorbidities, arrest conditions and laboratory measurements (i.e., all variables contained in Table 1), first in the entire group of 50 patients, and then separately in the good and poor outcome groups. A threshold of 0.6 was used to select significant correlations between miRNAs and continuous clinical variables, and an adjusted *p*-value below 0.05 was used for categorical variables.

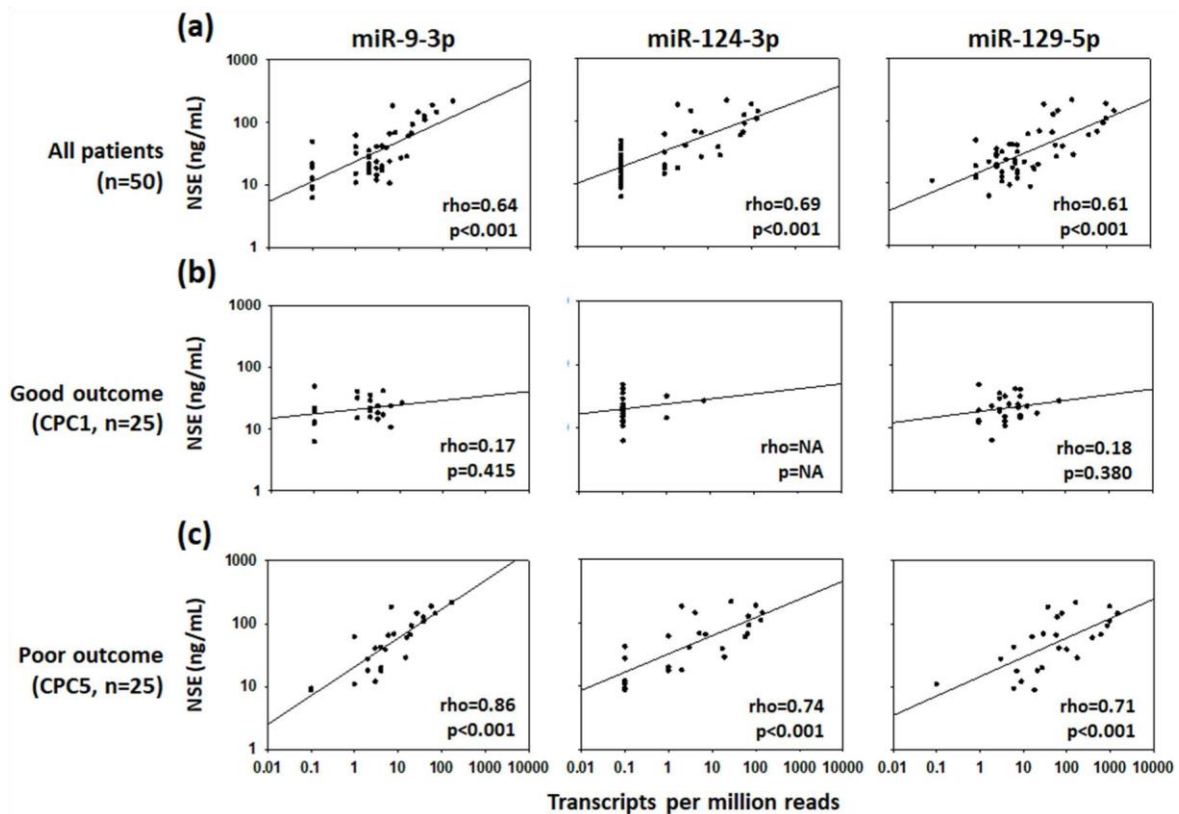
**Table 1.** Demographic and clinical characteristics of the study population.

Characteristic	ALL (n = 50)	Good (n = 25)	Poor (n = 25)	p-Value
<b>Age</b>	<b>63 (59–74)</b>	<b>62 (59–69)</b>	<b>70 (60–80)</b>	<b>0.039</b>
Sex	41 (82%)	21 (84%)	21 (84%)	1
COMORBIDITIES				
Arterial hypertension	21 (42%)	10 (40%)	11 (44%)	1
Chronic heart failure	3 (6%)	1 (4%)	2 (8%)	1
Diabetes	3 (6%)	1 (4%)	2 (8%)	1
Ischemic heart disease	11 (22%)	3 (12%)	8 (32%)	0.17
Transient ischemic attack or stroke	4 (8%)	2 (8%)	2 (8%)	1
Asthma or chronic obstructive pulmonary disease	5 (10%)	1 (4%)	4 (16%)	0.35
<b>Previous arrhythmia</b>	<b>11 (22%)</b>	<b>2 (8%)</b>	<b>9 (36%)</b>	<b>0.04</b>
Previous myocardial infarction	8 (16%)	2 (8%)	6 (24%)	0.25
ARREST CONDITIONS				
Bystander witnessed arrest	41 (82%)	22 (88%)	19 (76%)	0.46
Bystander cardiopulmonary resuscitation	37 (74%)	19 (76%)	18 (72%)	1
<b>Time from CA to ROSC (minutes)</b>	<b>22 (19–30)</b>	<b>20 (17–22)</b>	<b>30 (22–37)</b>	<b>0.001</b>
Shock on admission	8 (16%)	3 (12%)	5 (20%)	0.7
ST segment elevation myocardial infarction	29 (58%)	16 (64%)	13 (52%)	0.57
Shockable rhythm	46 (92%)	25 (100%)	21 (84%)	0.11
First monitored rhythm	44 (88%)	24 (96%)	20 (80%)	0.19
LABORATORY MEASUREMENTS				
pH	7.25 (7.15–7.32)	7.29 (7.18–7.33)	7.21 (7.13–7.29)	0.221
Lactate (mmol/L)	4.9 (2.9–8.7)	4.8 (3.1–7.2)	5 (2.9–9.5)	0.992
<b>Brain natriuretic peptide (NT-proBNP, pg/mL)</b>	<b>1856 (946–2932)</b>	<b>1327 (407–1872)</b>	<b>2324 (1494–4009)</b>	<b>0.005</b>
Copeptin (pmol/L)	48.74 (25.4–112.87)	53.43 (27.43–119.73)	31.63 (23.63–82.95)	0.491
<b>Creatinine (mg/dL)</b>	<b>0.99 (0.82–1.47)</b>	<b>0.9 (0.71–1.08)</b>	<b>1.33 (0.89–1.55)</b>	<b>0.007</b>
C-reactive protein (µg/mL)	143 (102–201)	142 (115–192)	144 (100–205)	0.961
Interleukin 6 (pg/mL)	166 (74–337)	120 (73–295)	196 (77–545)	0.332
<b>Neuron specific enolase (ng/mL)</b>	<b>27 (17–57)</b>	<b>20 (15–29)</b>	<b>60 (20–110)</b>	<b>0.003</b>
Procalcitonin (µg/L)	<b>1.11 (0.4–3.61)</b>	<b>0.64 (0.34–1.38)</b>	<b>3 (0.57–5.27)</b>	<b>0.015</b>
<b>S100 (S100A1B and S100BB, µg/L)</b>	<b>0.12 (0.07–0.21)</b>	<b>0.09 (0.07–0.14)</b>	<b>0.16 (0.1–0.26)</b>	<b>0.035</b>

Median (range) or number (percentage) are shown for continuous and categorical variables, respectively. Laboratory measurements were performed at 48 h after return of spontaneous circulation (ROSC) except for pH and lactate, which were measured at admission. Comparisons between good and poor outcome have been performed using the Wilcoxon signed-rank test for continuous variables or the Fisher exact test for categorical variables. *p*-values < 0.05 are considered significant and are in bold. CA: cardiac arrest; ROSC; return of spontaneous circulation.

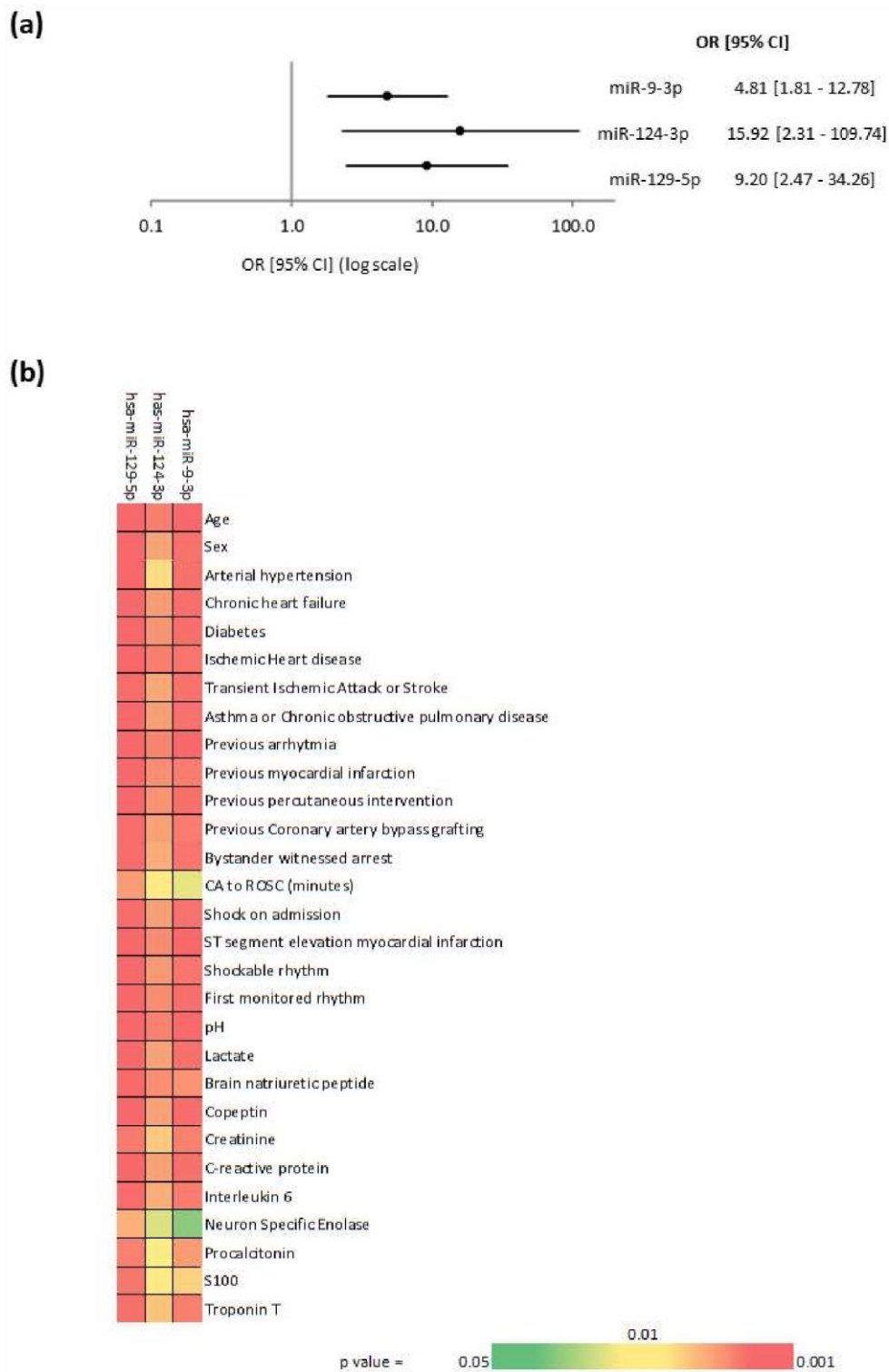
In all patients, a positive correlation was found between the expression levels of three miRNAs (miR9-3p, miR124-3p and miR129-5p) and NSE measurements at 48 h after ROSC with correlation coefficients of 0.64, 0.69 and 0.61, respectively (Figure 1a). Among the 673 detected miRNAs, these three miRNAs were the only ones correlated with NSE with a correlation coefficient above 0.6. When the neurological outcome at 6 months was taken into account, the correlation coefficients between the three miRNAs and NSE were far below 0.60 in the good outcome group (Figure 1b). Notably, in the poor outcome group, the correlations between the three miRNAs and NSE were even stronger than in all patients, reaching correlation coefficients of 0.86 for miR9-3p, 0.74 for miR124-3p and 0.71 for miR129-5p (all with *p* < 0.001; Figure 1c).

In addition, miR124-3p and miR129-5p were correlated with the time from cardiac arrest to ROSC in the poor outcome group ( $\rho = 0.66$ ,  $p = 3 \times 10^{-4}$ ;  $\rho = 0.67$ ,  $p = 3 \times 10^{-4}$ ; respectively). In the good outcome group, miR124-3p was detectable only in four patients with a number of reads ranging from one to seven compared to the CPC 5 group where the number of reads raised until 140 per patient in a total of 19 patients. Also in the good outcome, miR129-5p was not correlated with the time from cardiac arrest to ROSC ( $\rho = -0.04$ ,  $p = 0.863$ ). MiR9-3p was not correlated with the time from cardiac arrest to ROSC, either in the poor outcome group ( $\rho = 0.53$ ,  $p = 0.006$ ) or in the good outcome group ( $\rho = -0.19$ ,  $p = 0.355$ ). Remarkably, no significant correlation was found between the three miRNAs and the comorbidities shown in Table 1, either in the fifty patients or in the separate outcome groups (all adjusted *p*-values above 0.05).



**Figure 1.** Correlations between miRNAs and neuron-specific enolase (NSE). Scatter plot and linear regression lines show the correlation between NSE and levels of miR9-3p, miR124-3p, and miR129-5p, (a) measured 48 h after ROSC in 50 patients, (b) 25 patients with good neurological outcome (CPC 1) and (c) 25 patients with poor neurological outcome or died (CPC 5) at 6 months after cardiac arrest. Spearman correlation coefficients ( $\rho$ ) and  $p$ -values are indicated. NA = Not applicable as only few patients have miRNA values above the level of detection.

Logistic regression was subsequently used to address a possible association between the three miRNAs and neurological outcome of the 50 patients, as determined by 6-month CPC. All three miRNAs were univariate predictors of neurological outcome (Figure 2a). This prediction was maintained (all  $p < 0.05$ ) after adjustment with demographic and clinical variables (Figure 2b).



**Figure 2.** Association between miRNAs and neurological outcome. The association between levels of miR9-3p, miR124-3p and miR129-5p measured 48 h after ROSC in 50 patients and neurological outcome as attested by CPC score (1 vs. 5) at 6 months after cardiac arrest was addressed using univariate and multivariate logistic regression. **(a)** Forest plot with univariate odds ratios (OR)  $\pm$  95% confidence intervals (CI) for the prediction of neurological outcome. **(b)** Heat-map representing the statistical significance of multivariate logistic regression models containing one miRNA and one demographic or clinical variable. The coloured scale is as follows:  $p = 0.001$  (red) and  $p = 0.05$  (green),  $p = 0.01$  being used as a middle point for the colour gradient. All values represented had a  $p$ -value below 0.05, and  $p$ -values below 0.001 were displayed as the maximum intensity of red.

### 3. Discussion

This study was designed to address the correlation between circulating miRNAs and brain-injury in patients after cardiac arrest. We report strong correlations between the circulating levels of three brain-enriched miRNAs—miR9-3p, miR124-3p and miR129-5p—and NSE, suggesting that these miRNAs might reflect the extent of brain damage. In addition, these miRNAs were associated with neurological outcome and survival at 6 months. These observations support the value of brain-enriched miRNAs to aid in outcome prediction after cardiac arrest.

The correlation between miRNAs and NSE was only observed in patients with poor neurological outcome, i.e., in patients with severe brain injury. This observation strengthens the assumption that circulating levels of brain-enriched miRNAs reflect the extent of brain damage. The absence of significant correlation between miRNAs and comorbidities suggests that levels of miRNAs are not affected by the studied comorbidities, supporting a clinically relevant prognostic value, as shown in logistic regression analyses.

When adjusting with NSE in multivariate analyses, the statistical significance of each predictive model including miRNAs was reduced, especially for miR9-3p which was very close to the threshold for significance ( $p = 0.040$ ), consistently with the strong correlation with NSE observed in Figure 1. Similarly, the prediction capacity of the miRNAs was reduced after adjustment with the time from cardiac arrest to ROSC, strengthening the correlation between circulating levels of miRNAs and brain damage. However, the adjustment did not cancel the predictive capacity of miRNAs, which supports an added predictive value of miRNAs to existing predictive variables and biomarkers in multimodal approaches, as previously reported [13,15].

MiR9-3p, miR124-3p and miR129-5p are involved in different physiological and/or pathological processes such as brain development, differentiation, plasticity and cancer [17–21]. Hence, their presence— or increased levels—in the blood after cardiac arrest most probably mirrors the disruption of the blood brain barrier and cellular dysfunction or death in the brain after cardiac arrest.

This short study has some limitations. The number of patients enrolled was limited to a subset of 50 patients selected from the Targeted Temperature Management (TTM) cohort who were enrolled in a short RNA sequencing experiment. This low patients' number prevented adjusting for all demographic and clinical variables simultaneously in multivariate analysis, hence dampening the statistical power of the study. To avoid model overfitting, we conducted sequential adjustments with only one variable at a time. MiRNAs were measured in plasma samples while NSE was measured in the serum. However, miRNA levels are comparable in serum and plasma in these patients. The correlation between miRNAs and brain damage was assessed at a single time-point, 48 h after ROSC, which was chosen for consistency with previous studies [13,15,22] and because NSE reaches maximal levels at this time-point and achieves the highest prognostic value [3]. Some patients with comorbidities may have died from other causes than brain injury which might impact the correlation between miRNAs and NSE. Angiography was performed in 66% of the studied patients at the discretion of the physician. An association between severe coronary stenosis and mortality cannot be ruled out. Lastly, the 50 patients enrolled in this study were treated at 33 °C and it would be interesting to address the correlation with NSE in patients treated at 36 °C, although NSE has not been shown to be significantly affected by target temperature [3].

### 4. Materials and Methods

#### 4.1. Patients

A subgroup of patients from the Targeted Temperature Management trial (TTM-trial) was used in the present study. Detailed information about the TTM-trial's design, recruitment, protocol and results has been published elsewhere [23,24]. The trial is registered at [www.clinicaltrials.gov](http://www.clinicaltrials.gov) (NCT01020916) and was approved by ethical committees of the different participating countries. Informed consent was waived or obtained from each participant or relatives, according to the legislation in each country and in line with the declaration of Helsinki. The primary end-point of the TTM-trial was survival until end of trial and the main secondary outcome was neurological outcome at 6 months after cardiac arrest, as defined by the cerebral performance category (CPC) score. Patients with 6-month CPC scores of 1 or 2 were considered as having a good neurological outcome and patients with 6-month CPC scores of 3 to 5 were considered as having a poor neurological outcome [25].



For the present study, we considered a subset of fifty patients that exhibited either a good (CPC 1) or a poor neurological outcome or died (CPC 5) within the 6 months after cardiac arrest (25 patients per group). These two groups of patients have been used in a previous study and had similar demographic and clinical features than the entire TTM cohort [13]. The fifty patients received targeted therapeutic treatment at 33 °C.

#### 4.2. Small RNA Sequencing

Small RNA sequencing was performed in the groups of 25 patients at Exiqon Services following in-house protocols. Detailed methods have been previously published [13]. Briefly, total RNA was extracted from 400 µL of plasma obtained 48 h after ROSC, digested with proteinase K, checked for quality, and used to prepare sequencing libraries. Libraries were subjected to single-end sequencing of 50 nucleotide fragments on the NextSeq 500 Illumina platform. Sequencing reads were mapped to miRBase version 20 containing 1871 human precursor sequences and 2772 human mature miRNAs [26]. Sequencing data were filtered, considering only miRNAs expressed with more than 5 counts in at least 12 samples of at least one of the outcome groups. MiRNA levels are expressed as number of transcripts per million reads.

#### 4.3. Neuron-Specific Enolase

Measurements of NSE levels in serum samples obtained 48 h after ROSC have been conducted six months after completion of the trial in a core laboratory of the Centre Hospitalier de Luxembourg. Haemolysis was assessed and all samples had a haemolysis index below 500 ng/mL of haemoglobin. NSE levels were determined using a COBAS e601 apparatus with an Electro-Chemi-Luminescent-Immuno-Assay kit from Roche Diagnostics (Rotkreuz, Switzerland). The measuring range was 0.05–370 ng/mL and samples above the upper limit were diluted and reassessed. Assay sensitivity was 0.25 ng/mL and normal values were <17.0 ng/mL.

#### 4.4. Statistical Analysis

Correlation analyses were performed using Spearman correlation for continuous variables and logistic regression for categorical variables. For continuous variables, a correlation coefficient below or above 0.6 was used as threshold for significance. For categorical variables, an adjusted *p*-value (Benjamini-Hochberg step-up false discovery rate) below 0.05 was used for statistical significance. For univariate and multivariate analyses, missing values were imputed using the R package MICE with 10 imputations. All skewed continuous variables were log<sub>2</sub> transformed and scaled. Logistic regression was used to estimate the predictive value of the independent variables for neurological outcome. Univariate models were generated with each miRNA candidate. Multivariate models were generated with one miRNA and one clinical parameter at a time. The models were generated using the *lrm* function of the *rms* R package.

### 5. Conclusions

In conclusion, circulating levels of brain-enriched miRNAs are associated with NSE levels and hence reflect the extent of brain injury in patients after cardiac arrest. This observation strengthens the potential of brain-enriched miRNAs to aid in outcome prognostication after cardiac arrest.

**Author Contributions:** Conceptualization, F.M.S., N.N., L.Z., J.D., P.S., P.G., D.E., C.H., M.P.W., M.K., H.F., Y.D., and A.S.-S.; software and analysis, F.M.S., L.Z., and A.S.-S.; resources, N.N., D.E., and Y.D.; data curation, L.Z., Y.D., and A.S.-S.; writing—original draft preparation, F.M.S., Y.D., and A.S.-S.; writing—review and editing, all authors; visualization, F.M.S. and A.S.-S.; supervision, N.N., Y.D., and A.S.-S.; project administration, P.S., P.G., D.E., and Y.D.; funding acquisition, N.N., D.E., Y.D.; All authors have read and agreed to the published version of the manuscript.

**Funding:** This research was supported by COST (European Cooperation in Science and Technology) Action EU-CardioRNA CA17129. F.M.S., Y.D. and A.S.S. are funded by the National Research Fund (grants # C14/BM/8225223 and C17/BM/11613033), the Ministry of Higher Education and Research, and the Heart Foundation—Daniel Wagner of Luxembourg.

**Acknowledgments:** We thank all the patients, their relatives and all staff from the recruitment sites involved in the biomarker studies.

**Conflicts of Interest:** The authors declare no conflict of interest.



## Abbreviations

CA	Cardiac arrest
CI	Confidence intervals
CPC	Cerebral Performance Category
miRNAs	MicroRNAs
NSE	Neuron-specific enolase
OR	Odds ratio
ROSC	Return of spontaneous circulation
TTM	Targeted Temperature Management trial

## References

1. Kim, J.H.; Kim, M.J.; You, J.S.; Lee, H.S.; Park, Y.S.; Park, I.; Chung, S.P. Multimodal approach for neurologic prognostication of out-of-hospital cardiac arrest patients undergoing targeted temperature management. *Resuscitation* **2019**, *134*, 33–40. [[CrossRef](#)] [[PubMed](#)]
2. Sandroni, C.; Cariou, A.; Cavallaro, F.; Cronberg, T.; Friberg, H.; Hoedemaekers, C.; Horn, J.; Nolan, J.P.; Rossetti, A.O.; Soar, J. Prognostication in comatose survivors of cardiac arrest: An advisory statement from the European Resuscitation Council and the European Society of Intensive Care Medicine. *Intensive Care Med.* **2014**, *40*, 1816–1831. [[CrossRef](#)] [[PubMed](#)]
3. Stammet, P.; Collignon, O.; Hassager, C.; Wise, M.P.; Hovdenes, J.; Åneman, A.; Horn, J.; Devaux, Y.; Erlinge, D.; Kjaergaard, J.; et al. Neuron-specific enolase as a predictor of death or poor neurological outcome after out-of-hospital cardiac arrest and targeted temperature management at 33 °C and 36 °C. *J. Am. Coll. Cardiol.* **2015**, *65*, 2104–2114. [[CrossRef](#)] [[PubMed](#)]
4. Samaniego, E.A.; Mlynash, M.; Caulfield, A.F.; Eyngorn, I.; Wijman, C.A. Sedation confounds outcome prediction in cardiac arrest survivors treated with hypothermia. *Neurocrit. Care* **2011**, *15*, 113–119. [[CrossRef](#)]
5. Isgro, M.A.; Bottoni, P.; Scatena, R. Neuron-specific enolase as a biomarker: Biochemical and clinical aspects. *Adv. Exp. Med. Biol.* **2015**, *867*, 125–143.
6. Mlynash, M.; Buckwalter, M.S.; Okada, A.; Caulfield, A.F.; Venkatasubramanian, C.; Eyngorn, I.; Verbeek, M.M.; Wijman, C.A. Serum neuron-specific enolase levels from the same patients differ between laboratories: Assessment of a prospective post-cardiac arrest cohort. *Neurocrit. Care* **2013**, *19*, 161–166. [[CrossRef](#)]
7. Rundgren, M.; Cronberg, T.; Friberg, H.; Isaksson, A. Serum neuron specific enolase-impact of storage and measuring method. *BMC Res. Notes* **2014**, *7*, 726. [[CrossRef](#)]
8. Marchi, N.; Rasmussen, P.; Kapural, M.; Fazio, V.; Kight, K.; Mayberg, M.R.; Kanner, A.; Ayumar, B.; Albensi, B.; Cavaglia, M.; et al. Peripheral markers of brain damage and blood-brain barrier dysfunction. *Restor. Neurol. Neurosci.* **2003**, *21*, 109–121.
9. Devaux, Y.; Stammet, P.; Cardioline, N. What's new in prognostication after cardiac arrest: microRNAs? *Intensive Care Med.* **2018**, *44*, 897–899. [[CrossRef](#)]
10. Izzotti, A.; Longobardi, M.; La Maestra, S.; Micalè, R.T.; Pulliero, A.; Camoirano, A.; Geretto, M.; D'Agostini, F.; Balansky, R.; Miller, M.S.; et al. Release of microRNAs into body fluids from ten organs of mice exposed to cigarette smoke. *Theranostics* **2018**, *8*, 2147–2160. [[CrossRef](#)]
11. de Gonzalo-Calvo, D.; Iglesias-Gutierrez, E.; Llorente-Cortes, V. Epigenetic biomarkers and cardiovascular disease: Circulating microRNAs. *Rev. Esp. Cardiol. (Engl. Ed.)* **2017**, *70*, 763–769. [[CrossRef](#)] [[PubMed](#)]
12. Kim, Y.K. Extracellular microRNAs as biomarkers in human disease. *Chonnam Med. J.* **2015**, *51*, 51–57. [[CrossRef](#)] [[PubMed](#)]
13. Devaux, Y.; Dankiewicz, J.; Salgado-Somoza, A.; Stammet, P.; Collignon, O.; Gilje, P.; Gidlof, O.; Zhang, L.; Vausort, M.; Hassager, C.; et al. Association of circulating microRNA-124-3p levels with outcomes after out-of-hospital cardiac arrest: A substudy of a randomized clinical trial. *JAMA Cardiol.* **2016**, *1*, 305–313. [[CrossRef](#)] [[PubMed](#)]
14. Gilje, P.; Gidlof, O.; Rundgren, M.; Cronberg, T.; Al-Mashat, M.; Olde, B.; Friberg, H.; Erlinge, D. The brain-enriched microRNA miR-124 in plasma predicts neurological outcome after cardiac arrest. *Crit. Care* **2014**, *18*, R40. [[CrossRef](#)]

15. Devaux, Y.; Salgado-Somoza, A.; Dankiewicz, J.; Boileau, A.; Stammet, P.; Schritz, A.; Zhang, L.; Vausort, M.; Gilje, P.; Erlinge, D.; et al. Incremental value of circulating mir-122-5p to predict outcome after out of hospital cardiac arrest. *Theranostics* **2017**, *7*, 2555–2564. [[CrossRef](#)]
16. Park, J.S.; You, Y.; Min, J.H.; Yoo, I.; Jeong, W.; Cho, Y.; Ryu, S.; Lee, J.; Kim, S.W.; Cho, S.U.; et al. Study on the timing of severe blood-brain barrier disruption using cerebrospinal fluid-serum albumin quotient in post cardiac arrest patients treated with targeted temperature management. *Resuscitation* **2019**, *135*, 118–123. [[CrossRef](#)]
17. Ma, Q.; Zhang, L.; Pearce, W.J. MicroRNAs in brain development and cerebrovascular pathophysiology. *Am. J. Physiol. Cell Physiol.* **2019**, *317*, C3–C19. [[CrossRef](#)]
18. Sim, S.E.; Lim, C.S.; Kim, J.I.; Seo, D.; Chun, H.; Yu, N.K.; Lee, J.; Kang, S.J.; Ko, H.G.; Choi, J.H.; et al. The brain-enriched microRNA mir-9-3p regulates synaptic plasticity and memory. *J. Neurosci.* **2016**, *36*, 8641–8652. [[CrossRef](#)]
19. Zeng, A.; Yin, J.; Li, Y.; Li, R.; Wang, Z.; Zhou, X.; Jin, X.; Shen, F.; Yan, W.; You, Y. MiR-129-5p targets Wnt5a to block PKC/ERK/NF-kappaB and JNK pathways in glioblastoma. *Cell Death Dis.* **2018**, *9*, 394. [[CrossRef](#)]
20. Wu, C.; Zhang, X.; Chen, P.; Ruan, X.; Liu, W.; Li, Y.; Sun, C.; Hou, L.; Yin, B.; Qiang, B.; et al. MicroRNA-129 modulates neuronal migration by targeting Fmr1 in the developing mouse cortex. *Cell Death Dis.* **2019**, *10*, 287. [[CrossRef](#)]
21. Rajman, M.; Metge, F.; Fiore, R.; Khudayberdiev, S.; Aksoy-Aksel, A.; Bicker, S.; Ruedell Reschke, C.; Raoof, R.; Brennan, G.P.; Delanty, N.; et al. A microRNA-129-5p/Rbfox crosstalk coordinates homeostatic downscaling of excitatory synapses. *EMBO J.* **2017**, *36*, 1770–1787. [[CrossRef](#)] [[PubMed](#)]
22. Stammet, P.; Goretti, E.; Vausort, M.; Zhang, L.; Wagner, D.R.; Devaux, Y. Circulating microRNAs after cardiac arrest. *Crit. Care Med.* **2012**, *40*, 3209–3214. [[CrossRef](#)] [[PubMed](#)]
23. Nielsen, N.; Wetterslev, J.; Al-Subaie, N.; Andersson, B.; Bro-Jeppesen, J.; Bishop, G.; Brunetti, I.; Cranshaw, J.; Cronberg, T.; Edqvist, K.; et al. Target temperature management after out-of-hospital cardiac arrest—A randomized, parallel-group, assessor-blinded clinical trial—rationale and design. *Am. Heart J.* **2012**, *163*, 541–548. [[CrossRef](#)]
24. Nielsen, N.; Wetterslev, J.; Cronberg, T.; Erlinge, D.; Gasche, Y.; Hassager, C.; Horn, J.; Hovdenes, J.; Kjaergaard, J.; Kuiper, M.; et al. Targeted temperature management at 33 degrees C versus 36 degrees C after cardiac arrest. *N. Engl. J. Med.* **2013**, *369*, 2197–2206. [[CrossRef](#)] [[PubMed](#)]
25. Jennett, B.; Bond, M. Assessment of outcome after severe brain damage: A practical scale. *Lancet* **1975**, *305*, 480–484. [[CrossRef](#)]
26. Kozomara, A.; Griffiths-Jones, S. MiRBase: Integrating microRNA annotation and deep-sequencing data. *Nucleic Acids Res.* **2011**, *39*, D152–D157. [[CrossRef](#)] [[PubMed](#)]



© 2020 by the authors. Licensee MDPI, Basel, Switzerland. This article is an open access article distributed under the terms and conditions of the Creative Commons Attribution (CC BY) license (<http://creativecommons.org/licenses/by/4.0/>).

# Appendix III

## Circular RNAs to predict clinical outcome after cardiac arrest

Francesca M. Stefanizzi MSc<sup>a</sup>, Lu Zhang MSc<sup>a</sup>, Antonio Salgado-Somoza PhD<sup>a</sup>, Josef Dankiewicz MD, PhD<sup>b</sup>, Pascal Stammet MD, PhD<sup>c</sup>, Christian Hassager MD-DMSc<sup>d</sup>, Matthew P. Wise MD, DPhil<sup>e</sup>, Hans Friberg MD, PhD<sup>f</sup>, Tobias Cronberg MD, PhD<sup>g</sup>, Alexander Hundt PhD<sup>h</sup>, Jesper Kjaergaard MD-DMSc, PhD<sup>d</sup>, Niklas Nielsen MD, PhD<sup>i</sup>, Yvan Devaux PhD<sup>a</sup>

<sup>a</sup> Cardiovascular Research Unit, Department of Population Health, Luxembourg Institute of Health, Strassen, Luxembourg.

<sup>b</sup> Department of Cardiology, Clinical Sciences, Lund University and Skane University Hospital, Lund SE-221 85, Sweden.

<sup>c</sup> Department of Intensive Care Medicine, Centre Hospitalier de Luxembourg, Luxembourg L-1210, Luxembourg and Department of Life Sciences and Medicine, Faculty of Science, Technology and Medicine, University of Luxembourg, Esch-sur-Alzette L-4365, Luxembourg

<sup>d</sup> Department of Cardiology B, The Heart Centre, Rigshospitalet University Hospital, Copenhagen 2100, Denmark.

<sup>e</sup> Department of Intensive Care, University Hospital of Wales, Cardiff CF14 4XW, United Kingdom.

<sup>f</sup> Department of Anesthesia and Intensive Care, Clinical Sciences, Lund University and Skane University Hospital, Malmö SE-221 85, Sweden.

<sup>g</sup> Department of Neurology and Rehabilitation Medicine, Clinical Sciences, Lund University and Skane University Hospital, Lund SE-221 85, Sweden.

<sup>h</sup> Integrated BioBank of Luxembourg, Luxembourg Institute of Health, Dudelange, Luxembourg.

<sup>i</sup> Department of Anesthesia and Intensive Care, Clinical Sciences, Lund University and Helsingborg Hospital, Lund SE-25187, Sweden.

### Address for correspondence

Yvan Devaux, Cardiovascular Research Unit, Luxembourg Institute of Health, 1A-B rue Edison, L-1445 Strassen, Luxembourg. Tel: +352 26970300. Fax: +352 26970396. Email: [yvan.devaux@lih.lu](mailto:yvan.devaux@lih.lu)

### Abstract

**Background:** Cardiac arrest (CA) represents the third leading cause of death worldwide. Among patients resuscitated and admitted to hospital, death and severe neurological sequelae are frequent but difficult to predict. Blood biomarkers offer clinicians the potential to improve prognostication. Previous studies suggest that circulating non-coding RNAs constitute a reservoir of novel biomarkers. Therefore, this study aims to identify circulating circular RNAs (circRNAs) associated with clinical outcome after CA.

**Results:** Whole blood samples obtained 48h after return of spontaneous circulation in 588 survivors from CA enrolled in the Target Temperature Management trial (TTM) were used in this study. Whole transcriptome RNA sequencing in 2 groups of 23 sex-matched patients identified 28 circRNAs associated with neurological outcome and survival. The circRNA circNFAT5 was selected for further analysis using quantitative PCR. In the TTM-trial (n=542), circNFAT5 was upregulated in patients with poor outcome as compared to patients with good neurological outcome ( $p < 0.001$ ). This increase was independent of TTM regimen and sex. The adjusted odds-ratio of circNFAT5 to predict neurological outcome was 1.39 [1.07-1.83] (OR [95% confidence interval]). CircNFAT5 predicted 6-month survival with an adjusted hazard ratio of 1.31 [1.13-1.52].

**Conclusion:** We identified circulating circRNAs associated with clinical outcome after CA, among which circNFAT5 may have potential to aid in predicting neurological outcome and survival when used in combination with established biomarkers of OHCA.

## Keywords

Out-of-hospital cardiac arrest, biomarkers, prognostication, circular RNAs.

## Abbreviations

AIC	Akaike information criterion
CA	Cardiac arrest
cDNA	Complementary DNA
CI	confidence interval
circNFAT5	Circular NFAT5
circRNA	Circular RNA
COPD	Chronic obstructive pulmonary disease
CPC	Cerebral performance category
CPR	Cardiopulmonary resuscitation
HR	Hazard ratio
IBBL	Integrated Biobank of Luxembourg
IDI	Integrated discrimination improvement index
LRT	Likelihood-ratio test
mRS	modified Rankin Score
ncRNA	Non-coding RNA
NFL	Neurofilament light chain
NRI	Net reclassification improvement
NSE	Neuron-specific enolase
OHCA	Out of hospital cardiac arrest
OR	Odd ratio
PEA	Pulseless electrical activity
qPCR	Quantitative PCR
RNA-seq	RNA sequencing
ROSC	Return of spontaneous circulation
RT	Reverse transcription
TTM	Target temperature management trial
VF	Ventricular fibrillation
VT	Ventricular tachycardia

## Introduction

Cardiac arrest (CA) remains one of the major public health burdens worldwide, causing up to 20% of deaths in Europe [1]. Furthermore, among comatose patients admitted to the intensive care unit on average only 40-50% survive to hospital discharge [2]. Therefore, being able to

predict the outcome of these patients would aid in delivering personalized medicine, focusing on prioritization of resources and informing relatives at an earlier stage.

Current guidelines recommend the use of multiple prognostic approaches that combine neurophysiological tests, neuroimaging and biomarker assessment to predict the outcome of patients after CA [3-5]. The majority of the current biomarkers are brain-enriched markers released in the bloodstream after disruption of the blood-brain barrier such as neuron specific enolase (NSE) [6-8], neurofilament light chain (Nfl) [9] and S100 [10, 11]. Although the predictive value of these biomarkers has been reported in several studies [10-12] they do not seem to be accurate enough, as some of them may reflect other clinical disorders independent of CA [13-15]. Therefore, the identification of new biomarkers with additional prognostic power to be used in combination with the already established predictive modalities could improve the prognostication of CA patients.

Given the ubiquitous roles revealed in both physiological and pathological conditions, RNAs are emerging as promising biomarker candidates [16, 17]. Particularly a class of non-coding RNAs (ncRNAs), called circular RNAs (circRNAs), seem to represent the optimal intrinsic characteristics to function as biomarkers [18]. CircRNAs present a closed loop-ended structure, which originates from backsplicing [19]. This structure makes this class of RNA particularly stable when compared to any other class of linear RNAs, as they are resistant to exonuclease degradation [20]. Typically, circRNAs are more than 200 nucleotides long and lack a 5'-terminal cap and 3'-terminal poly A tail [19-21]. They also show a high cell type and tissue specificity and are abundantly expressed in numerous evolutionarily-conserved human genes [22]. In addition, circRNAs are widely distributed in body fluids, where biomarkers can easily be detected. The study of this class of RNAs is still in its infancy; however, it is becoming clear that they are relevant during disease initiation and progression [23, 24] and present some potential as disease biomarkers [25-27]. Furthermore, the stability, specificity, and abundant

expression in body fluids of circRNAs make them particularly advantageous as biomarkers to be assessed by minimally invasive and low-cost methodologies such as quantitative PCR (qPCR) [28].

The current work represents a substudy of the Target Temperature Management after out-of-hospital cardiac arrest trial, whose purpose was to evaluate the beneficial effect of two different targeted temperature regimens on the outcome of patients after OHCA, 33°C versus 36°C [29, 30]. Here, we report the potential biomarker value of a circulating circRNA, hsa\_circ\_0006845 (named herein circNFAT5), in OHCA prognostication.

## Methods

See online supplement for additional methods.

### Patients

The TTM-trial enrolled 950 unconscious adults admitted at the intensive care unit after OHCA of presumed cardiac cause. The recruitment occurred between November 11, 2010 and January 10, 2013 in 10 countries. The trial compared the effects of two targeted temperature regimens (33°C and 36°C) on survival until the end of the trial and 6-month neurological outcome. Neurological outcome was assessed with the Cerebral Performance Category (CPC) score and the modified Rankin Scale (mRS). A good neurological outcome was defined as patients with none or mild to moderate neurological damage (CPC1-2 or mRS 0-3), while a poor outcome was defined as patients with severe neurological damage, comatose or dead (CPC3-5 or mRS 4-6).

Informed consent was waived and obtained from each patient or relatives in line with the declaration of Helsinki and the legislation of each of the participating countries. The TTM-trial



is registered at [www.clinicaltrials.gov](http://www.clinicaltrials.gov) (NCT01020916). The details of the design, protocol, statistical analyses and results of the trial have been discussed elsewhere [29, 31, 32].

Whole blood samples were collected in PAXgene™ Blood RNA tubes (PreAnalytiX, cat n. 762165) 48h after return of spontaneous circulation (ROSC). Following collection, the samples were stored at the Integrated Biobank of Luxembourg (IBBL) in compliance with the International Society for Biological and Environmental Repositories Best Practices. RNA extractions were performed and quantified using accredited methods (ISO 17025:2005). Each recruiting center in the trial decided independently whether or not to participate in the biobank study. Among the patients recruited, PAXgene™ Blood RNA samples 48h after ROSC were available for 643 patients and RNA samples for 588 patients (Supplemental Figure 1).

### Statistical analyses

Sigma Plot software (version 12.5) was used to perform statistical analyses. The T-test and Mann-Whitney U test were used to measure the differential expression levels of circNFAT5 according to the neurological outcome, targeted temperature regimen or sex. Chi-squared test or Fisher's exact test were used to compare the categorical characteristics of TTM patients according to their neurological outcome (good vs. poor outcome). Mann-Whitney U test was used for continuous variables.

The neurological outcome of patients was assessed 6 months after OHCA. Patients were dichotomised as good or poor neurological outcome according to the CPC score and mRS score.

From 588 TTM patients used in this study, two sex-matched groups of 23 patients, one group with CPC1 and one with CPC5, were selected in the discovery phase for whole transcriptome RNA-seq. CircRNAs having differential expression profiles with  $p < 0.05$  and  $\log_2$  fold change  $> 0.5$  or  $< -0.5$  between the good (CPC 1) and bad (CPC 5) outcome groups were selected for further validation. A logistic regression analysis assessed the association of circNFAT5 levels

with 6-month neurological outcome while Kaplan-Meier survival curves and Cox proportional hazards models estimated the association between circNFAT5 and 6-month survival.

In the logistic regression analysis, patients were dichotomized in two groups, according to their CPC score and mRS score. Patients with a CPC 1-2 or mRS 0-3 were considered as having a good neurological outcome. Patients with a CPC 3-5 or mRS 4-6 belonged to the group with a poor neurological outcome. Both univariate and multivariable logistic regression analyses were performed. In multivariable analyses, the same clinical covariates used in previous publications [6, 33, 34] were considered: age, sex, first monitored rhythm, bystander cardiopulmonary resuscitation (CPR), circulatory shock on admission, targeted temperature regimen, time from CA to ROSC, initial serum lactate levels and NSE levels. Missing data were imputed using missForest R package (<https://doi.org/10.1093/bioinformatics/btr597>). Forest plots showing the odds ratios (OR) with 95% confidence interval (CI) were generated. The Akaike Information Criterion (AIC) and Hosmer & Lemeshow test were used to estimate the goodness of fit for the models. The lower AIC value, the better model fit. The Likelihood Ratio Test (LRT) was used to compare models. The net reclassification improvement (NRI) and the integrated discrimination improvement (IDI) were computed to evaluate the ability of circNFAT5 to reclassify patients misclassified by a clinical model. These analyses were performed using R version 4.0.3 with the following packages: ROCR, Hmisc, rms, lmtree, matrixStats and glmtoolbox.

Cox proportional hazards regression models were used in survival analyses. We calculated the Harrell's C-index (the concordance index) to evaluate the univariate and multivariable Cox models. We estimated the goodness of fit of the Cox models with AIC and Grønnesby & Borgan test. We compared different Cox models using LRT. The survival analysis was performed using survival, survMisc and lmtree R packages. Kaplan-Meier curves were generated for circNFAT5 using the Youden index at the cut-off value of 0.55.

## Results

### Study flow chart

RNA extracts from whole blood samples collected in PAXgene RNA tubes and obtained 48h after ROSC from a total of 588 patients from the TTM-trial were used in the present study (Supplemental Figure 1). We first conducted a discovery phase using RNA-seq in two sex-matched groups of 23 patients from the TTM-trial. The first 2 groups of 23 patients with sufficient RNA for RNA-seq and qPCR validation were selected. The first group consisted of patients who survived and recovered without neurological sequelae at 6 months after OHCA (CPC 1), while the second group included patients who died (CPC 5) (Supplemental Figure 1). Demographics and clinical characteristics of these 46 patients can be found in table 1.

**Table 1. Demographic and clinical characteristics of the discovery cohort.**

Characteristics	Neurological outcome		p-value
	CPC1 (n=23)	CPC5 (n=23)	
Age, years	61 (41 - 80)	74 (53- 90)	<b>0.002</b>
Sex			1
Male	20 (87 %)	19 (82.6 %)	
Female	3 (13 %)	4 (17.4 %)	
<b>Co-morbidities</b>			
Hypertension	7 (30.4 %)	11 (47.8 %)	0.19
Diabetes mellitus	2 (8.7 %)	5 (21.7 %)	1
Known IHD	3 (13 %)	12 (52.2 %)	0.093
Previous MI	2 (8.7 %)	9 (39.1 %)	0.502
Heart failure	1 (4.3 %)	2 (8.7 %)	1
COPD	1 (4.3 %)	4 (17.4 %)	0.174
Previous cerebral stroke	1 (4.3 %)	3 (13 %)	1
<b>First monitored rhythm</b>			0.865
VF or non-perfusing VT	22 (95.7 %)	18 (78.3 %)	
Asystole or PEA	1 (4.3 %)	4 (17.4 %)	
ROSC after bystander defibrillation	-	1 (4.3 %)	
<b>Witnessed arrest</b>	20 (87 %)	20 (87 %)	0.356
<b>Bystander CPR</b>	16 (69.6 %)	17 (74 %)	0.318

<b>Time from CA to ROSC, min</b>	20 (8 - 45)	29 (11 - 65)	<b>0.02</b>
<b>Initial serum lactate (mmol/l)</b>	3.2 (0 - 17)	4.7 (0 - 16)	0.244
<b>NSE 48h after ROSC (ng/ml)</b>	15 (6.6 - 49.2)	62.1 (8.8 - 291.2)	<b>&lt;0.001</b>
<b>Shock on admission</b>	2 (8.7 %)	8 (34.8 %)	0.111

Demographic and clinical characteristics of two groups of 23 TTM patients in the RNA-seq study according to neurological outcome established with CPC score. Continuous variables are indicated as median (range), while categorical characteristics are reported as number (frequency). A p-value<0.05 was considered as statistically significant (in bold). Abbreviations: COPD = chronic obstructive pulmonary disease; CPR = cardio-pulmonary resuscitation; PEA = pulseless electric activity; VF = ventricular fibrillation; VT= ventricular tachycardia; NSE= Neuron specific enolase.

The remaining 542 TTM patients were used in a validation phase with measurement of candidate circRNA by quantitative PCR. Therefore, in the validation phase 256 patients with CPC 3-5 and 253 patients with mRS 4-6 showed a poor neurological outcome 6 months after OHCA, while 286 with CPC 1-2 and 289 with mRS 0-3 had a good outcome (Supplemental figure 1).

#### Discovery phase: selection of circRNA candidates from RNA-seq data

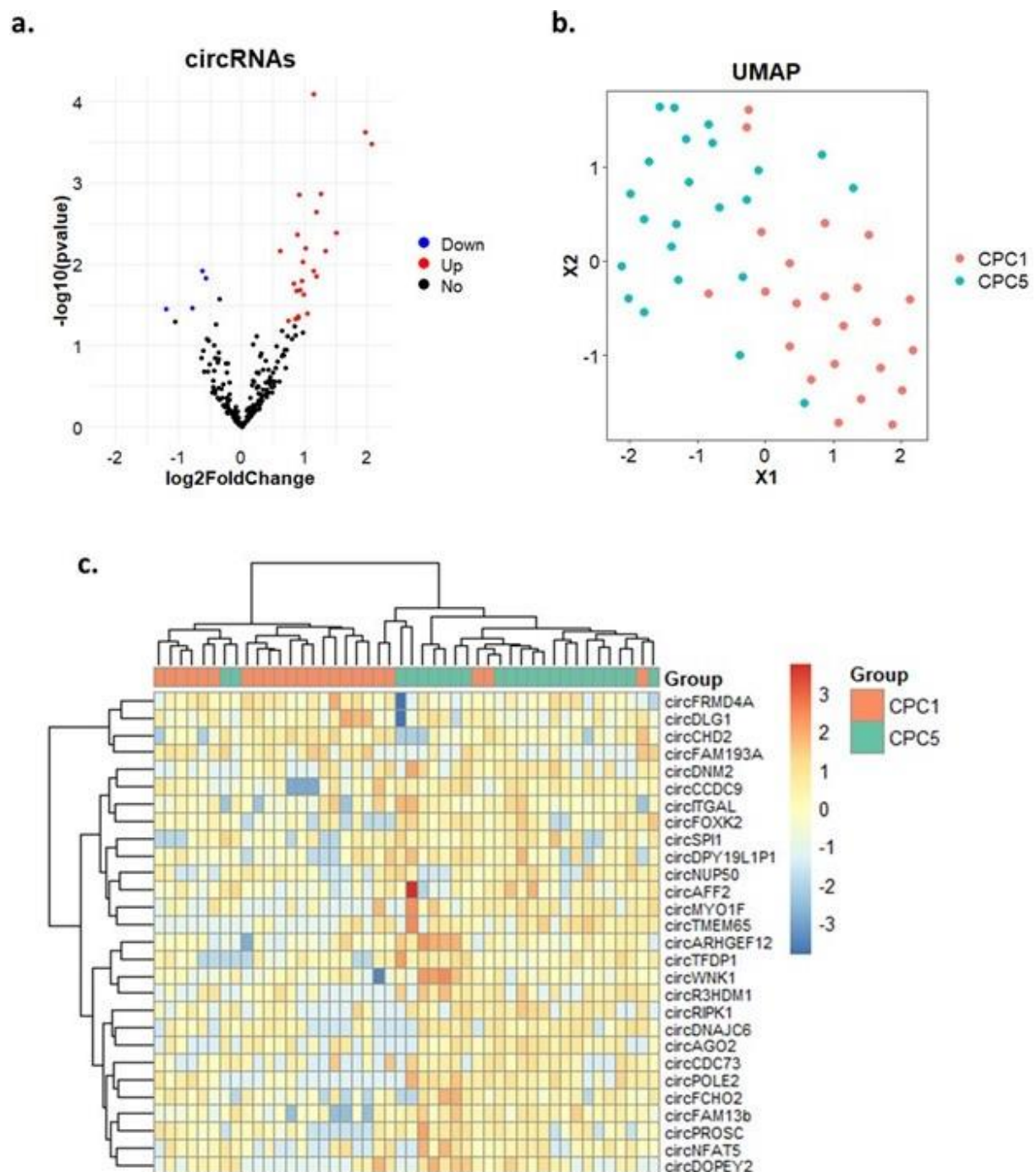
Whole transcriptome RNA sequencing of the 46 patients enrolled in the discovery phase allowed the identification of 28 candidate circRNAs with differential expression profiles with  $p < 0.05$  and  $\log_2$  fold change  $> 0.5$  or  $< -0.5$  between good (CPC 1) and poor (CPC 5) outcome groups (Table 2). Among these circRNAs, 24 were upregulated and 4 were downregulated in the CPC 5 group, as displayed by the volcano plot of Figure 1a. These circRNAs were able to reasonably distinguish the two groups of patients as showed by the uniform manifold approximation and projection (UMAP) clustering technique (Figure 1b). A heatmap shown in

Figure 1c displays the clusters of patients and standardized expression levels of the 28 circRNAs for each patient.

**Table 2. List of 28 circRNAs selected from RNA-seq.**

<b>Name</b>	<b>FPKM</b>	<b>Log2 fold-change</b>	<b>p-value</b>
circAFF2	28.88	0.62	0.007
circARHGEF12	9.13	1.02	0.006
circFRMD4A	8.6	-0.57	0.015
circDLG1	8.49	-0.62	0.012
circWNK1	5.87	0.92	0.001
circFAM13b	5.74	1.15	< 0.001
circITGAL	4.87	0.83	0.017
circTFDP1	4.15	0.98	0.009
circFCHO2	4.01	0.88	0.021
circDPY19L1P1	3.98	0.92	0.021
circCCDC9	3.72	0.88	0.004
circPROSC	3.09	0.95	0.016
circDNAJC6	2.72	0.74	0.049
circCHD2	2.63	-0.78	0.034
circFOXK2	2.35	1.19	0.002
circNFAT5	2.17	0.99	0.024
circSPI1	2.05	1.26	0.001
circPOLE2	2.04	1.19	0.014
circRIPK1	2	1.15	0.012
circCDC73	1.95	0.89	0.044
circNUP50	1.9	0.86	0.047
circDNM2	1.77	1.34	0.007
circMYO1F	1.74	1.5	0.004
circR3HDM1	1.69	1.04	0.04
circDOPEY2	1.63	1.97	< 0.001
circAGO2	1.52	0.9	0.045
circTMEM65	1.32	2.07	< 0.001
circFAM193A	1.13	-1.19	0.036

A positive log<sub>2</sub> fold-change indicates a higher level in poor outcome patients (CPC 5) as compared to good outcome (CPC 1) patients. Abbreviation: FPKM (Fragments Per Kilobase of transcript per Million mapped reads).



**Figure 1. RNA-seq results from the discovery study in 46 TTM-trial patients.**

**a.** Volcano plot showing the differential expression of the circRNAs in the CPC5 group as magnitude of change (log<sub>2</sub> fold change) on the X-axis versus statistical significance (-log<sub>10</sub>)

on the Y-axis. Color code: red, circRNAs significantly upregulated in the CPC5 group; blue, circRNAs significantly downregulated in the CPC5 group; black, circRNAs with no significant change. **b.** UMAP analysis showing the clustering of the patients with X1 and X2 representing the distance between samples. Color code: red, patients with CPC1; blue, patients with CPC5. **c.** Heatmap representing the expression levels of 28 circRNAs in each of the 46 RNA-seq samples. Color code: red, higher expression; blue, lower expression.

Pairs of divergent primers for qPCR were designed and tested for the 28 circRNAs listed in Table 1. Detectability of the circRNAs in blood samples (cut-off set at Ct value < 31) as well as amplification of the corrected product was confirmed for 5 circRNAs (Supplemental Figure 2). Among these 5 circRNAs, circNFAT5 was selected for further analysis as it represented the best compromise between PCR primers efficiency (supplementary methods), expression levels in Paxgene samples, confirmed circularity, with 76% resistance to RNase R treatment (Supplemental Figure 3) and confirmed product amplification by Sanger sequencing using divergent primers (Supplemental Figure 4a) with the junction point present in the middle of the sequence (Supplemental Figure 4b).

#### Validation phase: assessment of the biomarker potential of circNFAT5

Circulating levels of circNFAT5 were measured by qPCR in whole blood samples collected 48h after ROSC in the patients of the TTM-trial not enrolled in the discovery phase (n=542; Supplemental figure 1). 241 patients were subjected to a targeted temperature regimen of 33°C and 301 patients were assigned to 36°C. 134 patients treated at 33°C and 155 treated at 36°C showed a good neurological outcome with CPC 1-2. Demographic and clinical characteristics of these patients are gathered in Table 3 using CPC score and Supplemental Table 1 using mRS score. As compared to patients in the good outcome group (CPC 1-2), patients with poor outcome (CPC 3-5) were older, had more often co-morbidities (hypertension, diabetes mellitus,

heart failure and chronic obstructive pulmonary disease), had a higher delay between CA and ROSC, had higher levels of lactate, and had more often a shock on admission (Table 3).

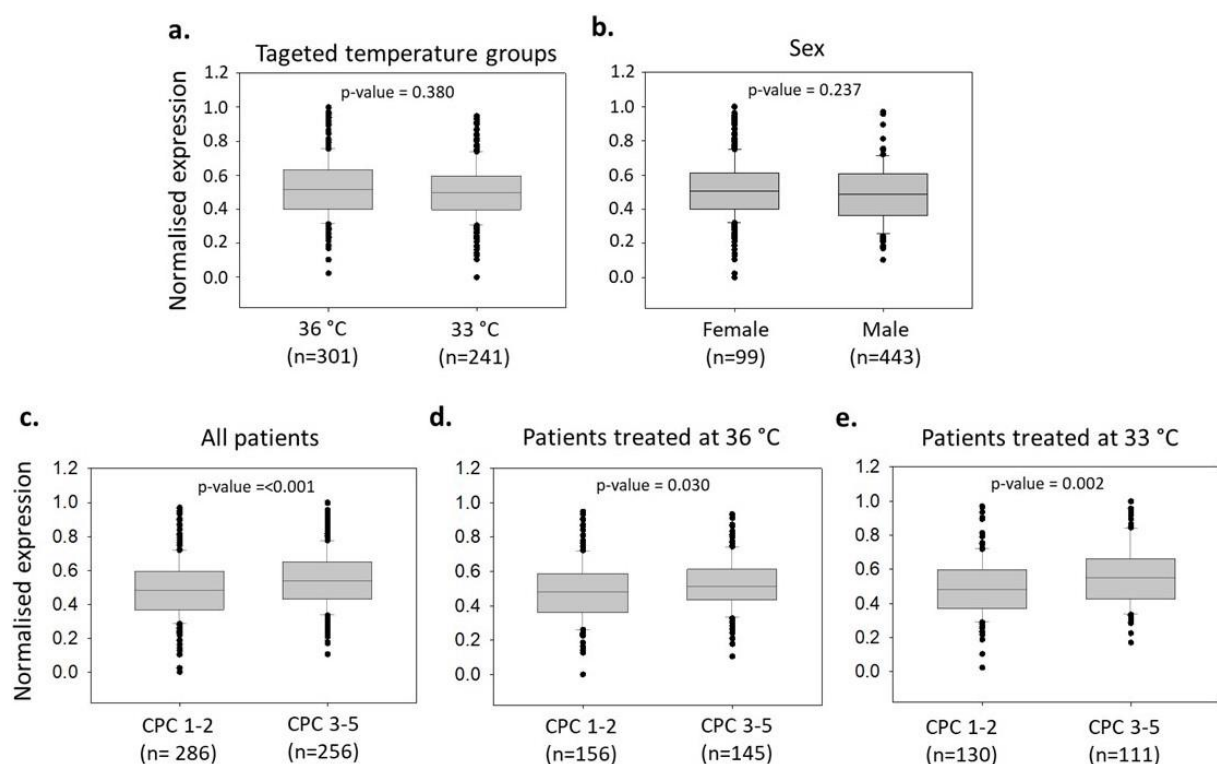
**Table 3. Demographic and clinical characteristics of TTM cohort using CPC score.**

Characteristics	Neurological outcome		p-value
	CPC1-2 n=286	CPC3-5 n=256	
<b>Age, years</b>	60 (20-90)	68 (35-94)	<b>&lt;0.001</b>
<b>Sex</b>			0.405
Male	238 (83.2%)	205 (80.1%)	
Female	48 (16.8%)	51 (19.9%)	
<b>Co-morbidities</b>			
Hypertension	101 (35.3%)	124 (48.4%)	<b>0.003</b>
Diabetes mellitus	31 (10.8%)	44 (17.2%)	<b>0.044</b>
Heart failure	7 (2.4%)	20 (7.8%)	<b>0.008</b>
COPD	18 (6.3%)	31 (12.1%)	<b>0.027</b>
<b>First monitored rhythm</b>			<b>&lt;0.001</b>
VF or non-perfusing VT	260 (90.9%)	170 (66.4%)	
Asystole or PEA	17 (5.9%)	77 (30.1%)	
ROSC after bystander defibrillation	7 (2.4%)	1 (0.4%)	
unknown	2 (0.7%)	8 (3.1%)	
<b>Witnessed arrest</b>	262 (91.6%)	223 (87.1%)	0.118
<b>Bystander CPR</b>	229 (80.1%)	168 (65.6%)	<b>&lt;0.001</b>
<b>Time from CA to ROSC, min</b>	20 (0 - 160)	30 (0 - 170)	<b>&lt;0.001</b>
<b>Initial serum lactate (mmol/l)</b>	4.4 (0 - 20)	6.5 (0 - 21.3)	<b>&lt;0.001</b>
<b>NSE 48h after ROSC (ng/ml)</b>	15 (2.5 - 119.1)	63.3 (3.1 - 782)	<b>&lt;0.001</b>
<b>Shock on admission</b>	23 (8%)	38 (14.8%)	<b>0.01</b>

Demographic and clinical characteristics of 542 patients of the TTM-trial according to neurological outcome established with CPC score. Continuous variables are indicated as median (range), while categorical characteristics are reported as number (frequency). Statistically significant p-values (< 0.05) are highlighted in bold in the table. Abbreviations as in table 1.



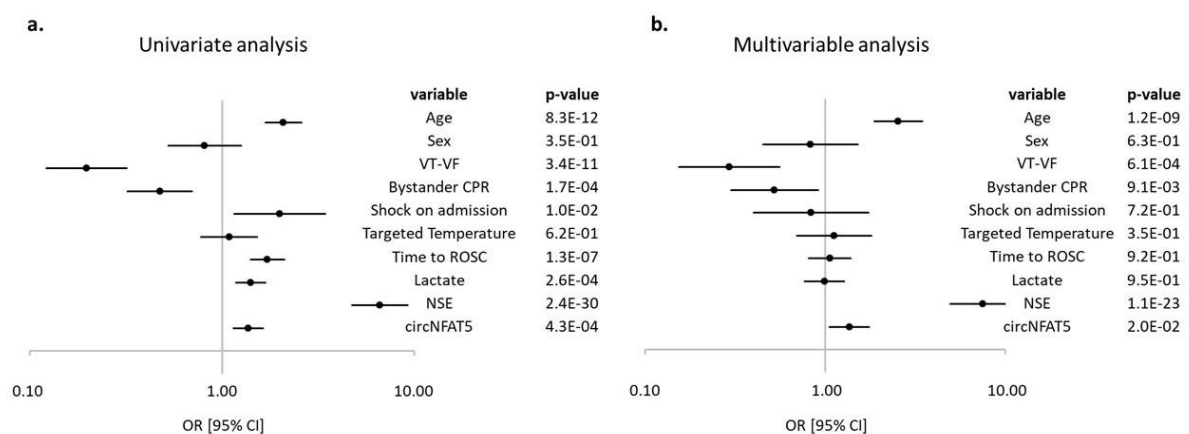
Higher levels of circNFAT5 in poor outcome patients (CPC 3-5) compared to good outcome patients (CPC 1-2) measured by qPCR (Figure 2c) confirmed the results of the RNA-seq data (Table 1). This difference persisted when separating patients by temperature treatment at 33°C or 36°C (Figure 2d-e). Targeted temperature regimen did not affect circNFAT5 levels, and males and females had comparable levels of circNFAT5 (Figure 2a-b). These results were confirmed also when patients were dichotomized according to mRS score (Supplemental Figure 5).



**Figure 2. CircNFAT5 expression levels in 542 patients of the TTM-trial.**

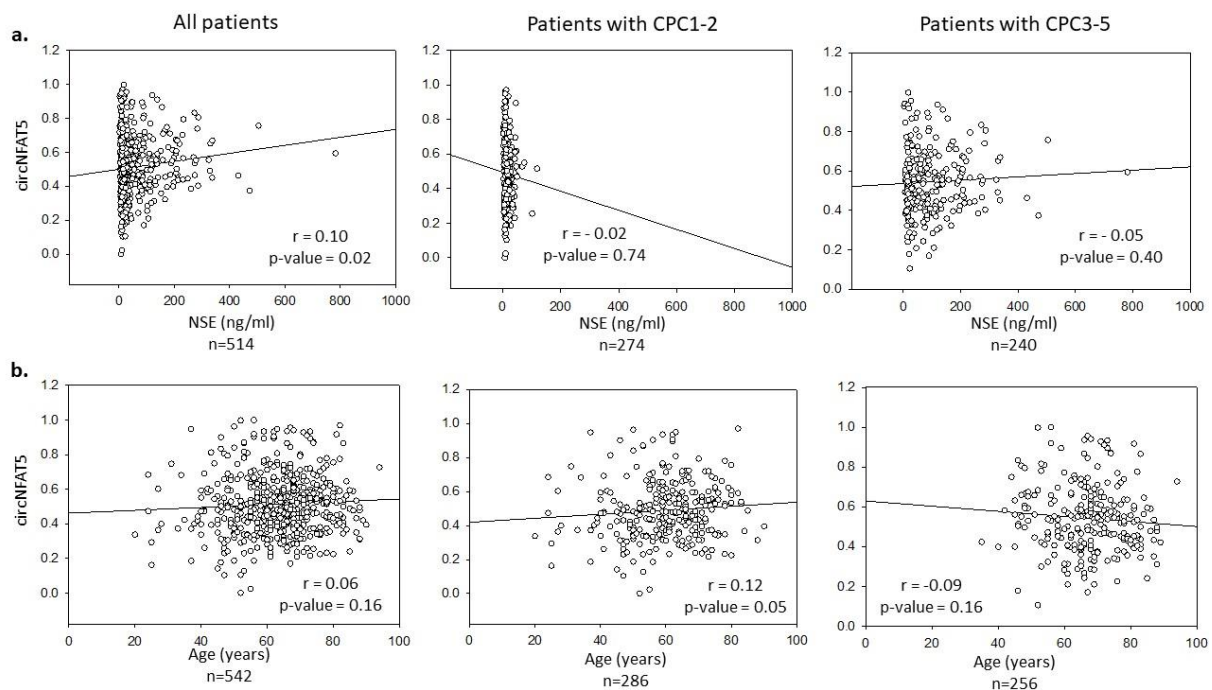
CircNFAT5 levels were compared according to the temperature regimen and regardless of the neurological outcome (a), between females and males (b), between good (CPC 1-2) and poor (CPC 3-5) neurological outcome regardless of the temperature regimen (c), and separately in patients treated at 36°C or 33°C (d-e). The expression levels of circNFAT5 were normalised, log<sub>2</sub> transformed and scaled. P-values are from Mann-Whitney U test.

To assess the potential of circNFAT5 to predict the neurological outcome of patients in the TTM-trial 6 months after OHCA, we conducted univariate and multivariable logistic regression analyses using both CPC score (Figure 3) and mRS score (Supplemental Figure 6) to classify patients. Consistently with previous studies in this trial, the following parameters were included in the multivariable clinical model: age, sex, first monitored rhythm, bystander cardiopulmonary resuscitation (CPR), circulatory shock on admission, targeted temperature regimen, time from CA to ROSC, initial serum lactate levels and NSE levels at 48h [33, 34]. As indicated in Figure 3 and supplemental table 2, circNFAT5 was a univariate predictor of the neurological outcome and this prediction remained significant after adjustment with clinical parameters (univariate OR [95% CI]: 1.37 [1.15-1.63] and 1.39 [1.07-1.83] after adjustment). In the multivariable analysis, age, first monitored rhythm, bystander CPR and NSE levels were also independent predictors of neurological outcome (Figure 3b and supplemental table 2). The results were also confirmed when using mRS instead of CPC as dichotomisation score (supplemental figure 6). Furthermore, correlation analyses showed no association between circNFAT5, NSE and age (Figure 4) both considering all patients ( $r= 0.10$  and  $r= 0.06$ , respectively) or only patients with good ( $r= 0.02$  and  $r= 0.12$ , respectively) or poor ( $r= 0.05$  and  $r= 0.09$ , respectively) neurological outcome.



### Figure 3. Logistic regression models to predict 6-month neurological outcome

Forest plots showing the odds ratio (OR) with  $\pm$  95% confidence interval [95% CI] for the prediction of 6-month neurological outcome in TTM-trial patients. **a)** Univariate logistic regression analysis. **b)** Multivariable logistic regression analysis.

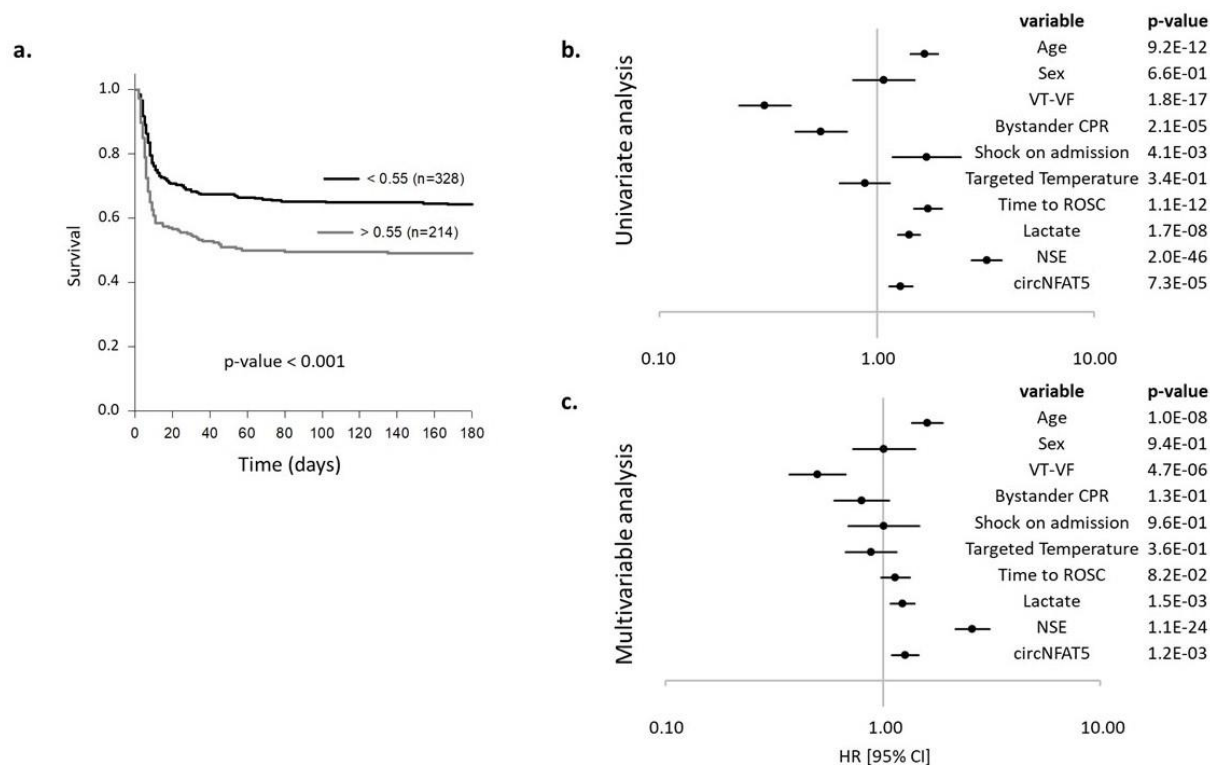


### Figure 4. Correlation analyses of circNFAT5 with NSE and age

Scatter plots and linear regressions showing the correlations between circNFAT5, NSE (a.) and age (b.). Correlations were conducted considering all patients or patients dichotomized according to neurological outcome as CPC1-2 and CPC-3-5. The expression levels of circNFAT5 used for these analyses were normalised, log2 transformed and scaled. circNFAT5 and NSE levels were measured 48h after OHCA. Spearman correlation coefficients (r) and p-value are indicated in each plot.

Kaplan-Meier survival curves and Cox proportional hazards models were then used to estimate the ability of circNFAT5 to predict 6-month survival. Kaplan-Meier survival curves generated

using the Youden's index as cutoff value indicate a higher chance of survival ( $p < 0.001$ ) in patients with expression levels of circNFAT5 below 0.55 (Figure 5a). In Cox proportional hazards models, a HR [95% CI] of 1.29 [1.14-1.46] indicated that the increase of circNFAT5 was associated with a higher risk of death at 6 months (Figure 5b and Supplemental Table 3) and this association remained significant after adjustment with demographic and clinical parameters (HR [95% CI]: 1.31 [1.13-1.52]; Figure 5c and Supplemental Table 3). After adjustment, age, first monitored rhythm, lactate and NSE levels were also independent predictors of 6-month survival (Figure 5c).



**Figure 5. Survival analyses in TTM-trial patients at 6 months**

6-month survival of TTM-trial patients using Kaplan-Meier curves and Cox proportional hazards. **a)** Kaplan-Meier curves using the Youden's index as cut-off value. **b)** Univariate Cox proportional hazards for 9 independent variables and circNFAT5. **c)** Multivariable Cox proportional hazards model. Data are presented as hazards ratio (HR) with  $\pm$  95% confidence interval [95% CI] and p-values are indicated for each variable.

The incremental value of circNFAT5 to predict neurological outcome and survival was assessed using the Akaike Information Criterion (AIC). For neurological outcome prediction using CPC score, a decrease of AIC was observed when integrating circNFAT5 in the model (LRT p-value= 0.015; Hosmer-Lemeshow p-value < 2.22E-16). This was associated with an IDI of

0.005 (p=0.15), a NRI of 0.27 (p=0.001) and an AUC of 0.91 (Table 4). Similar results were obtained for neurological outcome prediction using mRS score (Supplemental Table 4).

CircNFAT5 was able to improve the survival model as attested by a decrease of AIC (LRT p-value=3.91E-04; Gronnesby and Borgan p-value=8.62E-74), and this was associated with a C-index of 0.85 (Table 4).

**Table 4. CircNFAT5 performance to predict patient outcome in TTM cohort.**

<b>Neurological outcome</b>	<i>AIC</i>	<i>HL_p</i>	<i>AUC</i>	<i>lr_p</i>	<i>NRI</i>	<i>NRI_p</i>	<i>IDI</i>	<i>IDI_p</i>
<i>basal model</i>	433	< 2.22E-16	0.91	-	-	-	-	-
<i>basal model + circNFAT5</i>	429	< 2.22E-16	0.91	1.49E-02	0.27	1.37E-03	5.34E-03	0.15

<b>Survival</b>	<i>AIC</i>	<i>GB_p</i>	<i>C_idx</i>	<i>lr_p</i>
<i>basal model</i>	2373	1.57E-03	0.85	-
<i>basal model + circNFAT5</i>	2362	1.71E-03	0.85	3.91E-04

Incremental value of circNFAT5 to predict neurological and survival in TTM-trial patients. The basal model included age, sex, first monitored rhythm, bystander cardiopulmonary resuscitation (CPR), circulatory shock on admission, targeted temperature regimen, time from CA to ROSC, initial serum lactate levels and NSE levels at 48h. Abbreviations: AIC = Akaike Information Criterion; HL = Hosmer-Lemeshow; AUC = Area Under the Curve; GB = Gronnesby and Borgan; C\_idx = Harrell's C-index; IDI = Integrated Discrimination Improvement; IDI\_p = Integrated Discrimination Improvement p-value; lr\_p = Likelihood Ratio Test p-value; NRI = Net Reclassification Improvement; NRI\_p = Net Reclassification Improvement p-value.

## Discussion

The present study aimed to identify and validate the prognostic potential of circulating circRNAs after OHCA. In a discovery phase using whole transcriptome sequencing, one

circRNA named circNFAT5 (hsa-circ-0006845) was identified and selected for validation of its prognostic ability in the TTM-trial. Our study showed that patients with elevated circulating levels of circNFAT5 48h after OHCA were at higher risk of poor neurological outcome and death.

Although circRNAs are believed to have many regulatory functions within the cells [35-37], the mode of action of most of them including circNFAT5, remains to be determined. It is believed that different cell types can express clusters of genes in response to diverse insults [38, 39]. Therefore, the study of neighbouring genes could be an indicator of the function of a specific circRNA. CircNFAT5 is located in the last coding exon of the transcription factor NFAT5 which is expressed in several tissues such as skeletal muscle, heart, brain and peripheral blood leukocytes [40-43]. Its activation after stress and its tissue distribution makes it appealing and provides a potential link between the heart, brain and leukocytes, with all three of them contributing to clinical outcome after cardiac arrest. Importantly, leukocytes are the cells where the measurements of circNFAT5 are taking place and we have observed that circNFAT5 was expressed in lymphocytes and monocytes but was not detectable in serum (not shown). Additionally, several studies have previously reported that NFAT5 plays a key role in inflammatory processes of pathologies associated with cardiovascular diseases such as hypertension, atherosclerosis and diabetes mellitus [44-47]. Therefore, it would be interesting to investigate a hypothetical involvement of circNFAT5 in inflammatory pathways associated with CA and its clinical outcome and sequelae, in relationship with NFAT5. In addition to this, we observed a low correlation between circNFAT5 and NSE levels (Figure 4) which suggests an involvement of circNFAT5 in processes occurring after OHCA other than brain injury. This supports the incremental prognostic potential of circNFAT5 to be used in combination with established markers of OHCA such as NSE. Although NSE or more recently discovered biomarkers such as Nfl, are good predictors of neurological outcome after CA, novel

biomarkers reflecting other pathways (than neuronal death) involved in outcome after CA could provide some incremental predictive value to ensure a maximal prediction accuracy. Along with that, it would be interesting to conduct further post-hoc analysis to define whether circNFAT5 can better predict the outcome of specific subpopulations of patients, such as patients with shock on admission. However, this requires larger population than the TTM cohort included in the present study. This study has the strength of being a predefined sub-study of a large multicenter clinical trial on OHCA. Blood collection, processing and storage was performed homogeneously in each center according to standard operating procedures implemented and validated by our central biobank. Furthermore, the measurements of circNFAT5 were conducted in a single laboratory according to pre-established protocols [25], limiting the inter-laboratory variability of sample processing. All together, these measures ensure sample quality and robustness of the results. The present study also has some limitations. Firstly, the predictive value of only one circRNA from our discovery study has been extensively tested and reported, which does not exclude the presence of other circRNAs that can aid in the prognostication of OHCA patients. Combination of several circRNAs in prediction models remains to be tested. Secondly, the cellular origin of circNFAT5 was not accurately determined and neither was the mechanism that links circNFAT5 with outcome after OHCA. Finally, circNFAT5 was measured at a single time point, 48h after OHCA, and it is unknown whether it can be detected at an earlier stage. Despite these limitations, our study is the first to highlight the potential and unexplored biomarker ability of circRNAs for outcome prediction after OHCA and therefore represents the starting point for future biomarker and functional studies focusing on the role played by circRNAs in CA pathophysiology.

## Conclusions

In the present study, elevated circulating levels of the circular RNA, circNFAT5, measured 48h after ROSC were associated with a higher risk of poor neurological outcome and death after



OHCA. The incremental predictive value of circNFAT5 may emanate from its association with other post-cardiac arrest mechanisms than neurological damage, such as inflammation. However, the exact functional association between cNFAT5 and outcome after OHCA remains to be determined.

#### Availability of data and materials

The circRNAs metadata in TTM can be accessed using the GEO code GSE197764.

#### References

1. Wong CX, Brown A, Lau DH, Chugh SS, Albert CM, Kalman JM, Sanders P, (2019) Epidemiology of Sudden Cardiac Death: Global and Regional Perspectives. *Heart Lung Circ* 28: 6-14
2. Grasner JT, Herlitz J, Tjelmeland IBM, Wnent J, Masterson S, Lilja G, Bein B, Bottiger BW, Rosell-Ortiz F, Nolan JP, Bossaert L, Perkins GD, (2021) European Resuscitation Council Guidelines 2021: Epidemiology of cardiac arrest in Europe. *Resuscitation* 161: 61-79
3. Link MS, Berkow LC, Kudenchuk PJ, Halperin HR, Hess EP, Moitra VK, Neumar RW, O'Neil BJ, Paxton JH, Silvers SM, White RD, Yannopoulos D, Donnino MW, (2015) Part 7: Adult Advanced Cardiovascular Life Support: 2015 American Heart Association Guidelines Update for Cardiopulmonary Resuscitation and Emergency Cardiovascular Care. *Circulation* 132: S444-464
4. Ryoo SM, Jeon SB, Sohn CH, Ahn S, Han C, Lee BK, Lee DH, Kim SH, Donnino MW, Kim WY, Korean Hypothermia Network I, (2015) Predicting Outcome With Diffusion-Weighted Imaging in Cardiac Arrest Patients Receiving Hypothermia Therapy: Multicenter Retrospective Cohort Study. *Crit Care Med* 43: 2370-2377

5. Karapetkova M, Koenig MA, Jia X, (2016) Early prognostication markers in cardiac arrest patients treated with hypothermia. *Eur J Neurol* 23: 476-488
6. Stammet P, Collignon O, Hassager C, Wise MP, Hovdenes J, Aneman A, Horn J, Devaux Y, Erlinge D, Kjaergaard J, Gasche Y, Wanscher M, Cronberg T, Friberg H, Wetterslev J, Pellis T, Kuiper M, Gilson G, Nielsen N, Investigators TT-T, (2015) Neuron-Specific Enolase as a Predictor of Death or Poor Neurological Outcome After Out-of-Hospital Cardiac Arrest and Targeted Temperature Management at 33 degrees C and 36 degrees C. *J Am Coll Cardiol* 65: 2104-2114
7. Luescher T, Mueller J, Isenschmid C, Kalt J, Rasiah R, Tondorf T, Gamp M, Becker C, Sutter R, Tisljar K, Schuetz P, Marsch S, Hunziker S, (2019) Neuron-specific enolase (NSE) improves clinical risk scores for prediction of neurological outcome and death in cardiac arrest patients: Results from a prospective trial. *Resuscitation* 142: 50-60
8. Streitberger KJ, Leithner C, Wattenberg M, Tonner PH, Hasslacher J, Joannidis M, Pellis T, Di Luca E, Fodisch M, Krannich A, Ploner CJ, Storm C, (2017) Neuron-Specific Enolase Predicts Poor Outcome After Cardiac Arrest and Targeted Temperature Management: A Multicenter Study on 1,053 Patients. *Crit Care Med* 45: 1145-1151
9. Moseby-Knappe M, Mattsson N, Nielsen N, Zetterberg H, Blennow K, Dankiewicz J, Dragancea I, Friberg H, Lilja G, Insel PS, Rylander C, Westhall E, Kjaergaard J, Wise MP, Hassager C, Kuiper MA, Stammet P, Wanscher MCJ, Wetterslev J, Erlinge D, Horn J, Pellis T, Cronberg T, (2019) Serum Neurofilament Light Chain for Prognosis of Outcome After Cardiac Arrest. *JAMA Neurol* 76: 64-71
10. Stammet P, Dankiewicz J, Nielsen N, Fays F, Collignon O, Hassager C, Wanscher M, Unden J, Wetterslev J, Pellis T, Aneman A, Hovdenes J, Wise MP, Gilson G, Erlinge

- D, Horn J, Cronberg T, Kuiper M, Kjaergaard J, Gasche Y, Devaux Y, Friberg H, Target Temperature Management after Out-of-Hospital Cardiac Arrest trial i, (2017) Protein S100 as outcome predictor after out-of-hospital cardiac arrest and targeted temperature management at 33 degrees C and 36 degrees C. *Crit Care* 21: 153
11. Kleissner M, Sramko M, Kohoutek J, Kautzner J, Kettner J, (2021) Serum S100 Protein Is a Reliable Predictor of Brain Injury After Out-of-Hospital Cardiac Arrest: A Cohort Study. *Front Cardiovasc Med* 8: 624825
  12. Rundgren M, Karlsson T, Nielsen N, Cronberg T, Johnsson P, Friberg H, (2009) Neuron specific enolase and S-100B as predictors of outcome after cardiac arrest and induced hypothermia. *Resuscitation* 80: 784-789
  13. Pelinka LE, Hertz H, Mauritz W, Harada N, Jafarmadar M, Albrecht M, Redl H, Bahrami S, (2005) Nonspecific increase of systemic neuron-specific enolase after trauma: clinical and experimental findings. *Shock* 24: 119-123
  14. Burghuber OC, Worofka B, Schernthaner G, Vetter N, Neumann M, Dudczak R, Kuzmits R, (1990) Serum neuron-specific enolase is a useful tumor marker for small cell lung cancer. *Cancer* 65: 1386-1390
  15. DeGiorgio CM, Gott PS, Rabinowicz AL, Heck CN, Smith TD, Correale JD, (1996) Neuron-specific enolase, a marker of acute neuronal injury, is increased in complex partial status epilepticus. *Epilepsia* 37: 606-609
  16. Lu D, Thum T, (2019) RNA-based diagnostic and therapeutic strategies for cardiovascular disease. *Nat Rev Cardiol* 16: 661-674
  17. Gomes CPC, Schroen B, Kuster GM, Robinson EL, Ford K, Squire IB, Heymans S, Martelli F, Emanuelli C, Devaux Y, Action EU-CC, (2020) Regulatory RNAs in Heart Failure. *Circulation* 141: 313-328

18. Zhang Z, Yang T, Xiao J, (2018) Circular RNAs: Promising Biomarkers for Human Diseases. *EBioMedicine* 34: 267-274
19. Memczak S, Jens M, Elefsinioti A, Torti F, Krueger J, Rybak A, Maier L, Mackowiak SD, Gregersen LH, Munschauer M, Loewer A, Ziebold U, Landthaler M, Kocks C, le Noble F, Rajewsky N, (2013) Circular RNAs are a large class of animal RNAs with regulatory potency. *Nature* 495: 333-338
20. Szabo L, Salzman J, (2016) Detecting circular RNAs: bioinformatic and experimental challenges. *Nat Rev Genet* 17: 679-692
21. Jeck WR, Sorrentino JA, Wang K, Slevin MK, Burd CE, Liu J, Marzluff WF, Sharpless NE, (2013) Circular RNAs are abundant, conserved, and associated with ALU repeats. *RNA* 19: 141-157
22. Jeck WR, Sharpless NE, (2014) Detecting and characterizing circular RNAs. *Nat Biotechnol* 32: 453-461
23. Aufiero S, Reckman YJ, Pinto YM, Creemers EE, (2019) Circular RNAs open a new chapter in cardiovascular biology. *Nat Rev Cardiol* 16: 503-514
24. Lee ECS, Elhassan SAM, Lim GPL, Kok WH, Tan SW, Leong EN, Tan SH, Chan EWL, Bhattamisra SK, Rajendran R, Candasamy M, (2019) The roles of circular RNAs in human development and diseases. *Biomed Pharmacother* 111: 198-208
25. Vausort M, Salgado-Somoza A, Zhang L, Leszek P, Scholz M, Teren A, Burkhardt R, Thiery J, Wagner DR, Devaux Y, (2016) Myocardial Infarction-Associated Circular RNA Predicting Left Ventricular Dysfunction. *J Am Coll Cardiol* 68: 1247-1248
26. Salgado-Somoza A, Zhang L, Vausort M, Devaux Y, (2017) The circular RNA MICRA for risk stratification after myocardial infarction. *Int J Cardiol Heart Vasc* 17: 33-36

27. Devaux Y, Creemers EE, Boon RA, Werfel S, Thum T, Engelhardt S, Dimmeler S, Squire I, Cardioline n, (2017) Circular RNAs in heart failure. *Eur J Heart Fail* 19: 701-709
28. Gratz C, Bui MLU, Thaqi G, Kirchner B, Loewe RP, Pfaffl MW, (2022) Obtaining Reliable RT-qPCR Results in Molecular Diagnostics-MIQE Goals and Pitfalls for Transcriptional Biomarker Discovery. *Life (Basel)* 12
29. Nielsen N, Wetterslev J, Cronberg T, Erlinge D, Gasche Y, Hassager C, Horn J, Hovdenes J, Kjaergaard J, Kuiper M, Pellis T, Stammet P, Wanscher M, Wise MP, Aneman A, Al-Subaie N, Boesgaard S, Bro-Jeppesen J, Brunetti I, Bugge JF, Hingston CD, Juffermans NP, Koopmans M, Kober L, Langorgren J, Lilja G, Moller JE, Rundgren M, Rylander C, Smid O, Werer C, Winkel P, Friberg H, Investigators TTMT, (2013) Targeted temperature management at 33 degrees C versus 36 degrees C after cardiac arrest. *N Engl J Med* 369: 2197-2206
30. Dankiewicz J, Cronberg T, Lilja G, Jakobsen JC, Levin H, Ullen S, Rylander C, Wise MP, Oddo M, Cariou A, Belohlavek J, Hovdenes J, Saxena M, Kirkegaard H, Young PJ, Pelosi P, Storm C, Taccone FS, Joannidis M, Callaway C, Eastwood GM, Morgan MPG, Nordberg P, Erlinge D, Nichol AD, Chew MS, Hollenberg J, Thomas M, Bewley J, Sweet K, Grejs AM, Christensen S, Haenggi M, Levis A, Lundin A, During J, Schmidbauer S, Keeble TR, Karamasis GV, Schrag C, Faessler E, Smid O, Otahal M, Maggiorini M, Wendel Garcia PD, Jaubert P, Cole JM, Solar M, Borgquist O, Leithner C, Abed-Maillard S, Navarra L, Annborn M, Uden J, Brunetti I, Awad A, McGuigan P, Bjorkholt Olsen R, Cassina T, Vignon P, Langeland H, Lange T, Friberg H, Nielsen N, Investigators TTMT, (2021) Hypothermia versus Normothermia after Out-of-Hospital Cardiac Arrest. *N Engl J Med* 384: 2283-2294

31. Nielsen N, Wetterslev J, al-Subaie N, Andersson B, Bro-Jeppesen J, Bishop G, Brunetti I, Cranshaw J, Cronberg T, Edqvist K, Erlinge D, Gasche Y, Glover G, Hassager C, Horn J, Hovdenes J, Johnsson J, Kjaergaard J, Kuiper M, Langorgen J, Macken L, Martinell L, Martner P, Pellis T, Pelosi P, Petersen P, Persson S, Rundgren M, Saxena M, Svensson R, Stammet P, Thoren A, Unden J, Walden A, Wallskog J, Wanscher M, Wise MP, Wyon N, Aneman A, Friberg H, (2012) Target Temperature Management after out-of-hospital cardiac arrest--a randomized, parallel-group, assessor-blinded clinical trial--rationale and design. *Am Heart J* 163: 541-548
32. Nielsen N, Winkel P, Cronberg T, Erlinge D, Friberg H, Gasche Y, Hassager C, Horn J, Hovdenes J, Kjaergaard J, Kuiper M, Pellis T, Stammet P, Wanscher M, Wise MP, Aneman A, Wetterslev J, (2013) Detailed statistical analysis plan for the target temperature management after out-of-hospital cardiac arrest trial. *Trials* 14: 300
33. Devaux Y, Dankiewicz J, Salgado-Somoza A, Stammet P, Collignon O, Gilje P, Gidlof O, Zhang L, Vausort M, Hassager C, Wise MP, Kuiper M, Friberg H, Cronberg T, Erlinge D, Nielsen N, for Target Temperature Management After Cardiac Arrest Trial I, (2016) Association of Circulating MicroRNA-124-3p Levels With Outcomes After Out-of-Hospital Cardiac Arrest: A Substudy of a Randomized Clinical Trial. *JAMA Cardiol* 1: 305-313
34. Devaux Y, Salgado-Somoza A, Dankiewicz J, Boileau A, Stammet P, Schritz A, Zhang L, Vausort M, Gilje P, Erlinge D, Hassager C, Wise MP, Kuiper M, Friberg H, Nielsen N, investigators TT-t, (2017) Incremental Value of Circulating MiR-122-5p to Predict Outcome after Out of Hospital Cardiac Arrest. *Theranostics* 7: 2555-2564
35. Shao T, Pan YH, Xiong XD, (2021) Circular RNA: an important player with multiple facets to regulate its parental gene expression. *Mol Ther Nucleic Acids* 23: 369-376

36. Chen LL, (2020) The expanding regulatory mechanisms and cellular functions of circular RNAs. *Nat Rev Mol Cell Biol* 21: 475-490
37. Qu S, Liu Z, Yang X, Zhou J, Yu H, Zhang R, Li H, (2018) The emerging functions and roles of circular RNAs in cancer. *Cancer Lett* 414: 301-309
38. Ghanbarian AT, Hurst LD, (2015) Neighboring Genes Show Correlated Evolution in Gene Expression. *Mol Biol Evol* 32: 1748-1766
39. Michalak P, (2008) Coexpression, coregulation, and cofunctionality of neighboring genes in eukaryotic genomes. *Genomics* 91: 243-248
40. O'Connor RS, Mills ST, Jones KA, Ho SN, Pavlath GK, (2007) A combinatorial role for NFAT5 in both myoblast migration and differentiation during skeletal muscle myogenesis. *J Cell Sci* 120: 149-159
41. Adachi A, Takahashi T, Ogata T, Imoto-Tsubakimoto H, Nakanishi N, Ueyama T, Matsubara H, (2012) NFAT5 regulates the canonical Wnt pathway and is required for cardiomyogenic differentiation. *Biochem Biophys Res Commun* 426: 317-323
42. Loyher ML, Mutin M, Woo SK, Kwon HM, Tappaz ML, (2004) Transcription factor tonicity-responsive enhancer-binding protein (TonEBP) which transactivates osmoprotective genes is expressed and upregulated following acute systemic hypertonicity in neurons in brain. *Neuroscience* 124: 89-104
43. Trama J, Lu Q, Hawley RG, Ho SN, (2000) The NFAT-related protein NFATL1 (TonEBP/NFAT5) is induced upon T cell activation in a calcineurin-dependent manner. *J Immunol* 165: 4884-4894
44. Machnik A, Neuhofer W, Jantsch J, Dahlmann A, Tammela T, Machura K, Park JK, Beck FX, Muller DN, Derer W, Goss J, Ziomber A, Dietsch P, Wagner H, van Rooijen N, Kurtz A, Hilgers KF, Alitalo K, Eckardt KU, Luft FC, Kerjaschki D, Titze J, (2009) Macrophages regulate salt-dependent volume and blood pressure by a

- vascular endothelial growth factor-C-dependent buffering mechanism. *Nat Med* 15: 545-552
45. Ma P, Zha S, Shen X, Zhao Y, Li L, Yang L, Lei M, Liu W, (2019) NFAT5 mediates hypertonic stress-induced atherosclerosis via activating NLRP3 inflammasome in endothelium. *Cell Commun Signal* 17: 102
  46. Neuhofer W, (2010) Role of NFAT5 in inflammatory disorders associated with osmotic stress. *Curr Genomics* 11: 584-590
  47. Cen L, Xing F, Xu L, Cao Y, (2020) Potential Role of Gene Regulator NFAT5 in the Pathogenesis of Diabetes Mellitus. *J Diabetes Res* 2020: 6927429

### Acknowledgements

The authors would like to thank all patients of TTM-trial, their relatives and all staff at the recruiting centers. In addition, the authors would like to thank Andrew Lumley for proofreading the manuscript.

### Funding

This work is supported by independent research grants from nonprofit or governmental agencies (the Swedish Research Council [Vetenskapsrådet], Swedish Heart–Lung Foundation, Stig and Ragna Gorthon Foundation, Knutsson Foundation, Laerdal Foundation, Hans-Gabriel and Alice Trolle-Wachtmeister Foundation for Medical Research, and Regional Research Support in Region Skåne) and by governmental funding of clinical research within the Swedish National Health Service.

YD is supported by the National Research Fund of Luxembourg (grants # C14/BM/8225223 and C17/BM/11613033), the Ministry of Higher Education and Research of Luxembourg, and



the Heart Foundation - Daniel Wagner. FMS is supported by the National Research Fund of Luxembourg (grant # C17/BM/11613033).

#### Authors' contributions

FMS carried out the molecular studies, helped with the statistical analyses and drafted the manuscript. LZ carried out the sequencing alignment and the statistical analyses. ASS participated in the design of the study and selection of the candidates for the molecular studies. J.D., P.S., C.H., M.P.W., H.F., T.C., J.K. and N.N. recruited patients into the TTM-trial. A.H. was responsible for the storage and RNA extraction of the TTM samples at IBBL. N.N. was also involved in the critical review of the manuscript. YD conceived the study, participated in its design and coordination and helped in the drafting of the manuscript. All authors read and approved the manuscript.

#### Ethics declarations

#### Ethics approval and consent to participate

The trial has received ethical approval from each participating country. Informed consent was obtained from each participant or relatives, according to the legislation in each country. The study was conducted in accordance with the declaration of Helsinki. The trial is registered at [www.clinicaltrials.gov](http://www.clinicaltrials.gov) (NCT01020916).

#### Ethical approvals

Czech Republic: Ethics committee of the General University Hospital of Prague, c/j 193-11 S 17.2.2011.

Denmark: De vitenskabetiske Komiteer i Region Hovedstaden, H-1-2010-059.

Italy: Comitato Etico Indipendente, Hospedaliera S Maria degli Angeli Pordenone, No 9.

Luxembourg: Comité National d'Ethique de Recherche CNER No 201007/05 Ver 1.0.

The Netherlands: Medisch Etische Toetsingscommissie MEC 10/107 # 10.17.0921.

Norway: Regional komité for medisinsk och helsefaglig forskningsetikk Sør-øst C Ref 2010/384.

Sweden: Regional Ethical Review Board Lund, Protocol 2009/6 Dnr 2009/324 (TTM-Trial).

Switzerland: Comité d’Ethique de Recherche CER 10-254 (NAC 10-088).

United Kingdom: Cardiff and Vale Research Review Service, Project ID 10/AIC/4927,  
Research Ethics Committee for Wales: 10/MRE09/41.

#### Consent for publication

Not applicable.

#### Competing interests

All authors declare no conflict of interest.

## Supplemental methods

### RNA extraction

Total RNA was extracted from PAXgene™ Blood RNA tubes using the PAXgene™ Blood miRNA Kit (Qiagen), according to the manufacturers' protocol, followed by spectrophotometric quantification.

### RNA sequencing (RNA-seq)

A strand-specific RNA-Seq library was prepared using the Ovation Human Blood RNA-Seq Library Systems (NuGEN Technologies, San Carlos, USA) from 46 human whole blood samples from TTM-trial. The sequencing was performed using the HiSeq platform (Illumina, San Diego, CA) with 2 x 50 bp. After trimming the adapters, quality control of the RNA-seq data was performed using the FastQC tool (<https://www.bioinformatics.babraham.ac.uk/projects/fastqc/>). The reads were aligned to the human reference genome (GRCh38) using STAR with default set-up (34). DCC was used with default set-up for circRNA identification (35) and DESeq2 (36) to identify differentially expressed circRNAs. The circRNAs detected with at least 2 reads in at least half samples of CPC1 or CPC5 group were kept in differential expression analysis. The circRNAs with p-value < 0.05 and log<sub>2</sub> fold change > 0.5 or < -0.5 were kept for candidate selection and validation by quantitative PCR (qPCR).

A volcano plot was generated using ggplot (37) to show the  $-\log_{10}$  p-values versus log<sub>2</sub> fold change of detected circRNAs. A UMAP (Uniform Manifold Approximation and Projection) plot (38) was used to show the separation of CPC1 and CPC5 groups with the normalized counts of differentially expressed circRNAs. The heatmap of differentially expressed circRNAs was

generated using pheatmap R package (<https://CRAN.R-project.org/package=pheatmap>) with Euclidean distance.

### Reverse transcription

Reverse transcription (RT) was performed on 300 ng of RNA per sample with the SuperScript™ II Reverse Transcriptase kit following the manufacturer's protocol (ThermoFisher scientific cat n. 18064071) with the addition of random primers (Invitrogen, P/N 58875) and dNTPs (Invitrogen, cat n.18427088). Controls without reverse transcriptase allowed verifying the absence of genomic DNA amplification in each RT series. The resulting cDNA was diluted 10-fold before measuring the expression levels of circNFAT5 by qPCR.

### Quantitative PCR

Pairs of divergent PCR primers were designed using Beacon Designer software version 8.0 (Premier Biosoft) for circRNAs engaged in qPCR experiments. Divergent primers allow a specific amplification of circular and not linear RNAs. Primers for circNFAT5 were as follows: circNFAT5-H-S1: AGATTGATTTGCTTGTTTC and circNFAT5-H-AS1: TGAGAAAGAAGTGTTGTC. The optimal annealing temperature selected for circNFAT5 was 58 °C with a PCR efficiency of 93.9%. PCR product sequencing and melt curve analysis confirmed the specificity of the amplification. Each PCR plate contained an internal standard calibrator and a cDNA pool originated from five PAXgene™ Blood RNA tubes of CA patients. The internal standard calibrator allowed interplate variability to be corrected. Furthermore, each plate contained appropriate negative controls in order to check for potential mastermix or sample contamination. Quantitative PCRs were performed using CFX96 thermocycler (Bio-Rad). SF3a1 was used as housekeeping gene for normalisation. The expression values were determined using the relative quantification method ( $\Delta\Delta C_t$ ) with CFX Maestro 1.1 software (Bio-Rad), followed by log<sub>2</sub> transformation and scaling.

### RNaseR treatment

The circularity of 5 circRNAs was confirmed in PAXgene blood samples of CA patients. Eight samples were selected for the RNase R treatment: four samples from patients with a CPC1 and four from patients with a CPC5. 500 ng of total RNA were used for the treatment with RNaseR enzyme (Epicentre; cat n. RNR07250) and another 500 ng was used for the mock. The RNaseR treatment was performed following the manufacturer's protocol. Thus, RT and qPCRs were performed following the same previously described protocol. SF3a1 is a linear transcript and therefore considered as a negative control of the experiment while, MICRA, a known circular RNA, was used as a positive control to confirm circRNAs circularity. RNase R resistance was quantified as the average of the 8 samples reported as a percentage of  $(2^{-Cq\_RNaseR}) / (2^{-Cq\_mock})$  for each candidate circRNA.

## Supplemental results

### Supplemental tables

Supplemental Table 1. Demographic and clinical characteristics of TTM cohort using mRS score.

Characteristics	Outcome patients		p-value
	mRS 0-3 n=289	mRS 4-6 n=253	
<b>Age, years</b>	60 (20-90)	<b>68 (35-94)</b>	<b>&lt;0.001</b>
<b>Sex</b>			0.464
Male	240 (83%)	203 (80.2%)	
Female	49 (17%)	50 (19.8%)	
<b>Co-morbidities</b>			
Hypertension	105 (36.3%)	120 (47.4%)	<b>0.032</b>
Diabetes mellitus	30 (10.4%)	45 (17.8%)	<b>0.044</b>
Heart failure	7 (2.4%)	20 (7.9%)	<b>0.008</b>
COPD	19 (6.6%)	30 (11.9%)	<b>0.047</b>
<b>First monitored rhythm</b>			<b>&lt;0.001</b>
VF or non-perfusing VT	262 (90.7%)	168 (66.4%)	
Asystole or PEA	17 (5.9%)	77 (30.4%)	
ROSC after bystander defibrillation	7 (2.4%)	1 (0.4%)	
unknown	3 (1%)	7 (2.8%)	
<b>Witnessed arrest</b>	265 (91.7%)	220 (87%)	0.1
<b>Bystander CPR</b>	234 (81%)	163 (64.4%)	<b>&lt;0.001</b>
<b>Time from CA to ROSC, min</b>	20 (0 - 160)	30 (0 - 170)	<b>&lt;0.001</b>
<b>Initial serum lactate (mmol/l)</b>	5 (1 - 20)	7 (1 - 21)	<b>&lt;0.001</b>
<b>NSE 48h after ROSC (ng/ml)</b>	15 (2.5 - 119.1)	64.8 (3.1 - 782)	<b>&lt;0.001</b>
<b>Shock on admission</b>	25 (8.7%)	36 (14.2%)	0.056

Demographic and clinical characteristics of 542 patients of the TTM-trial according to neurological outcome established with mRS score. Same analyses as described in Table 3.

Supplemental Table 2. Univariate and multivariable logistic regression analyses to predict 6-month neurological outcome

	<b>Univariate logistic regression</b>			
	<i>OR</i>	<i>Lower 95% CI</i>	<i>Upper 95% CI</i>	<i>p-value</i>
<i>Age</i>	2.00	1.65	2.46	8.3E-12
<i>Sex</i>	0.81	0.52	1.25	3.5E-01
<i>VT-VF</i>	0.20	0.12	0.32	3.4E-11
<i>Bystander CPR</i>	0.48	0.32	0.70	1.7E-04
<i>Shock on admission</i>	1.99	1.16	3.49	1.0E-02
<i>Targeted Temperature</i>	0.92	0.65	1.29	6.2E-01
<i>Time to ROSC</i>	1.72	1.41	2.12	1.3E-07
<i>Lactate</i>	1.39	1.17	1.66	2.6E-04
<i>NSE</i>	7.50	5.40	10.78	2.4E-30
<i>circNFAT5</i>	1.37	1.15	1.63	4.3E-04

	<b>Multivariable logistic regression</b>			
	<i>OR</i>	<i>Lower 95% CI</i>	<i>Upper 95% CI</i>	<i>p-value</i>
<i>Age</i>	2.42	1.84	3.25	1.2E-09
<i>Sex</i>	0.86	0.46	1.60	6.3E-01
<i>VT-VF</i>	0.31	0.15	0.60	6.1E-04
<i>Bystander CPR</i>	0.46	0.26	0.82	9.1E-03
<i>Shock on admission</i>	0.87	0.41	1.84	7.2E-01
<i>Targeted Temperature</i>	0.79	0.48	1.30	3.5E-01
<i>Time to ROSC</i>	0.99	0.74	1.31	9.2E-01
<i>Lactate</i>	1.01	0.77	1.31	9.5E-01
<i>NSE</i>	9.17	6.08	14.48	1.1E-23
<i>circNFAT5</i>	1.39	1.07	1.83	2.0E-02

Univariate and multivariable logistic regression analyses reporting the odd ratio (OR) coefficients, 95% confidence intervals (Lower 95% CI and Upper 95% CI) and p-values for the different parameters tested.

Supplemental Table 3. Univariate and multivariable Cox proportional hazards models to predict 6-month survival.

<b>Univariate Cox proportional hazards</b>				
	<i>HR</i>	<i>Lower 95% CI</i>	<i>Upper 95% CI</i>	<i>p-value</i>
<i>Age</i>	1.65	1.43	1.91	9.2E-12
<i>Sex</i>	0.93	0.67	1.29	6.6E-01
<i>VT-VF</i>	0.31	0.23	0.40	1.8E-17
<i>Bystander CPR</i>	0.55	0.42	0.73	2.1E-05
<i>Shock on admission</i>	1.70	1.18	2.43	4.1E-03
<i>Targeted Temperature</i>	0.88	0.68	1.15	3.4E-01
<i>Time to ROSC</i>	1.72	1.48	2.00	1.1E-12
<i>Lactate</i>	1.43	1.24	1.65	1.7E-08
<i>NSE</i>	3.54	3.09	4.07	2.0E-46
<i>circNFAT5</i>	1.29	1.14	1.46	7.3E-05

<b>Multivariable Cox proportional hazards</b>				
	<i>HR</i>	<i>Lower 95% CI</i>	<i>Upper 95% CI</i>	<i>p-value</i>
<i>Age</i>	1.60	1.36	1.89	1.0E-08
<i>Sex</i>	1.01	0.73	1.41	9.4E-01
<i>VT-VF</i>	0.50	0.37	0.67	4.7E-06
<i>Bystander CPR</i>	0.80	0.60	1.06	1.3E-01
<i>Shock on admission</i>	1.01	0.70	1.47	9.6E-01
<i>Targeted Temperature</i>	0.88	0.68	1.15	3.6E-01
<i>Time to ROSC</i>	1.14	0.98	1.33	8.2E-02
<i>Lactate</i>	1.23	1.08	1.40	1.5E-03
<i>NSE</i>	2.58	2.15	3.09	1.1E-24
<i>circNFAT5</i>	1.27	1.10	1.46	1.2E-03

Univariate and multivariable Cox proportional hazards models reporting the hazard ratio (OR) coefficients, 95% confidence intervals (Lower 95% CI and Upper 95% CI) and p-values for the different parameters tested.



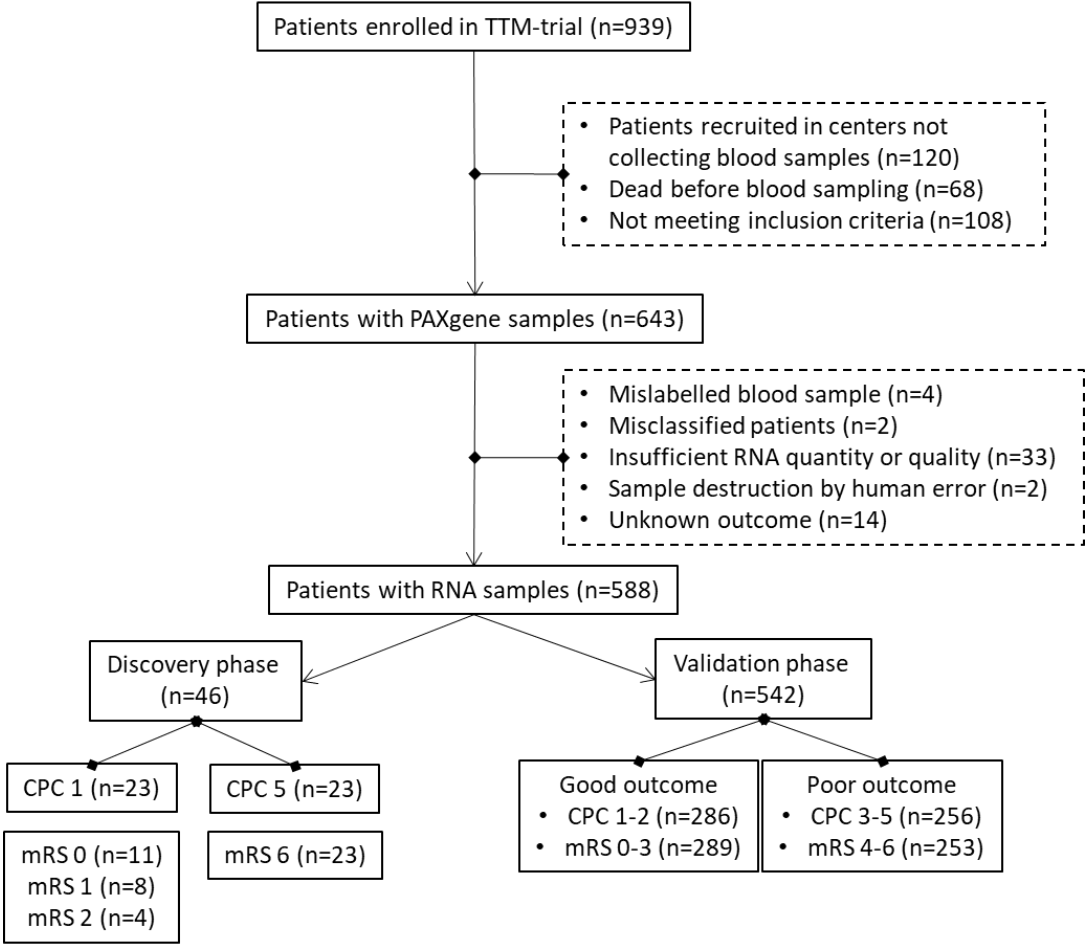
Supplemental Table 4. CircNFAT5 performance to predict patient outcome in TTM cohort using mRS score.

<b>Neurological outcome</b>	<i>AIC</i>	<i>HL<sub>p</sub></i>	<i>AUC</i>	<i>lr<sub>p</sub></i>	<i>NRI</i>	<i>NRI<sub>p</sub></i>	<i>IDI</i>	<i>IDI<sub>p</sub></i>
<i>basal model</i>	424	< 2.22E-16	0.91	-	-	-	-	-
<i>basal model + circNFAT5</i>	420	< 2.22E-16	0.91	0.015	0.285	7.97E-04	0.005	0.163

Incremental value of circNFAT5 to predict neurological outcome in TTM-trial patients using mRS score. Clinical model included in the analyses, analyses performed and abbreviations as in table 4.

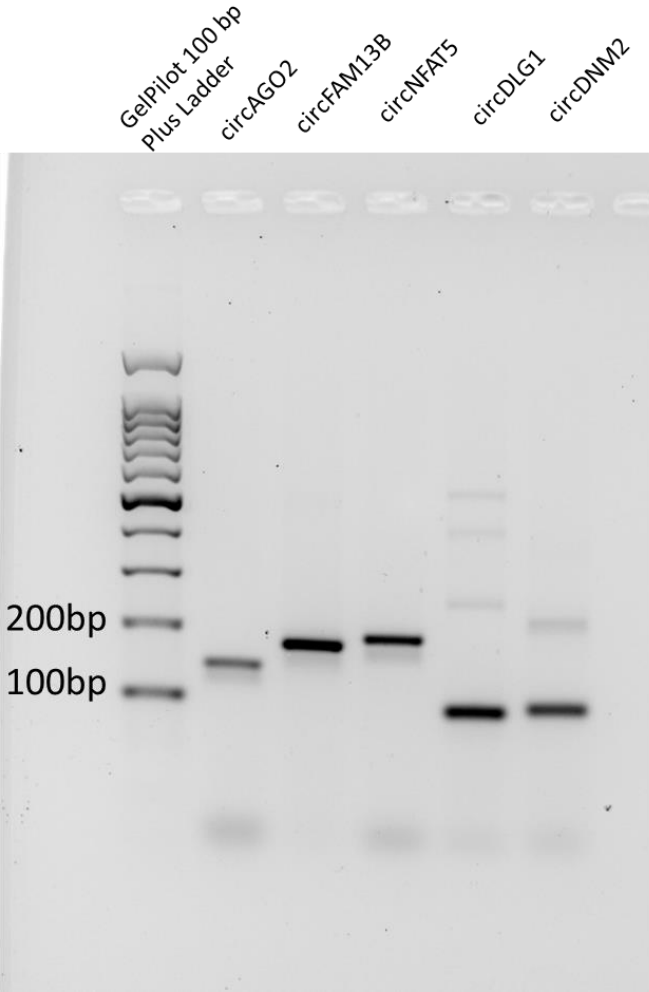
Supplemental figures

Supplemental Figure 1. Study flow-chart of TTM-trial.



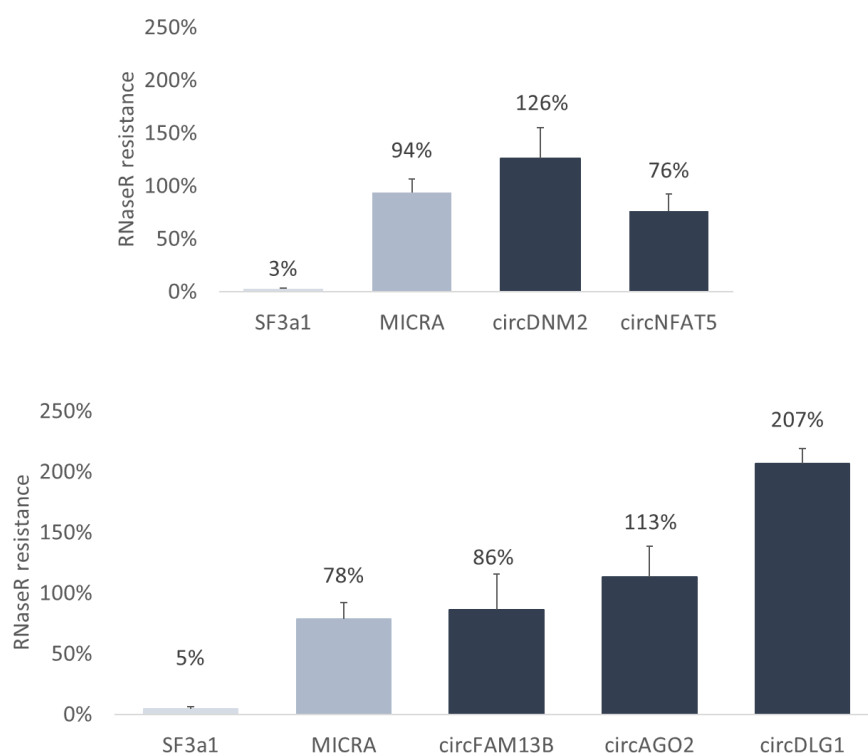
Abbreviations: TTM (Targeted Temperature Management); IBBL (International Biobank of Luxembourg); CPC (Cerebral Performance Category) mRS (modified Rankin Scale).

Supplemental Figure 2. PCR products of 5 circRNAs used for sequencing



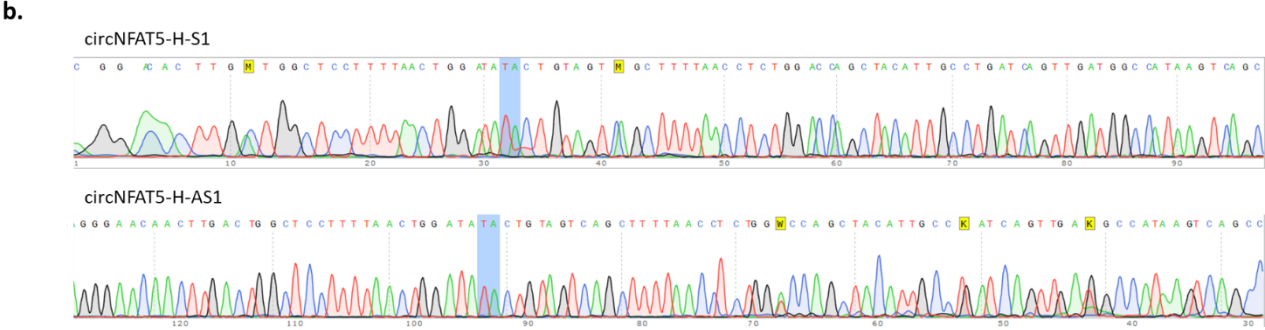
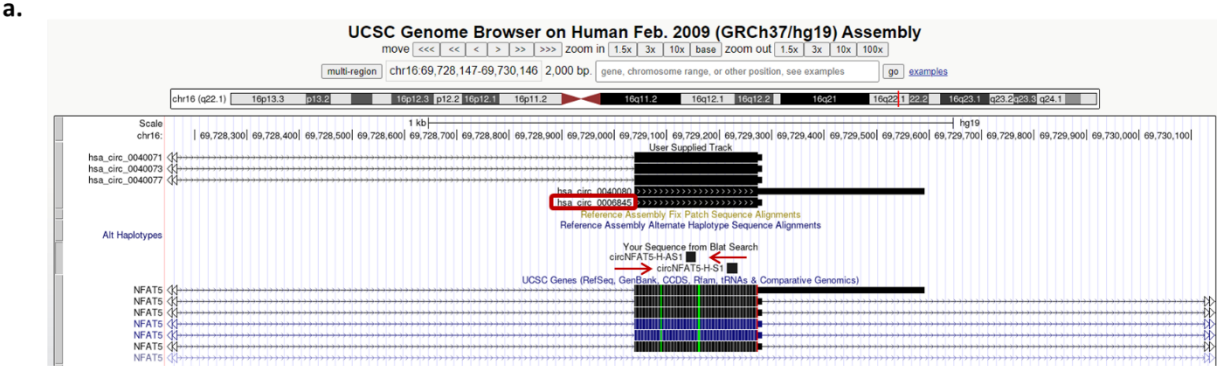
Electrophoretic gel showing the PCR products of the 5 circRNAs used for sequencing. The product size of each circRNA, circFAM13b (173 bp), circNFAT5 (185bp), circDLG1 (88 bp), circDNM2 (90 bp) and circAGO2 (139 bp) was confirmed. The electrophoretic run was performed on a 2% agarose gel. The ladder used was the GelPilot 100 bp Plus (cat. no. 239045).

Supplemental Figure 3. Confirmed circularity of the 5 circRNAs.



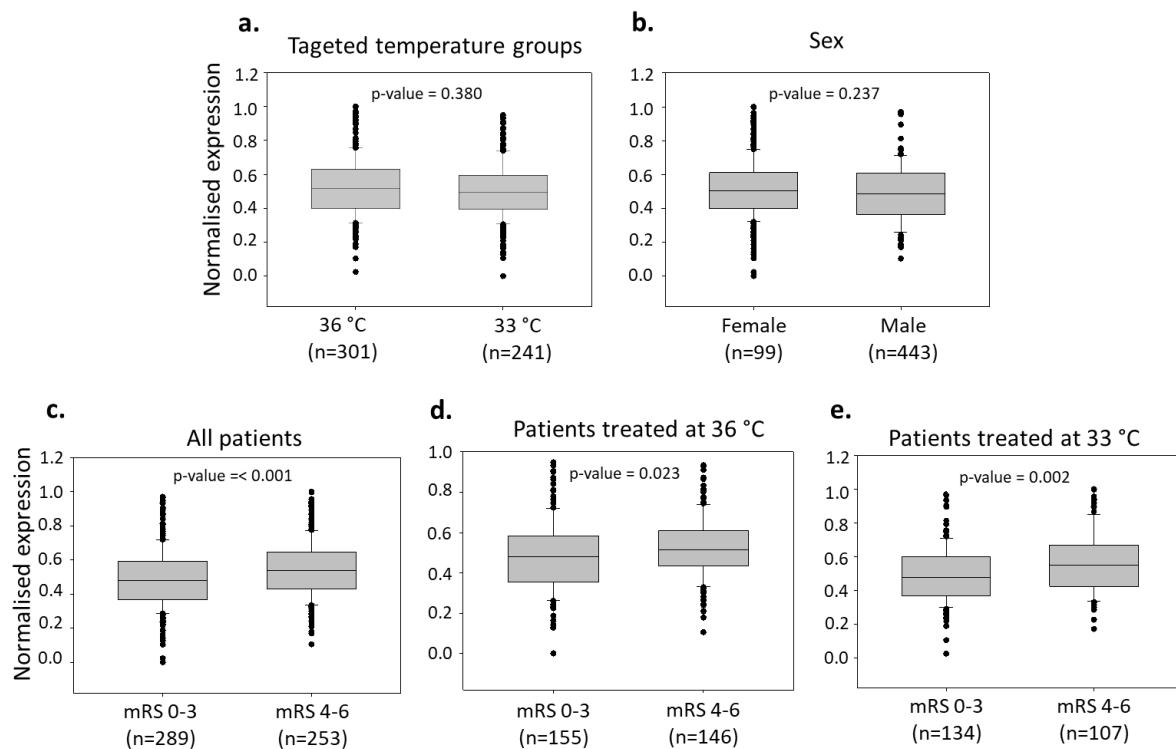
Bar chart showing resistance to RNase R treatment of 5 circRNAs. The resistance to RNase R of circDNM2 and circNFAT5 was measured in a first set of 8 patients, whereas the resistance of circFAM13b, circAGO2 and circDLG1 was measured in a different set of patients and therefore represented in a separate chart. SF3a1 linear RNA was used as a negative control of the experiment showing a 3-5% resistance to the treatment, while the circRNA MICRA (cZNF609) was used as positive control (78-94% resistance to the enzyme). Details on the protocol can be found in supplementary materials and methods section.

Supplemental Figure 4. Location and amplification circNFAT5.



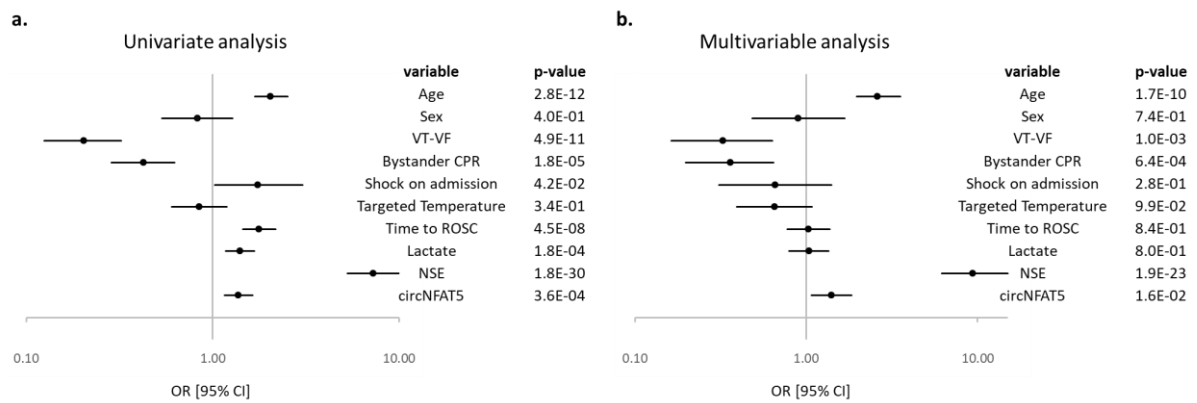
**a.** UCSB representation showing the location of circNFAT5 PCR divergent primers (red arrows), circNFAT5 (hsa\_circ\_0006845; red square) and linear NFAT5 isoforms. **b.** PCR product of Sanger sequencing using circNFAT5 divergent primers with the junction site highlighted in blue.

Supplemental Figure 5. CircNFAT5 expression levels in 542 patients of the TTM-trial using mRS score



CircNFAT5 levels were compared according to the temperature regimen and regardless of the neurological outcome (a), between females and males (b), between good (mRS 0-3) and poor (mRS 3-5) neurological outcome regardless of the temperature regimen (c), and separately in patients treated at 36°C or 33°C (d-e). The analyses have been performed as described in figure 2.

Supplemental Figure 6. Logistic regression models to predict neurological outcome in TTM-trial patients.



Forest plots showing the odds ratio (OR) with  $\pm$  95% confidence interval [95% CI] for the prediction of 6-month neurological outcome in TTM-trial patients using mRS score. **a)** Univariate logistic regression analysis. **b)** Multivariable logistic regression analysis.

## Abstract

Cardiac arrest is one of the leading causes of death worldwide, affecting on average 100 out of 100,000 people per year in Europe. Of these, resuscitation is attempted in 50-60% of cases, and survivors to hospital discharge average 8%. Accurate prediction of the outcome of these patients would help adapt health care. However, despite progress in this field, the prognosis of these patients remains poor. Therefore, the discovery of new specific biomarkers could improve current multimodal prediction approaches. Non-coding RNAs (ncRNAs) detected in blood represent a reservoir of novel biomarkers. Among them, circulating levels of micro RNAs (miRNA) have already been shown to be associated with outcome prediction of patients after out-of-hospital cardiac arrest (OHCA).

In light of this, an initial study was designed to determine whether the levels of miRNAs identified in patients after OHCA may indeed reflect the extent of brain damage. To this end, circulating levels of miRNAs were assessed by sequencing plasma samples collected 48h after ROSC of 50 patients from the Targeted Temperature Management (TTM) trial grouped according to their favourable or unfavourable neurological outcome, 6 months after OHCA. These miRNAs were correlated with neuron-specific enolase (NSE), a marker of brain damage. Among miRNAs, brain-enriched miR9-3p, miR124-3p and miR129-5p showed significant positive correlation with NSE. Furthermore, all 3 miRNAs showed to be predictors of neurological outcome. Thus, these results indicated that circulating levels of brain-enriched microRNAs may indeed reflect the extent of brain damage, strengthening their potential to aid in the outcome prognostication after OHCA.

In a second study, the goal was to identify potential long ncRNAs (lncRNA) and circular RNAs (circRNA) able to predict the outcome of patients after OHCA. To this end, whole blood samples of 46 TTM patients grouped according to their neurological outcome were sequenced. Among the lncRNAs and circRNAs identified, 5 circRNAs (circAGO2, circDLG1, circDNM2, circFAM13b and circNFAT5) and 1 lncRNA (lnc-IL1R1-1:2) were selected and measured by qPCR in the remaining TTM samples (n=542). The ability of candidates to predict neurological outcome was assessed by logistic regression and survival with Kaplan-Meier and Cox proportional hazards curves. Among the selected candidates, circNFAT5 performed best in predicting neurological outcome and survival 6 months after OHCA. Therefore, this circRNA was selected for preliminary *in-vitro* functional studies. Among the *in-vitro* treatments mimicking a post-cardiac arrest syndrome, circNFAT5 was found to be significantly modulated upon activation of T-cells and monocytes, suggesting an association of this circRNA with the inflammatory process occurring after OHCA. Furthermore, preliminary experiments suggested an independent relationship of circNFAT5 expression with its parental gene, strengthening the belief of a functional regulatory role of circNFAT5. Although, different attempts were made to elucidate the regulatory mechanisms of action of circNFAT5, no potential functions could be delineated in this work. Therefore, future explorations are needed to shed light on the possible biological functions performed by circNFAT5. Finally, the 3 best performing circRNAs identified in the TTM-trial were also measured by qPCR in 674 patients of the TTM2-trial. Following the same analyses presented in TTM, the three circRNAs were confirmed as independent predictors of neurological outcome and survival, but only in the normothermia group of TTM2, with circDNM2 as best performing candidate.

In conclusion, this project aimed to deepen the understanding of the potential use of ncRNAs as biomarkers after OHCA and represented a starting point for future studies focusing on the clinical utility and mechanisms of action of the identified candidates in the outcome prognostication of patients after OHCA.



## Résumé

L'arrêt cardiaque extra-hospitalier (ACHE) est l'une des principales causes de décès, touchant environ 100 personnes sur 100 000 par an en Europe. Une réanimation a été tentée dans 50 à 60 % des cas, et en moyenne, 8 % des survivants sont sortis de l'hôpital. Un pronostic précis de l'évolution de ces patients permettrait de mieux adapter les soins de santé. Malgré les progrès réalisés, le pronostic post-ACEH reste encore trop peu fiable. De ce fait, la découverte de nouveaux biomarqueurs spécifiques pourrait améliorer les approches actuelles. Les ARN non-codants détectés dans le sang représentent un réservoir de nouveaux biomarqueurs. Parmi eux, certains microARN (miARN) ont déjà été associés au pronostic des patients après un ACEH.

Sur cette base, une première étude a pour but de déterminer si des miARN circulants pourraient refléter l'étendue des lésions cérébrales post-ACEH. À cette fin, des miARN ont été identifiés par séquençage du plasma prélevé 48h post-ACEH chez 50 patients provenant de l'essai TTM (Targeted Temperature Management) et sélectionnés selon leur évolution neurologique favorable ou défavorable, 6 mois post-ACEH. Ces miARN ont été corrélés avec l'énolase spécifique des neurones (NSE), un marqueur de lésions cérébrales. Parmi ces miARN, les miR-9-3p, miR-124-3p et miR-129-5p, connus comme étant enrichis dans le cerveau, ont montré une corrélation positive significative avec la NSE. De plus, ces 3 miARN se sont avérés être des prédicteurs de l'évolution neurologique post-ACEH. Ces résultats suggèrent que les niveaux circulants de ces miARN peuvent refléter l'étendue des lésions cérébrales, renforçant ainsi leur potentiel pour aider au pronostic de l'évolution post-ACEH.

Dans une deuxième étude, l'objectif était d'identifier des longs ARN non-codants (ARNlnc) et des ARN circulaires (ARNcirc) capables de prédire l'évolution des patients après un ACEH. À cette fin, les échantillons sanguins prélevés 48h post-ACEH chez 46 patients TTM sélectionnés en fonction de leur évolution neurologique à 6 mois ont été séquencés. Parmi les candidats identifiés, 5 ARNcirc (circAGO2, circDLG1, circDNM2, circFAM13b et circNFAT5) et 1 ARNlnc (lnc-IL1R1-1:2) ont été sélectionnés et mesurés par qPCR chez les 542 patients restants de l'étude TTM. La capacité de ces 6 candidats à prédire l'évolution neurologique a été évaluée par régression logistique, et la survie grâce aux courbes de Kaplan-Meier et aux modèles de Cox. Parmi les candidats étudiés, circNFAT5 fût le meilleur pour prédire l'évolution neurologique et la survie 6 mois post-ACEH. Par conséquent, cet ARNcirc fût sélectionné pour des études fonctionnelles *in-vitro*. Dans les modèles *in-vitro* imitant un syndrome post-arrêt cardiaque, circNFAT5 fût modulé lors de l'activation des cellules T et des monocytes, suggérant un lien possible entre cet ARNcirc et le processus inflammatoire post-ACEH. De plus, des expériences préliminaires ont suggéré une relation indépendante de l'expression de circNFAT5 de celle de son gène parental, renforçant un rôle fonctionnel indépendant de circNFAT5. Après avoir investigué plusieurs pistes, aucune d'entre elles n'a permis d'identifier formellement les fonctions de circNFAT5. Par conséquent, des explorations futures seront nécessaires pour comprendre les fonctions biologiques de circNFAT5. Enfin, les 3 ARNcirc les plus performants identifiés dans l'étude TTM ont également été mesurés par qPCR chez les 674 patients de l'essai TTM2. Les 3 ARNcirc ont confirmés leur capacité de prédiction de l'évolution neurologique et de la survie, mais uniquement dans le groupe de patients traités en normothermie. CircDNM2 fût le candidat le plus performant dans cette étude.

En conclusion, ce projet visait à investiguer l'utilisation potentielle des ARNnc comme biomarqueurs après un ACEH et représente un point de départ pour de futures études sur l'utilité clinique et les mécanismes d'action des candidats identifiés pour le pronostic des patients après un ACEH.